

THÈSE DE DOCTORAT

présentée et soutenue publiquement le

26 septembre 2025

pour l'obtention du diplôme de

Docteur de l'Université Gustave Eiffel

spécialité : Informatique

par

Loïc DUBOIS

Algorithms for Topological and Metric Surfaces

MEMBRES DU JURY

Marthe BONAMY	<i>Examinateuse</i>
Jérémie CHALOPIN	<i>Président</i>
Éric COLIN DE VERDIÈRE	<i>Directeur de thèse</i>
Vincent DESPRÉ	<i>Co-encadrant de thèse</i>
Jeff ERICKSON	<i>Rapporteur</i>
Louis ESPERET	<i>Rapporteur</i>
Federica FANONI	<i>Examinateuse</i>
Csaba TÓTH	<i>Rapporteur</i>

École Doctorale Mathématiques et STIC
Laboratoire d'Informatique Gaspard Monge
5 boulevard Descartes, Champs-sur-Marne, France

Abstract

In this thesis we provide algorithms for geometric and topological problems. This line of research, computational geometry, emerged in the 70s with the advent of computers.

We consider the problem of untangling graphs on surfaces: given a drawing of a graph on a surface, possibly with crossings, remove all crossings by deforming the drawing continuously, or correctly assert that this is not possible. We give the first polynomial time algorithms for this problem. To do so we introduce a new kind of triangulations of surfaces that discretize negative-curvature surfaces in a better way than the state of the art. On these triangulations, we provide a combinatorial analog of the celebrated barycentric embeddings of Tutte.

In a more geometric setting, we give a new efficient algorithm for computing a Delaunay triangulation of an abstract piecewise-flat surface (a generalization of meshes). We also study the classical Delaunay flip algorithm, and prove, when the surface is a flat torus, the first worst-case bound that is tight up to a constant factor. On hyperbolic surfaces, we provide an implementation of the Delaunay flip algorithm, collected in a package of the standard library of computational geometry CGAL, along with convenient generation and visualization tools.

Keywords: computational geometry, computational topology, surface, graph, homotopy, Delaunay triangulation.

Résumé

Dans cette thèse, nous fournissons des algorithmes pour des problèmes géométriques et topologiques. Cette ligne de recherche, la géométrie algorithmique, a émergé dans les années 70 avec l'avènement des ordinateurs.

Nous considérons le problème du démêlage de graphes sur les surfaces : étant donné un dessin d'un graphe sur une surface, éventuellement avec des croisements, nous devons supprimer tous les croisements en déformant le dessin continuement, ou affirmer correctement que ce n'est pas possible. Nous donnons les premiers algorithmes en temps polynomial pour ce problème. Pour ce faire, nous introduisons un nouveau type de triangulations de surfaces qui discrétilisent les surfaces à courbure négative d'une façon meilleure que l'état de l'art. Sur ces triangulations, nous fournissons un analogue combinatoire des célèbres plongements barycentriques de Tutte.

Dans un cadre plus géométrique, nous donnons un nouvel algorithme efficace pour calculer une triangulation de Delaunay d'une surface abstraite plate par morceaux (une généralisation des maillages). Nous étudions également l'algorithme classique de bascule de Delaunay et prouvons, lorsque la surface est un tore plat, la première borne dans le pire cas qui soit optimale à facteur constant près. Sur les surfaces hyperboliques, nous fournissons une implémentation de l'algorithme de bascule de Delaunay, collectée dans un package de la bibliothèque standard de géométrie algorithmique CGAL, et accompagnée d'outils de génération et de visualisation pratiques.

Mots clefs: géométrie algorithmique, topologie algorithmique, surface, graphe, homotopie, triangulation de Delaunay.

Acknowledgements

I would like to thank first my two advisors, Éric Colin de Verdière and Vincent Despré. They introduced me to interesting and fruitful research topics, improved my ability in writing, accompanied me as co-authors, and motivated me when writing this document. Special thanks also to Monique Teillaud. She guided my first steps in computational geometry, hosted me many times in Nancy, and supported me in various ways. Lots of thanks to my other co-authors, especially Marc Pouget, without whom our software would not have become a proper package, and Guillem Perarnau, for his determinant role in my first publication. Let me express my gratitude to Stefan Felsner and his group for having hosted me in Berlin, and to Hugo Parlier and Peter Buser for having boosted my interest in hyperbolic geometry. I would like to thank also the reviewers and examiners of this thesis, and all the people I met during my stays in Marnes-la-Vallée and Nancy. Last but not least, I am very grateful to my family for their tireless support.

Contents

Contents	6
1 Introduction	9
1.1 Untangling graphs on surfaces	10
1.2 Computing Delaunay triangulations of surfaces	11
2 Introduction en Français	13
2.1 Démêler des graphes sur les surfaces	14
2.2 Calculer des triangulations de Delaunay de surfaces	15
3 Geometric and Topological Background	17
3.1 Topology of graphs on surfaces	17
3.2 Homotopy	22
3.3 Geometry of surfaces	26
I Untangling Graphs on Surfaces	31
4 Related Works	37
4.1 Drawing graphs on surfaces	38
4.2 Perturbing drawings	41
4.3 Embedding graphs rectilinearly in the plane	42
4.4 Untangling graphs on surfaces	46
5 Preliminaries	55
5.1 Limit points of lifted curves	55
5.2 Intersection number, primitivity, and lifts	59
5.3 Perturbing drawings into embeddings	60
5.4 Perturbing closed walks minimally	61
6 Untangling Graphs on Reducing Triangulations	67
6.1 Reducing triangulations	68
6.2 Reduced walks	69
6.3 Making closed curves cross minimally	77
6.4 Untangling loop graphs	79
6.5 Untangling graphs	86
6.6 Efficient factorization	90

7 Untangling Graphs on Surfaces	97
7.1 Untangling graphs on the canonical system of loops of the torus	99
7.2 Untangling graphs on the loop systems of surfaces with boundary	103
7.3 Model conversions	106
7.4 Untangling graphs on surfaces	110
7.5 Application to the punctured plane	112
8 A Discrete Analog of Tutte Embeddings	115
8.1 Harmonious drawings	116
8.2 A Tutte theorem on reducing triangulations	119
8.3 Harmonizing a drawing monotonically	135
8.4 Extensions to reducing triangulations with boundary	146
II Computing Delaunay Triangulations of Surfaces	149
9 Background and Related Works	155
9.1 Portalgons versus meshes	155
9.2 Measuring distances, and tracing shortest paths	156
9.3 Voronoi diagrams and Delaunay tessellations	156
9.4 Computing Voronoi diagrams and Delaunay tessellations	158
10 Computing the Delaunay Tessellation of a Closed Piecewise-Flat Surface	161
10.1 Introduction	161
10.2 Tubes and bifaces	164
10.3 Algorithm	165
10.4 Combinatorial analysis of the algorithm: proof of Proposition 10.5	170
10.5 Enclosure	174
10.6 Geometric analysis of the algorithm: proof of Proposition 10.1	181
10.7 Extension to non-flat surfaces: proof of Proposition 10.2	183
10.8 Appendix: proof of Proposition 10.4	185
10.9 Appendix: Voronoi diagram and Delaunay tessellation	188
10.10 Appendix: Computing the Delaunay tessellation	190
11 Bounds for Delaunay Flips on Flat Tori	201
11.1 Background: stereographic projection	201
11.2 Lower bound	202
11.3 Upper bound	205
12 Implementation of Delaunay Triangulations of Closed Hyperbolic Surfaces	211
12.1 Introduction	211
12.2 Data structures	212
12.3 Generation of domains in genus two	213
13 Conclusion	217
13.1 Untangling graphs on surfaces	217
13.2 Computing Delaunay triangulations of surfaces	219

Contributions	221
Bibliography	223

Chapter 1

Introduction

This thesis grew out of a fascination for surfaces. Surfaces appear in many contexts. They occur naturally in the physical world, and are represented in computer softwares and video games. Mathematicians have studied surfaces for centuries, from various points of view reflected by famous results: the Gauss–Bonnet formula, the uniformization theorem, the topological classification of surfaces, the Dehn–Thurston classification of their homeomorphisms, or more recently the spectacular geometric study of Mirzakhani. Tools have been developed on surfaces before being transposed to other contexts, by Dehn and Gromov in group theory, or by Thurston in the study of 3-manifolds and knots. In theoretical computer science, mixing surfaces with graphs led to structural results like the graph minor theory of Robertson and Seymour, and to a very active line of research concerned with the design of algorithms for graphs embedded on surfaces.

Strikingly, surfaces take various forms, from their topological abstractions to their geometric realizations. In this thesis we navigate between different types of surfaces to provide efficient algorithms for discrete problems. For example we consider a problem stated on topological surfaces which admits a non-algorithmic solution on hyperbolic surfaces, and we transform this solution into an algorithm on a more combinatorial notion of surfaces.

The design and analysis of efficient algorithms for geometric problems crystallized in the 70s as a line of research, computational geometry, in response to the needs of computer graphics, computer-aided design, robotics, and geographic information systems. Populated by traditional geometric notions, the field has equipped itself with unique algorithms and paradigms, and has developed interactions with other areas of computer science.

Even though most of our contributions are theoretical results, we also implemented a package in the standard library of computational geometry CGAL. Our implementation can be used by mathematicians for exploring conjectures on hyperbolic surfaces. Moreover, CGAL is widely used, not only by academics, but also in the industry, and this package is a good way to disseminate algorithms on surfaces more broadly.

We provide some background in Chapter 3, and a conclusion in Chapter 13. The other chapters are divided into two parts, concerned with two different problems on surfaces: untangling graphs, and computing Delaunay triangulations. We now provide a brief account of the problems and contributions of each part. More detailed introductions are given at the beginning of each part.

1.1 Untangling graphs on surfaces

The first part of the thesis is concerned with the problem of untangling graphs on surfaces. In this problem we are given a drawing of a graph on a surface, possibly with crossings. We have to remove all these crossings by deforming the drawing continuously, or correctly assert that this is not possible. To illustrate, consider Figure 1.1. Here the surface is the usual Euclidean plane, minus a finite set of obstacle points. Two graphs are drawn. By deforming the drawing on the left continuously, avoiding the obstacle points, we can remove all its crossings. Observe, informally, how the edges and vertices of the drawing can go “through” each other while deforming the drawing. Is it possible to untangle the drawing on the right this way? For a drawing on a surface more general than the plane, consider Figure 1.2.

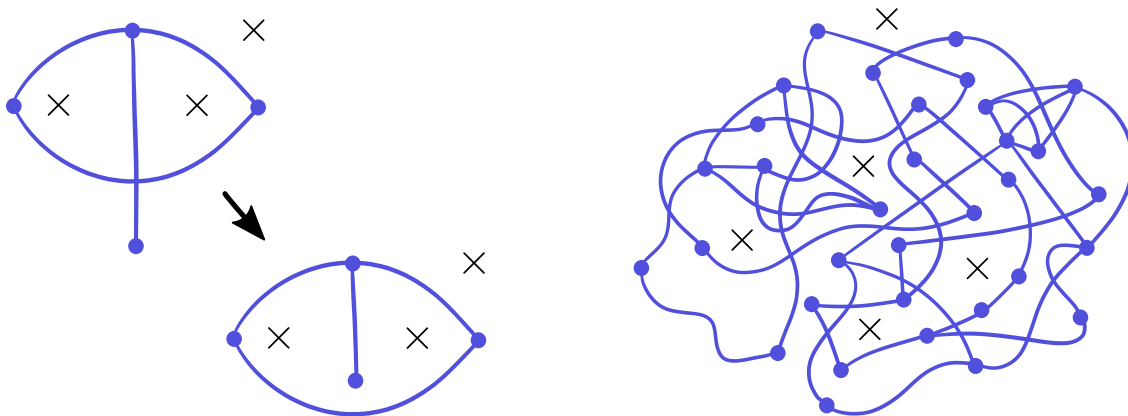


Figure 1.1: In the Euclidean plane, obstacle points are represented by crosses, and graphs are drawn in blue. The drawing on the left can be untangled while avoiding the obstacle points. What about the drawing on the right?

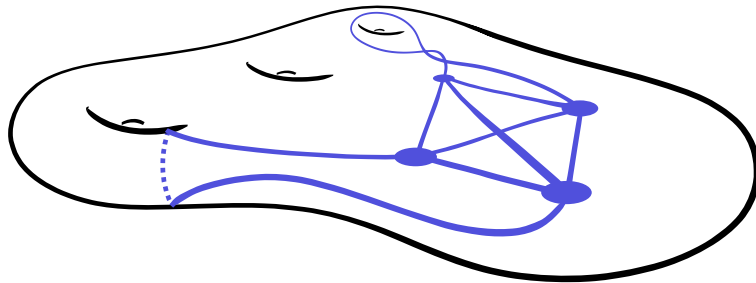


Figure 1.2: A drawing of a graph on a surface that cannot be untangled.

This problem is a variation of the problem of drawing a graph on a surface with few, if not zero, crossings, which has been extensively studied. The novelty is the constraint of having to deform an input drawing continuously.

This constraint, in addition to being very natural, stems from the topological study of curves on surfaces, which has been an important field of study in the mathematical communities for more than one hundred years. As early as 1911, Dehn obtained combinatorial characterizations of whether a closed curve on a surface is contractible (can be continuously moved to a point), or whether two closed curves are homotopic (can be continuously

deformed into each other). Even earlier, in 1904, Poincaré described a characterization of whether a closed curve can be untangled. Such questions have since been considered by numerous mathematicians, and have been extensively revisited under a more algorithmic lens since the 1990s. Many of them extend from curves to drawings of graphs, but surprisingly the literature studying them on graphs is rather scarce, in stark contrast with the central importance of graphs in computer science.

We provide the first polynomial time algorithms for the untangling problem, in a natural discrete model. To do so we crucially introduce a new kind of triangulations of surfaces that build upon many previous works for discretizing properties of negatively curved surfaces. They are likely of independent interest. On those triangulations, we also provide a combinatorial analog of the celebrated barycentric embedding theorem of Tutte from 1963, and its polynomial time algorithmic counterpart. This allows to produce many different untangled versions of a drawing, and even allows vertices of the graph to be attached to the boundary of the surface in the drawing. Incidentally, we provide algorithms to minimize the crossings of a collection of closed curves that generalize, improve, and simplify the state of the art.

This section corresponds to the three papers [1], [2], and [5]. The first two papers are co-authored with Éric Colin de Verdière and Vincent Despré.

1.2 Computing Delaunay triangulations of surfaces

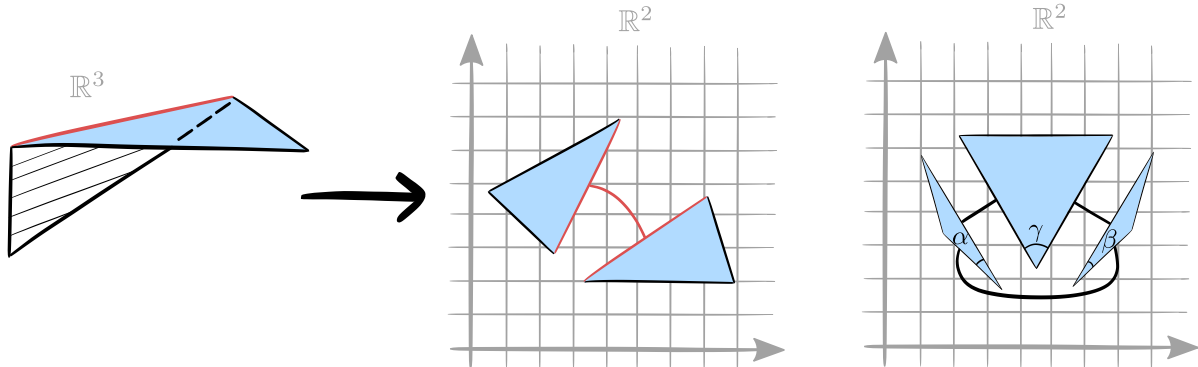


Figure 1.3: (Left) The mesh is cut along a red edge, and the resulting triangles are laid out in the plane. (Right) It is not possible to form a mesh by cutting out the three triangles from the plane and identifying the three pairs of matched sides, since the angles α , β , and γ satisfy $\alpha + \beta < \gamma$.

The second part of the thesis is concerned mainly with piecewise-flat surfaces, and more specifically with their *triangulations*. Such surfaces are commonly obtained from *meshes*, namely flat triangles in \mathbb{R}^3 glued along their edges. And every mesh carries a triangulation of its surface. However triangulations are far more general, they are generically not issued of a mesh this way. To see that consider Figure 1.3. On the left, a mesh with two triangles is cut along its interior red edge, and the two resulting triangles are laid out in the plane. On the right, cutting out the triangles from the plane and identifying the matched sides defines a triangulation of a piecewise-flat surface, but this triangulation is not issued of any mesh, as is easily observed.

There is a recent development of algorithms that advantageously operate on triangulations without the assumption that they are issued of a mesh. On the other hand, triangulations are so general that not all of them are suited to computation, compared to meshes. Prominently, algorithms for such a fundamental problem as measuring the distance between two points on the surface are affected by the *happiness* of the triangulation, a natural parameter which is unbounded on triangulations while bounded on meshes. This raises the problem of computing, from an input triangulation, another triangulation representing the same surface, but whose happiness is bounded. This problem has been observed, in this form or another, by several computational geometers over the last few decades.

Specifically, we consider computing a Delaunay triangulation, for those triangulations not only have bounded happiness, but they also enjoy some level of unicity, and they are naturally related to distances and shortest paths on the surface.

We have several contributions. First, we provide an efficient algorithm for computing a Delaunay triangulation of a closed piecewise-flat surface from any other triangulation of the surface. Then, we depart from looking for an efficient algorithm, and we consider instead a classical algorithm that computes a Delaunay triangulation simply by flipping the edges of an input triangulation. The asymptotics of the number of flips are vastly open. In the particular case where the surface is a flat torus, we provide the first worst-case bound that is tight up to a constant factor. Finally, our third contribution is an implementation of the Delaunay flip algorithm on triangulations of closed *hyperbolic* surfaces, a fundamental building block for computing with such surfaces. Our implementation is collected in a package of the standard library of computational geometry CGAL, along with convenient generation and visualization tools.

This section corresponds to the two papers [6] and [4], and to the package [3] to appear in the next release of CGAL. At the time of writing this thesis, the first paper is a preprint. The package is co-authored with Vincent Despré, Marc Pouget, and Monique Teillaud.

Chapter 2

Introduction en Français

Ce chapitre est une traduction en français de l'introduction de la thèse, à savoir du Chapitre 1.

Cette thèse est née d'une fascination pour les surfaces. Les surfaces apparaissent dans de nombreux contextes. Elles se produisent naturellement dans le monde physique et sont représentées dans les logiciels informatiques et les jeux vidéo. Les mathématiciens ont étudié les surfaces pendant des siècles, sous des angles divers reflétés par des résultats célèbres : la formule de Gauss-Bonnet, le théorème d'uniformisation, la classification topologique des surfaces, la classification de Dehn-Thurston de leurs homéomorphismes, ou plus récemment la spectaculaire étude géométrique de Mirzakhani. Des outils ont été développés sur des surfaces avant d'être transposés à d'autres contextes, par Dehn et Gromov dans la théorie des groupes, ou par Thurston dans l'étude des 3-variétés et des noeuds. En informatique théorique, le mélange de surfaces et de graphes a conduit à des résultats structurels comme la théorie des graphes mineurs de Robertson et Seymour, et à une ligne de recherche très active concernée par la conception d'algorithmes pour les graphes plongés sur les surfaces.

Il est frappant de constater que les surfaces prennent des formes diverses, de leurs abstractions topologiques à leurs réalisations géométriques. Dans cette thèse, nous naviguons entre différents types de surfaces afin de fournir des algorithmes efficaces pour des problèmes discrets. Par exemple, nous considérons un problème énoncé sur des surfaces topologiques qui admet une solution non algorithmique sur des surfaces hyperboliques, et nous transformons cette solution en un algorithme sur une notion plus combinatoire de surfaces.

La conception et l'analyse d'algorithmes efficaces pour des problèmes géométriques se sont cristallisées dans les années 70 en une ligne de recherche, la géométrie algorithmique, en réponse aux besoins de l'infographie, de la conception assistée par ordinateur, de la robotique et des systèmes d'information géographique. Peuplé de notions géométriques traditionnelles, le domaine s'est doté d'algorithmes et de paradigmes uniques, et a développé des interactions avec d'autres domaines de l'informatique.

Même si la plupart de nos contributions sont des résultats théoriques, nous avons également implémenté un package dans la bibliothèque standard de géométrie algorithmique CGAL. Notre implémentation peut être utilisée par les mathématiciens pour explorer des conjectures sur les surfaces hyperboliques. De plus, CGAL est largement utilisée, non seulement par les universitaires, mais aussi dans l'industrie, et ce package est un bon moyen de diffuser des algorithmes sur des surfaces plus largement.

Nous fournissons un peu de contexte dans le Chapitre 3, et une conclusion dans le Chapitre 13. Les autres chapitres sont divisés en deux parties, qui s'intéressent à deux

problèmes différents sur les surfaces : démêler des graphes et calculer des triangulations de Delaunay. Nous présentons maintenant un bref compte rendu des problèmes et contributions de chaque partie. Des introductions plus détaillées sont données au début de chaque partie.

2.1 Démêler des graphes sur les surfaces

La première partie de la thèse s'intéresse au problème du démêlage de graphes sur les surfaces. Dans ce problème, on nous donne un dessin d'un graphe sur une surface, éventuellement avec des croisements. Nous devons supprimer tous ces croisements en déformant le dessin continuellement, ou affirmer correctement que ce n'est pas possible. Pour illustrer, regardez Figure 2.1. Ici, la surface est le plan Euclidien habituel, moins un ensemble fini de points servant d'obstacles. Deux graphes sont dessinés. En déformant le dessin de gauche continuellement, tout en évitant les points d'obstacle, on peut supprimer tous les croisements. Observez, de manière informelle, comment les arêtes et les sommets du dessin peuvent "se passer au travers" durant la déformation du dessin. Est-il possible de démêler le dessin de droite de cette façon? Pour un dessin sur une surface plus générale que le plan, regardez Figure 2.2.

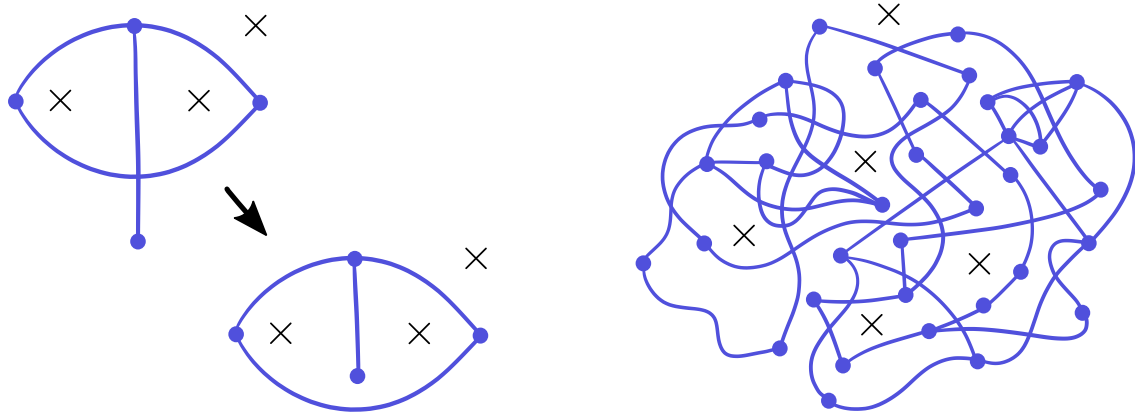


Figure 2.1: Dans le plan Euclidien, des points servant d'obstacles sont représentés par des croix et des graphes sont dessinés en bleu. Le dessin sur la gauche peut être démêlé tout en évitant les points d'obstacle. Qu'en est-il du dessin de droite?

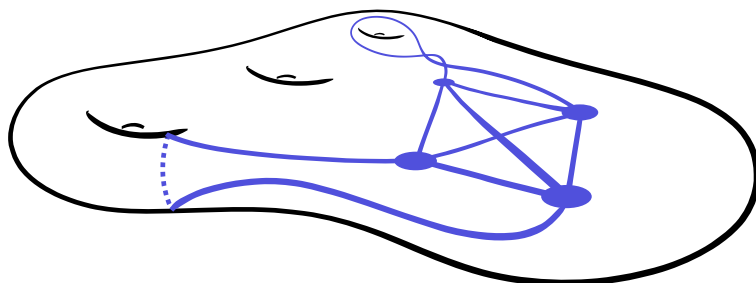


Figure 2.2: Un dessin d'un graphe sur une surface qui ne peut pas être démêlé.

Ce problème est une variante du problème de dessiner un graphe sur une surface avec peu, voire aucun, croisements, qui a été largement étudié. La nouveauté est la contrainte de devoir déformer continuellement un dessin donné en entrée.

Cette contrainte, en plus d'être très naturelle, découle de l'étude topologique des courbes sur les surfaces, qui est un domaine d'étude important dans les communautés mathématiques depuis plus de cent ans. Dès 1911, Dehn a obtenu des caractérisations combinatoires permettant de savoir si une courbe fermée sur une surface est contractible (peut être déplacée continuellement vers un point), ou si deux courbes fermées sont homotopes (peuvent être continuellement transformées l'une en l'autre). Encore plus tôt, en 1904, Poincaré a décrit une caractérisation des courbes fermées démêlables. De telles questions ont depuis été considérées par de nombreux mathématiciens, et on a été largement réexaminées sous une lentille plus algorithmique depuis les années 1990. Beaucoup d'entre elles s'étendent des courbes aux dessins de graphes, mais étonnamment, la littérature qui les étudie sur les graphes est plutôt éparsse, en contraste frappant avec l'importance centrale des graphes en informatique.

Nous fournissons les premiers algorithmes en temps polynomial pour le problème de démêlage, dans un modèle discret naturel. Pour ce faire, nous introduisons de manière cruciale un nouveau type de triangulations de surfaces, s'appuyant sur de nombreux travaux antérieurs pour discréteriser les propriétés des surfaces à courbure négative. Ces triangulations sont probablement d'intérêt indépendant. Sur ces triangulations, nous fournissons également un analogue combinatoire du célèbre théorème de plongement barycentrique de Tutte de 1963, et de sa contre-partie algorithmique. Cela nous permet de produire de nombreuses versions démêlées différentes d'un dessin, et permet même d'attacher les sommets du graphe au bord de la surface dans le dessin. Au passage, nous fournissons des algorithmes pour minimiser les croisements d'un ensemble de courbes fermées qui généralisent, améliorent et simplifient l'état de l'art.

Cette section correspond aux trois articles [1], [2], et [5]. Les deux premiers articles ont pour co-auteurs Éric Colin de Verdière et Vincent Despré.

2.2 Calculer des triangulations de Delaunay de surfaces

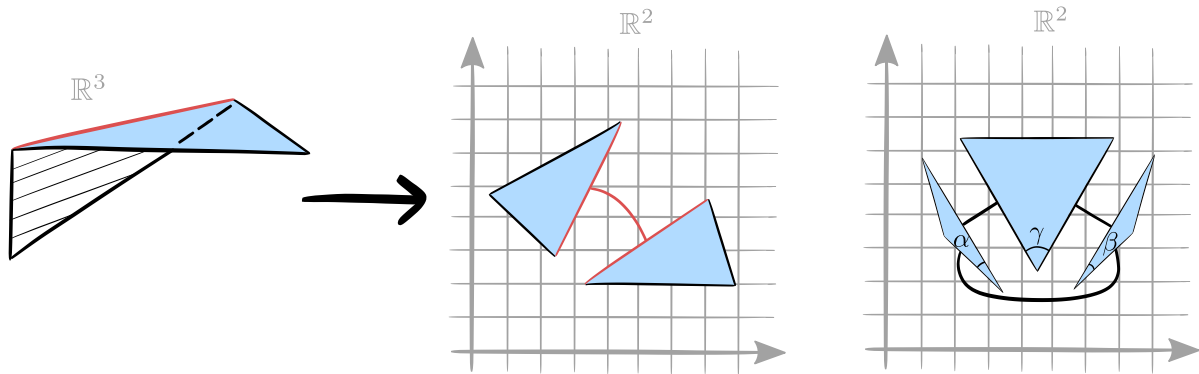


Figure 2.3: (À gauche) Le maillage est coupé le long d'une arête rouge et les triangles résultants sont disposés dans le plan. (À droite) Il n'est pas possible de former un maillage en découpant les trois triangles du plan et en identifiant les côtés appariés, car les angles α , β , et γ satisfont $\alpha + \beta < \gamma$.

La deuxième partie de la thèse s'intéresse principalement aux surfaces plates par morceaux, et plus particulièrement à leurs *triangulations*. De telles surfaces sont couramment obtenues à partir de *maillages*, à savoir des triangles plats dans \mathbb{R}^3 collés le long de leurs bords. Et

chaque maillage porte une triangulation de sa surface. Cependant, les triangulations sont beaucoup plus générales, elles ne sont généralement pas issues d'un maillage. Pour voir cela, regardez Figure 2.3. Sur la gauche, un maillage comportant deux triangles est coupé le long de son arrête rouge intérieure, et les deux triangles résultants sont disposés dans le plan. Sur la droite, découper les triangles dans le plan et identifier les côtés appariés définit bien une triangulation d'une surface plate par morceaux, mais cette triangulation n'est issue d'aucun maillage, comme on peut facilement l'observer.

Il y a un développement récent d'algorithmes opérant avantageusement sur des triangulations qui ne sont pas issues d'un maillage. D'un autre côté, les triangulations sont si générales qu'elles ne sont pas toutes adaptées au calcul, par rapport aux maillages. En particulier, les algorithmes pour un problème aussi fondamental que la mesure de la distance entre deux points sur la surface sont affectés par la *happiness* de la triangulation, un paramètre naturel qui n'est pas borné sur les triangulations alors qu'il est borné sur les maillages. Cela pose le problème de calculer, à partir d'une triangulation d'entrée, une autre triangulation représentant la même surface, mais dont la happiness est bornée. Ce problème a été observé, sous une forme ou une autre, par plusieurs géomètres algorithmiciens au cours des dernières décennies.

Plus spécifiquement, nous voulons calculer une triangulation de Delaunay, car ces triangulations ont non seulement une happiness bornée, mais elles jouissent également d'un certain niveau d'unicité, et elles sont naturellement liées aux distances et aux plus courts chemins sur la surface.

Nous avons plusieurs contributions. Tout d'abord, nous fournissons un algorithme efficace pour calculer une triangulation de Delaunay d'une surface fermée plate par morceaux à partir de toute autre triangulation de la surface. Ensuite, nous laissons de côté la recherche d'un algorithme efficace, et considérons plutôt un algorithme classique qui calcule une triangulation de Delaunay simplement en basculant les arêtes d'une triangulation d'entrée. Le comportement asymptotique du nombre de bascules est une question vastement ouverte. Dans le cas particulier où la surface est un tore plat, nous fournissons la première borne dans le pire cas qui soit optimale à facteur constant près. Enfin, notre troisième contribution est une implémentation de l'algorithme de bascule sur les triangulations de surfaces fermées *hyperboliques*, un outil fondamental pour caluler avec de telles surfaces. Notre implémentation est regroupée dans un package de la bibliothèque standard de géométrie algorithmique CGAL, accompagné d'outils de génération et de visualisation pratiques.

Cette section correspond aux deux articles [6] et [4], et au package [3] qui doit apparaître dans la prochaine version de CGAL. Au moment où cette thèse est écrite, le premier article est une prépublication. Le package a pour co-auteurs Vincent Despré, Marc Pouget, et Monique Teillaud.

Chapter 3

Geometric and Topological Background

In this chapter we present some of the main notions of this thesis. We focus on the geometric and topological background, assuming without review some basic algorithmic knowledge. We keep the presentation short and simple, referencing to textbooks for the details.

3.1 Topology of graphs on surfaces

The main characters of this thesis are surfaces, graphs, and drawings of graphs on surfaces. In this section we present these geometric objects from a coarse point of view, that of topology. Topology is the branch of mathematics concerned with the properties of geometric objects that are preserved under continuous deformations such as stretching, twisting, or bending; that is without tearing or gluing. A common example is the deformation of a rubber band. An introduction to topology is provided by Armstrong [16]. See also Stillwell [177] and Hatcher [115].

A **topology** is a structure that allows to define the notion of continuous deformation by relating spatially the points of a set. Formally, on a set X , a topology can be defined as a collection of subsets of X , called **open sets**, such that (1) the empty set is an open set, (2) every union of open sets is an open set, and (3) every finite intersection of open sets is an open set. A set X equipped with a topology is a **topological space**. We illustrate this definition with a classical topology. Given $d \geq 1$, $x \in \mathbb{R}^d$, and $r > 0$, the set of points of \mathbb{R}^d whose Euclidean distance to x is strictly smaller than r is an **open metric ball** of \mathbb{R}^d . The arbitrary unions of open metric balls are the open sets of a topology of \mathbb{R}^d . This is the smallest topology in which every open metric ball is an open set. It is the only topology of \mathbb{R}^d considered in this thesis. We mention that there are different but equivalent formulations of the notion of topology, for example whose axioms are the properties of the **closed sets**, the complements of the open sets.

A function $f : X \rightarrow Y$ between topological spaces X and Y is **continuous** if for every open set O of Y , $f^{-1}(O)$ is an open set of X . A continuous function is also called a **map**. An injective map is an **embedding**. A bijective map whose inverse is also a map is a **homeomorphism**. Two topological spaces related by a homeomorphism are **homeomorphic**, in which case they are often regarded as equal.

We use without review standard operations on topological spaces such as taking a subspace or a quotient. For example we equip every subspace of \mathbb{R}^d with the subspace topology. We also use notions such as compactness and connectedness. All the connected spaces con-

sidered in this thesis are also path-connected, meaning that every two points are related by a path. And every topological space considered is Hausdorff, meaning that for every two distinct points $x \neq x'$ there exist two disjoint open sets O and O' such that $x \in O$ and $x' \in O'$.

3.1.1 Surfaces

The first characters of this thesis are surfaces. Typical surfaces are the **plane** \mathbb{R}^2 and the (closed) **half plane** $\mathbb{R} \times [0, +\infty)$. In general a topological space S is a **surface** if S locally resembles the plane or the half plane. Formally, if each point of S has a neighborhood homeomorphic to the plane or to the half plane. By definition a surface S can have two types of points. The **interior** of S contains the points having a neighborhood homeomorphic to the plane, while the **boundary** of S , denoted ∂S , contains the points having a neighborhood homeomorphic to the half plane. The interior and the boundary of S are disjoint. For example the interior of the half plane is $\mathbb{R} \times (0, +\infty)$, its boundary is $\mathbb{R} \times \{0\}$.

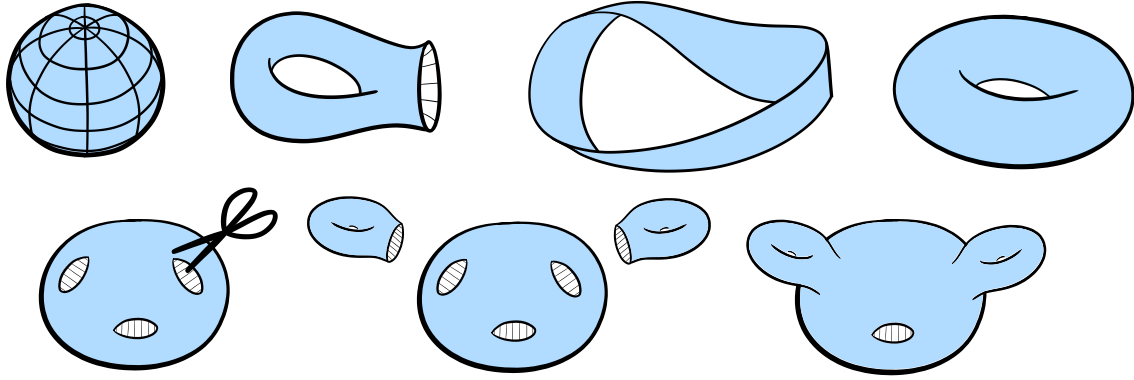


Figure 3.1: (Top, from left to right) The sphere, the handle, the Möbius strip, and the torus. (Bottom) Construction of the surface $S_{2,1}$ by cutting holes from the sphere and attaching handles.

So what are all the possible surfaces? Of course, there are other surfaces than the plane and the half plane. For example the **sphere** and the **handle** depicted in Figure 3.1. Already, the sphere and the handle suffice to construct an entire family of surfaces $S_{g,b}$ for every $g, b \geq 0$, by cutting holes from the sphere and attaching handles. See Figure 3.1. To construct $S_{g,b}$ consider g copies of the handle and one copy of the sphere, remove the interiors of $g+b$ disjoint closed disks from the sphere, and identify g of their boundary circles with the boundaries of the handles. Some of the resulting surfaces have names, like the **torus** $S_{1,0}$ (Figure 3.1), the **disk** $S_{0,1}$, and the **annulus** $S_{0,2}$. In general the numbers g and b are respectively the **genus** of $S_{g,b}$ and its number of boundary components. And $S_{g,b}$ is said **closed** if it has no boundary, that is if $b = 0$. There are other surfaces, for example the **Möbius strip** depicted in Figure 3.1. However in this thesis we consider only **orientable** surfaces, which can be defined as those not containing a Möbius strip. Among them the surfaces $S_{g,b}$ are quite generic:

Theorem 3.1 (Classification of orientable surfaces). *Every connected, compact, and orientable surface is homeomorphic to $S_{g,b}$ for some $g \geq 0$ and $b \geq 0$. No two of these surfaces are homeomorphic.*

In this thesis most surfaces are connected and compact, in addition of being orientable, so this is assumed unless explicitly stated otherwise. Yet we occasionally consider disconnected surfaces, and even non-compact surfaces obtained from a compact surface S by removing a discrete subset $X \subset S$. The points in X are called **punctures** in this context, and $S \setminus X$ is a **punctured surface**. For example the plane is a punctured surface, obtained by removing a single puncture from the sphere. The interior of a surface with boundary is also a punctured surface.

3.1.2 Obtaining surfaces by gluing polygons

We saw that complicated surfaces can be constructed from simpler ones by cutting and gluing. While using the sphere and the handle as the basic surfaces helps to grasp the classification theorem, surfaces can more simply be obtained by gluing polygons. See Figure 3.2.

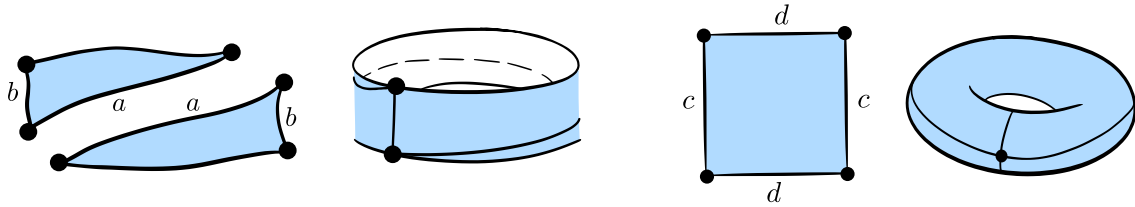


Figure 3.2: (Left) Construction of the annulus by gluing sides of two topological triangles. (Right) Construction of the torus from its canonical polygonal schema. In both figures the pairs of sides with the same label are glued.

From the point of view of topology a **polygon** is a surface S homeomorphic to a disk, together with $n \geq 1$ points on the boundary of S . Technically a topological polygon can have only one or two vertices but the reader can assume $n \geq 3$ if this helps the reading. Consider a disjoint collection of *oriented* polygons together with a partial matching of the sides of the polygons. Identifying the matched sides *while respecting the orientations* of the polygons provides a surface S . Observe that S is oriented but not necessarily connected. Also S may not be compact if infinitely many polygons are glued, but it is compact otherwise. And S may have boundary. Every (orientable) surface can be obtained by gluing polygons this way.

Some of these gluings of polygons are particularly important. For example a (oriented) **polygonal schema** consists in a single polygon whose sides are all matched. The corresponding surface is closed. The **canonical** polygonal schema of the closed surface of genus $g \geq 1$ is the one in which the sides of the polygon can be labeled $a_1 b_1 a_1 b_1 \dots a_g b_g a_g b_g$ in order in such a way that two sides are matched when they have the same label. For example, the canonical polygonal schema of the torus is depicted in Figure 3.2.

3.1.3 Graphs

The second characters of this thesis are graphs. There are several notions of graphs. A graph is commonly a set, whose elements are called vertices, together with a set of unordered pairs of distinct vertices, called edges. In this thesis however, we consider a related but more topological notion of graph. See Figure 3.3.

Roughly, we obtain our graphs by considering a set of points for the vertices and a set of strings for the edges, and by attaching the ends of the strings to vertices. There are infinitely

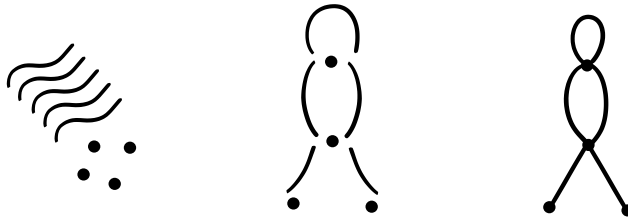


Figure 3.3: Construction of a graph from points and closed intervals.

many points in a string, so an edge is more than just a pair or vertices. It is possible, but unnecessary, to think of each graph as a subset of \mathbb{R}^3 , so that a vertex is a point of \mathbb{R}^3 and an edge a path in \mathbb{R}^3 . Formally, a **graph** is any topological space G obtained from a discrete set V and a collection of closed intervals by identifying each endpoint of each interval with a point in V . Note that a single point of V can be identified with several endpoints of intervals. The points of V become the **vertices** of G . The intervals become the **edges** of G .

It is important to understand that this definition of graph is rather permissive. For example an edge can be incident to only one vertex, in which case it is called a **loop**. To illustrate consider the graph with a single vertex to which is attached a single loop edge. This graph is homeomorphic to a circle. In fact it may be convenient to think of the circle itself as a graph without any vertex, but this is incidental for the circle can be turned into a graph by inserting a vertex anyway. In a graph several edges can have the same end-vertices, in which case they are called **parallel edges** (or multiple edges). A graph is **simple** if it has no loops nor parallel edges.

Also graphs can have infinitely many vertices or edges. However the graphs considered in this thesis have *countably* many vertices and edges, and every vertex has *finite* degree. Those with finitely many vertices and edges are called **finite**.

We will use standard notions of graph theory such as **walks**. We refer to the textbook of Diestel [74]. We will repeatedly use the notion of **spur**, a walk of length two that takes an edge e and then the reversal of e .

3.1.4 Curves

Before drawing graphs on a surface S we draw curves on S . In this section the surface S can be replaced by any topological space, but thinking of S as a surface may help the intuition. There are several topological types of curves. Among the simplest ones are the **paths**, the maps $p : [0, 1] \rightarrow S$. The points $p(0)$ and $p(1)$ are the **endpoints** of p . Paths can be concatenated and reversed. Importantly, we do not care too much about the parameterization of the curves. For example we usually consider two paths p and q equal if there is an orientation-preserving homeomorphism $\tau : [0, 1] \rightarrow [0, 1]$ such that $p = q \circ \tau$. With this definition a path is distinct from its reversal, the direction of the path matters. When the direction of the path is of no matter to us we allow τ to be orientation-reversing. A path p for which $p(0) = p(1)$ is called a **loop**, $p(0)$ is the **basepoint** of p .

Some curves do not have endpoints. For example the **bi-infinite paths** are the maps $\mathbb{R} \rightarrow S$. More important to us are the **closed curves**. Informally, closed curves are like loops but without basepoint, they are drawings of a circle on S . Formally, they are the maps $\mathbb{R}/\mathbb{Z} \rightarrow S$, where \mathbb{R}/\mathbb{Z} is the quotient of \mathbb{R} by the equivalence relation \sim such that $x \sim x'$ if and only if $x - x' \in \mathbb{Z}$. Note that \mathbb{R}/\mathbb{Z} is homeomorphic to a circle. Closed curves are

related to loops since, informally, forgetting the basepoint of a loop ℓ provides a closed curve c . Formally c is the composition of the natural map $\mathbb{R}/\mathbb{Z} \rightarrow [0, 1)$ by ℓ . We say that c is obtained by **closing** ℓ .

Of particular importance are the curves that are also embeddings, equivalently are injective. These curves are commonly called **simple**, with the exception of paths p which are simple when their restriction to the interval $(0, 1)$ is an embedding, so that it is possible for a loop to be simple. Then the image of $(0, 1)$ by p is the **relative interior** of p . Sometimes we identify a simple curve with its image, when the direction of the curve is of no matter to us.

3.1.5 Drawings of graphs on surfaces

The third characters of this thesis are drawings of graphs on surfaces. From the point of view of topology, a drawing of a graph G on a surface S is just a map $f : G \rightarrow S$. Observe that f maps each vertex of G to a point of S , and each edge to a path between the image points of its end-vertices.

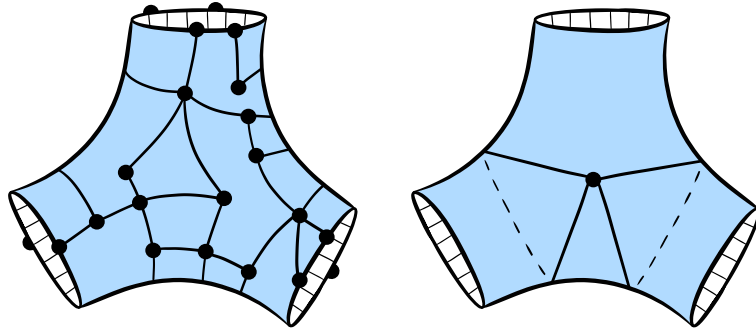


Figure 3.4: (Left) A graph cellularly embedded on the surface $S_{0,3}$. (Right) A loop system of the surface $S_{0,3}$.

If a drawing $f : G \rightarrow S$ is an embedding then the image $H = f(G)$ is a graph **embedded on** S , a graph that is also a subspace of S . The fact that H is embedded on S provides additional information. For example, any orientation of S induces a **rotation system** on H : the data, for each vertex v of H , of a cyclic ordering of the ends of edges incident to v in H . Also, the connected components of $S \setminus H$ are the **faces** of H . Observe that faces can be quite complicated topologically. If every face of H is homeomorphic to the interior of a disk then H is **cellularly** embedded on S , see Figure 3.4 (Left). Note that H then contains the boundary of S . And H is a **triangulation** if every face of H is a “triangle”: it has three incidences with edges of H . Importantly, each graph cellularly embedded on S can be represented uniquely by finite data, provided that we regard two such graphs as equal whenever one can be obtained by applying an orientation-preserving homeomorphism of S to the other. We mention the combinatorial map, the doubly-connected edge list, the half-edge data structure, or the gem representation [82, 127].

The graphs embedded on fixed surface have strong properties. For example, the numbers n , e , and f of respectively vertices, edges, and faces of a graph embedded on the surface of genus g with b boundary components are related via the classical Euler formula $n - e + f = 2 - 2g - b$.

The graphs embedded on a surface can be modified with folklore operations. For example any edge that is not a loop can be contracted. Also, given two graphs H and H' embedded on the same surface S , in general position, the **overlay** of H and H' is the graph H'' embedded on S that is the union of H and H' . The vertices of H'' are exactly the vertices of H , the vertices of H' , and the intersection points between H and H' .

We provide two important examples of graphs embedded on surfaces, in order to fix the intuition. On a closed surface S , a **system of loops** is a graph cellularly embedded on S that has exactly one vertex and exactly one face. On a surface S with boundary, while it is possible to embed a graph cellularly, it is usually impossible for this graph to have only one face and only vertex at the same time. Instead, a **loop system** is a set Y of pairwise-disjoint simple loops with a common basepoint b on S , such that each face of Y has genus zero and contains exactly one component of the boundary of S , see Figure 3.4 (Right). This is very different from a system of loops. Here the surface S *deform-retracts* to Y . One can think of S as a “thickening” of Y .

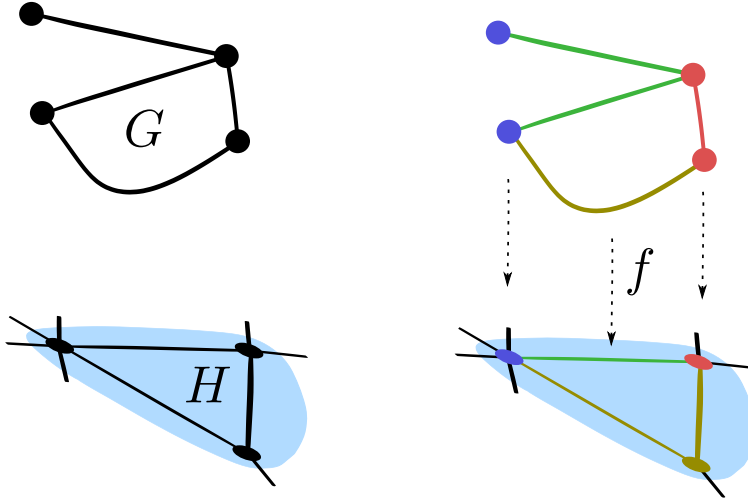


Figure 3.5: A graph G , a graph H embedded on a surface, and a drawing $f : G \rightarrow H$.

Assume that we have a graph H embedded on a surface S . Then we can draw other graphs G on S in a discrete way. See Figure 3.5. Here a **drawing** is a map $f : G \rightarrow H$ that sends each vertex of G to a vertex of H , and each edge of G to a walk (possibly a single vertex) in H . Observe the overlaps that f may have along the edges of H , and the entire subgraphs of G that may be mapped to a single vertex of H . The **size** of f is the number of edges and vertices of G plus the sum of the lengths of the walks $f(e)$ over the edges e of G . The **depth** of f is the maximum length of the image walks $f(e)$ over the edges e of G .

3.2 Homotopy

In this section we introduce a topological notion central to this thesis: homotopy.

3.2.1 Homotopy and fundamental group

Homotopy formalizes the intuitive notion of continuous deformation. Formally, given topological spaces X and Y , a **homotopy** is a sequence of maps $f_t : X \rightarrow Y$ that varies contin-

uously with $t \in [0, 1]$. It is a continuous deformation of f_0 into f_1 . Equivalently, it is a map $H : [0, 1] \times X \rightarrow Y$, with $H(t, x) = f_t(x)$ for all $t \in [0, 1]$ and $x \in X$. We emphasize that homotopy is a general concept: X and Y can be any topological spaces.

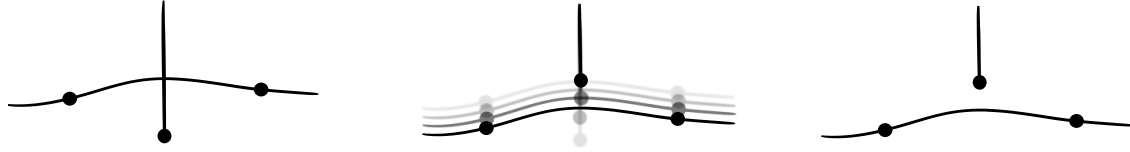


Figure 3.6: Continuous deformation of a drawing of a graph.

Of particular importance to us are the homotopies $f_t : G \rightarrow S$ of drawings of a graph G on a surface S . See Figure 3.6. Observe that the images of the vertices and edges of G are free to move and overlap during the homotopy. A homotopy that fixes a subgraph $G_0 \subset G$ is **relative** to G_0 . Two more classical cases are the homotopies of closed curves $c_t : \mathbb{R}/\mathbb{Z} \rightarrow S$ and paths $p_t : [0, 1] \rightarrow S$. The case of paths is particular for we usually require of the homotopy that it fixes the endpoints: $p_t(0)$ and $p_t(1)$ are constant over t . Equivalently, we consider homotopies relative to $\{0, 1\}$, without further mention. In contrast the homotopies of closed curves are sometimes called free for they are not required to fix any point.

A particular case of the homotopy of paths is that of loops. In S consider a point x_0 and the loops based at x_0 . The loops are classified by homotopy. For example a loop is **contractible** if it is homotopic to the constant loop. More generally the equivalence relation “is homotopic to” partitions the loops into **homotopy classes**: two loops belong to the same homotopy class if and only if they are homotopic. We already saw the homotopy class of the constant loop. In general denote by $\pi_1(S, x_0)$ the set of homotopy classes of loops. If ℓ and ℓ' are homotopic loops, and if γ is a loop, then the concatenation of ℓ and γ is homotopic to the concatenation of ℓ' and γ . So concatenation defines an operation on $\pi_1(S, x_0)$. With this operation $\pi_1(S, x_0)$ is a group whose unit element is the homotopy class of the constant loop. If S is connected this group does not depend on x_0 up to group isomorphism. In this case it is abbreviated $\pi_1(S)$, and called the **fundamental group** of S . From there we use standard notions of group theory. For example an element $a \in \pi_1(S)$ is **primitive** if there is no integer $n \geq 2$ and $b \in \pi_1(S)$ such that $a = b^n$ (this implies $a \neq 1$). Then a loop is primitive if its homotopy class is primitive.

On S paths and closed curves are also classified by homotopy. For example a closed curve is contractible if it is freely homotopic to a constant closed curve. And it is primitive if it is not freely homotopic to a power of another closed curve. There is a relation between loops and closed curves. Indeed recall that closing a loop ℓ based at x_0 provides a closed curve c . Then ℓ is contractible if and only if c is contractible, and ℓ is primitive if and only if c is primitive. More generally closing the loops defines a correspondence between the conjugacy classes of $\pi_1(S)$ and the free homotopy classes of closed curves. Indeed every closed curve is freely homotopic to a closed curve intersecting x_0 , which is then the closing of a loop. Moreover, given a loop ℓ' based at x_0 , and the closed curve c' obtained by closing ℓ' , the two closed curves c and c' are freely homotopic if and only if there is a loop γ based at x_0 such that $\gamma \cdot \ell \cdot \gamma^{-1} = \ell'$.

Finally, we mention that there are connected surfaces S in which all the loops and closed curves are contractible, for example the sphere and the disk. These surfaces are called

simply connected. Equivalently there is a unique homotopy class of paths connecting any two points of S .

3.2.2 Isotopy

If two maps f_0 and f_1 satisfy some property we may ask for a homotopy between f_0 and f_1 whose intermediate maps all satisfy this property. Typically, an **isotopy** is a homotopy whose intermediate maps are all *embeddings*. Two embeddings are **isotopic** if they are related by an isotopy. Of particular importance are the isotopies of homeomorphisms $\varphi_t : S \rightarrow S$ for a surface S . Such isotopy is called an **ambient isotopy**. Informally, because it is a deformation of the *ambient* space, the surface S . Ambient isotopies are often applied to the drawings of graphs in S , so that two drawings $f_0, f_1 : G \rightarrow S$ are **ambient isotopic** if there is an ambient isotopy $\varphi_t : S \rightarrow S$ such that φ_0 is the identity map $S \rightarrow S$ and $\varphi_1 \circ f_0 = f_1$. Observe that f_0 and f_1 need not be embeddings.

If two embeddings $f_0, f_1 : G \rightarrow S$ are ambient isotopic, then they are isotopic, and if they are isotopic then they are homotopic. The reader should be careful with the converse however, which is usually false, even for curves. For example in a surface S if a simple closed curve c is contractible then c bounds a disk [83, Theorem 1.7]. In that case c is isotopic to an arbitrarily small curve. In the particular case where c is disjoint from the boundary of S , it is also *ambient* isotopic to an arbitrarily small curve. However this is false if c intersects two distinct boundary components of S . In that case no ambient isotopy can detach c from any of the two boundary components.

3.2.3 Universal cover

Homotopy is strongly related to the *universal cover*, a construction that we now present on surfaces. It is possible to *cover* the torus with the plane. See Figure 3.7. First wrap the plane around an infinite tube. Then wrap the tube around the torus. Note that the plane wraps infinitely many times around the torus. Now, this is perhaps difficult to imagine, but it is possible to wrap the plane around every closed surface of higher genus. In all these cases, the plane and its wrapping around the surface constitute a **universal cover** of the surface.

Formally, a universal cover of a surface S is a simply connected surface \tilde{S} , together with a **covering map**, a surjective map $\rho : \tilde{S} \rightarrow S$ that satisfies the following. There is a cover of S by open sets $(U_i)_i$ such that for every i , $\rho^{-1}(U_i)$ is a disjoint union of open sets in \tilde{S} , each of which is mapped by ρ homeomorphically onto S_i . By a slight abuse, we may call \tilde{S} a universal cover of S , when ρ is unambiguous. It turns out that S has a unique universal cover, up to some trivial changes that are irrelevant here.

Each point in S has representatives in the universal cover of S . To grasp this intuition think of the cover of the torus by the plane. For each point x of the torus there are infinitely many points \tilde{x} of the plane that are sent to x by the covering map. Formally, a point \tilde{x} of \tilde{S} **lifts** (or is a lift of) a point x of S if $\rho(\tilde{x}) = x$. It is not just points that can be lifted, but also paths and more generally maps: a map $\tilde{f} : X \rightarrow \tilde{S}$ lifts a map $f : X \rightarrow S$ if $\rho \circ \tilde{f} = f$.

The universal cover has a general property called the **lifting property**. This property describes how the homotopies in S are lifted by homotopies in \tilde{S} : for any topological space X , homotopy $f_t : X \rightarrow S$, and map $\tilde{f}_0 : X \rightarrow \tilde{S}$ lifting f_0 , there exists a unique homotopy $\tilde{f}_t : X \rightarrow \tilde{S}$ of \tilde{f}_0 that lifts f_t . Let us give two important cases of this property to illustrate. The first case is when X is a single point. In this case the property says that for every path

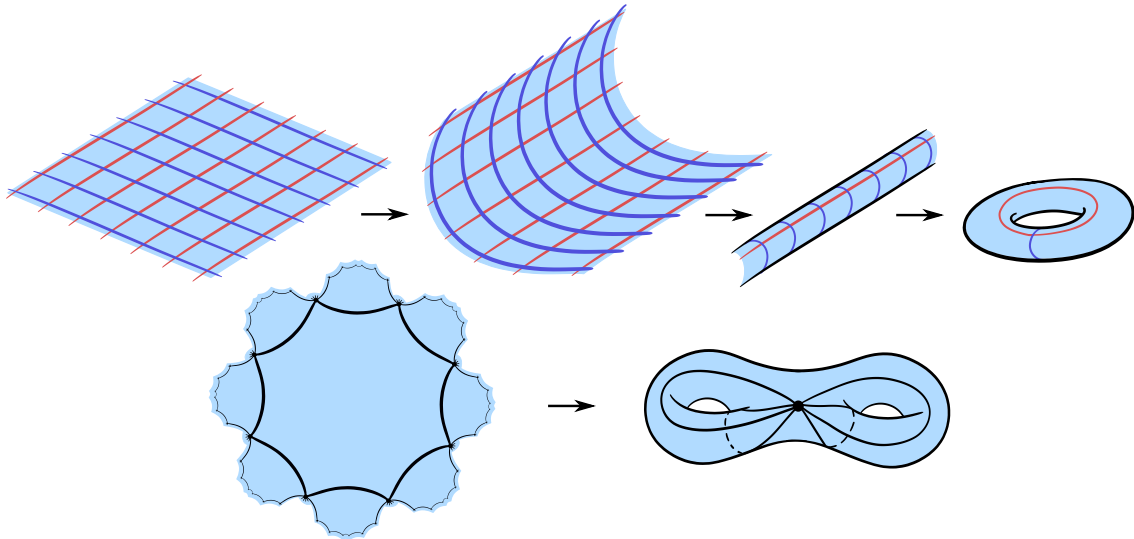


Figure 3.7: (Top) The plane is wrapped around an infinite tube, itself wrapped around a torus. (Bottom) The plane is wrapped around the closed surface of genus two.

p in S , and for every point $\tilde{x}_0 \in \tilde{S}$ that lifts the starting point of p , there is a unique path \tilde{p} in \tilde{S} that starts at \tilde{x}_0 and lifts p . The second case is when $X = [0, 1]$, each map f_t is a path. In this case the property says that for every path p in S , every lift \tilde{p} of p in \tilde{S} , and every continuous deformation of p , there is a unique continuous deformation of \tilde{p} that lifts the continuous deformation of p .

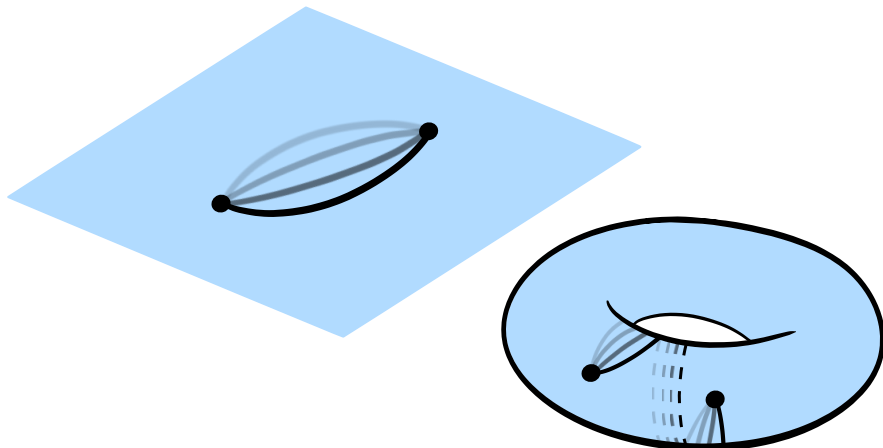


Figure 3.8: Two paths in a surface S are homotopic if and only if they admit lifts with the same endpoints in the universal cover of S .

The universal cover is strongly related to homotopy in several ways, in particular by the lifting property, but also because it is simply connected by definition. This has useful consequences. For example a loop ℓ of S is contractible if and only if some lift of ℓ in \tilde{S} is a loop, in which case all the lifts are loops. Also two paths p and q are homotopic if and only if they admit respective lifts with the same endpoints: lifts \tilde{p} and \tilde{q} such that $\tilde{p}(0) = \tilde{q}(0)$ and $\tilde{p}(1) = \tilde{q}(1)$ (Figure 3.8).

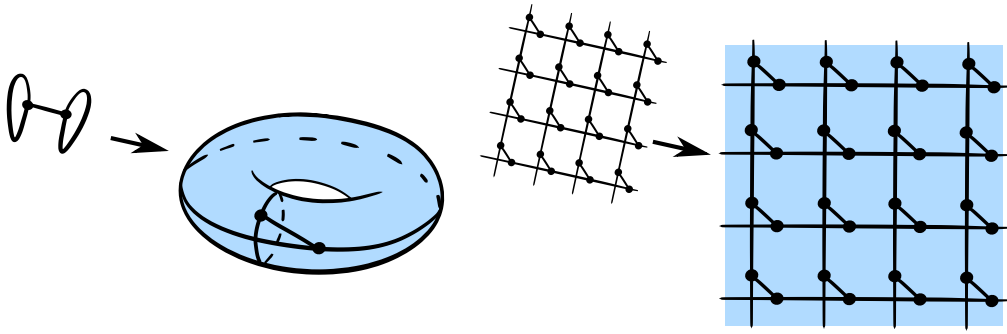


Figure 3.9: (Left) Drawing of a graph in the torus. (Right) Lift of the drawing in the universal cover of the torus.

We mention here that it is possible to define more covers of a surface S without the requirement that \tilde{S} be simply connected. With this definition every surface is a cover of itself. Another example is the infinite-tube in the previous construction, which is a cover of the torus. There is even a classification of the covers but in this thesis we mostly consider the universal cover, the simply connected one. Also, the notion of universal cover immediately generalizes from surfaces to topological spaces. For example the universal cover of a connected graph is an infinite tree.

Importantly, lifting maps in general is slightly more delicate than lifting paths. This is for example the case when lifting a closed curve $c : \mathbb{R}/\mathbb{Z} \rightarrow S$. The reason is that if c is non-contractible there is no closed curve lifting c properly speaking: there is no $\tilde{c} : \mathbb{R}/\mathbb{Z} \rightarrow S$ such that $\rho \circ \tilde{c} = c$. So instead one considers the bi-infinite path $p : \mathbb{R} \rightarrow S$ that “wraps around” c infinitely many times, formally the composition of c and the natural map $\mathbb{R} \rightarrow \mathbb{R}/\mathbb{Z}$, and considers a lift $\tilde{p} : \mathbb{R} \rightarrow \tilde{S}$ of p . This idea can be refined to lift drawings of graphs; we will not need the exact definition, and the concept is the one the reader has in mind, illustrated in Figure 3.9.

3.3 Geometry of surfaces

In this section we focus on surfaces and refine our presentation from the finer point of view of geometry. Geometry is concerned in particular with the measure of distances. This requires additional structure on a surface, other than the topology. We use the notion of Riemannian 2-manifold, or **Riemannian surface** (not to be confused with the related but different notion of *Riemann* surface). We cannot reasonably attempt a review of the foundations of Riemannian geometry, so instead we refer to the textbook of do Carmo [76]. In a nutshell, a Riemannian surface is a smooth surface together with an object called a **Riemannian metric** which allows to measure area, angle, and length for example.

It is tempting to think of surfaces as smoothly embedded in \mathbb{R}^3 , and to measure the length of a path on a surface as its usual length in \mathbb{R}^3 . However the reference to \mathbb{R}^3 disappears in the definition of a Riemannian surface S , and in fact this definition is so general that it is possible for S to have no such embedding in \mathbb{R}^3 . It is possible however to think of *small* portions of S in \mathbb{R}^3 .

In this thesis we focus on a very particular, yet important, class of Riemannian surfaces S that “locally look the same everywhere”, more formally, in which every two points admit

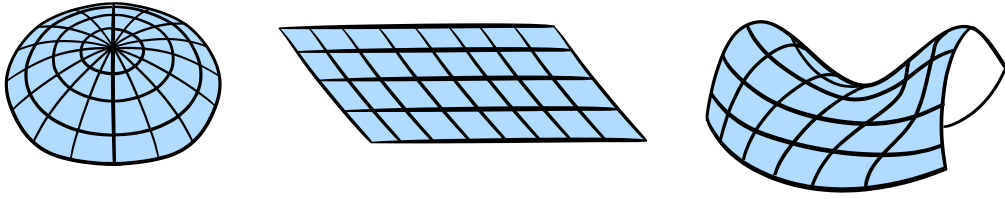


Figure 3.10: (Left) Spherical surface. (Middle) Flat surface. (Right) Hyperbolic surface.

respective neighborhoods that are isometric. Up to rescaling the Riemannian metric of S (multiplying all distances by a positive real), there is for every point x a neighborhood of x isometric to one of the three Riemannian surfaces depicted in Figure 3.10. This classifies S into spherical, flat, and hyperbolic. Spherical surfaces are incidental in this thesis, we are mostly concerned with flat and hyperbolic surfaces. In particular the flat plane and the hyperbolic plane, which we will see in a moment. Technically some of the surfaces we consider will not locally look the same everywhere, for example because a boundary point and an interior point cannot have isometric neighborhoods. Nevertheless they are all obtained by cutting and pasting portions of the flat plane and the hyperbolic plane.

We use standard notions of Riemannian geometry without review. We only mention that a curve is **geodesic** if it is locally distance minimizing. Technically, for a curve to be geodesic it should also have “constant speed”, but the exact parameterization of the curve is of no matter to us. Importantly, geodesics are not necessarily shortest paths, even though all shortest paths are geodesic.

3.3.1 Piecewise-flat surfaces

The simplest flat surface is the **flat plane**. This is the usual plane, also called Euclidean plane, whose point set is often identified with \mathbb{R}^2 . Some surfaces can be obtained as subsets of the flat plane. Typically, a **flat polygon** is a topological polygon (Section 3.1.2) that lies in the flat plane and whose sides are geodesic. We use folklore facts on flat polygons. For example the classical Gauss–Bonnet formula implies that the number n of vertices of a flat polygon and the sum a of its angles satisfy $(n - 2)\pi = a$.

We construct other surfaces from the flat plane by gluing polygons with the construction described in Section 3.1.2. Here instead of using arbitrary topological polygons we use flat polygons. The gluing of polygons is encoded by a data structure, and it will be convenient for us to have a name for this data structure. We could not find a consistent name in the literature. We chose the name *portalgon*, introduced by Löffler, Ophelders, Silveira, and Staals [141]. See Figure 3.11. A **portalgon** T is a disjoint collection of oriented flat polygons together with a partial matching of the sides of the polygons. It is **triangular** if all polygons are triangles. Given a portalgon T , any subset of the polygons defines a **sub-portalgon** T' of T : two sides of polygons are matched in T' if and only if they are matched in T .

In a portalgon T , identifying the matched sides while respecting the orientations of the polygons provides the **surface of T** , denoted $\mathcal{S}(T)$. It is a Riemannian surface but the Riemannian metric may have singularities, we will see that in a moment. The sides of the polygons of T correspond to a graph T^1 cellularly embedded on $\mathcal{S}(T)$, called the **1-skeleton** of T . In general a **piecewise-flat surface** is any Riemannian surface S isometric to the surface of a portalgon. And when we say that a portalgon T is a **portalgon of S** , we implicitly fix

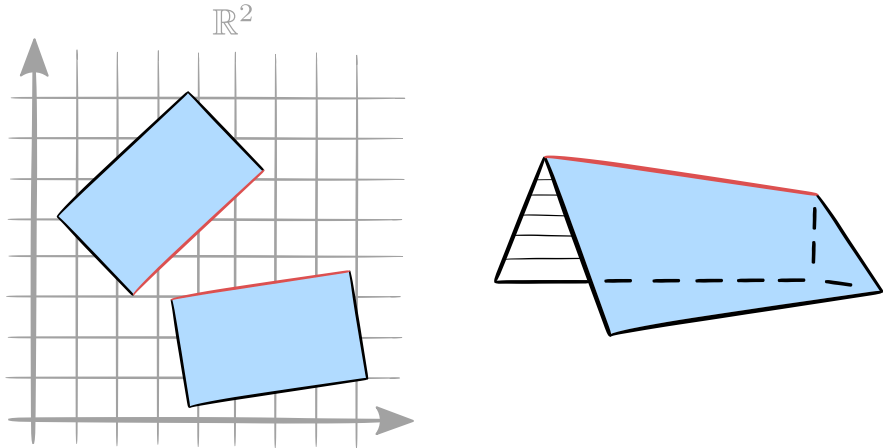


Figure 3.11: (Left) A portalgon T : two flat polygons with two sides matched, in red. (Right) The surface $S(T)$.

an isometry between $S(T)$ and S . A **tessellation** of S is the 1-skeleton of a portalgon of S . It is a **triangulation** if the portalgon is triangular. Such a “geometric” triangulation is also a “topological” triangulation as defined in Section 3.1.5, but the converse does not hold in general. There should be no confusion between the two notions of triangulation in the thesis.

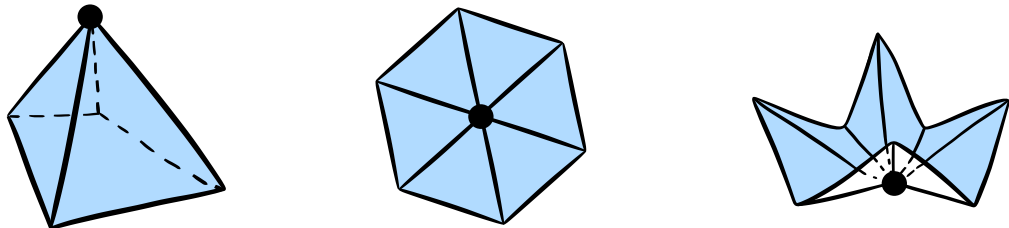


Figure 3.12: (Left) The surface $S(T)$ of a portalgon T , on which is represented the 1-skeleton T^1 of T . The vertex of T^1 in the interior of $S(T)$, represented by a black disk, is a singularity of $S(T)$. (Middle) The vertex is a flat point. (Right) The vertex is a singularity.

Let us detail the singularities that a piecewise-flat surface S can have. Consider a triangulation T of S , a vertex x of T , and the sum a of the angles of faces of T around x . The point x is a **singularity** if x lies in the boundary of S and $a \neq \pi$, or if x lies in the interior of S and $a \neq 2\pi$. Every other point of S is **flat**. Equivalently, a point $x \in S$ is flat if there is a neighborhood of x isometric to a plane disk, or half-disk if x lies on the boundary of S . This does not depend on any particular triangulation of S . To help the intuition observe that on S a geodesic p is straight outside of the singularities and does the following at each singularity x . If x lies in the interior of S , then p forms at x an angle greater than or equal to π on both sides. Otherwise, if x lies on the boundary of S , p forms an angle greater than or equal to π on the side that does not contain the boundary of S . In S , a **segment** is a simple geodesic path, usually not a single point, whose relative interior is disjoint from any singularity of S .

A piecewise-flat surface is **flat** if its interior has no singularity. The closed flat surfaces are called **flat tori**. They are all homeomorphic to a torus but there are infinitely many of them. They are obtained by identifying the opposite sides of a flat parallelogram.

3.3.2 Hyperbolic surfaces

We have just described flat surfaces, starting off from the flat plane. The metric of the flat plane is defined by the equation $ds^2 = dx^2 + dy^2$, where ds is the length of an infinitesimally small line segment and dx and dy are the infinitesimal variations of its coordinates. We now describe hyperbolic surfaces, starting off from the **hyperbolic plane**. A model of the hyperbolic plane is the **Poincaré disk**. It is the open unit disk of the complex plane $\mathbb{D} = \{u + iv \in \mathbb{C} \mid u^2 + v^2 < 1\}$ with the metric defined by

$$ds^2 = \frac{4(du^2 + dv^2)}{(1 - (u^2 + v^2))^2}.$$

In the Poincaré disk the geodesics are the circle arcs and rectilinear paths meeting $\partial\mathbb{D}$ at right angle. See Figure 3.13. We refer to the textbook of Buser [30]. Similarly to flat polygons, a **hyperbolic polygon** is a topological polygon that lies in the hyperbolic plane and whose sides are geodesic. Here the Gauss-Bonnet formula implies that the number n of vertices of a hyperbolic polygon and the sum a of its angles satisfy $(n - 2)\pi \geq a$.

It is no surprise that we construct other surfaces by gluing hyperbolic polygons. Importantly, in this thesis we only consider the case where the resulting surface has no singularity in its interior: every vertex point in the interior of the surface is surrounded by an angle of 2π . Such a Riemannian surface is a **hyperbolic surface**. The sides of the hyperbolic polygons define a (hyperbolic) **tessellation** of S . It is a (hyperbolic) **triangulation** if all polygons are triangles.

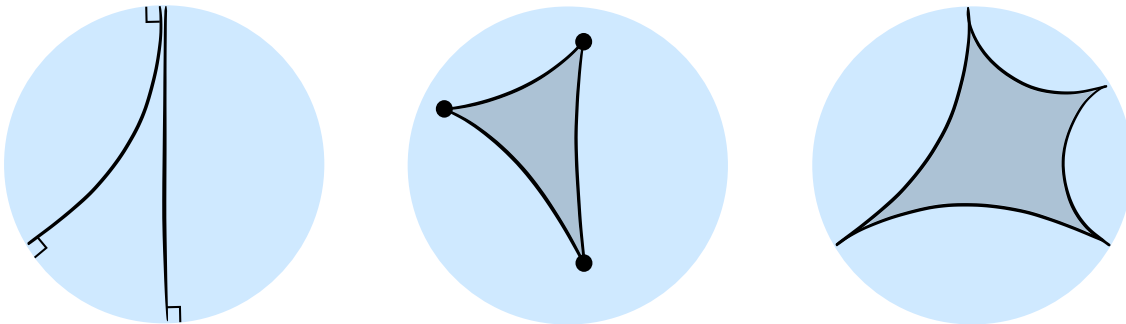


Figure 3.13: (Left) In the Poincaré disk, two geodesic lines. (Middle) A triangle with geodesic sides of finite length. (Right) An ideal quadrilateron with geodesic sides of infinite length.

Every closed hyperbolic surface has genus at least two. For every $g \geq 2$ there are infinitely many closed hyperbolic surfaces of genus g .

We will also consider a construction of non-compact hyperbolic surfaces from **ideal** hyperbolic polygons, the sides of which are geodesics of infinite length (Figure 3.13). Such polygons do not exist in the flat plane, they are specific to the hyperbolic plane. Pair the sides of a collection of ideal hyperbolic polygons, and identify the two sides in each pair in a way that respects the orientations of the polygons. The result is a hyperbolic surface whose topological type is that of a punctured surface, but punctures are relegated to infinity.

Part I

Untangling Graphs on Surfaces

In this part of the thesis

In this part of the thesis we consider the problem of untangling a drawing of a graph on a surface. The review of the related works is postponed to Chapter 4. Here we provide an informal account of our contributions, then we describe the organization of the chapters.

Curves. Our problem naturally generalizes to graphs another problem on curves, which we revisit as a starting point. In this problem we are given a collection of closed curves C on a surface S . The curves may cross themselves and each other. We must minimize the number of crossings by continuously deforming the curves, or at least compute the minimum number of crossings $i_S(C)$. The case we consider is when the surface S is obtained from a closed surface by removing the interiors of finitely many (possibly zero) disjoint closed disks. Then S is topologically determined by its genus and its number of boundary components.

This problem on curves has been extensively studied for more than a century by numerous mathematicians, see for example Poincaré [155, Section 4]. From these works emerges the following key insight. Generally, the most difficult case is when the surface S has no boundary, and has genus at least two. In this case S can be endowed with a hyperbolic metric, in which all the curves in C can be made geodesic by continuous deformation. Afterward, roughly but not exactly, the number of crossings of C is the minimum of its homotopy class. This is a solution to our problem, but it is not discrete so it does not immediately give an algorithm.

In order to obtain an algorithm, we must first discretize the problem. To do so, as is done classically, we decompose S along a graph H (cellularly) embedded on S (Chapter 3), part of the input, and we require that each curve in C be given as a closed walk in H . We output another collection of closed walks C' in H . It is possible that the walks in C' overlap by using several times an edge of H . We make sure that C' is in *minimal position*: there is an infinitesimal perturbation of C' after which C' does not overlap and the number of crossings of C' is the minimum of its homotopy class. One could then construct such a perturbation of C' using a recent algorithm of Fulek and Tóth [101]. Their work allows for this neat decomposition of our problem. In detail we prove:

Theorem 3.2. *Let S be a surface of genus smaller than s , with less than s boundary components. Let H be a graph of size m cellularly embedded on S . Let C be a collection of closed walks of total length n in H . One can compute $i_S(C)$ in $O(m + s^2 + sn \log(sn))$ time. One can construct in additional $O(s^2 mn)$ time a collection of closed walks C' in H , freely homotopic to C in S , in minimal position.*

To obtain Theorem 3.2, we provide a discrete analog of the hyperbolic construction. Assuming that S has no boundary, and has genus at least two, we replace the hyperbolic metric by a carefully chosen triangulation T of S , which we call *reducing triangulation*, and we replace the geodesics in the hyperbolic metric by particular walks and closed walks in T ,

which we call *reduced* (closed) walks. Then we prove that every collection of reduced closed walks is in minimal position.

To define the reduced walks (and closed walks), informally, we are inspired by the fact that on a hyperbolic surface a curve is geodesic if and only if every *small portion* of the curve is geodesic, this property is *local*. Analogously, we define reduced walks in such a way that a walk is reduced if and only if all its *length two subwalks* are reduced. We are also inspired by the fact that on a hyperbolic surface a curve can be made geodesic homotopically (albeit not in finite time) by straightening *portions* of the curve *greedily*. Analogously, we show that a walk can be turned into a reduced walk homotopically by straightening portions of the walk greedily. *Reduced* walks are the results of this *reduction* process, and *reducing* triangulations are the object on which the process happens.

In general, the input walks are in a graph H that is not a reducing triangulation, so (1) we construct a reducing triangulation T on S , (2) we push the walks in H by homotopy into walks in T , (3) we reduce the walks in T , and (4) we push the result back into H . At this point we only handled the surfaces without boundary of genus at least two. Fortunately, the techniques we developed for those surfaces extend similarly to the other surfaces, leading to Theorem 3.2.

The strategy of greedily reducing walks originates in a classical algorithm of Dehn from 1912 [64], since refined by Erickson and Whittlesey [88] for testing curves for homotopy, and by Despré and Lazarus [69] for minimizing the crossings of curves by homotopy. The latter reduce walks in particular graphs embedded on S , called *systems of quads*, previously introduced by Lazarus and Rivaud [134], which inspired reducing triangulations. On systems of quads the reduced walks are close to being in minimal position, but an infinitesimal perturbation of the walks may not suffice to realize the minimum number of crossings. In this way the systems of quads and their reduced walks do not allow for a neat decomposition with the algorithm of Fulek, and Tóth [101]. Despré and Lazarus [69], who obtained their results before Fulek, and Tóth [101], deployed considerable efforts due to this deficiency of the systems of quads. On the other hand, by introducing reducing triangulations, we easily obtain Theorem 3.2, improving, generalizing, and simplifying the results of Despré and Lazarus [69]. This is due to very strong properties of reducing triangulations that previous models did not have all at once. For example, in a reducing triangulation, the reduced walks are stable upon taking a subwalk and reversing the walk, and each homotopy class of walks contains exactly one reduced walk.

Graphs. More importantly, reducing triangulations allow us to pivot from closed curves to general drawings of graphs, which is our main concern in this thesis. Again, the surface S is decomposed along a graph H cellularly embedded on S . This time we are given a graph G , and a map $f : G \rightarrow S$, and we require that f maps each vertex of G to a vertex of H , and each edge of G to a walk in H . Determining, given an integer k , whether there is a drawing homotopic to f in S with less than k of crossings is NP-hard, for this contains the classical *crossing number* problem. So instead we ask whether there is an *embedding* homotopic to f , a drawing without any crossing. If so, we output a *weak embedding*, a drawing $f' : G \rightarrow H$, not necessarily an embedding, but such that there is an infinitesimal perturbation of f' after which f' is an embedding. One could then construct such a perturbation of f' using a recent algorithm of Akitaya, Fulek and Tóth [10], similar to the algorithm of Fulek and Tóth [101] for curves. In detail we prove:

Theorem 3.3. *Let S be a surface of genus smaller than s , with less than s boundary components. Let H be a graph of size m cellularly embedded on S . Let G be a graph, and let $f : G \rightarrow H$ be a drawing of size n . One can determine in $O(m + s^2n \log(sn))$ time whether f can be untangled in S . If so, one can construct in additional $O(s^2mn^2)$ time a weak embedding $f' : G \rightarrow H$, homotopic to f in S , of depth $O(s^2mn)$.*

In order to obtain Theorem 3.3, we first provide an algorithm for untangling the drawings of very simple graphs in a reducing triangulation. Basically, the algorithm reduces walks and closed walks. We then provide a rather generic framework to reduce the untangling problem to those particular graphs.

Tutte embeddings. In the end, we move away from the design of the most efficient and complete algorithms, to obtain our most involved and insightful results, on reducing triangulations. We consider a classical theorem of Tutte [184] from 1963, generalized by Yves Colin de Verdière [52] in 1991. As far as we are concerned, the essence of those results is roughly that, on non-positively curved surfaces, “straightening” a drawing suffices to untangle the drawing, at least if it can be untangled. In other words, a “straightened” drawing is homotopic to an embedding if and only if it is itself an embedding. Analogously, we define “straightened” drawings of graphs in reducing triangulations, which we call *harmonious drawings*, and prove:

Theorem 3.4. *Let S be a surface of genus $g \geq 2$ without boundary. Let T be a reducing triangulation of S . Let G be a graph, and let $f : G \rightarrow T$ be a harmonious drawing. There is an embedding homotopic to f in S if and only if f is a weak embedding.*

We emphasize surfaces without boundary, as they constitute the hardest cases, but we also obtain results for surfaces with boundary, allowing vertices of the graph to be attached to the boundary of the surface in the drawing. In contrast, the case of the sphere is not relevant in this context, and our results are not valid on the torus.

We also provide an algorithm for transforming an arbitrary drawing into a harmonious drawing, without increasing the length of any edge in the drawing, which allows to build many harmonious drawings:

Theorem 3.5. *Let S be a surface of genus $g \geq 2$ without boundary. Let T be a reducing triangulation of S , with m edges. Let G be a graph, and let $f : G \rightarrow T$ be a drawing of size n . We can compute in $O((m+n)^2n^2)$ time a drawing $f' : G \rightarrow T$, harmonious, homotopic to f in S , such that for every edge e of G , the image of e under f' is not longer than under f .*

Theorem 3.5 gives another algorithm for untangling graphs, less efficient, but with the advantage of being flexible concerning the choice of the output embedding, making it a powerful tool. The algorithm mimics the reduction of walks and closed walks by straightening portions of the drawing, but in a carefully chosen order this time, not greedily.

Organization of the chapters. We review the related works in Chapter 4, and detail some preliminary results in Chapter 5. We introduce reducing triangulations, reduced walks, and their properties in Chapter 6. In the same chapter we show, on reducing triangulations, how to put closed walks in minimal position, and how to untangle drawings of graphs. In Chapter 7 we extend our results from drawings in reducing triangulations to drawings in

cellularly embedded graphs, obtaining Theorem 3.2 and Theorem 3.3. In the same chapter, we also describe an application of our results in the particular case where the surface is the Euclidean plane minus a finite set of obstacle points, and the drawing is piecewise-linear. Finally, in Chapter 8, we go back to reducing triangulations, on which we introduce harmonious drawings and prove Theorem 3.4 and Theorem 3.5.

Chapter 4

Related Works

In this chapter we review works related to untangling graphs on surfaces. Recall that in this problem, broadly, we are given a drawing f of a graph G on a surface S , and we must remove crossings from f by deforming f continuously, in other words by applying a homotopy to f . By untangling, we usually mean removing all crossings, but sometimes we mean removing as many crossings as possible, by abuse of terminology. We ultimately review this problem in Section 4.4, but first we consider three other problems related to it.

Attempting to solve an example by hand, it is difficult to guess which deformations of f remove the most crossings. This prompts at deleting the homotopy constraint from the problem. Then we can replace f by any drawing of G on S , so there is no need for f in the input. We are just given a graph G and a surface S , and we must produce a drawing of G on S with few crossings. This is the broad problem of drawing a graph on a surface, reviewed in Section 4.1.

In Section 4.2 we consider an intermediate problem in which the homotopy constraint is weakened but not completely removed. We are given f , G , and S , and for the problem to be interesting we assume that f has overlaps. We must remove crossings from f by homotopy, but this time the homotopy is not allowed to move f all around the surface. Instead f can just be perturbed infinitesimally. This is the problem of perturbing a drawing. Some of the results of this section will be used as black boxes in the rest of the thesis, they are also detailed in the next chapter, Chapter 5.

In Section 4.3 we consider again the problem of drawing a graph on a surface, but we introduce a new geometric constraint. For simplicity we focus on the particular case where the surface is the plane, and where the graph G admits a drawing without crossings in the plane, an embedding. The novelty is that we ask for an embedding f that draws the edges of G as straight-line segments. This is the problem of embedding graphs rectilinearly in the plane. The main technique reviewed in this section is influential in our work.

We emphasize that even though some of the works reviewed handle non-orientable surfaces, we will only present the results for orientable surfaces, the only surfaces considered in this thesis. In order to ease the reading, we do not name the authors of a paper when the paper has more than five authors.

4.1 Drawing graphs on surfaces

In this section we review the broad problem of drawing a graph on a surface with few crossings. First we ask for a drawing without any crossing, an embedding. We review this problem on the plane in Section 4.1.1, and then on surfaces in Section 4.1.2. Arises the problem of telling two embeddings apart, that we review in Section 4.1.3. We finally review in Section 4.1.4 the problem of drawing a graph with a minimum number of crossings, but only on the plane for this case is already difficult.

4.1.1 Embedding on the plane

As announced we first ask for a drawing without any crossing, an embedding. The first problem is to determine if a given graph G admits an embedding on a given surface S . This problem is refined by asking for either an embeddding of G on S , or a “smallest” subgraph of G that cannot be embedded on S , certifying that G cannot be embedded on S . Historically the first case considered is when the surface S is the plane.

A graph is planar if it admits an embedding in the plane. The first characterizations of planar graphs were found almost 100 years ago. A simple application of Euler’s formula shows that K_5 , the complete graph on five vertices, is not planar. Clearly if a graph G is not planar, and if G is homeomorphic to a subgraph of another graph H , then H is not planar either. So the search began for graphs G that are not planar, and are minimal in the sense that all proper subgraphs of G are planar. Clearly K_5 is such a minimal non planar graph as every proper subgraph of K_5 is planar. In 1930, Kuratowski [130] added $K_{3,3}$ to the list, and found out that there is no other minimal non planar graph. In detail, he proved that a graph G is planar if and only if no subgraph of G is homeomorphic to K_5 or $K_{3,3}$. This result is now known as Kuratowski’s theorem, but was announced independently and around the same time by Frink and Smith, although their paper was never published due to the fact that Kuratowski’s paper was already in press [126]. Also, Menger concurrently proved the special case that a cubic graph is planar if and only if none of its subgraphs is homeomorphic to $K_{3,3}$ [147], in relation to a problem on colorings of maps that he had encountered in Reidemeister’s Vienna seminar of 1924 [126].

There are algorithms that determine if a graph G with n vertices is planar, and either produce a combinatorial description of an embedding of G in the plane or find a Kuratowksi subgraph of G , all in $O(n)$ time. See for the example the relatively recent algorithm of Myrvold [25], and the clear exposition of Brandes [26] of the algorithm of De Fraysseix and Rosenstiehl [61, 58]. We now present the historical development of this result. As a preliminary note that by the Euler’s formula planar graphs with n vertices have less than $3n$ edges so in any planarity test one may preliminarily throw any graph with too many edges. The naive approach of looking for Kuratowski subgraphs in the input graph G by exhaustive search does not provide an efficient planarity test. Instead the most fruitful approaches try to compute an embedding of G in the plane. Note however that the original papers do not always take care of extracting a Kuratowski subgraph when G is found to be not planar. The two most commonly cited approaches that lead to linear time algorithms are the “path addition” method and the “vertex addition” method. The first method, “path addition”, was initiated in 1961 by Auslander and Parter [18], and then by Goldstein [104]. Roughly, the method is to cut the graph into several pieces along a cycle, to recursively embed each piece with the cycle, and then to combine the embeddings of the pieces, halting if some subgraph is

found that is not planar, or if the graph is trivially planar. In 1974 Hopcroft and Tarjan [118] combined this method with depth first search to design the first and celebrated linear time planarity test. The second method, “vertex addition”, was introduced in 1967 by Lempel, Even and Cederbaum [136]. Roughly, one maintains a data structure that represents all possible embeddings of an induced subgraph, and adds vertices to this data structure one at a time in a specific order. This method was later proved to achieve linear time with two refinements. The first refinement is an algorithm of Even and Tarjan [90] that computes the specific order of the vertices in linear time. The second refinement is a data structure introduced by Booth and Lueker [24], called a PQ tree, that represents a particular set of permutations, and is here applied to represent the possible embeddings of a graph.

4.1.2 Embedding on surfaces

On closed surfaces S the characterization of the graphs that can be embedded on S has its roots in a variation of Kuratowski’s theorem, proved by Wagner [187] in 1937, in which the subgraph relationship is replaced by minor containment. A graph G is a minor of a graph H if G can be obtained from H by deleting edges and vertices, and by contracting edges. Wagner proved that a graph G is planar if and only if no minor of G is isomorphic to K_5 or $K_{3,3}$. Every minor of every planar graph is itself planar. This led Wagner to ask more generally whether every minor-closed class of graphs is determined by a finite set forbidden minors. This is now the Robertson-Seymour theorem, also called graph minor theorem, proved by Robertson and Seymour in a long series of papers from 1983 to 2004, a cornerstone of graph theory. The class of graphs that can be embedded on a given surface S being minor-closed, this theorem implies that the set X_S of *forbidden minors* of S , the graphs that cannot be embedded on S but whose proper minors can all be embedded on S , is finite. Unfortunately, this set is currently unknown for surfaces S other than the plane and the projective plane, and the torus has at least 17 535 minimal forbidden minors [153].

Robertson and Seymour undertook their graph minor theory in parallel of the development of algorithms for embedding graphs on surfaces. The first thing to notice is that, if a graph G can be embedded on the closed surface of genus $g \geq 0$ then G can be embedded on every closed surface of higher genus. The *genus* of G is the minimum genus of a closed surface on which G can be embedded. There are variants such that the maximum genus of a closed surface on which G admits a cellular embedding, we refer to the survey of Ringeisen [160]. Only particular graphs have known genus, among which the complete graph on $n \geq 4$ vertices whose genus is $\lceil (n - 3)(n - 4)/12 \rceil$ [161, 162, 163]. In 1989 Thomassen [181] proved that the genus problem, of checking that the genus of a given graph is equal to a given integer, is NP-hard. In 1991 Mohar [150] gave a fixed-parameter-tractable $O(f(S) \cdot n)$ time algorithm, for some computable function f , that embeds a graph of n vertices on a closed surface S , or returns a minimal non-embeddable subgraph. The function f seems to be doubly exponential in the genus of S , but this is not explicit in Mohar’s paper. This algorithm has since been revisited by Kawarabayashi, Mohar, and Reed [124]. The basic idea is to embed a subgraph, then try to extend this partial embedding, and recursively work with discovered forbidden subgraphs for smaller genus surfaces. Mohar’s result is subsequent to previous works, in particular by Juvan, Marinček, and Mohar [121] when S is the torus. Even earlier, in 1979, Filotti, Miller, and Reif [95] claimed the first algorithm with polynomial running time for fixed surface S , but where the degree of the polynomial depends on S , although their algorithm

has since been shown incorrect [152]. Just before Mohar published his result, Djidjev and Reif [75] gave a fixed-parameter-tractable algorithm, although not linear in n .

There is another approach to determine if a graph can be embedded on a surface, using graph minors more directly. This approach has not given the most efficient algorithms, nor the first ones, but deserves a presentation. Recall that the Robertson-Seymour theorem implies that every surface has a finite number of forbidden minors. Moreover Robertson and Seymour [164, 56] provided an algorithm to determine whether a fixed graph H is a minor of an input graph G , in time $O(n^3)$ if G has size n . The running time hides a constant that depends super-polynomially on the size of H . This result has since been improved to $O(n^2)$ by Kawarabayashi, Kobayashi, and Reed [123], and recently to $O(n^c)$ for any $c > 1$ by Korhonen, Pilipczuk, and Stamoulis [129]. This result can serve to determine if an input graph G embeds on a fixed surface S in almost-linear time simply by listing the forbidden minors of S , and determining if one of them is a minor of G (again, the running time hides a constant that depends on S). Recall however that the set of forbidden minors of S is unknown in general. Moreover the approach does not tell how to construct an embedding if there is one.

4.1.3 Telling embeddings apart

We now consider the problem of telling embeddings apart. On a closed surface S , one can think of several notions of equivalence between two embeddings $f_1, f_2 : G \rightarrow S$ of a graph G . For example one can consider f_1 and f_2 as *congruent* if there is a homeomorphism $\varphi : S \rightarrow S$ such that $f_1 = \varphi \circ f_2$. A finer equivalence restricts φ to being homotopic to the identity map of S . This the same as f_1 and f_2 being *isotopic*, prominently because all homotopic homeomorphisms of S are isotopic. (If S was not the sphere, an intermediate notion of equivalence would be obtained by considering *orientation-preserving* homeomorphisms, but we will not use that.)

On the sphere there are only two classes of homeomorphisms up to homotopy, the orientation-preserving ones, all homotopic to the identity map, and the orientation-reversing ones. Yet even on this simple surface there are embeddings of the same graph that are congruent but not isotopic, or even that are not congruent at all. To understand what are the possible embeddings of a graph the key tool is connectivity. A graph is k -connected, $k \geq 1$, if it has at least $k + 1$ vertices and cannot be disconnected by removing at most $k - 1$ vertices. On the sphere all the embeddings of a 3-connected graph are congruent, and are thus isotopic up to composition by an orientation-reversing homeomorphism. This rigidity theorem is completed by a natural decomposition of every graph into 3-connected graphs. We do not detail, but roughly every graph is a disjoint union of 1-connected subgraphs, every 1-connected graph decomposes into maximal 2-connected subgraphs (and some edges) articulated by a tree-like structure, and every 2-connected graph decomposes into 3-connected subgraphs articulated by a *SPQR tree*. The point is that the articulations of those decompositions describe the possible embeddings of the graph on the sphere.

Algorithmically, an embedding, cellular say, for simplicity, of a graph G on a surface S can be encoded by a graph isomorphism between G and the 1-skeleton of a combinatorial map whose surface is homeomorphic to S . Determining whether two embeddings encoded this way are congruent then boils down to an isomorphism test of combinatorial maps. Isotopy testing however is more challenging, and involves a correspondence between the surfaces of the two embeddings. Colin de Verdière and de Mesmay [47] give an algorithm to determine

whether two embeddings of a graph G in the interior of a surface S are isotopic. The input embeddings $f_1, f_2 : G \rightarrow S$ are given separately, in general position with respect to a common graph H cellularly embedded on S . Given the two arrangements of f_1 and f_2 with H , of complexities k_1 and k_2 , they determine whether f_1 and f_2 are isotopic in $O(k_1 + k_2)$ time. Note that H and S are part of the input. They extend their results to a different model where the surface is the Euclidean plane with some points removed and the embeddings are piecewise linear. Their approach is the continuity of previous work by Ladegaillerie [132], and relies on the fact that if a homeomorphism $\varphi : S \rightarrow S$ with $f_1 = \varphi \circ f_2$ is homotopic to the identity map of S , then for every closed walk C in G the image closed curves $f_1 \circ C$ and $f_2 \circ C$ are freely homotopic, and this can be tested using known algorithms (see Section 4.4.1).

4.1.4 Drawing with few crossings in the plane

In this section we consider the more general problem of computing the minimum number of crossings that a drawing of a graph can have. This is already difficult in the particular case where the surface is the plane, so we review only this case. The *crossing number* of a graph G is the minimum number of crossings that a plane drawing of G can have. During World War II, Turán [183] asked what are the crossing numbers of the complete bipartite graphs $K_{n,m}$. The same problem arose at the same time in sociology [28]. A simple drawing gives the upper bound $\lfloor n/2 \rfloor \lfloor (n-1)/2 \rfloor \lfloor m/2 \rfloor \lfloor (m-1)/2 \rfloor$, and this formula is conjectured to be the exact value, but this is still open [84]. In general researchers have tried to compute the crossing numbers of very simple graphs with limited success. Variants of the crossing number have also been considered [154, 167].

The crossing number problem, of determining whether the crossing number of a given graph is smaller than a given integer, is in NP, for a drawing of the graph with a minimum number of crossings would provide a certificate. In 1983 Garey and Johnson [103] proved that the problem is NP-hard, and thus NP-complete. Hliněný [117] and Cabello [33] later proved that the problem remains NP-hard on smaller classes of graphs: the cubic graphs, and the graphs obtained by adding only one edge to the planar graphs. On the positive side, Grohe [109] gave a $O(f(k) \cdot n^2)$ time algorithm to determine if a graph with n vertices has crossing number smaller than k , for some computable function f , using Courcelle's theorem. This has been improved to $O(f(k) \cdot n)$ by Kawarabayashi and Reed [125], and the function f has recently been brought to $f(k) = 2^{O(k \log k)}$ by several authors [142, 50]. Concerning approximation, Cabello [31] proved that, unless $P = NP$, there is a constant $s > 1$ such that no polynomial time algorithm can approximate the crossing number of a graph with n vertices within a factor s , even when restricted to 3-regular graphs. Whether constant factor approximation is achievable is open. Approximating the crossing number is notoriously difficult [89, 45].

We note that the crossing number problem is generalized by the problem of determining whether a graph can be embedded on a simplicial complex [50, 51].

4.2 Perturbing drawings

In this section we consider a variation of the problem of drawing a graph G with few crossings on a surface S . Informally this variation considers an initial drawing f that has “overlaps”, and asks for a “perturbation” of f into a drawing with few crossings. We first ask for a

drawing without any crossing, an embedding, in Section 4.2.1. We consider minimizing the number of crossings in Section 4.2.2.

4.2.1 Perturbing drawings into embeddings

First we ask for a drawing without any crossings, an embedding. We are given a graph H embedded on S , and a drawing $f : G \rightarrow H$ that maps the vertices of G to vertices of H , and the edges of G to walks in H . We must determine if there are embeddings $G \rightarrow S$ “arbitrarily close” to f , or equivalently but more formally if f is the limit of some sequence of embeddings $G \rightarrow S$ in the compact-open topology. Such a drawing is a *weak embedding*. The problem is already interesting when G is a cycle. Cortese, Di Battista, Patrignani, and Pizzonia [55] gave the first polynomial time algorithm to determine whether a given closed walk C in an embedded graph H is a weak embedding. Their result has then been improved by Chang, Erickson, and Xu [40], and finally by Akitaya, Fulek and Tóth [9] with a $O(n \log n)$ time algorithm, where n is the length of C . In 2017 Fulek and Kynčl [100] gave the first algorithm for general graphs, by generalizing the classical Hanani-Tutte theorem. And their result was then improved by Akitaya, Fulek, and Tóth [10] who determine whether a drawing $f : G \rightarrow H$ of complexity n is a weak embedding in $O(n \log n)$ time. If f is a weak embedding, their algorithm constructs a combinatorial representation of embeddings arbitrarily close to f . We will detail their result in Chapter 5, and we will use it afterward.

The initial motivation of Cortese, Di Battista, Patrignani, and Pizzonia [55] for considering weak embeddings was the study of clustered planarity, a problem introduced in 1995 by Feng, Cohen, and Eades [93, 94, 53] in which a graph is given together with a hierarchical clustering of its vertices, and one has to provide an embedding of the graph in the plane together with a collection of disjoint simple closed curves surrounding the clusters. At the time no polynomial time algorithm was known for testing clustered planarity, only particular cases were solved [54, 105, 13]. Recently Fulek and Tóth [102] gave the first polynomial time algorithm for testing clustered planarity.

4.2.2 Perturbing closed walks minimally

Now we ask for a drawing with few crossings instead of an embedding. We are given G , H , $f : G \rightarrow H$, and an integer k , and we must determine if there are drawings arbitrarily close to f with less than k crossings. This problem is clearly in NP, and contains the classical crossing number problem, when H is a single vertex, so it is NP-complete. Perhaps surprisingly, Fulek and Tóth [101] showed that the problem remains NP-complete even when G is a cycle, that is when f is a closed walk, by a reduction from 3-SAT. On the other-hand, they provide a quasi-linear time algorithm when f is a collection of closed walks that have no *spur*, that never take an edge of H and its reversal consecutively. Their algorithm even constructs curves realizing the minimum number of crossings. Again, we will detail their result in Chapter 5 to use it afterward.

4.3 Embedding graphs rectilinearly in the plane

In this section we consider drawing graphs in the plane, but with the additional geometric constraint that all edges are drawn as geodesic segments for the Euclidean metric. Such a

drawing is called a *Fáry* drawing, and a Fáry embedding if it is also an embedding. For such an embedding to exist, the graph must have no loop, nor any two parallel edges, in addition of being planar. In 1948 Fáry [92] proved that there is no other obstruction, every planar graph without loops nor parallel edges has a Fáry embedding. This result was independently discovered by Stein [175] and Wagner [186]. In this section graphs have no loop nor parallel edges, without further mention.

In Section 4.3.1 we review a classical method of Tutte for producing Fáry embeddings of planar graphs. The resulting embeddings may have high resolution so we review in Section 4.3.2 other methods that produce embeddings whose vertices have small integer coordinates. Finally in Section 4.3.3 we consider the refined problem of transforming a Fáry embedding into another Fáry embedding via an isotopy whose intermediate maps are all Fáry embeddings. This will be the occasion for us to see that the method of Tutte does not just produce Fáry embeddings, but also generalizes to produce isotopies of Fáry embeddings.

4.3.1 Tutte embeddings

In 1963 Tutte [184] proved that every 3-connected planar graph has a Fáry embedding whose inner faces are all strictly convex: the angles at the corners are all strictly smaller than π . And he gave a method to construct such embeddings.

A *Tutte* drawing is a Fáry drawing $f : G \rightarrow \mathbb{R}^2$ that satisfies the following, where some face of the unique embedding of G on the sphere is singularized as the *outer face*:

- (i) The $k \geq 3$ vertices x_1, \dots, x_k along the boundary of the outer face are mapped by f to the vertices of a strictly convex polygon in order.
- (ii) For every vertex $y \notin \{x_1, \dots, x_k\}$ the image of y under f is a barycenter with strictly positive coefficients of the images of the neighbours of y .

The first result of Tutte is a theorem:

Theorem 4.1 (Tutte, 1963). *Let G be a 3-connected planar graph. If $f : G \rightarrow \mathbb{R}^2$ is a Tutte drawing then f is an embedding and every inner face of f is strictly convex.*

In Theorem 4.1 the assumption that the graph is 3-connected is crucial. To see that consider a cycle C of four vertices v, x, w, y . In a Fáry embedding $f : C \rightarrow \mathbb{R}^2$ the vertices x and y cannot be both embedded as barycenters with strictly positive coefficients of their neighbours, for otherwise $f(x)$ and $f(y)$ would both be contained in the line supporting $f(v)$ and $f(w)$, contradicting the fact that f is an embedding.

The second result of Tutte is an algorithm to construct a Tutte embedding of a 3-connected planar graph G . Fix an outer face and its $k \geq 3$ boundary vertices x_1, \dots, x_k . Fix the image points $f(x_1), \dots, f(x_k)$ as the vertices of a strictly convex polygon so that f satisfies (i). Fix strictly positive barycentric coefficients to serve in (ii). Tutte proved that there is a unique assignment of positions $f(y)$ to the vertices $y \notin \{x_1, \dots, x_k\}$ that satisfies (ii) for the chosen barycentric coefficients, and that those are obtained by solving in polynomial time a system of linear equations.

The initial work of Tutte [184] has been revisited many times; see, in particular, Richter-Gebert [159, Section 12.2], Thomassen [182], or Edelsbrunner [79, Section I.4].

4.3.1.1 Spring embeddings

Importantly, the method of Tutte has flexibility in the choice of the outer polygon, and in the barycentric coefficients. Fixing those determines a unique Tutte embedding. In Tutte's original work the coefficients are all equal to one, but the proofs extend readily, and the generalization to arbitrary positive coefficients is detailed for example by Floater [96, 97].

A particular kind of Tutte embedding is obtained by a *symmetric* set of barycentric coefficients: if y and z are neighbor inner vertices, the coefficient of $f(z)$ in the barycentric decomposition of $f(y)$ is equal to the coefficient of $f(y)$ in the barycentric decomposition of $f(z)$. This is equivalent to assigning a weight $\omega_e > 0$ to each inner edge e of G . The associated Tutte embedding $f : G \rightarrow \mathbb{R}^2$ is then the unique Fáry drawing with the given outer polygon that minimizes the function $\sum_e \omega_e |f(e)|^2$, summing over the inner edges e of G , and where $|\cdot|$ denotes length. This function is the energy of a physical system that fixes the outer polygon and models the image $f(e)$ of each inner edge e by an ideal spring of rigidity ω_e . Upon this interpretation Tutte embeddings are sometimes called *spring embeddings*, although we emphasize that this interpretation applies only to the Tutte embeddings defined by a symmetric set of barycentric coefficients. Simulating the evolution of this physical system from arbitrary initial conditions is another method for obtaining those particular Tutte embeddings. This method has been generalized, in particular by including repulsive forces, to the field of force-directed graph drawing.

4.3.1.2 Application and generalization

The results of Tutte can be used to prove a classical theorem of Steiniz, that a graph is planar and 3-connected if and only if it is the 1-skeleton of a convex polytope in \mathbb{R}^3 . The “only if” part can be proved constructively in two steps. Consider a 3-connected planar graph G . The first step constructs a Fáry embedding $f : G \rightarrow \mathbb{R}^2$, and assigns a non-zero (possibly negative) weight $\omega(e) \in \mathbb{R} \setminus \{0\}$ to each edge e of G , in such a way that every vertex v of G (possibly on the outer polygon) is mapped to $f(v) = \sum_w \omega(vw)f(w)$, summing over the neighbours of v . Such assignment ω is called an *equilibrium stress*. The second step makes use of ω and lifts f to an isomorphism from G to the 1-skeleton of a convex polytope in \mathbb{R}^3 . This lifting in the second step is called the *Maxwell Cremona correspondence*. Our interest lies in the first step, constructing f and ω , where the results of Tutte can be used. Here one reduces to the case where the outer face is a triangle, in a way that we do not describe here, and constructs the Fáry embedding f with the method of Tutte, after fixing barycentric coefficients that are symmetric, so that they correspond to an assignment ω of *positive* reals on the *inner* edges of G . The outer face being a triangle, it is then easily seen that ω can be extended to an equilibrium stress by assigning *negative* reals to the three *outer* edges.

Part of the work of Tutte has been generalized to higher dimensions by Linial, Lovász, and Wigderson [137], who proved that a graph G with n vertices is k -connected, $1 < k < n$, if and only if every tuple of k vertices of G can be placed at the vertices of a simplex in \mathbb{R}^{k-1} , and the other vertices at points in \mathbb{R}^{k-1} , such that for every vertex v not in the tuple the convex hull of the neighbors of v is full dimensional and contains v in its interior. Such a mapping can then be found by fixing the simplex and solving a system of equations to place the other vertices at some average of their neighbors. This is similar to the method of Tutte.

4.3.2 Grid embeddings

The *resolution* of an embedding can be defined as the ratio between the smallest and the largest distance between two distinct, non-incident, and non-adjacent geometric objects representing vertices or edges. Unfortunately, there are graphs with n vertices, for arbitrarily large n , whose Tutte embeddings all have resolution $1/2^{\Omega(n)}$ [73].

A line of research considers the problem of producing Fáry embeddings whose vertices have *integer coordinates*, equivalently are placed at the vertices of an integer grid. It quickly became clear that every planar graph admits such an embedding, so research focused on finding how *small* the grid can be. Rosenstiehl and Tarjan [165] asked whether the planar graphs with n vertices admit Fáry embeddings with integer coordinates bounded by a polynomial in n (earlier work [174] considered drawing edges as piecewise-linear segments). Unaware of the problem, Schnyder [170] gave a first construction solving the problem with a $2n - 5$ by $2n - 5$ grid (excluding a few small values of n). The problem was really answered by De Fraysseix, Pach, and Pollack [59, 60], who gave an algorithm that constructs a Fáry embedding of a graph with n vertices on the $2n - 4$ by $n - 2$ grid in $O(n \log n)$ time and $O(n)$ space, and who also proved that the grid size is optimal up to constant factor. Their approach is based on a canonical representation of plane graphs, providing an ordering of the vertices. They proceed by induction, embed the graph induced by the first vertices, then move some of the vertices in the embedding in a controlled way, to allow for the next vertex to be placed. Subsequent work by Schnyder [171] computes in optimal $O(n)$ time on a $n - 2$ by $n - 2$ grid. More recent work produces Fáry embeddings with small integer coordinates and with convex faces and outer polygon [189, 23] (even *strictly* convex [166]).

4.3.3 Morphing

A morph between two embeddings f_0 and f_1 is an isotopy that preserves some property of f_0 and f_1 . In this section we consider two isotopic Fáry embeddings $f_0, f_1 : G \rightarrow \mathbb{R}^2$, and the problem of building an isotopy $(f_t)_{t \in [0,1]}$ in which all embeddings are Fáry.

A priori, it is not even clear that such a morph between f_0 and f_1 exists. A natural attempt is to let for every $t \in [0, 1]$ the map f_t be the Fáry drawing that maps each vertex v to $f_t(v) = (1 - t)f_0(v) + tf_1(v)$. If the resulting homotopy $(f_t)_{t \in [0,1]}$ is an isotopy, that is if all intermediate maps are embeddings, this is the *linear morph* between f_0 and f_1 . But unfortunately, intermediate maps are not always embeddings. The difficulty is to find trajectories for the vertices so that all intermediate Fáry drawings are embeddings.

Any two isotopic Fáry embeddings are related by a *sequence* of linear morphs. This was first proved in 1944 by Cairns [34], but only for triangulations. Thomassen [180] then extended Cairns's result to all Fáry embeddings. His approach is to augment both embeddings to *compatible triangulations*, isotopic triangulations with the same outer face, reducing to Cairns's result. The idea of compatible triangulations has also been explored by Aronov, Seidel, and Souvaine [17]. The number of linear morphs produced by those works is exponential in the number n of vertices. An efficient version of Cairns's algorithm has been given in which the number of linear morphs is polynomial in n [12]. This has since been improved [14], and it is now established [11] that $O(n)$ linear morphs suffice (even if all vertices have to move along parallel lines in each linear morph), and that this is worst case optimal.

Importantly, Floater and Gostman [98] described a morph between Tutte embeddings $f_0, f_1 : G \rightarrow \mathbb{R}^2$ with the same outer face, based on Tutte's method. They construct the

barycentric coefficients for which f_0 and f_1 are Tutte embeddings. Then they interpolate between the coefficients linearly and consider the associated Tutte embeddings. Note that the vertex trajectories are not piecewise-linear anymore. Gotsman and Surazhsky [107, 178] applied the method to morph between more general Fáry embeddings, in particular between planar polygons (Fáry embeddings of cycles). Their approach is the one taken by Thomassen and Aronov, Seidel, and Souvaine [17] to extend Cairns's result: they augment both embeddings to compatible triangulations.

We note that allowing to bend the edges of the intermediate embeddings gives more freedom in moving vertices, by bending edges to avoid collision, leading to an efficient morphing algorithm of Lubiw and Petrick [144].

4.4 Untangling graphs on surfaces

In this section we review works related to untangling graphs on surfaces. In comparison with drawing graphs the novelty is the homotopy constraint: we must deform the input drawing continuously. To understand this constraint we start in Section 4.4.1 by reviewing a problem that is just about homotopy, not about removing crossings. And only in the particular case of closed curves, instead of general drawings of graphs. This problem is to determine whether a given closed curve can be deformed into another given closed curve. In Section 4.4.2 we consider removing crossings, and we review the problem of minimizing the number of crossings of a collection of closed curves by deforming it. We finally consider untangling drawings of graphs in Section 4.4.3.

4.4.1 Testing curves for homotopy

In this section we review the *transformability problem*: To determine, given two closed curves C_0 and C_1 on a surface S , whether C_0 and C_1 are (freely) homotopic, in other words whether C_0 and C_1 can be continuously deformed into each other. The transformability problem has a special case in which one of the two closed curves is contractible. This is the *contractibility problem*, to determine whether a given closed curve C is contractible, in other words whether C can be continuously shrunk to a point.

The similar problems on loops reduce to the problems on closed curves: A loop ℓ is contractible if and only if the closed curve obtained by joining the ends of ℓ is contractible, and two loops ℓ_0 and ℓ_1 are homotopic with basepoint fixed if and only if the concatenation of ℓ_0 by the reversal of ℓ_1 is contractible.

The algorithms for the transformability problem on closed surfaces are easily generalized to surfaces with boundary. Indeed every surface with boundary S extends to a closed surface S' by attaching a handle on each boundary component. And two closed curves in S are homotopic in S if and only if they are homotopic in S' ; this intuitive fact is an immediate consequence of the classical Seifert–Van-Kampen theorem. Nevertheless, we will review a simple algorithm for surfaces with boundary that closed surfaces do not have.

4.4.1.1 Approach by covering space

Concerning the contractibility problem, according to Stillwell [176], the first method of resolution can be traced back to Schwartz. Our presentation focuses on a closed surface S of

genus $g \geq 1$. Transform the input closed curve C into a loop by fixing a basepoint, and lift this loop to a path in the universal covering space \tilde{S} of S . The key property is that the endpoints of the lifted path are equal if and only if C is contractible. Moreover this property can be decided constructively. Consider a canonical system of loops L embedded on S . Assume without loss of generality that C is a closed walk in L . Cut S along L into a canonical polygonal schema. Attach copies of the schema along the appropriate sides to construct a large portion \tilde{S}_0 of \tilde{S} , and lift C in it.

Schipper [169] revisited the solution of Schwartz under a more algorithmic length. The closed walk C is now given in a triangulation T of S that is also part of the input, instead of a fixed canonical system of loops. He determines whether C is contractible in S in $O(g^2k + gn)$ time if $g \geq 2$, and in $O(k^2 + n)$ time if $g = 1$, if T has size n , and if C has length k . His algorithm first uses a fundamental algorithm of Vegter and Yap [185] to embed a canonical system of loops L in general position with T , controlling the number of crossings between L and T . Then it pushes C to a closed walk in L , and uses the method of Schwartz. Dey and Schipper [71] subsequently proved that $O(n + k \log g)$ time is achievable with similar techniques. They push the curve into a system of loops that may not be canonical, although it still has a minimum number of $2g$ loops, and provide a more efficient encoding.

In the same vein Lazarus and Rivaud [134] obtained an optimal algorithm. They preprocess any graph G of size n cellularly embedded on S in $O(n)$ time and then determine in $O(k)$ time whether a closed walk of length k in G is contractible in S . Their first contribution is to push the closed walk not in a system of loops but in a new kind of graph Q embedded on S , a *system of quads*, that they obtain from the input graph G as follows. They construct a subgraph of G whose complement in S is an open disk, and contract some edges of this graph to get a system of loops embedded on S . Then they insert a vertex in the face of this system of loops, and link this new vertex to the corners of the face. Finally they delete the loops to obtain Q . Every face of Q has four corners, and Q has two vertices of degree $4g$ each. To solve the contractibility problem they basically use the method of Schwartz, lifting the curve in a portion \tilde{S}_0 of \tilde{S} , but they construct \tilde{S}_0 by gluing faces of Q .

Lazarus and Rivaud [134] also obtained an optimal algorithm for the transformability problem. They determine whether two non-contractible closed walks C_1 and C_2 in G are freely homotopic, in $O(k_1 + k_2)$ time if C_1 and C_2 have lengths k_1 and k_2 . Here again they push the closed walks into a system of quads Q , but their approach of this problem has an additional component. They define a unique closed walk in Q among each non-contractible homotopy class of closed curves in S , to serve as a representative. They compute this representative in a portion of an intermediate covering space homeomorphic to an open annulus (not the universal covering space), and project the result back to the surface.

4.4.1.2 Torus

Before going further, we mention that when the surface S is a torus the transformability problem has a simple solution. On S a canonical system of loops L consists in loops L_1 and L_2 . Given a walk W in L and $i \in \{1, 2\}$ we denote by W_i the number of times W traverses L_i minus the number of times it traverses the reversal of L_i . Then two walks W and W' are homotopic in S if and only if $W_1 = W'_1$ and $W_2 = W'_2$. Moreover the two closed walks obtained by closing W and W' at their basepoint are freely homotopic if and only if W and W' are homotopic. There is no analog on higher genus surfaces.

4.4.1.3 Approach by shortening: surfaces with boundary

We now consider another approach, that also lead to optimal algorithms. Informally, to *shorten* the input curves in some suitably chosen metric. We illustrate this approach with a very simple algorithm in the special case where the surface S has boundary. In this case S can be realized as a thickening of a graph H . Every closed curve in S is homotopic to a closed walk in H , and two closed walks are homotopic in H if and only if they are homotopic in S . In H removing all spurs greedily from a contractible closed walk C shrinks C to a point. And every non-contractible closed walk is homotopic to a *unique* closed walk without spur. So telling whether two closed walks are freely homotopic boils down to removing all spurs greedily and comparing the resulting walks. This is a very simple solution to the transformability problem! Observe that removing a spur is a *local* shortening of the curve, and that spurs are removed *greedily*. Observe also that this technique does not construct a portion of the universal cover, but operates directly on the surface.

4.4.1.4 Approach by shortening: closed surfaces

The shortening technique does not immediately generalize to closed surfaces S of genus $g \geq 2$ for those cannot be obtained as a thickening of a graph. However S can be given a hyperbolic metric. And in such a metric the shortening technique applies. Indeed shortening a contractible closed curve shrinks the curve to a point. And there is a unique shortest closed curve in each homotopy class of non-contractible closed curves. Those remarkable properties of hyperbolic surfaces are false on other Riemannian surfaces. Methods exist to shorten a curve, but they are not discrete. The discretization of the shortening technique took a century.

The first step was taken in 1912 by Dehn [64] (translated by Stillwell [66]). He considers a system of loops L , that we assume canonical for simplicity, and a closed walk C in L . His algorithm is based on two observations. First, in the same way as for surfaces with boundary, every spur can be removed from C by homotopy, and this shortens C . Second, and this is new, consider the boundary closed walk R of the face of L , or its reversal. Assume that a subwalk X of C is also a subwalk of R , so that R is the concatenation of X and a walk Y . Then X can be replaced by the reversal of Y in C , and doing so only if X is longer than Y shortens C . Dehn's algorithm applies greedily those two *reductions* until none applies anymore, at which point the closed walk is *reduced*. Dehn proved that every reduced closed walk is either non-contractible or a single vertex. This allows to determine whether a closed walk of length k in L is contractible in S in $O(\kappa \cdot k)$ time, where $\kappa > 0$ depends on the genus of S .

For the transformability problem, Dehn [63, 65] had first provided a reduction to the contractibility problem. Two closed walks C_0 and C_1 in L are freely homotopic in S if and only if they satisfy the following. There are basepoints for C_0 and C_1 and a walk X in L such that the concatenation of C_0 , X , the reversal of C_1 , and the reversal of X is contractible. Dehn provided an upper bound on the minimal length of X , so one tries all possibilities for X , and for the basepoints of C_0 and C_1 . In his 1912 paper Dehn [64, 66] then gave a better solution, without reduction to the contractibility problem. He proved that if two freely homotopic non-contractible closed walks C_0 and C_1 are *reduced* then either they are equal (up to cyclic permutation), or they are related by a *single* loop of L . Ultimately this allows to determine whether two closed walks of lengths k_1 and k_2 are freely homotopic in

$O(\kappa \cdot (k_1 + k_2))$ time.

The first optimal algorithms for both the contractibility problem and the transformability problem were announced by Dey and Guha [72] in 1999, and they were Dehn type algorithms. However it has since been claimed that their work contains errors [134, 88]. In 2013 Erickson and Whittlesey [88] recasted the optimal algorithms of Lazarus and Rivaud into Dehn type algorithms. They use the same systems of quads, and consider the same representative closed walk in each homotopy class of non-contractible closed curves, but they compute this representative differently. Instead of computing in a covering space, they operate directly on the surface and reduce portions of the walks greedily, in the spirit of Dehn's algorithm. Similarly, they determine if a closed walk is contractible by reducing it and seeing if it shrinks to a point.

4.4.1.5 Side note on group theory

We cannot conclude this section without a side note on group theory. Indeed the contractibility problem is a particular case of the more general *word problem*, one of three fundamental problems on groups studied by Dehn [63, 65, 67], for which Dehn's algorithm was originally formulated. In this problem a finite presentation P is given of a group G , and one must determine whether a given product W over the generators of P and their inverses represents the unit element of G . The contractibility problem is transformed into a word problem as follows. The homotopy classes of the directed loops of L are labeled $a_1, b_1, \dots, a_g, b_g$, so that the fundamental group $\pi_1(S)$ is the free group generated by $a_1, b_1, \dots, a_g, b_g$ and quotiented by the relation $R = 1$ where $R := a_1 b_1 a_1^{-1} b_1^{-1} \dots a_g b_g a_g^{-1} b_g^{-1}$ corresponds to the boundary walk of the face of L . A word over the generators and their inverses encodes a contractible loop if and only if it represents the unit element of $\pi_1(S)$. Dehn's algorithm can be defined to operate directly on those words. His algorithm can even be defined for more general group presentations. However there are finite presentations whose word problem is undecidable [176]. Finding sufficient conditions for a finite presentation to have its word problem solved by Dehn's algorithm is at the root of *small cancellation theory*. In a similar manner, the transformability problem is a special case of the more general *conjugacy problem* on groups.

4.4.2 Computing the intersection number of curves

On a surface S , a collection C of closed curves is in **general position** if no point of S is the image of more than two points of C , and if every self-intersection of C is a crossing. In addition, C is in **minimal position** if no continuous deformation, in other words no homotopy, can decrease its number of crossings. In general the (geometric) **intersection number** $i_S(C)$ is the number of crossings of a collection of closed curves in minimal position homotopic to C .

In this section we review the *intersection number problem*, of computing $i_S(C)$ given S and C . The problem is further restricted by just asking whether $i_S(C) = 0$. This is the *simplicity problem*, of determining whether C can be deformed into a disjoint collection of simple closed curves. In both cases one can further ask not only to compute $i_S(C)$ but actually to compute a collection C' realizing the minimum.

4.4.2.1 Preliminary observations

Before going further, there are two things to understand about the problem. The first thing is that if we just want to compute $i_S(C)$, without actually constructing curves realizing the minimum number of crossings, then we can reduce to C containing only one or two closed curves. To see that first consider two closed curves c and d on S . For any two curves c' and d' homotopic to c and d the collection $\{c', d'\}$ has three types of crossings: the self-crossings of c' , the self-crossings of d' , and the crossings between c' and d' . So $i_S(\{c, d\}) \geq i_S(c) + i_S(d) + i_S^*(c, d)$, where $i_S^*(c, d)$ denotes the minimum number of crossings between any two curves in general position homotopic to c and d . We emphasize that $i_S^*(c, d)$ does *not* count the self-crossings of the curves, contrarily to $i_S(\{c, d\})$. Perhaps surprisingly, the inequality is actually an equality, and it holds more generally for any number of curves. Given an arbitrary collection of closed curves C there is a collection homotopic to C in which every curve c crosses itself $i_S(c)$ times and every two curves $c \neq d$ cross each other $i_S^*(c, d)$ times. In other words, if a collection of closed curves is in minimal position, then every single curve in the collection is in minimal position, and every pair of curves too. This is folklore, and follows for example from a result of de Graaf and Schrijver [62, Theorems 1]. From there computing $i_S(C)$ for an arbitrary C boils down to computing $i_S(C)$ when C contains at most two curves, via a simple formula. We emphasize however that an algorithm that can put one or two curves in minimal position would not necessarily extend to an arbitrary number of curves.

The second thing to understand about the problem is that it reduces to the case where all the curves in C are primitive, and where no two of them are homotopic. We will detail in the next chapter, Chapter 3. Roughly, the idea is that to put C in minimal position contractible curves can be pushed into arbitrarily small disks, homotopic curves can be drawn parallel to each other, and powers of a curve c can be drawn in a neighborhood of c . This time, we can actually put C in minimal position this way, we are not restricted to computing $i_S(C)$. However we must be able to determine whether two curves are homotopic, and also, given a non-contractible curve c , to compute a curve \hat{c} and an integer $n \geq 1$ such that c is homotopic to the n -th power of \hat{c} .

For those reasons, the results that we are going to review sometimes focus on one or two curves, or on primitive non-homotopic curves. We insist however that the reductions are not perfect, as we already said: focusing on one or two curves does not allow to put more than two curves in minimal position, and focusing on primitive curves subsumes that we can test curves for homotopy and compute the primitive ones.

4.4.2.2 An early result by Poincaré

Several approaches were developed to untangle curves. For example Chillingworth [43, 44] used the notion of winding number to determine if a closed curve can be made simple by homotopy, and if a set of simple closed curves can be made disjoint. We selected only some of these approaches for review.

As early as 1904 Poincaré [155, Section 4] described a necessary and sufficient condition for a primitive closed curve C on a closed surface S to be homotopic to a simple closed curve. When S has genus greater than or equal to two he puts a hyperbolic metric on S and identifies the universal cover of S with the Poincaré disk \mathbb{D} . Any lift of C in \mathbb{D} is a bi-infinite line \tilde{C} with two limit points a and b on the boundary circle $\partial\mathbb{D}$. The infinitely many lifts of

C correspond to infinitely many pairs of limit points on $\partial\mathbb{D}$. Crucially, all the closed curves homotopic to C have the same pairs of limit points than C . Poincaré leveraged this invariant of the homotopy class of C to show that this class contains a simple closed curve if and only no two pairs of limit points are interlaced on $\partial\mathbb{D}$. Note that two pairs $\{a, b\}$ and $\{a', b'\}$ of limit points are either equal or disjoint. The approach of Poincaré was turned into an algorithm by Reinhart [158], but without precise complexity analysis.

4.4.2.3 Approach by shortening

Prominently, the technique of shortening curves, used to test the curves for homotopy (Section 4.4.1), has also successfully been used to compute their intersection number. For example Birman and Series [20] determine if a closed curve C is homotopic to a simple closed curve, on a surface S with boundary. The surface S is a thickening of a loop system Y and C is a closed walk in Y . Roughly, they prove that shortening C as much as possible suffices to untangle C if C can be untangled. In detail they prove that if the homotopy class of C contains a simple closed curve, and if C has no spur, then C is what we call today a weak embedding. They also exhibit a necessary and sufficient condition for C to be a weak embedding, leading to a polynomial algorithm. Their proof is impregnated by previous work in topology of surfaces and hyperbolic geometry, in particular by the above construction of Poincaré. The result of Birman and series was extended by Lustig [146] to compute the intersection number of one or several curves.

On closed surfaces also, the curve shortening technique applies. For example on a closed hyperbolic surface every collection of primitive non-homotopic geodesic closed curves is in minimal position [91, Section 1.2.4]. This holds also on flat tori. A discrete algorithm was given by Cohen and Lustig [46]. The current state of the art is a recent algorithm of Despré and Lazarus [69]. They use some of the curve shortening tools developed for homotopy testing, but apply them to compute the intersection number. More precisely Despré and Lazarus apply the algorithm Erickson and Whittlesey [88] to reduce closed walks, and they show that the reduced closed walks are close to being in minimal position. However an infinitesimal perturbation may not suffice, reduced closed walks can have excess crossings. Their main contribution is to retrieve the intersection number anyway. In detail they proved:

Theorem 4.2 (Despré, Lazarus, 2019). *Let M be a graph with m edges cellularly embedded on a surface S . Let C be a collection of either one or two closed walks of total length n in M . One may compute $i_S(C)$ in $O(m + n^2)$ time.*

When S has negative Euler characteristic, Despré and Lazarus also provide an algorithm to compute a closed curve γ' in minimal position, homotopic to a given closed walk C . They derive from M a system of quad Q , and return γ' as a perturbation of a closed walk C' in Q . They proved:

Theorem 4.3 (Despré, Lazarus, 2019). *Let M be a graph with m edges cellularly embedded on a surface S of negative Euler characteristic. Let C be a closed walk of length n in M . One may construct in $O(m + n^4)$ time a quadrangulation Q , a closed walk C' of length $O(n)$ in Q , homotopic to C , and a perturbation of C' with $i_S(C)$ self-crossings.*

We stress that Theorem 4.3 does not cope with more than one closed walk. Although Despré and Lazarus do not mention it, their output can easily be turned by isotopy into a

perturbed closed walk of length $O(mn)$ in M (instead of Q), at an additional cost of $O(mn)$ time.

4.4.2.4 Approach by homotopy moves

Another approach is pioneered by Hass and Scott [113], who prove that if a *single* closed curve has excess crossing, then it must have a monogon or a bigon: a disk in the surface bounded by one or two portions of the curve. Removing this monogon or bigon from the curve decreases the number of crossings. However Hass and Scott do not tell how to find the monogons and bigons. Interestingly, their proof uses variants of a curve shortening technique of Grayson [108], Shepard [173], and Angenent [15].

On a collection of *arbitrarily many* curves, de Graaf and Schrijver [62] proved that the number of crossings can be minimized by applying a few types of moves, that include but are not limited to the removal of monogons and bigons. Those moves are monotonic, they do not increase the number of crossings. But some do not decrease the number of crossings either, and the authors do not provide an upper bound on the number of moves required to put the curves in minimal position. By considering homotopy moves that may increase the number of crossings, some authors [39] provide a polynomial time algorithm for a single closed curve. Then Chang and de Mesmay [38] provide a polynomial time algorithm for arbitrarily many curves, using only the original monotonic moves.

4.4.2.5 Compactly encoded simple curves

On surfaces the *simple* curves have a compact encoding that other curves do not have. Let S be a surface, and T be a triangulation of S . A simple closed curve C on S is *normal* with respect to T if C is in general position with T , and if C never leaves a triangle Δ of T via the same side it entered Δ . For each pair of sides of Δ we count the number of times C enters and leaves Δ consecutively via those two sides. Those $3n$ non-negative integers, assuming T has n triangles, are the *normal coordinates* of C with respect to T . If C intersects m times the edges of T then the vector of normal coordinates is encoded on $O(n + \log m)$ bits, which is generically more compact than listing the intersections of C with edges of T for example.

Operating on normal coordinates allows for more efficient algorithms, usually considered efficient when polynomial in n and $\log m$, instead of m . For example determining whether a closed curve is connected is non-trivial in this setting. More related to us, Lackenby [131] recently computed the intersection number of a collection of *simple* closed curves on a surface S . The approach, borrowed to Bell and Webb [19], is to decrease the number of intersections between the curves and the triangulation by modifying the triangulation, working out the corresponding change of normal coordinates. This completes previous works [168, 19, 78] in the particular case where S has boundary. Unsurprisingly, this case is considerably simpler. The reason is that the interior of S can be realized as the surface of a triangulation T punctured at its vertices, and that then each homotopy class of simple closed curves contains a *unique* curve realizing the minimum number of crossings with the edges of T .

4.4.3 Untangling graphs

In this section we finally review the works related to untangling drawings of graphs on surfaces. A first problem is the following. We are given a map $f : G \rightarrow S$, for example given

as a drawing $G \rightarrow T^1$ into the 1-skeleton of a triangulation T of S , and an integer k . We must determine whether there is a drawing homotopic to f , in general position, with less than k crossings. If S is the sphere this is the same as asking whether the crossing number of G is smaller than k , which is NP-hard.

So instead we consider the problem of determining whether there exists an embedding homotopic to f . With the variation of actually constructing an embedding if there is one. There is no discrete algorithm to do that. However there is a method generalizing the spring embeddings of Tutte (Section 4.3.1), obtained by Y. Colin de Verdière [52]. He first considers a closed Riemannian surface S of non-positive curvature. In particular S can be a closed hyperbolic surface of a flat torus, and the reader can think of only those surfaces if this helps the understanding, but technically S can have non-constant curvature. He further considers a topological triangulation T of S , its 1-skeleton $T^1 \subset S$, and a map $f : T^1 \rightarrow S$ homotopic to the inclusion map $T^1 \rightarrow S$. The map f , while homotopic to an embedding by definition, may not be embedding itself. And f draws the edges of G as arbitrary paths. Y. Colin de Verdière provides a method to deform f into an embedding whose edges are geodesic. First he considers only the drawings f whose edges are geodesic, by making each edge geodesic in the drawing without moving the images of the vertices. We call those the *Fary* drawings, by analogy with the classical setting. The problem is now to move the images of the vertices around, keeping the edges geodesic, to make f an embedding. To do so he considers the Fary drawings f that minimize a potential $\sum_e \omega_e |f(e)|^2$ for some arbitrary assignment of positive coefficients ω_e on the edges e of T^1 . We call those the *spring* drawings. The first result of Y. Colin de Verdière [52, Theorem 1] is:

Theorem 4.4 (Y. Colin de Verdière, 1991). *Let S be a closed Riemannian surface of non-positive curvature. Let G be the 1-skeleton of a triangulation of S . Let $f : G \rightarrow S$ be homotopic to the inclusion map $G \rightarrow S$. If f is a spring drawing then f is an embedding.*

Theorem 4.4 is analogous to the classical theorem of Tutte (Theorem 4.1). The assumption that the graph G is 3-connected and planar is replaced by the assumption that G is the 1-skeleton of a triangulation of S , and that f is homotopic to the inclusion map $G \rightarrow S$. The role of homotopy is now clearly visible. The main difference is that the classical theorem fixes the outer face of the graph to a polygon while Theorem 4.4 does not fix anything, for this is not necessary on surfaces. Y. Colin de Verdière considers fixing a cycle of the graph to a boundary component of the surface in a second result [52, Theorem 3].

Contrarily to the classical setting, the homotopy class of f may contain several spring embeddings. This is easily seen on a flat torus, where every spring embedding can be translated along the surface. Nonetheless there is “generically” only one, for example if S is negatively curved everywhere [52, Theorem 2].

To transform the initial drawing f into a spring drawing the only method that seems to work in this context is the simulation of the physical system modeling the image $f(e)$ of each edge e by an ideal spring of rigidity ω_e . In particular the method of Tutte, solving equations, does not seem to extend, except in the particular case of flat tori [37].

We mention that similar results were later independently described by several authors, including Hass and Scott [114, Lemma 10.12], Delgado-Friedrichs [68], Gortler, Gotsman, and Thurston [106], Lovász [143, p.98], and Luo, Wu, and Zhu [145, Theorem 1.6].

Chapter 5

Preliminaries

In this chapter we present some results that will be used in the next chapters, and we provide proofs for some of them. In Section 5.1 and Section 5.2, we present folklore results about curves on surfaces. In Section 5.3 and Section 5.4 we detail the results of Akitaya, Fulek, and Tóth [10], and of Fulek and Tóth [101], mentioned in Chapter 3.

5.1 Limit points of lifted curves

In this section we present a classical construction that will be used in Section 6.4. This construction dates back to Poincaré [155] and was briefly mentioned in Section 4.4.2. A good overview is provided by Farb and Margalit [91, Chapter 1], but we need a few more properties, so we provide details and proofs. Consider a surface S of genus at least two without boundary. We shall see that the universal cover \tilde{S} of S can be compactified into a topological space $\tilde{S} \cup \partial\tilde{S}$, by adding a set $\partial\tilde{S}$ of **limit points**, such that the compactified space is homeomorphic to the closed disk, and under this homeomorphism \tilde{S} is represented by the open disk and $\partial\tilde{S}$ is represented by the circle. Moreover, we shall see that such a construction exists that satisfies each of the following:

Lemma 5.1. *If $\tilde{c} : \mathbb{R} \rightarrow \tilde{S}$ is a lift of a non-contractible closed curve on S , then $\lim_{+\infty} \tilde{c}$ and $\lim_{-\infty} \tilde{c}$ exist (in $\tilde{S} \cup \partial\tilde{S}$) and are distinct points of $\partial\tilde{S}$.*

Lemma 5.2. *Lift a homotopy $c \simeq d$ between non-contractible closed curves on S to a homotopy $\tilde{c} \simeq \tilde{d}$ between lifts of c and d . Then \tilde{c} and \tilde{d} have the same limit points.*

Lemma 5.3. *Let c and d be two non-contractible closed curves on S . If c and d admit lifts with the same pairs of limit points, there is a closed curve e such that c and d are homotopic to powers of e .*

Lemma 5.4. *Consider lifts \tilde{c} and \tilde{d} of non-contractible closed curves on S . Assume either that \tilde{c} and \tilde{d} intersect exactly once, or that they are disjoint lifts of the same curve on S . Then the four limit points of \tilde{c} and \tilde{d} are pairwise distinct.*

In the rest of this section we detail this compactification of \tilde{S} , and we prove the associated four lemmas. This is folklore, and can be skipped by the reader without impacting the reading of the thesis.

Interestingly, although the properties of the compactification and of the limit points are expressed purely topologically above, they all follow from folklore arguments in hyperbolic geometry: One endows S with a hyperbolic metric and lifts this metric to the universal cover \tilde{S} ; then \tilde{S} is isometric to the hyperbolic plane, which has a classical compactification in the Poincaré model (by adding the boundary of the open disk), the limit points are then naturally defined, and the properties follow, as we shall see.

5.1.1 Compactification of the hyperbolic plane and fixed points of translations

We first present the compactification of the hyperbolic plane that we use. Let \mathbb{H} be the hyperbolic plane, corresponding to the open unit disk in the Poincaré model. One can compactify \mathbb{H} by considering the set $\partial\mathbb{H}$ of “points at infinity”, corresponding to the unit circle (in the Poincaré model) with its usual topology. Equivalently [91, Chapter 1], the points in $\partial\mathbb{H}$ are the equivalence classes of unit speed geodesic rays, where two rays are equivalent if they stay at bounded distance from each other; the union $\bar{\mathbb{H}}$ of \mathbb{H} and $\partial\mathbb{H}$ is topologized via the basis containing the open sets of \mathbb{H} plus one open set U_P for each open half-plane P of \mathbb{H} , where $U_P \cap \mathbb{H} = P$ and $U_P \cap \partial\mathbb{H}$ contains the equivalence class ℓ of unit speed geodesic rays if all the rays in ℓ eventually end up in P .

We shall need some definitions and a lemma, that we now present. Isometries of \mathbb{H} extend naturally to $\bar{\mathbb{H}}$, and the **hyperbolic translations** are those with exactly two fixed points on $\partial\mathbb{H}$. In particular the identity is not considered a hyperbolic translation here. Any hyperbolic translation f admits a unique geodesic line A , its **axis**, such that $f(A) = A$ and such that f is a real translation on A . A hyperbolic translation is uniquely determined by its axis and by the image of a point on this axis. Iterating any point of \mathbb{H} under f makes it converge to one of the two fixed points of f in $\partial\mathbb{H}$, the **fixed point at $+\infty$** of f , while iterating under f^{-1} makes it converge to the **fixed point at $-\infty$** of f . See [122, p. 13-14] for more details. We will need the following lemma in the next section:

Lemma 5.5. *Fix any $x \in \mathbb{H}$. Two hyperbolic translations $f, g : \mathbb{H} \rightarrow \mathbb{H}$ have the same fixed point at $+\infty$ if and only if they satisfy the following for some $D > 0$: there exist arbitrarily large values of $i, j \geq 0$ for which $f^i(x)$ and $g^j(x)$ are at distance less than D .*

Our proof of Lemma 5.5 relies on the following lemma, which is standard and results from simple computations in the Poincaré model of the hyperbolic plane, so we omit the proof:

Lemma 5.6. *In the hyperbolic plane \mathbb{H} let $L \subset \mathbb{H}$ be a geodesic line and $a : \mathbb{R} \rightarrow \mathbb{H}$ be a unit speed geodesic ray. The distance between $a(t)$ and L either tends to ∞ as $t \rightarrow \infty$ or it tends to zero. In the latter case there is a direction of L that satisfies the following. For every unit speed parametrization $c : \mathbb{R} \rightarrow L$ respecting the direction of L , $c(t)$ and $a(t)$ remain at bounded distance over $t \geq 0$.*

Proof of Lemma 5.5. Let $\ell \in \partial\mathbb{H}$ and $\ell' \in \partial\mathbb{H}$ be the fixed point at $+\infty$ of respectively f and g . First assume the existence of some $D > 0$ such that there exist arbitrarily large values of $i, j \geq 0$ for which $f^i(x)$ and $g^j(x)$ are at distance less than D . To prove $\ell = \ell'$ we consider any open set O of $\bar{\mathbb{H}}$ that contains ℓ and we claim the existence of $i_0 \geq 0$ such that for every $i \geq i_0$ the ball of radius D centered at $f^i(x)$ is contained in O . This claim, combined with

our assumption, implies that there exist arbitrarily large values of $j \geq 0$ for which $g^j(x) \in O$. Since $g^j(x)$ tends to ℓ' as x goes to $+\infty$, we have $\ell = \ell'$.

To prove this claim, and without loss of generality, we assume that O belongs to the basis described above to define the topology of $\bar{\mathbb{H}}$. Then, and since $\ell \in O$, there is an open half plane P of \mathbb{H} such that $O = U_P$. Parameterize the axis of f by some unit speed geodesic $a : \mathbb{R} \rightarrow \mathbb{H}$. By definition (up to reversing a) there is $\alpha > 0$ such that $f \circ a(t) = a(t + \alpha)$ on every $t \in \mathbb{R}$. Since f is an isometry the distance between $f^i(x)$ and $a(i\alpha)$ remains constant over $i \in \mathbb{Z}$. By construction a eventually ends up in P . Let L be the geodesic line that bounds P in \mathbb{H} . If the distance between $a(t)$ and L goes to infinity as $t \in \mathbb{R}$ goes to $+\infty$, then the claim is proved. Otherwise this distance goes to zero by Lemma 5.6 and there is some unit speed parameterization $c : \mathbb{R} \rightarrow \mathbb{H}$ of L such that $c(t)$ and $a(t)$ remain at bounded distance over $t \geq 0$. Thus $c(t)$ tends to ℓ as $t \in \mathbb{R}$ goes to $+\infty$, contradicting the fact that $c(t) \notin P$ for every $t \in \mathbb{R}$.

Conversely, assume $\ell = \ell'$. Consider unit speed parametrizations $a : \mathbb{R} \rightarrow \mathbb{H}$ and $b : \mathbb{R} \rightarrow \mathbb{H}$ of their respective axes such that $a(t)$ and $b(t)$ tend to ℓ as t goes to $+\infty$. By definition of the limit points, there exists $D > 0$ such that for every $t \geq 0$ the distance between $a(t)$ and $b(t)$ is less than D . Let $\alpha > 0$ and $\beta > 0$ be the translation lengths of respectively f and g on their axes. There exists $D' > 0$ for which there exist $i, j \geq 0$ arbitrarily large such that $|\alpha i - \beta j| < D'$ and thus such that $a(\alpha i)$ and $b(\beta j)$ are at distance less than $D + D'$. Moreover the distance between $a(\alpha i) = f^i(a(0))$ and $f^i(x)$ does not depend on i since f is an isometry. The same holds for the distance between $b(\beta j)$ and $g^j(x)$. \square

5.1.2 Limit points of lifted curves

Now, every surface S of genus at least two without boundary is homeomorphic to the quotient of the hyperbolic plane \mathbb{H} by the action of some (actually, many) group Γ of isometries of \mathbb{H} . The elements of Γ other than the identity are hyperbolic translations [91, p. 22]. The action is free, in the sense that if $f \in \Gamma$ satisfies $f(x) = x$ on some $x \in \mathbb{H}$, then f is the identity. The action is also properly discontinuous in the sense that every $x \in \mathbb{H}$ admits a neighborhood whose intersection with the Γ -orbit of x is $\{x\}$. The surface S then admits a unique hyperbolic metric for which the quotient map $\mathbb{H} \rightarrow S$ is a local isometry. Also, the hyperbolic plane \mathbb{H} is a universal covering space of S , where the quotient map $\mathbb{H} \rightarrow S$ is the covering map.

In the rest of this section we identify our surface S with a quotient $S = \mathbb{H}/\Gamma$, with the construction presented in the previous paragraph, thus identifying its universal cover \tilde{S} with \mathbb{H} . We are going to prove our four initial lemmas, but first we need two preliminary lemmas:

Lemma 5.7. *Consider a lift $\tilde{c} : \mathbb{R} \rightarrow \mathbb{H}$ of a non-contractible closed curve on S . There is $f \in \Gamma \setminus \{1\}$ such that $\tilde{c}(t+1) = f(\tilde{c}(t))$ on every $t \in \mathbb{R}$. Moreover $\lim_{t \rightarrow \infty} \tilde{c}$ and $\lim_{t \rightarrow -\infty} \tilde{c}$ exist and are the fixed points of f in $\partial\mathbb{H}$, at respectively $+\infty$ and $-\infty$.*

Proof. For every $t \in \mathbb{R}$, there exists some $f_t \in \Gamma$ such that $f_t(\tilde{c}(t)) = \tilde{c}(t+1)$. Moreover every such f_t is not the identity as $\tilde{c}(t) \neq \tilde{c}(t+1)$ since \tilde{c} is a lift of a non-contractible closed curve. We claim that f_t does not depend on t . This claim concludes the proof. We prove the claim by contradiction so assume the existence of some $t \in \mathbb{R}$ fixed and of some $t' \in \mathbb{R}$ arbitrarily close to t such that $f_t \neq f_{t'}$. By choosing t' close enough to t we make the distance between $f_{t'}^{-1} \circ f_t(\tilde{c}(t))$ and $\tilde{c}(t)$ go to zero, contradicting the fact that Γ acts properly discontinuously on \mathbb{H} . \square

Lemma 5.8. *Assume that $f, g \in \Gamma \setminus \{1\}$ have the same fixed point at $+\infty$. There are $h \in \Gamma \setminus \{1\}$ and $n, m \geq 1$ such that $f = h^n$ and $g = h^m$. In particular, they have the same fixed point at $-\infty$.*

Proof. Consider some arbitrary fixed $x \in \mathbb{H}$. We claim the existence of $a, b \geq 1$ such that $f^a(x) = g^b(x)$. Indeed by Lemma 5.5 there is $D > 0$ that satisfies the following. There are $i, j \geq 0$ arbitrarily large such that $f^i(x)$ and $g^j(x)$ are at distance less than D . For every such i, j the point $f^{-i} \circ g^j(x)$ belongs to the closed ball B_x of radius D centered at x . Since Γ acts properly discontinuously on \mathbb{H} the Γ -orbit $\Gamma \cdot x$ of x intersects B_x in finitely many points. Indeed every such point $y \in B_x \cap \Gamma \cdot x$ admits a neighborhood whose intersection with $\Gamma \cdot x$ is $\{y\}$, and finitely many such neighborhoods suffice to cover the compact ball B_x . In particular there exist $i, j \geq 0$, $i' > i$ and $j' > j$ such that $f^{-i'} \circ g^{j'}(x) = f^{-i} \circ g^j(x)$. Letting $a := i' - i \geq 1$ and $b := j' - j \geq 1$ proves the claim.

Our claim implies that f and g have the same fixed points both at $+\infty$ and $-\infty$ and thus the same axis, say A , oriented from $-\infty$ to $+\infty$. Without loss of generality we assume that x was chosen so that $x \in A$. Recall that f and g are real translations on A and let $\alpha > 0$ and $\beta > 0$ be their respective periods.

We consider the hyperbolic translation h whose oriented axis is A and whose period γ is defined as follows. We proved $a\alpha = b\beta$ since $f^a(x) = g^b(x)$ and since $f^a(x)$ and $g^b(x)$ are the translations of x along A by a distance of respectively $a\alpha$ and $b\beta$. There are $n, m \geq 1$ relatively prime such that $na = mb$. By Bézout's theorem, there are $u, v \in \mathbb{Z}$ such that $un + vm = 1$. We let $\gamma = u\alpha + v\beta$.

We claim that $h = f^u \circ g^v$, and thus $h \in \Gamma$. To prove this claim observe that the point $h(x)$ is the translation of the point x by a distance γ along the oriented axis A of h . The point $g^v(x)$ is the translation of x by a distance $v\beta$ along the same oriented axis A , and the point $f^u(g^v(x))$ is the translation of $g^v(x)$ by a distance of $u\alpha$ along A . Thus $h(x) = f^u \circ g^v(x)$. That proves the claim since hyperbolic translations are defined by their axis, here A , and by the image of any point on this axis, here x .

In the same way we have $h^n = f$ and $h^m = g$ since these hyperbolic translations have the same oriented axis by construction, and since their periods satisfy $n\gamma = \alpha$ and $m\gamma = \beta$, as seen by a straightforward computation. \square

Finally, we prove our four initial lemmas:

Proof of Lemma 5.1. The result is given by Lemma 5.7. \square

Proof of Lemma 5.2. Consider the hyperbolic translations, say f and g , given by Lemma 5.7 for \tilde{c} and \tilde{d} respectively. Since the homotopy $\tilde{c} \simeq \tilde{d}$ lifts the homotopy $c \simeq d$, the distance between the points $\tilde{c}(k) = f^k(\tilde{c}(0))$ and $\tilde{d}(k) = g^k(\tilde{d}(0))$ does not depend on $k \in \mathbb{Z}$. By Lemma 5.5 f and g have the same fixed points. \square

Proof of Lemma 5.3. Let \tilde{c} and \tilde{d} be lifts of respectively c and d and assume that \tilde{c} and \tilde{d} have the same limit points. In a first step, if \tilde{c} and \tilde{d} are disjoint, we apply a homotopy of c to make \tilde{c} intersect \tilde{d} ; this does not change the limit points of \tilde{c} by Lemma 5.2.

So we can assume without loss of generality that \tilde{c} and \tilde{d} intersect, and thus also that $\tilde{c}(0) = \tilde{d}(0) = x \in \mathbb{H}$. Consider the hyperbolic translations, say f and g , given by Lemma 5.7 for \tilde{c} and \tilde{d} respectively. By Lemma 5.8 there exist $n, m \geq 1$ and $h \in \Gamma \setminus \{1\}$ such that $f = h^n$ and $g = h^m$. Thus $f(x) = h^n(x)$ and $g(x) = h^m(x)$. Let ℓ be a loop on S that lifts to a path

from x to $h(x)$. Based at zero, c and d are homotopic as loops to respectively the n th power and the m th power of the loop ℓ . \square

Proof of Lemma 5.4. By Lemma 5.1, the two limit points of \tilde{c} are distinct, and similarly for \tilde{d} . Assume, for a contradiction, that \tilde{c} and \tilde{d} have the same limit point at $+\infty$ (up to reversing c or d). There are two cases.

First assume that \tilde{c} and \tilde{d} intersect exactly once in some point $x \in \mathbb{H}$. Without loss of generality assume $\tilde{c}(0) = \tilde{d}(0) = x$. Consider the hyperbolic translations, say f and g , given by Lemma 5.7 for \tilde{c} and \tilde{d} respectively. Then f and g have the same fixed point at $+\infty$. Thus by Lemma 5.8 there exist $i, j \geq 1$ such that $f^i = g^j$. Then $\tilde{c}(i) = f^i(x) = g^j(x) = \tilde{d}(j)$ and this point is distinct from x since, for example, \tilde{c} is non-contractible. This is a contradiction.

Now assume that \tilde{c} and \tilde{d} are disjoint lifts of the same curve c in S . There is a geodesic closed curve α homotopic to c [91, Proposition 1.3]. Lift the homotopy $c \simeq \alpha$ to homotopies $\tilde{c} \simeq \tilde{\alpha}$ and $\tilde{d} \simeq \tilde{\beta}$ for some lifts $\tilde{\alpha}$ and $\tilde{\beta}$ of α . By the preceding lemmas, $\tilde{\alpha}$ and $\tilde{\beta}$ have the same limit points. Thus $\tilde{\alpha}$ and $\tilde{\beta}$ have the same image (a geodesic line), so they are equal up to homeomorphism $\mathbb{R} \rightarrow \mathbb{R}$. By the uniqueness part of the lifting property, \tilde{c} and \tilde{d} are then equal up to homeomorphism $\mathbb{R} \rightarrow \mathbb{R}$. We proved that \tilde{c} and \tilde{d} intersect, a contradiction. \square

5.2 Intersection number, primitivity, and lifts

In this section we review some results about the intersection number of closed curves on surfaces that will be used in the next chapters. Recall from Chapter 4 that on a surface S , given a collection of closed curves C , the **intersection number** $i_S(C)$ is the minimum number of crossings of a collection of closed curves homotopic to C .

The intersection number of arbitrary closed curves is related to the intersection number of the primitive ones. In particular we will use the following result, proved by de Graaf and Schrijver [62, Theorems 6-7]. We need a definition. On a surface S , given two closed curves c and d , we denote by $i_S^*(c, d)$ the minimum number of crossings between any two closed curves in general position homotopic to c and d . We emphasize that $i_S^*(c, d)$ does *not* count the self-crossings of the curves, contrarily to $i_S(\{c, d\})$.

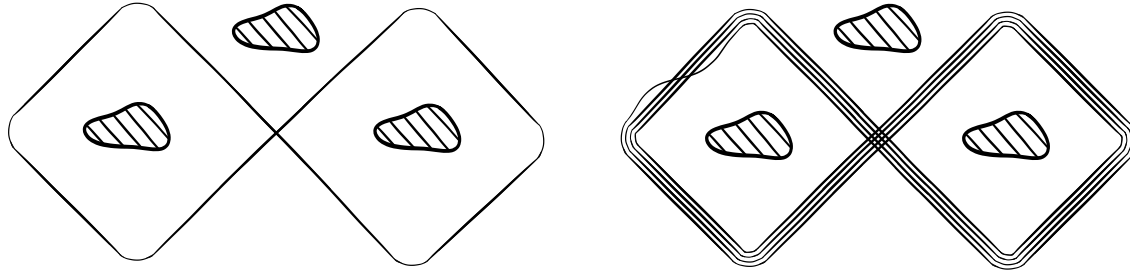


Figure 5.1: (Left) A primitive closed curve \hat{c} , in minimal position. (Right) The fourth power of \hat{c} in minimal position in a neighborhood of \hat{c} .

Lemma 5.9 (de Graaf and Schrijver, 1997). *Let S be the closed surface of genus $g \geq 1$. Let c and d be two closed curves on S homotopic to respectively the n th power of a primitive*

closed curve \hat{c} , and the m^{th} power of a primitive closed curve \hat{d} , for some $n, m \geq 1$. Then $i_S(c) = n^2 i_S(\hat{c}) + n - 1$ and $i_S^*(c, d) = nm \times i_S^*(\hat{c}, \hat{d})$.

In the setting of Lemma 5.9, assume that \hat{c} and \hat{d} are drawn in general position on S . Then draw c in the neighborhood of \hat{c} in the way described by Figure 5.1, and draw d in the neighborhood of \hat{d} the same way. The first part of Lemma 5.9 essentially says that if \hat{c} crosses itself minimally, then so does c . The second part of the lemma says that if \hat{c} and \hat{d} cross each other minimally, then so do c and d .

Now we review a sufficient condition for a collection of closed curves on a surface S to realize the minimum number of crossings of its homotopy class, based on the lifts of the curves in the universal cover of S :

Lemma 5.10. *Let S be the closed surface of genus $g \geq 1$. Let C be a collection of closed curves in general position in S . Assume that in the universal cover of S , every lift of every curve in C is injective, and no two lifts cross each other more than once. Then C has the minimum number of crossings of its homotopy class.*

Proof. We use a result of de Graaf and Schrijver [62, Theorem 1]. They described four moves that can be applied to C , labeled 0, I, II, and III. They proved that it is possible to make C have the minimum number of crossings of its homotopy class just by applying those moves to C . With our assumptions, only the moves 0 and III can be applied. Applying them preserves our assumptions, and does not decrease the number of crossings of C . So C already has $i_S(C)$ crossings initially. \square

5.3 Perturbing drawings into embeddings

In this section we present in more detail the result of Akitaya, Fulek, and Tóth. [10] mentioned in Chapter 3. They consider a graph H embedded on a surface S , a graph G , and a drawing $f : G \rightarrow H$. They are interesting in determining whether f is a **weak embedding**, namely, whether there are embeddings $G \rightarrow S$ “arbitrarily close” to f . To do so they formulate an alternative, more combinatorial definition of weak embeddings. We present a trivially equivalent variation, more suitable to our needs.

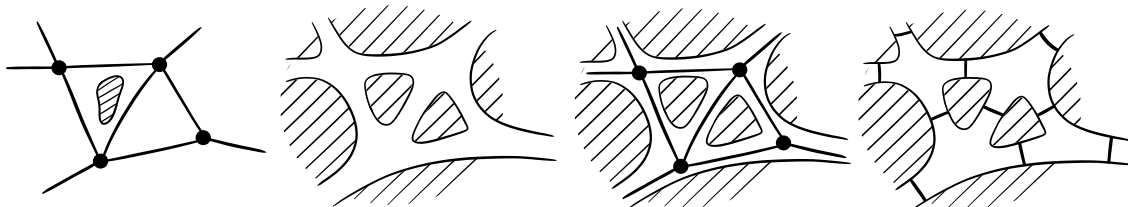


Figure 5.2: (Left) An embedded graph M . (Middle Left) The patch system Σ of M . (Middle Right) We usually think of Σ as a “closed neighborhood” of M . (Right) The arcs of Σ .

Consider an embedded graph H . We present the **patch system** of H , an adaptation of the strip system of Akitaya, Fulek, and Tóth [10], similar to the concept of fat graph [110] and ribbon graph [81]. See Figure 5.2. To ease the reading we assume that H has no loop and no multiple edges; the following extends readily to general graphs H . Consider an oriented closed disk D_v for each vertex v of G ; consider pairwise disjoint closed segments along the boundary

of D_v , one segment per edge incident to v , ordered along the boundary of D_v as prescribed by the rotation system of H . Now, for every edge uv of G , identify the corresponding segments of the disks D_u and D_v in a way that respects their orientations. Those identifications result in a surface Σ homotopically equivalent to H (informally, a “thickening” of H). If u is a vertex of H , then the interior of D_u is an open disk **dual to** u . If uv is an edge of H , then the intersection of D_u and D_v is a simple arc **dual to** uv . The surface Σ , the open disks and arcs dual to the vertices and edges of H , and the two one-to-one correspondences encoding the two dualities constitute the patch system of H . Slightly abusing, we may not make the distinction between the patch system of H and its surface Σ . The graph H embeds naturally in Σ in such a way that every vertex v of H lies in the interior of D_v , and every edge of H intersects the arcs of Σ exactly once, by crossing its dual arc.

An **approximation** of a drawing $f : G \rightarrow H$ is a map $g : G \rightarrow \Sigma$, in general position with itself and with the arcs of Σ , that satisfies both of the following. Firstly, for every vertex v of G , the point $g(v)$ lies in the interior of the disk D_v of Σ dual to v . Secondly, for every edge e of G , the arcs of Σ crossed by the path $g \circ e$ are the duals of the edges of H traversed by the walk $f \circ e$, in order. Note that g may have crossings.

Now, if H is embedded in a surface S and inherits its rotation system from the embedding, we usually think of Σ as a “closed neighborhood” of H in S . In that case, it is easily seen (and follows from considerations by Akitaya, Fulek, and Tóth [10]) that a drawing $f : G \rightarrow H$ is a weak embedding (once viewed as a map $G \rightarrow S$) if and only if there is an approximation $g : G \rightarrow \Sigma$ of f that is also an embedding. Note how the patch system Σ and the property for f to be a weak embedding do not depend on any embedding of H on S , but only on the rotation system of H .

We finally formulate the result of Akitaya, Fulek, and Tóth [10]:

Theorem 5.1 (Akitaya, Fulek, and Tóth, 2019). *Let G be a graph. Let H be an embedded graph. Let $f : G \rightarrow H$ be a drawing of length n . One can compute an embedding approximating f , or correctly report that no such embedding exists, in $O(n \log n)$ time.*

We note that the authors require that f maps each of edge G to either a vertex or an edge of H , not a walk in H , but we can assume this trivially by subdividing the graph G . The running time, in their theorem $O(m \log m)$ where m is the number of edges of G , becomes $O(n \log n)$. The algorithm returns the output embedding (if any) in the disks of Σ .

5.4 Perturbing closed walks minimally

In this section we present in more detail the result of Fulek and Tóth. [101] mentioned in Chapter 3. They consider an embedded graph H , and a collection C of closed walks in H , without spur. They construct curves “arbitrarily close” to C with a minimum number of crossings, and count the crossings. This is formalized as follows.

Recall that H is embedded in its patch system Σ . Assume that C is a single closed walk; the following paragraph trivially extends to collections of closed walks. Recall that an approximation of C is a closed curve γ , in general position in Σ , such that the arcs of Σ crossed by γ are the duals of the edges of H traversed by C , in order. From now on, every such approximating closed curve γ is implicitly assumed to intersect every disk of Σ as a collection of simple paths where every two such paths intersect at most once in the disk; this is without loss of generality, for otherwise γ clearly has excess crossings. Moreover, we

retain from γ only the following combinatorial information: For every arc a of Σ , we retain the order in which the crossings between γ and a occur along a . Dually, we retain, for every edge e of H , a linear order \prec_e on the occurrences of e in C . We say that $\Gamma := (C, (\prec_e)_e)$ is a **perturbed closed walk**, and that Γ is a **perturbation** of C . These ideas exist in the literature, see for example Chambers, Erickson, Fox, and Nayyeri [36, Section 2.4]. A single perturbation of C may correspond to several approximations of C , but it is easily seen that all those approximations have the same number of self-crossings, making the distinction between them irrelevant. In this setting Fulek and Tóth [101] proved:

Theorem 5.2 (Fulek and Tóth, 2020). *Let H be an embedded graph of size m . Let C be a collection of closed walks of total length n in H , without spur. One can construct a minimal perturbation of C in $O(m + n \log n)$ time.*

The number of crossings can then be computed efficiently:

Lemma 5.11 (Fulek and Tóth, 2020). *Let H be an embedded graph of size m . Let Γ be a perturbed collection of closed walks in H , of total length n . One can compute the number of self-crossings of Γ in $O(m + n \log n)$ time.*

Observe that there are embedded graphs with closed walks of arbitrarily large length n whose approximations have $\Omega(n^2)$ self-crossings. So computing any of those approximations would be too expensive for the above quasi-linear time algorithms. This is why those algorithms handle perturbations instead of approximations.

While the rest of the thesis uses Theorem 5.2 and Lemma 5.11 as black boxes, we think that the reader could benefit from proofs of both. Moreover, even though Theorem 5.2 and Lemma 5.11 follow from their work, Fulek and Tóth technically formulate their results differently, and even seem to describe a weaker result [101, Theorem 1] where the graph H is embedded in the plane, and only one closed walk is given as input. For all those reasons we here rephrase and extract the essence of the arguments of Fulek and Tóth [101, Section 3]. We insist that we do not introduce any new idea or result here, and that this section can be skipped without impacting the reading of the rest of the thesis.

Lemma 5.11 is easy to prove:

Proof of Lemma 5.11. One must count the number of self-crossings of Γ around each vertex of H , equivalently within each disk of the patch system of H . There is an immediate reduction to the following problem. Fix $n \geq 1$. Consider a perfect matching of the set $[2n]$, represented by its set E of edges. Write every edge $e \in E$ as $e = ij$, where i and j are the vertices of e , and $i < j$. Say that an edge $ij \in E$ crosses another edge $uv \in E$ if $i < u < j < v$, up to exchanging ij with uv . Let $\perp E$ be the number of unordered pairs of edges of E that cross. Our problem is to compute $\perp E$. We claim that we can compute $\perp E$ in $O(n \log n)$ time.

To prove this claim, we apply a divide-and-conquer strategy. The base cases (small values of n) are trivial. In general, we consider the unique $k \in [2n]$ for which exactly n edges $uv \in E$ satisfy $v \leq k$. We partition E into three sets E_0, E_1, E_2 as follows. An edge $uv \in E$ belongs to E_0 if it satisfies $v \leq k$. It belongs to E_1 if it satisfies $k < u$. And it belongs to E_2 otherwise, that is if $u \leq k < v$. By definition of k , each of the sets E_0, E_1, E_2 contains at most n edges. For every $\ell \leq k$, we let $\omega(\ell)$ be the number of edges $uv \in E_0$ that satisfy $u < \ell < v$. For every $\ell > k$, we let $\omega(\ell)$ be the number of edges $uv \in E_1$ that satisfy $u < \ell < v$. We have the recursion formula $\perp E = \perp E_0 + \perp E_1 + \perp E_2 + \sum_{uv \in E_2} (\omega(u) + \omega(v))$. We use this formula

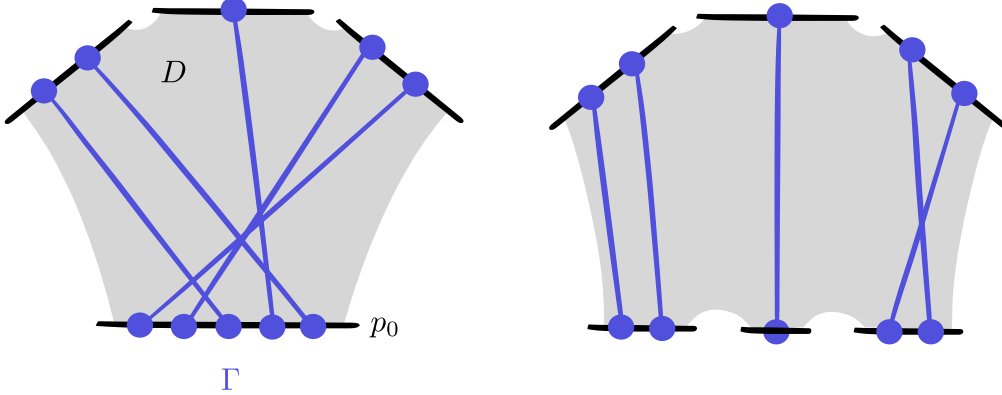


Figure 5.3: The split operation.

in our recursion step, as follows. First, we compute k , E_0 , E_1 , E_2 , and ω in $O(n)$ time. Then we recurse to compute $\perp E_0$, $\perp E_1$, and $\perp E_2$. And we deduce $\perp E$ in $O(n)$ time from the recursion formula. \square

The rest of this section is devoted to the proof of Theorem 5.2. We consider the setting of Theorem 5.2: an embedded graph H of size m , and a collection C of closed walks of total length n in H , without spur. We will prove Theorem 5.2 by constructing a minimal perturbation of C in $O(m + n \log n)$ time. We assume that H has no loop edge nor any parallel edges. This is without loss of generality, for the result trivially extends to a general graph H by inserting two vertices in each edge of H .

We start with any initial perturbation Γ of C . We call **pebbles** the crossings of the closed walks in Γ with the arcs of Σ , and we see the closed walks in Γ as cycles of pebbles. Remember that C has no spur. Along any arc a of Σ , the corresponding pebbles are linearly ordered along a . The problem is to reorder the pebbles along a , and that for every arc a of Σ , so that in the end Γ has the minimum of self-crossings of its homotopy class. We slightly modify the problem as follows. We gradually partition every arc into a concatenation of sub-arcs. The partition of the pebbles into the sub-arcs and the linear orderings of the pebbles along the sub-arcs constitute an **arrangement**. When reordering the pebbles, we are only allowed to reorder within the sub-arcs (pebbles cannot be exchanged between distinct sub-arcs). If reordering the pebbles this way can still make Γ have the minimum of crossings of its homotopy class, then the arrangement is **valid**.

The **split** operation modifies an arrangement as follows. See Figure 5.3. It plays the role of the “cluster expansion” and “pipe expansion” operations of Fulek and Tóth. Let D be a disk of Σ . Let p_0, \dots, p_r for some $r \geq 1$ be the sub-arcs of the arrangement that bound D , in clockwise order, where p_0 is arbitrary. For every $1 \leq i \leq r$, let X_i contain the pebbles of p_0 that are linked to a pebble of p_i via a portion of Γ that runs through D . If only one of the sets X_1, \dots, X_r is not empty, then the split is not defined. Otherwise, the split cuts p_0 into sub-arcs q_1, \dots, q_r , in counter-clockwise order with respect to the orientation of D . Also, for every $1 \leq i \leq r$, the split places the pebbles in X_i along q_i , in any order. Any newly-created sub-arc that does not contain a pebble is discarded.

Lemma 5.12. *If an arrangement is valid before a split, then it is valid after the split.*

Proof. Consider the arrangement before the split. In this arrangement, using the assumption that the arrangement is valid, reorder the pebbles within their sub-arcs so that Γ has minimum self-crossing. Name p_0 the sub-arc to be split; p_0 is to be divided into sub-arcs q_1, \dots, q_r for some $r \geq 2$. Assign an orientation to p_0 , so that q_1, \dots, q_r are in this order along p_0 . For every $1 \leq i \leq r$, let X_i contain the pebbles of p_0 that are to be placed in q_i . In our arrangement, consider the pebbles along p_0 , and let $f : [k] \rightarrow [r]$ be the correspondence that sends every $\ell \in [k]$ to the unique $f(\ell) \in [r]$ such that the ℓ -th pebble along p_0 belongs to $X_{f(\ell)}$. If $f(\ell) > f(\ell + 1)$ for some $1 \leq \ell < k$, then the ℓ -th and the $\ell + 1$ -th pebbles can be swapped in our arrangement without increasing the number of self-crossings of Γ . Thus, without loss of generality, f can be assumed non-decreasing. Then, the sub-arcs q_1, \dots, q_r can be realized on p_0 (without affecting the order of the pebbles on p_0) so that, for every $i \in [r]$, the sub-arc q_i contains the pebbles in X_i . \square

The **sub-arcs graph** of an arrangement is the graph whose vertices are the sub-arcs of the arrangement, and where two sub-arcs p_0 and p_1 are linked by an edge when there is a pebble in p_0 and a pebble in p_1 that are consecutive in some closed walk of Γ .

Lemma 5.13. *In a valid arrangement, if no split applies, then the pebbles can be re-ordered in $O(m + n \log n)$ time within their respective sub-arcs to make Γ have the minimum of self-crossings of its homotopy class.*

Proof. If no split applies, then the sub-arcs graph of the arrangement is a collection of disjoint cycles. Deal with the cycles independently. The sub-arcs along a cycle O contain the pebbles of a subset Γ_0 of closed walks from Γ . The closed walks in Γ_0 are all powers of the single closed walk that one obtains by making one loop around O . Re-order the pebbles within the sub-arcs of O , so that each closed walk in Γ_0 is as in Figure 5.1, and so that any two closed walks do not intersect more than necessary. In the end, no re-ordering of the pebbles within their respective sub-arcs could induce less self-crossings of Γ by Lemma 5.9. Thus, and since the arrangement is valid, Γ has minimum self crossing. \square

Proof of Theorem 5.2. We assume, without loss of generality, that H has no loop edge nor any parallel edges (see above). The overall algorithm is the following. Initialize an arrangement from an arbitrary perturbation of Γ , whose sub-arcs are the entire arcs of Σ . At this point, the arrangement is valid. Perform splits on it as long as possible. In the end, the arrangement is still valid by Lemma 5.12. Conclude by Lemma 5.13. All there remains to do is to describe how to perform all the splits in $O(m + n \log n)$ total time.

We maintain the sub-arcs graph A . Also, for every edge of A between two sub-arcs p_0 and p_1 , we maintain a list of the edges of Γ between pebbles in p_0 and pebbles in p_1 , and an integer that records the size of the list. Finally, we maintain the list of the sub-arcs that can be split. This data structure is easily initialized in $O(m + n \log n)$ time.

Suppose we split a sub-arc p_0 incident to a disk D of Σ . The $N \geq 2$ pebbles on p_0 are linked to pebbles in sub-arcs p_1, \dots, p_r bounding D , for some $r \geq 2$. For each $i \in \{1, \dots, r\}$, let X_i contain the pebbles of p_0 linked to a pebble in p_i , and let N_i be the cardinality of X_i . (X_i and N_i are the list and the integer recorded by the corresponding edge of the sub-arc graph A .) Naively, we could range over $i \in \{1, \dots, r\}$, remove the pebbles in X_i from the sub-arc p_0 , place those pebbles on a new sub-arc, and update the sub-arc graph A , the lists and the integers, all in $O(N)$ time. Unfortunately, that would lead to a quadratic time algorithm. To overcome this issue, Fulek and Tóth crucially suggest to find some $j \in \{1, \dots, r\}$ maximizing

N_j , and to range over $i \in \{1, \dots, r\} \setminus \{j\}$. In the end, the pebbles still remaining on p_0 are precisely the pebbles in X_j , we do not touch them. And now the split takes $O(N - N_j)$ time. Summing this $N - N_j$ quantity over all the splits results in a total of $O(n \log n)$. Indeed, transfer a weight of $N - N_j$ to the pebbles in $X \setminus X_j$, by attributing a weight of 1 to each pebble. After the split, each of these pebbles ends up in a sub-arc that contains no more than $N/2$ pebbles. Thus, the sequence of splits attributes $O(\log n)$ weight to each pebble. There are $O(n)$ pebbles. \square

Chapter 6

Untangling Graphs on Reducing Triangulations

In this chapter we start, in Section 6.1, by introducing reducing triangulations. Then, in Section 6.2, we define reduced (closed) walks, exhibit their main properties, and provide linear time algorithms to reduce (closed) walks. In Section 6.3, we provide an algorithm to make a collection C of closed curves cross minimally, when C is given as a collection of closed walks in a reducing triangulation (actually, in a δ -reducing triangulation, which is the kind of reducing triangulation we will be mostly concerned about, but we will see that in due time):

Theorem 6.1. *Let S be a surface of genus $g \geq 2$ without boundary. Let T be an δ -reducing triangulation of S . Let C be a collection of closed walks of total length n in T . One can compute in $O(n)$ time a collection C' of closed walks in T , freely homotopic to C in S , in minimal position.*

In Theorem 6.1, the output collection C' is usually not in general position. We say that such a collection C' is in *minimal position* if there exists an approximation of C' with $i_S(C')$ self-crossings. One could then apply the result of Fulek and Tóth, Theorem 5.2 to actually compute a minimum perturbation of C' .

To obtain Theorem 6.1, basically, we just reduce the closed walks in C , and we prove that the resulting collection C' has an approximation with a minimum number of crossings.

The last three sections of the chapter, Sections 6.4, 6.5, 6.6, are devoted to an algorithm that untangles drawings of graphs on (δ -)reducing triangulations:

Theorem 6.2. *Let S be a surface of genus $g \geq 2$ without boundary. Let T be an δ -reducing triangulation of S . Let G be a graph, and let $f : G \rightarrow T$ be a drawing of size n . One can determine in $O(gn \log(gn))$ time whether f can be untangled in S . If so, one can construct in additional $O(n^2)$ time a weak embedding $f' : G \rightarrow H$, homotopic to f in S , of depth $O(n)$.*

(Recall from Chapter 3 that the *depth* of a drawing f of a graph G is the maximum length of the image walks $f(e)$ over the edges e of G . The *size* of f is the number of edges and vertices of G plus the sum of the lengths of the walks $f(e)$ over the edges e of G .)

To obtain Theorem 6.2, roughly, we start in Section 6.4 by focusing on a particular class of graphs that have only one vertex per connected component, we call them *loop graphs* (as all their edges are loops). We provide an algorithm that untangles loop graphs, again, just a simple “straightening” procedure, but whose proof of correctness is more delicate, and relies

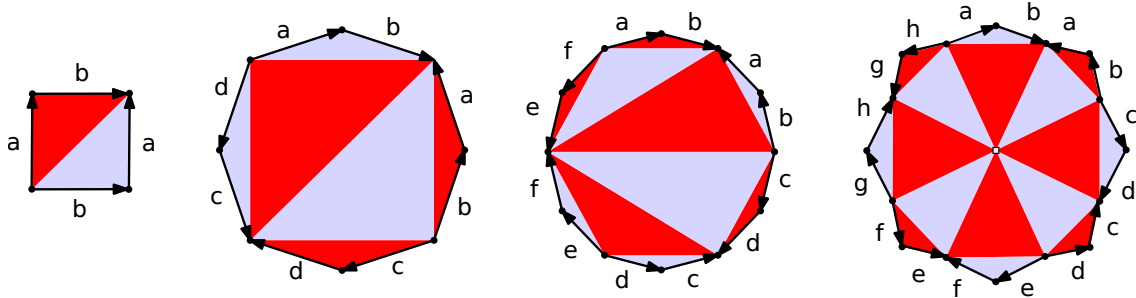


Figure 6.1: Building a reducing triangulation from a canonical polygonal schema of the surface of genus $g \geq 1$. The cases $g = 1, 2, 3$ use special constructions; the case $g = 4$ (right) trivially generalizes to higher genus. These reducing triangulations are 8-reducing except the one for the case $g = 1$ whose unique vertex has degree six.

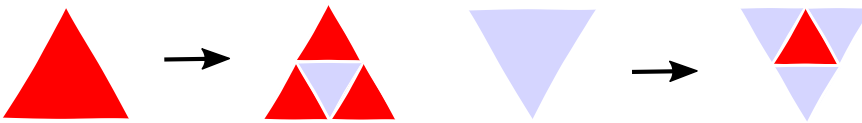


Figure 6.2: Subdividing the faces of a reducing triangulation.

on constructions from 2-dimensional hyperbolic geometry. In Section 6.5 we finally provide the general untangling algorithm. Crucially, the first phase of the algorithm transforms the initial drawing into the drawing of a loop graph, to be untangled by the algorithm of Section 6.4. The details of this phase are omitted when presenting the algorithm, and deferred to Section 6.6, the last section of the chapter.

6.1 Reducing triangulations

Consider a surface S *without boundary*. A triangulation T of S is **reducing** if its dual graph is bipartite, and if all its vertices have degree at least six. It is **8-reducing** if, in addition, all its vertices have degree at least eight. We color the faces of T red and blue so that adjacent faces have different colors.

A straightforward application of Euler's formula shows that the sphere does not admit any reducing triangulation, and that the torus does not admit any 8-reducing triangulation. Yet the torus admits a reducing triangulation with a single vertex of degree six, and every surface of higher genus admits an 8-reducing triangulation with at most two vertices, see Figure 6.1. Moreover, every reducing triangulation can be subdivided to obtain a reducing triangulation with more vertices, as in Figure 6.2, although this introduces degree six vertices. Note also that every reducing triangulation of a surface S lifts to a reducing triangulation of any covering space of S . Finally observe that while reducing triangulations may in general have loops, or several edges between two vertices, the reducing triangulations of the plane cannot; this is a straightforward consequence of the Euler's formula, and also an immediate corollary of Proposition 6.1 below.

Most of this chapter will be concerned with 8-reducing triangulations only, thus excluding the torus, but the first part of Section 6.2 handles general reducing triangulations, for later use in Chapter 8. Note that at the very end of Chapter 8 we will present an extension of the

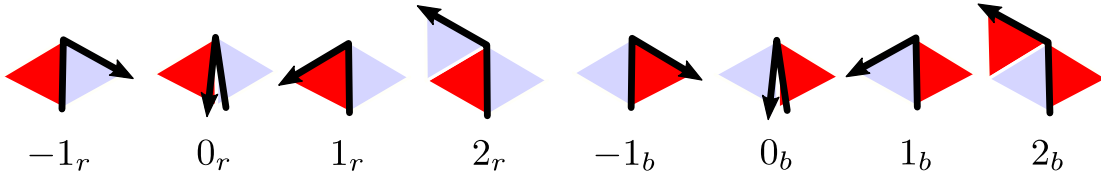


Figure 6.3: Some of the turns that a walk can make in a reducing triangulation.

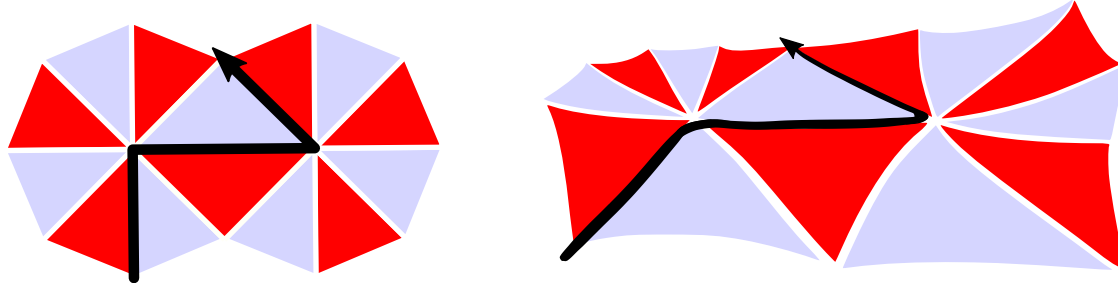


Figure 6.4: In a reducing triangulation, a portion of a walk that makes a -2_r -turn followed by a 1_b -turn (both are bad turns).

notion of reducing triangulations to surfaces with boundary, but this is only incidental to us, so for now we focus on surfaces without boundary.

6.2 Reduced walks

In a reducing triangulation T , let W be a walk (closed or not). Assume that a subwalk of W traverses a directed edge e , arrives at a vertex v , and from there traverses a directed edge e' . When traversing v , we say that W makes a k -**turn**, $k \geq 0$, if the walk of length two composed of edges e and e' , in this order, leaves exactly k triangles of T to its left in the cyclic ordering around v between e and e' . Similarly (and not exclusively), it makes a $-k$ -**turn**, $k \geq 1$, if that walk leaves exactly k triangles of T to its right. When a turn is not a 0-turn, the notation is ambiguous because it can be represented either by a positive integer or by a negative integer (whose absolute values sum up to the degree of the vertex in T). We always use an integer between -3 and 3 if possible. For a degree-six vertex, we prefer 3 over -3 . For turns that cannot be represented by any integer between -3 and 3 , we choose the positive integer.

We sometimes need to be more precise and refine the notation: For $k \in \mathbb{Z}$, a k_b -**turn**, respectively a k_r -**turn**, is a k -turn such that e (with the previous notation) has a blue, respectively red, triangle to its left. See Figures 6.3 and 6.4.

We call **bad turn** any 0-turn, 1-turn, -1 -turn, 2_r -turn or -2_r -turn. In T , a walk is **reduced** if it does not make any bad turn. Intuitively, reduced walks are discrete geodesics in the triangulation T where all triangles are equilateral: A reduced walk leaves an angle at least π on both sides at each interior vertex, except when the vertex makes a 2_b -turn or a -2_b -turn, which corresponds to an angle of $2\pi/3$ on one side. The bipartiteness of the triangulation then ‘breaks ties’ for determining the geodesic. We emphasize that the notion of reduced walks requires an orientation of the surface. A closed walk C is **reduced** if it

does not make any bad turn. It is **strongly reduced** if moreover not all vertices of C make a 3_r -turn, and not all of them make a -3_b -turn.

Here are a few immediate but crucial properties that we will use repeatedly. Any subwalk of a reduced walk (closed or not) is also reduced. The reversal of any reduced walk (closed or not) is also reduced, because reversing a walk exchanges 2_r -turns with -2_r -turns, and 3_r -turns with -3_b -turns.

The **turn sequence** of a (closed) walk is the list of turns made by the walk at its interior vertices; this is a cyclic sequence if the walk is closed. We use some straightforward notations for turn sequences: Exponents denote iterations, stars denote arbitrary nonnegative integers, and vertical bars denote “or”. For example, 23^*4 denotes a 2 followed by a nonnegative number of 3s, followed by a 4. $(23^*4)^*$ denotes a nonnegative number of concatenations of patterns of that form. $(2|4)$ denotes either a 2 or a 4.

6.2.1 Uniqueness of reduced walks

In this section we prove the key property of reduced walks, grounding the analogy between reduced walks in reducing triangulations and geodesic paths in non-positively curved surfaces. More precisely, we prove the following:

Proposition 6.1. *In a reducing triangulation T , any two homotopic reduced walks are equal.*

The proof of Proposition 6.1 goes by showing that any two distinct homotopic reduced walks would form a monogon or a bigon (a disk bounded by one or two subwalks, in the universal cover), and that this is impossible. It relies on the following two lemmas.

Lemma 6.1. *In a reducing triangulation T , any walk whose turn sequence is of the form 23^*2 contains a 2_r -turn. Any walk in T whose turn sequence is of the form 23^*4 or 43^*2 contains a 2_r -turn or a 4_r -turn.*

Proof. By bipartiteness of the reducing triangulation T , the color of the triangle of T located to the left of the walk changes when passing over an interior vertex that makes a 2-turn or 4-turn, and not when the interior vertex makes a 3-turn. \square

Lemma 6.2. *In a reducing triangulation T , let C be a simple closed walk that bounds a (non-empty) disk to its left. For every $k \geq 1$, let m_k be the number of vertices of C at which C has exactly k triangles to its left. Then $2m_1 + m_2 \geq 6 + \sum_{k \geq 4} m_k$.*

The proof can be viewed as a consequence of the Gauss–Bonnet theorem [88, Section 2.3]:

Proof. Let D be the restriction of the reducing triangulation to the closed disk bounded by C . Consider the following discharging argument. Give initial weight 6 to each vertex and each triangle of D , and weight -6 to each edge of D . By Euler’s formula, the weights initially attributed sum up to 6. Discharge as follows. For each incidence between a vertex v and an edge e , transfer 3 from v to e . For each incidence between a vertex v and a triangle t , transfer 2 from t to v . Now, edges and triangles all have weight 0, while every vertex v has weight $\kappa(v) := 6 - 3\deg(v) + 2\deg'(v)$ where $\deg(v)$ and $\deg'(v)$ denote respectively the number of edge incidences and triangle incidences of v in D . We proved $6 = \sum_v \kappa(v)$.

Every vertex v that lies in the interior of D (not on C itself) satisfies $\deg(v) = \deg'(v)$ and thus $\kappa(v) = 6 - \deg(v) \leq 0$, since each vertex of T has degree at least six. Every vertex v

that lies on C satisfies $\deg(v) = \deg'(v) + 1$ and thus $\kappa(v) = 3 - \deg'(v)$. Thus, we have $6 = \sum_v \kappa(v) \leq \sum_{k \geq 1} (3 - k)m_k$, implying the result. \square

Lemma 6.3. *In a reducing triangulation T , let C be a simple closed walk that bounds a (non-empty) disk to its left. There are at least three vertices at which C makes a 1-turn or a 2_r -turn.*

Proof. Let S be the set of vertices of C that make a 1-turn or a 2_r -turn. By contradiction, assume $|S| \leq 2$. Using the notations of Lemma 6.2, we have $m_1 \leq |S| \leq 2$; indeed, any vertex that makes a 1-turn belongs to S . We consider the subwalks with turn sequence of the form $2(1|3)^*2$. These subwalks may only share their first and last edges and are otherwise disjoint. Lemma 6.2 implies that $m_2 \geq (6 - 2m_1) + \sum_{k \geq 4} m_k$; thus, there are at least $6 - 2m_1$ such sequences. At most $|S| - m_1$ vertices in S make a 2-turn, and thus at most $2(|S| - m_1)$ such sequences start or end in S , because the sequences all start and end with a vertex that makes a 2-turn. There remains at least $(6 - 2m_1) - 2(|S| - m_1) = 6 - 2|S| \geq 1$ such sequences whose first and last elements are not in S . In such a sequence, exactly one of the two vertices that make a 2-turn actually makes a 2_r -turn by Lemma 6.1, which is impossible because the vertices of C that make a 2_r -turn are all in S . \square

Proof of Proposition 6.1. The reducing triangulation T lifts to an infinite reducing triangulation \tilde{T} in its universal cover. Assume that there exist two distinct homotopic reduced walks in T (possibly one of them being a single vertex). Let W_1 and W_2 be lifts of these walks in \tilde{T} , with the same endpoints; they are also reduced. We show below that this implies that there exists, in \tilde{T} , a simple closed walk C with at most two vertices that make a bad turn. This contradicts Lemma 6.3.

Indeed, if one of W_1 and W_2 is not simple, it contains a non-empty subwalk with the same starting and ending vertex v , and otherwise not repeating any vertices; since subwalks of reduced walks are also reduced, the claim holds (only at v the walk can make a bad turn). Otherwise, W_1 and W_2 are simple, distinct, and have the same first and last vertices, which implies that they admit non-empty subwalks that have the same endpoints and are otherwise disjoint. (Indeed: up to exchanging W_1 and W_2 , some edge in W_1 does not belong to W_2 . Consider the subwalk of W_1 of minimum length containing that edge and intersecting W_2 at its endpoints. The subwalks of W_1 and W_2 with these endpoints have the desired property.) Let C be the simple closed walk that is the concatenation of these subwalks (or their reversals) W'_1 and W'_2 . The subwalks W'_1 and W'_2 are also reduced, since subwalks and reversals of reduced walks are reduced. Hence, C has at most two vertices that make a bad turn, which concludes as desired. \square

6.2.2 Uniqueness of strongly reduced closed walks

From now on in this chapter, we focus on 8-reducing triangulations (except for Lemma 6.6 in the next section, for use in Chapter 8, but this will be precised in due course). In this section we prove a result similar to Proposition 6.1, but for *closed* walks. More precisely, we prove:

Proposition 6.2. *In a 8-reducing triangulation T , any two freely homotopic, non-contractible, strongly reduced closed walks are equal.*

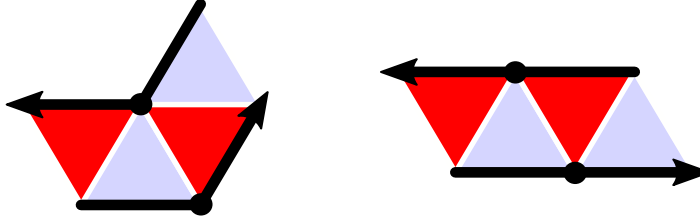


Figure 6.5: The cases leading to a contradiction at the end of the proof of Lemma 6.4.

(It is possible that Proposition 6.2 holds on all reducing triangulations, not just the 8-reducing ones, but again, we do need any of that, so we stick to 8-reducing triangulations.) The assumption of Proposition 6.2 that the closed walks are *strongly* reduced, and not just reduced, is necessary. Indeed, there exist freely homotopic non-contractible closed walks that are reduced and yet distinct, such as the ones depicted in Figure 6.10. This is analogous to the metric setting where it can happen that a flat portion of a non-positively curved surface contains two non-contractible geodesics that are freely homotopic and yet distinct: consider for example the two boundary curves of any flat annulus with geodesic boundary.

The proof of Proposition 6.2 relies on the following lemma:

Lemma 6.4. *Consider two disjoint simple closed walks C and C' that bound an annulus in T . Then C and C' are not both strongly reduced.*

Proof. We prove the claim by contradiction so assume that C and C' are both strongly reduced. Let A be the restriction of the 8-reducing triangulation to the closed annulus bounded by C and C' . Let i be the number of vertices in the interior of A , and let B be the vertex set of the boundary of A . For every vertex v of A let $\deg(v)$ and $\deg'(v)$ be the number of incidences of v with respectively the edges and the triangles of A .

We first claim that $2i \leq \sum_{v \in B} (3 - \deg'(v))$. We prove this claim with the same discharging rules as in the proof of Lemma 6.2. Give initial weight 6 to each vertex and each triangle of A , and weight -6 to each edge of A . By Euler's formula, the weights initially attributed sum up to 0. Discharge as follows. For each incidence between a vertex v and an edge e , transfer 3 from v to e . For each incidence between a vertex v and a triangle t , transfer 2 from t to v . Now, edges and triangles all have weight 0, while each vertex v has weight $\kappa(v) := 6 - 3\deg(v) + 2\deg'(v)$. We proved $0 = \sum_v \kappa(v)$. Every vertex v of A satisfies $\kappa(v) = 3 - \deg'(v)$ if $v \in B$ and $\kappa(v) = 6 - \deg(v) \leq -2$ otherwise. Therefore, $0 \leq \sum_{v \in B} (3 - \deg'(v)) - 2i$, proving the claim.

We orient C and C' so that A lies to their left. Let $C_1 \in \{C, C'\}$, and let $B_1 \subset B$ be the set of vertices of C_1 . We remark that, because C_1 has no bad turn, every $v \in B_1$ satisfies $\deg'(v) \geq 2$. Moreover, because C_1 is strongly reduced, by Lemma 6.1, its turn sequence does not contain 23^*2 as a subword, and it is not of the form 23^* . Thus, $\sum_{v \in B_1} (3 - \deg'(v)) \leq 0$, with equality if and only if the turn sequence of C_1 has the form $(23^*43^*)^*$ or 3^* .

From the above claim and the conclusion of the previous paragraph, we deduce that A has no interior vertices and that each of the turn sequences of C and C' is of the form $(23^*43^*)^*$ or 3^* , which must actually be $(2_b 3^* 4_r 3^*)^*$ (by Lemma 6.1 and because there is no 2_r) or 3_b^* (by definition of a strongly reduced closed walk).

Assume that the turn sequence of one boundary component of A has the form $(2_b 3^* 4_r 3^*)^*$. Let v be a vertex of B that makes a 2_b -turn. Then, the vertex across v in the other boundary

component of A makes a 4_b -turn (Figure 6.5, left), which is a contradiction since no 4_b appears in the allowed forms above. So the turn sequences of C and C' are both of the form 3_b^* ; however, for a similar reason as above, if v is a vertex of B that makes a 3_b -turn, the vertices across v make a 3_r -turn (Figure 6.5, right), a contradiction. \square

Proof of Proposition 6.2. Consider a 8-reducing triangulation T of a surface \mathcal{S} and two freely homotopic strongly reduced closed walks C and C' in T .

We consider the *annular cover* $\hat{\mathcal{S}}$ of \mathcal{S} defined by C [48, Section 1.1]. This is a covering space homeomorphic to an open annulus, in which C lifts to a closed curve \hat{C} , and every simple closed curve is either contractible or homotopic to \hat{C} or its reverse. Lifting the homotopy from C to C' yields a lift \hat{C}' that is homotopic to \hat{C} . Both \hat{C} and \hat{C}' are strongly reduced closed walks in \hat{T} , the lift of the 8-reducing triangulation T .

We claim that \hat{C} (and, for the same reasons, also \hat{C}') is simple. Indeed, lifting \hat{C} to the universal cover $\tilde{\mathcal{S}}$ of \mathcal{S} yields a lift, which is a bi-infinite path \tilde{P} , and is actually strongly reduced in the 8-reducing triangulation \tilde{T} obtained from lifting T . By Proposition 6.1, \tilde{P} is simple. Since it is the *only* lift of \hat{C} , this implies that \hat{C} is simple.

Now there are two cases. If \hat{C} and \hat{C}' are disjoint, Lemma 6.4 implies a contradiction. If they intersect, at vertex v say, then we transform \hat{C} and \hat{C}' into loops with starting and ending vertex v ; these two loops have the same turning number, and are thus homotopic strongly reduced walks, and equal by Proposition 6.1. Thus \hat{C} and \hat{C}' are equal, and so are C and C' by projection. \square

6.2.3 Reducing a walk

In this section we back Proposition 6.1 with an algorithm. More precisely, we prove the following:

Proposition 6.3. *Given a walk W of length n in a 8-reducing triangulation T , one can compute a reduced walk homotopic to W in $O(n)$ time.*

The techniques of the proof of Proposition 6.3 will be reused in Section 6.6. In particular, we need a few data structures here, which will be extended later.

Our 8-reducing triangulation T is stored as an embedded graph, but we need additional information. Specifically, for each vertex v of T , we number the directed edges with source v in clockwise order (starting at an arbitrary directed edge). This number is stored on each directed edge. Moreover, vertex v contains an array A_v of pointers such that $A_v[i]$ is the directed edge number i with source v . This array has size the degree of v , which is also stored in v . We note that this additional data can be computed in time linear in the size of the 8-reducing triangulation, so we assume that the 8-reducing triangulation incorporates this information. With this data structure, we can perform the following operations in constant time: (1) given two directed edges uv and vw , compute the integer i such that uvw forms an i -turn; (2) given a directed edge uv and an integer i , compute the directed edge vw such that the walk uvw forms an i -turn. Again, this can be done as a preprocessing step in time linear in the size of the 8-reducing triangulation.

We also need a data structure, called **compressed homotopy sequence**, that represents walks in a compact form, in the same spirit as Erickson and Whittlesey [88, Section 4.1] use run-length encoding to encode turn sequences. An **elementary subwalk** of W is an inclusionwise maximal subwalk of W whose turn sequence has the form 3^k or $(-3)^k$ for some

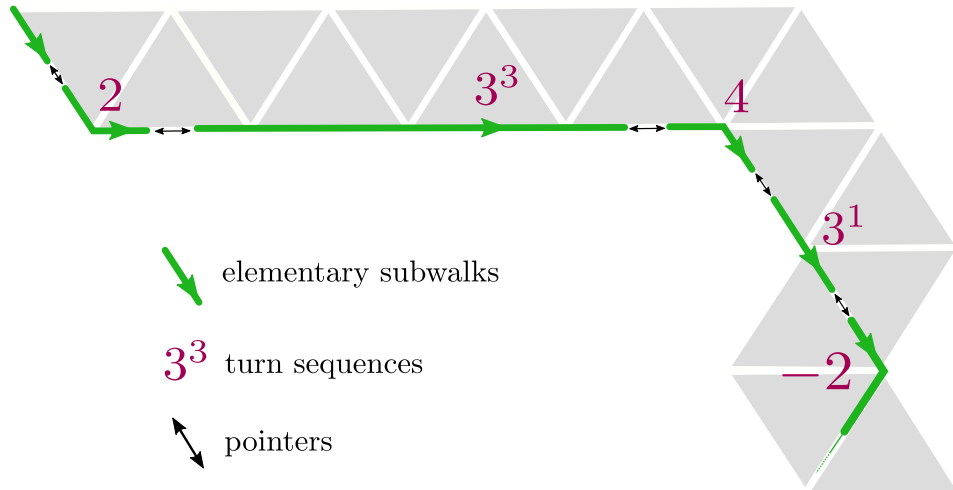


Figure 6.6: The compressed homotopy sequence data structure.

$k \geq 1$, or is a single symbol $a \notin \{-3, 3\}$. The elementary subwalks of W are naturally ordered along W and cover W , with overlaps because the last edge of an elementary subwalk appears as the first edge of the following one. We represent W by storing the elementary subwalks of W in a doubly linked list in order along W ; each elementary subwalk is described by the images in T of its first and last directed edges, as well as its turn sequence in compressed form, namely, whether it is of the form 3^k , $(-3)^k$, or a , and the integer k or the symbol a . (Walks W of length zero or one cannot be encoded in this data structure, but can be handled separately in a trivial manner.)

Proof of Proposition 6.3. The *extended turn sequence* of a walk W is its usual turn sequence, with a new symbol E appended before its first symbol and after its last letter. We consider the *reduction moves* depicted in Figure 6.7 that modify a walk W by homotopy. Each of them can be applied when a specific subsequence appears in the extended turn sequence of W or of its reversal:

- *spur move*: 0 ,
- *spike move*: 1 ,
- *bracket move*: 23^k2 for some $k \geq 0$,
- *flip move*: $a3^k2_r3^\ell b$ for some $k, \ell \geq 0$ and some symbols $a, b \notin \{-1, 0, 1, 2, 3\}$. (In particular, a and/or b can be equal to E .)

We observe that if no reduction move can be applied to W , then W is reduced. Moreover, for each walk W , let $\varphi(W)$ be equal to three times the length of W , plus the number of bad turns of W . We observe that $\varphi(W)$ strictly decreases at each move; indeed, a spur, spike, or bracket move decreases the length of W (by at least one) and creates at most two bad turns, while a flip move does not affect the length and removes at least one bad turn (no bad turn is created because the degree of each vertex is at least eight, and by the conditions on a and b). Thus, any sequence of moves has length $O(n)$.

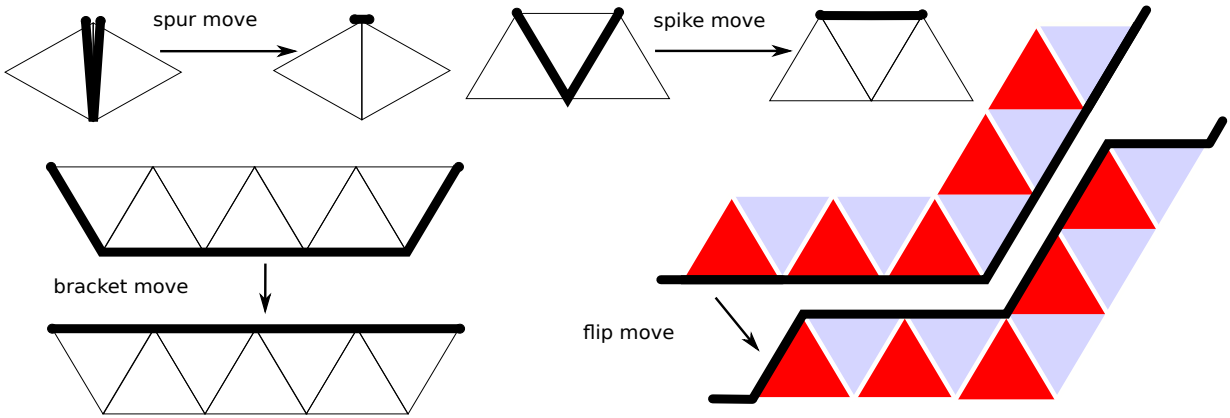


Figure 6.7: The reduction moves for the reduction of walks.

The algorithm is as follows. In a first step, we walk along W to initialize its compressed homotopy sequence in $O(n)$ time (using Operation (1) above). Then, in a second step, we traverse this sequence in order, and reduce W as soon as a possible move is encountered, maintaining the compressed homotopy sequence as it evolves. Each possible move involves at most six consecutive elementary subwalks, which are replaced by at most seven elementary subwalks. Then, before resuming the algorithm and looking for a possible move, we need to backtrack by at most five elementary subwalks in the compressed homotopy sequence, in order not to skip any possible move created by performing the previous one. Finally, in a third step, when we reach the end of the list, no move is possible any more; we convert our compressed homotopy sequence back to a walk on T (using Operation (2) above). All of this takes $O(n)$ time because the sequence of moves has length $O(n)$, and because the length of a walk does not increase when reducing it, so that the compressed homotopy sequence always has length $O(n)$. \square

6.2.4 Strongly reducing a closed walk

In this section we back Proposition 6.2 with an algorithm, similar to Proposition 6.3, but for *closed* walks. More precisely, we prove the following:

Proposition 6.4. *Given a closed walk C of length n in a 8-reducing triangulation T , one can compute a strongly reduced closed walk freely homotopic to C in $O(n)$ time.*

Before proving Proposition 6.4, we observe that the proposition does not hold on 6-reducing triangulations:

Lemma 6.5. *There are a reducing triangulation T of the torus, and a closed walk C in T , such that no closed walk freely homotopic to C is reduced.*

Proof. Consider the reducing triangulation T , and the closed walk C of Figure 6.8. Assume the existence of a reduced closed walk C' in T^1 . If at some point C' takes a directed edge of T that sees red on its left, then C' makes only 3_r -turns. Otherwise C' makes only 3_b -turns. In both cases C' is not freely homotopic to C . \square

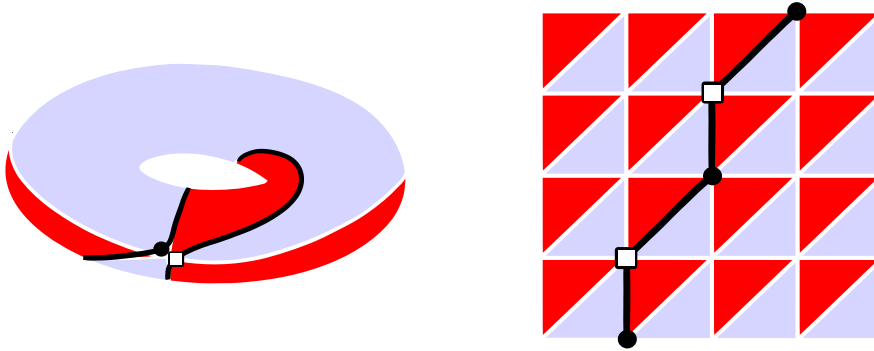


Figure 6.8: (Left) A reducing triangulation T of the torus, and a closed walk C of length two in T . (Right) A portion of the universal covering triangulation of T , and a portion of a lift of C . In T there is no reduced closed walk freely homotopic to C .

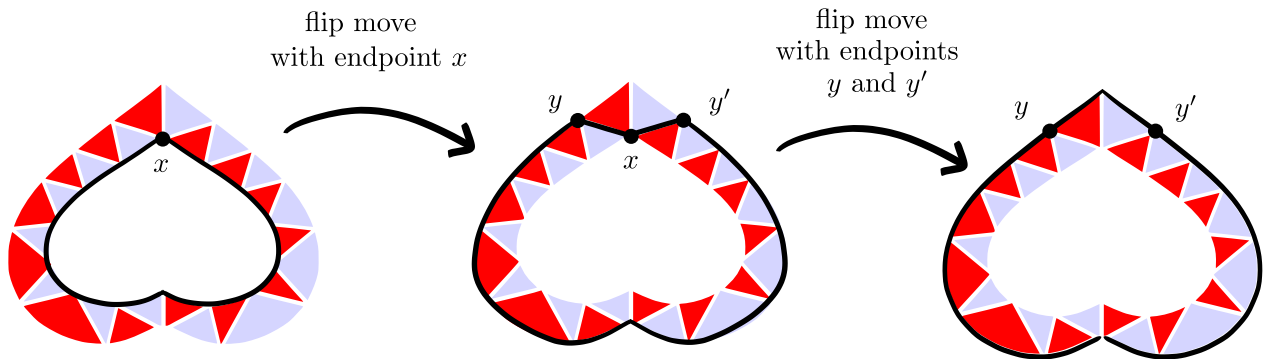


Figure 6.9: The situation in the proof of Proposition 6.4.

Proof of Proposition 6.4. We first remove the bad turns from C . For this purpose, we use the same reduction moves as in the proof of Proposition 6.3, but the turn sequence is now cyclic. We observe that, in each move, the part of C that is removed corresponds to an actual subwalk of C (and does not “wrap around” it). In particular, in a bracket move, the entire cyclic turn sequence of C cannot be 23^k , because the color of the triangle to the left of the walk changes after passing a 2. As a limit case, in a flip move, the symbols a and b in the sequence $a3^k2_r3^\ell b$ may correspond to the same vertex of the cyclic walk; see Figure 6.9, left for an illustration in the case where the turn at $a = b$ is a 4-turn.

As in the proof of Proposition 6.3, if no move is possible, then C has no bad turn. If $\varphi(C)$ is equal to three times the length of C , plus the number of bad turns of C , then $\varphi(C)$ decreases at each move, except in the very special “heart-like” case of Figure 6.9, corresponding to the case where the cyclic turn sequence of C (or its reversal) is $43^k2_r3^\ell$ for some $k, \ell \geq 0$. The flip move does not affect the length and removes the bad 2-turn, but both edges of C incident to the 4-turn are rotated by one triangle, which creates another bad 2-turn, see Figure 6.9. However, after this move, the only possible move flips the new bad 2-turn into a good one, at which point the closed walk is reduced. Thus, as in the proof of Proposition 6.3, any sequence of moves has length $O(n)$.

Finally, if the turn sequence of C is of the form $(3_r)^*$ or $(-3_b)^*$, then C can be turned into a *strongly* reduced closed walk in $O(1)$ time using the new move depicted in Figure 6.10. \square

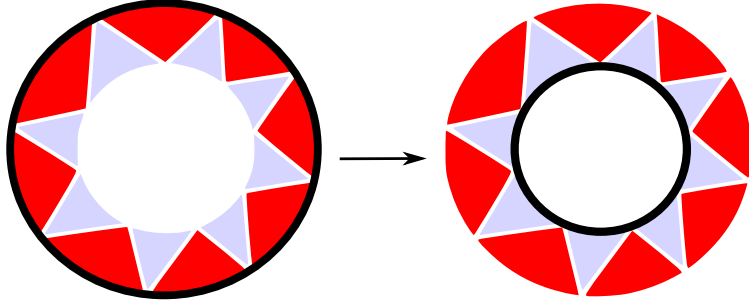


Figure 6.10: The last reduction move in the proof of Proposition 6.4.

6.3 Making closed curves cross minimally

We now begin to use reducing triangulations to attack our initial problems of making closed curves cross minimally, and of untangling graphs. We start with closed curves, by proving Theorem 6.1, which we now restate for convenience:

Theorem 6.1. *Let S be a surface of genus $g \geq 2$ without boundary. Let T be an 8-reducing triangulation of S . Let C be a collection of closed walks of total length n in T . One can compute in $O(n)$ time a collection C' of closed walks in T , freely homotopic to C in S , in minimal position.*

The rest of this section is dedicated to the proof of Theorem 6.1. We state our first lemma on reducing triangulations, not just the 8-reducing ones, for later use in Chapter 8:

Lemma 6.6. *Let S be a surface of genus $g \geq 2$ without boundary. Let T be a reducing triangulation of S . Let C be a collection of closed walks in T . Remove an open disk from each face of T , and consider the resulting surface $\Sigma \subset S$. If the closed walks in C are all reduced and primitive in S , then $i_S(C) = i_\Sigma(C)$.*

Proof. We have $i_S(C) \leq i_\Sigma(C)$ by the inclusion $\Sigma \subset S$. We will now prove the converse by exhibiting a collection of closed curves homotopic to C in Σ whose number of crossings is the minimum of its homotopy class in S . To do so we see Σ as the patch system of T (Section 5.3). Recall that each edge of T is dual to an arc in Σ . We endow the interior of Σ with a complete hyperbolic metric for which the arcs of Σ are complete geodesics. More precisely, we replace every face of the interior of Σ by an ideal hyperbolic polygon, and we identify the (infinitely long) sides of the polygons along the arcs of Σ . See Figure 3.13. For every $c \in C$, we let γ_c be the geodesic closed curve homotopic to c in Σ . We now see γ_c as a closed curve on S , by the inclusion $\Sigma \subset S$.

If a curve γ_c homotopic to a curve γ_d or to the reversal of γ_d then γ_c is actually equal to γ_d up to parameterization, since the two curves are geodesic. We consider each such set of overlapping curves, and we slightly perturb the curves into “parallel” curves. Afterward, the collection $\{\gamma_c \mid c \in C\}$ is in general position.

We claim that in the universal cover of S , the lifts of the closed curves in $\{\gamma_c \mid c \in C\}$ are injective, and no two of them cross more than once. Let us prove that the claim implies the lemma. The collection $\{\gamma_c\}_{c \in C}$ then has the minimum number of crossings of its homotopy class in S by Lemma 5.10, which is $i_S(C)$. So $i_\Sigma(C) \leq i_S(C)$, which proves the lemma.

Now let us prove the claim. We may assume that no curve γ_c is homotopic to γ_d or to the reversal of γ_d for some $c \neq d \in C$, for the claim trivially extends to the general case where some overlapping curves have been perturbed. We prove the claim by contradiction, so assume that one of those lifts is not injective. It contains a loop, which projects to a geodesic loop γ on Σ that is contractible on S . The sequence of crossings of γ with the arcs of Σ is that of a reduced walk. Thus, by Proposition 6.1, the loop γ does not cross any arc of Σ , which is impossible since γ is geodesic. Similarly, if two distinct lifts intersect twice without overlapping, then they form two paths with the same endpoints and otherwise disjoint, which project to geodesic paths p and q in Σ that are homotopic in S . The sequence of crossings of p and q with the arcs of Σ must be the same by Proposition 6.1, so p and q are homotopic in Σ , which is impossible since p and q are geodesics. The claim is proved. \square

Now, we focus again on 8-reducing triangulations, and we show that we can remove the assumption that the closed walks in C are primitive, if we assume that they are *strongly* reduced, not just reduced. In detail, we deduce the following from Lemma 6.6:

Proposition 6.5. *Let S be a surface of genus $g \geq 2$ without boundary. Let T be an 8-reducing triangulation of S . Let C be a collection of closed walks in T . Remove an open disk from each face of T , and consider the resulting surface $\Sigma \subset S$. If the closed walks in C are all strongly reduced, then $i_S(C) = i_\Sigma(C)$.*

Assuming that the closed walks are strongly reduced allows us to use Proposition 6.2 that, on 8-reducing triangulations, any two freely homotopic strongly reduced closed walk are equal (up to cyclic permutation). Note that, as for Proposition 6.2, it is entirely possible that Proposition 6.5 holds on all reducing triangulations, not just on the 8-reducing ones. It may even be possible that Proposition 6.2 holds on all reduced closed walks, not just on the strongly reduced ones, contrarily to Proposition 6.5. But we do not need any of that.

Proof of Proposition 6.5. We have $i_S(C) \leq i_\Sigma(C)$ by the inclusion $\Sigma \subset S$. Let us prove the converse. Assume without loss of generality that no closed walk in C is trivial, it does not consist in a single vertex. Then every $c \in C$ is non-contractible on S by Proposition 6.1, and is thus homotopic in S to the k^{th} power of a primitive closed curve d , for some $k \geq 1$. Let \hat{c} be the strongly reduced closed walk freely homotopic to d in S , which exists by Proposition 6.4. Proposition 6.2 implies that c is actually equal to the k^{th} power of \hat{c} , since the two are freely homotopic, non-contractible, and strongly reduced. Let \hat{C} contain the primitive strongly reduced closed walks issued this way of the collection C .

We consider, for every $\hat{c} \in \hat{C}$, a closed curve $\hat{\gamma}_{\hat{c}}$ homotopic to \hat{c} in Σ , such that the collection $\{\hat{\gamma}_{\hat{c}} \mid \hat{c} \in \hat{C}\}$ is in general position. By Lemma 6.6 there is such a collection whose number of crossings is the minimum of its homotopy class in S .

Now realize every $c \in C$ by a closed curve γ_c in the neighborhood of $\hat{\gamma}_{\hat{c}}$ like in Figure 5.1. By Lemma 5.9, the collection $\{\gamma_c\}_{c \in C}$ has the minimum number of crossings of its homotopy class in S , which is $i_S(C)$. \square

Proposition 6.6. *Let H be a graph embedded in its patch system Σ . Let C be a collection of closed walks in H . If the closed walks in C have no spur, then there is an approximation of C with $i_\Sigma(C)$ self-crossings.*

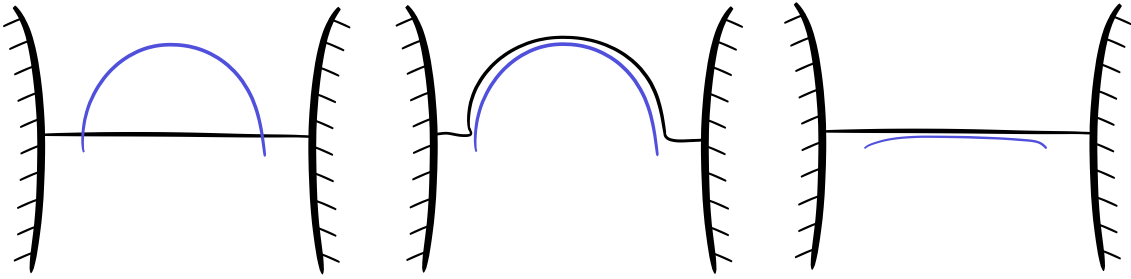


Figure 6.11: Removing a bigon in the proof of Proposition 6.6.

Proof of Proposition 6.6. We assume for clarity that C is a single closed walk, but the proof trivially extends to any collection of closed walks. There is a closed curve γ in general position in Σ , homotopic to C , with $i_\Sigma(C)$ self-crossings. Without loss of generality, assume that γ intersects the arcs of Σ a minimum number of times (among the closed curves that match its definition). Record the arcs crossed by γ by the corresponding closed walk C' in H , so that γ is an approximation of C' . We shall prove $C = C'$ (up to cyclic permutation). To do so, it is enough to prove that C' has no spur. Indeed, C and C' are homotopic in Σ , and Σ is homotopy equivalent to H , so C and C' are homotopic in H . Moreover, in a graph, every two homotopic closed walks without spur are equal.

We prove that C' has no spur by contradiction, so assume that C' has a spur. There is a portion of γ that crosses an arc a of Σ and then crosses a again consecutively, in the opposite direction. See Figure 6.11. Let γ_0 and a_0 be the respective portions of γ and a between the two crossing points. Let n and m be the number of crossings of γ with the interiors of γ_0 and a_0 , respectively. Redrawing γ_0 in a neighborhood of a_0 would not decrease the number of self-crossings of γ , so $n \leq m$. Redrawing a_0 in a neighborhood of γ_0 would not decrease the number of crossings between a_0 and γ , so $m + 2 \leq n$. This is a contradiction. \square

Proof of Theorem 6.1. Apply Proposition 6.4 to compute in $O(n)$ time a collection C' of strongly reduced closed walks in T , freely homotopic to C in S . Then $i_S(C) = i_\Sigma(C)$ by Proposition 6.5, where Σ is the surface obtained from S by removing an open disk from each face of T . And there is an approximation of C with $i_\Sigma(C)$ crossings by Proposition 6.6. \square

6.4 Untangling loop graphs

Now, for untangling graphs, one could mimick the strategy of the previous section (Section 6.3) for making closed curves cross minimally, i.e. one could generalize the notion of bad turns from closed walks to general graph drawings, then remove all bad turns from the initial drawing $f : G \rightarrow T$ by homotopy in S , and finally prove that the resulting drawing $f' : G \rightarrow T$ is a weak embedding whenever f can be untangled in S . This strategy is viable and will be detailed in Chapter 8. However we shall now present a different strategy, simpler, and more efficient.

In this other strategy, we first focus on a specific class of drawings. A **loop graph** is a graph L whose connected components have a single vertex. (Then every edge of L is a loop, hence the name.) Given a surface S , a map $\lambda : L \rightarrow S$ is **sparse** if, under λ , the edges of each connected component of L correspond to pairwise non-homotopic non-contractible loops in S . In this section we prove the following:

Proposition 6.7. *Let S be a surface of genus $g \geq 2$ without boundary. Let T be an 8-reducing triangulation of S . Let L be a loop graph. Let $\lambda : L \rightarrow T$ be a drawing of size n and depth N . Assume that λ is sparse in S . One can compute in $O(n)$ time a drawing $\lambda' : L \rightarrow T$, homotopic to λ in S , of depth $O(N)$, such that if λ can be untangled in S then λ' is a weak embedding.*

We emphasize that, in Proposition 6.7, the drawing λ is sparse as a map $L \rightarrow S$ (more formally, the composition of λ by the inclusion map $T \rightarrow S$ is sparse), not just as a map $L \rightarrow T$. This is important since, for example, a non-contractible loop in T may be contractible in S .

The rest of this section is devoted to the proof of Proposition 6.7. To do so, given a drawing $\lambda : L \rightarrow T$, we choose an edge in each connected component of L and declare it to be a **major edge**; the other edges of L (if any) are **minor edges**. We say that λ is **straightened** if, under λ , (1) each minor edge is mapped to a reduced walk, and (2) each major edge is mapped to a reduced *closed* walk. We emphasize that the reduced closed walks do not have any bad turn, even at the basepoint, contrarily to the reduced walks, which are allowed to have a bad turn at the basepoint. Informally, to prove Proposition 6.7, we will straighten the initial drawing λ , and then prove that this makes λ a weak embedding whenever λ can be untangled in S . In detail:

Lemma 6.7. *In the setting of Proposition 6.7, one can compute in $O(n)$ time a drawing $\lambda' : L \rightarrow T$, straightened, homotopic to λ in S , of size $O(n)$, and of depth $O(N)$.*

Proof. Assume without loss of generality that L is connected. Construct λ' from λ as follows. Choose the major edge e_0 of L such that the image walk $\lambda(e_0)$ has minimal length. As a first step, reduce *cyclically* the *closed* walk $\lambda(e_0)$ with Proposition 6.4. Note that this usually moves the image of the vertex v of L , and thus elongates the image walks of the minor edges of L (if any). As a second step, once $\lambda(e_0)$ is cyclically reduced, fix the image of v and reduce the image walks of the minor edges (not cyclically this time) with Proposition 6.3.

For the analysis observe that in the first phase of the algorithm Proposition 6.4 cyclically reduces $\lambda(e_0)$ in $O(m)$ time, where m denotes the initial length of $\lambda(e_0)$. Now for every minor edge e_1 the image walk $\lambda(e_1)$ was initially at least as long as $\lambda(e_0)$, by the choice of e_0 . So the length of $\lambda(e_1)$ cannot increase by more than a constant factor in the first step. This proves that the algorithm takes $O(n)$ time and produces the desired drawing. \square

The main technical ingredient of this section is the following:

Proposition 6.8. *If a drawing $\lambda : L \rightarrow T$ is sparse, straightened, and can be untangled in S , then λ is a weak embedding.*

Lemma 6.7 and Proposition 6.8 immediately imply Proposition 6.7:

Proof of Proposition 6.7, assuming Proposition 6.8. Apply Lemma 6.7 to compute in $O(n)$ time the drawing $\lambda' : L \rightarrow T$. If λ can be untangled in S , then λ' is a weak embedding by Proposition 6.8. \square

The rest of this section is devoted to the proof of Proposition 6.8. We need to start with some preliminaries.

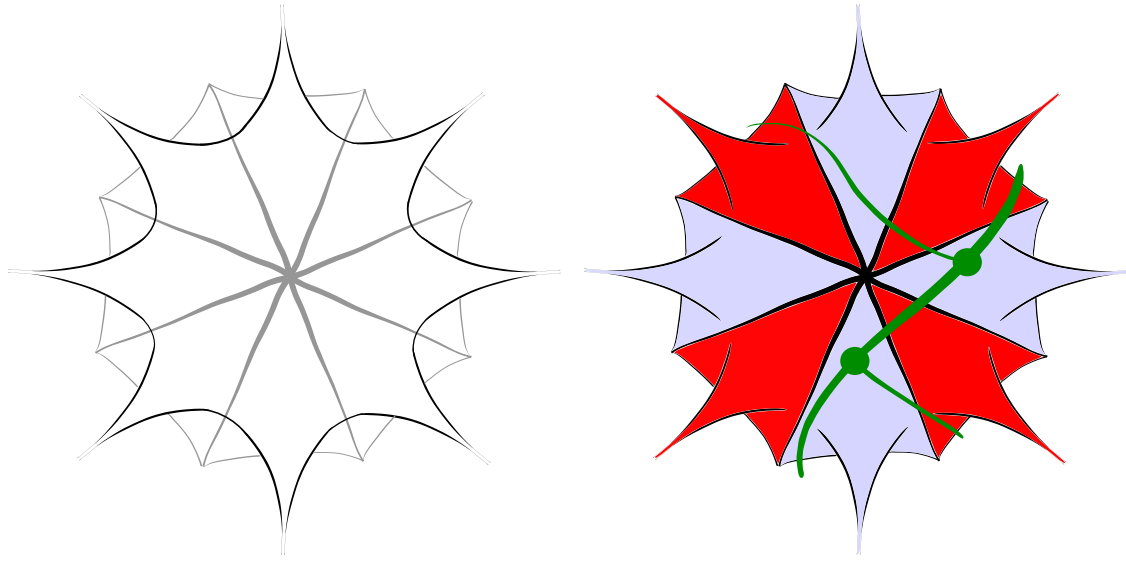


Figure 6.12: The map λ' (in green) in the hyperbolic patch system Σ of the reducing triangulation T , in the proof of Proposition 6.8.

6.4.1 Patch system and hyperbolic metric on the punctured surface

To prove Proposition 6.8, we assume that there is an embedding homotopic to λ in S , and we will prove that λ is a weak embedding. To do so we consider the patch system Σ of T , and we will exhibit an embedding $L \rightarrow \Sigma$ that approximates λ . Since T is cellularly embedded on S , we can think of the faces and arcs of Σ as the faces and edges of the dual graph of T in S . More precisely, we see the surface of Σ as open instead of closed by considering only the interior of Σ , and we realize Σ and its arcs in S as follows. Remove a point x_t from the interior of each triangle t of T ; then, for each edge e of T , consider the two distinct triangles t, t' incident to e in T , and draw a simple arc between x_t and $x_{t'}$ that crosses e exactly once and does not intersect any other edge or any vertex of T . Assume without loss of generality that the resulting arcs are pairwise disjoint. From now on we see Σ as realized in S in this way.

We construct our candidate $\lambda' : L \rightarrow \Sigma$ for an embedding that approximates λ as follows. Firstly, we endow Σ with a complete hyperbolic metric for which the arcs of Σ are geodesics, as follows. The arcs of Σ separate Σ into open disks. Each resulting connected component P has $k \geq 8$ incidences with arcs since the vertices of T have degree at least eight. We replace P by a hyperbolic polygon with k geodesic sides, with the particularity that these k geodesic sides all have *infinite* length (such polygons are called ideal polygons). Then we identify the sides of the polygons by pairs corresponding to the arcs of Σ .

Secondly, we see λ as a map from L to Σ and we construct λ' by modifying λ homotopically on every connected component L_0 of L , as follows. Let v be the vertex of L_0 and let e be the major edge of L_0 . We start by replacing homotopically the image of e by the geodesic closed curve c_e in its free homotopy class, thus possibly changing the image of v . Here we make use of the fact that $\lambda(e)$ is neither contractible nor homotopic to the neighborhood of a puncture in Σ , since it is non-contractible in S . We require that during this homotopy $\lambda \simeq \lambda'$ the image of v remains in the same disk of Σ (never belongs to an arc of Σ). We can do so since

the reduced closed walk $\lambda(e)$ makes no 0-turn and thus has the same sequence of crossings with the arcs of Σ as the geodesic closed curve c_e . Then, we replace for each minor edge e' of L_0 the image of e' by the geodesic segment in its homotopy class, this time holding the image of v fixed. The map λ' approximates λ since the images of the vertices of L remained in the same disks of Σ and since for every edge e'' of L the walk $\lambda(e'')$ makes no 0-turn.

Finally, we may ensure without loss of generality that the vertices of L are mapped by λ' to distinct points of Σ , and belong to no arc of Σ . That can be achieved by moving infinitesimally the image of each vertex of L along the image of its major edge.

At this point λ' is not necessarily an embedding; indeed, several major edges can overlap. The strategy is to prove that this is the only reason why λ' may fail to be an embedding, and that such overlaps can be eliminated by a small perturbation of λ' .

6.4.2 Proof of Proposition 6.8

In this section, we conclude the proof of Proposition 6.8. To ease the reading, we abuse the notation and write L to refer to the map λ' on L (defined in the previous section).

Recall from Section 5.1 that the universal cover \tilde{S} of S is homeomorphic to an open disk, which can be compactified into a closed disk $\tilde{S} \cup \partial\tilde{S}$, so that the properties of Section 5.1 can be applied. Note that, here, we view $\tilde{S} \cup \partial\tilde{S}$ as a purely topological space, and completely ignore any metric on it. In this section, we consider the subset $\tilde{\Sigma}$ of \tilde{S} made of the points that are lifts of Σ ; in other words, $\tilde{\Sigma}$ is obtained from \tilde{S} by removing the lifts of the punctures. (It turns out that $\tilde{\Sigma}$ is a covering space of Σ , but we will never use this property.) $\tilde{\Sigma}$ naturally inherits a hyperbolic metric, obtained by lifting the hyperbolic metric of Σ .

By construction, lifts of edges of L are geodesics under the metric of $\tilde{\Sigma}$. A **major lift** is a lift of a major edge; it is a bi-infinite geodesic path in $\tilde{\Sigma}$ with two distinct limit points on $\partial\tilde{S}$, by Lemma 5.1 and sparsity. A **minor lift** is a lift of a minor edge; it is a geodesic path in $\tilde{\Sigma}$.

If P and Q are minor lifts of distinct minor edges, then they may share one of their endpoints, but not both, since L is sparse and since the vertices of L are distinct points of Σ . In particular, the minor lifts of distinct minor edges are distinct. However, the situation is slightly more complicated for major lifts. Two major lifts obtained from different major edges are considered different. Recall that major edges are primitive (by Lemma 5.9 and sparsity). So any two major lifts $\tilde{c}, \tilde{d} : \mathbb{R} \rightarrow \tilde{\Sigma}$ of the same major edge that differ only by a homeomorphism of \mathbb{R} actually differ by an integer translation; in that case, we see them as equal.

The proof of Proposition 6.8 combines a long series of relatively easy lemmas on the lifts of the edges of L in $\tilde{\Sigma}$. Recall that by assumption L can be untangled.

Lemma 6.8. *Every lift of an edge is simple. Any two lifts of edges (possibly the same edge) that do not overlap intersect at most once, and if they intersect in their relative interiors, then they cross.*

Proof. If two portions of geodesic paths intersect in their relative interiors without overlapping, then they cross. Now assume, for a contradiction, that a lift is not simple; it contains a loop, which projects to a geodesic loop γ in Σ that is contractible in S . The sequence of crossings of γ with the arcs of Σ is that of a reduced walk. Thus, by Proposition 6.3, the

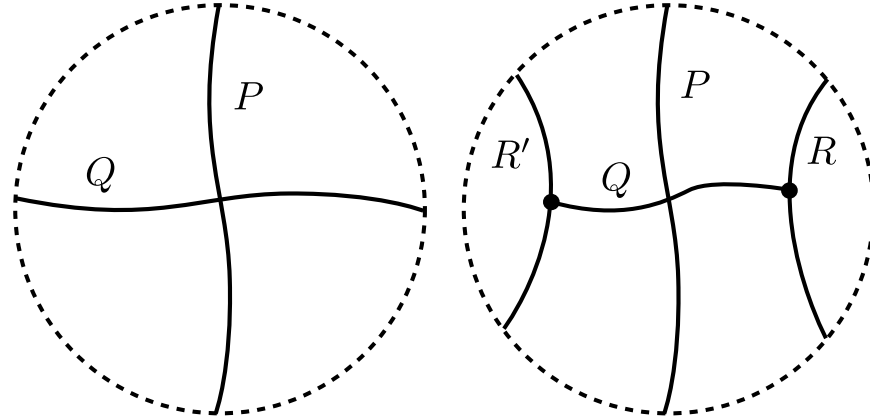


Figure 6.13: (Left) Proof of Lemma 6.9. (Right) Proof of Lemma 6.11.

loop γ does not cross any arc of Σ , and so γ is contractible in Σ , which is impossible since γ is geodesic.

Similarly, if two lifts intersect twice without overlapping, they form two paths with the same endpoints and otherwise disjoint, which project to geodesic paths p and q in Σ that are homotopic in S . The sequence of crossings of p and q with the arcs of Σ must be the same by Proposition 6.3, so p and q are homotopic in Σ , which is impossible since p and q are geodesics. \square

Lemma 6.9. *Any two major lifts either have the same image or are disjoint.*

Proof. Assume that two major lifts P and Q intersect and do not have the same image. They cross exactly once by Lemma 6.8. But then, their limit points are pairwise distinct by Lemma 5.4, and interleaved on $\partial\tilde{S}$ (see Figure 6.13 (left)), which implies that L cannot be untangled by Lemma 5.2. \square

Lemma 6.10. *Let P be a major lift and Q a minor lift such that P and Q are lifts of edges in the same connected component of L , and such that an endpoint of Q belongs to the image of P . Then no other point of Q lies on the image of P .*

Proof. Otherwise, P and Q overlap by Lemma 6.8. Let P' be the part of P that starts and ends at the endpoints of Q (which are both lifts of the vertex of the corresponding connected component L_0 of L). By Lemma 5.9, the projection of P' is the major edge of L_0 . Moreover, the projection of Q is a minor edge of L_0 . This contradicts the sparsity of L . \square

Before treating the other cases, we need a definition. Let P be a minor lift and let v and v' be the endpoints of P (they are distinct). Let p be the minor edge of L that is the projection of P , and let q be the major edge of L that lies in the same connected component of L as p . Let Q and Q' be the major lifts, starting at v and v' respectively, that are lifts of q . We say that Q and Q' form the **H-block** of P . Indeed, Q , P , and Q' together form the shape of the embedded letter “H”, because they touch only at v and v' by the preceding lemmas, and moreover the four limit points of Q and Q' are pairwise distinct by Lemma 5.4.

Lemma 6.11. *There is no intersection between a major lift P and the relative interior of a minor lift Q .*

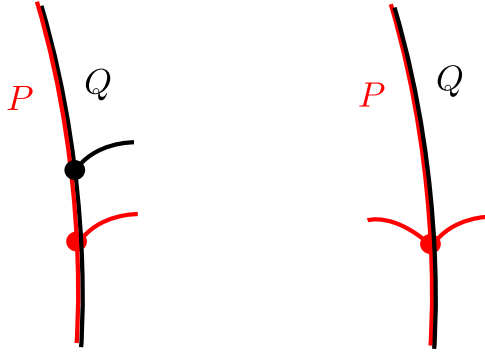


Figure 6.14: The two cases forbidden by Lemma 6.12.

Proof. Let R and R' be the major lifts forming the H-block of Q . Assume first that there is an intersection between P and the relative interior of Q that is not a crossing. Then P and Q overlap by Lemma 6.8. In particular, P intersects R and R' . However R and R' are disjoint, being part of the same H-block. This contradicts Lemma 6.9.

Now assume that there is an intersection between P and the relative interior of Q that is a crossing. By Lemma 6.8, there is exactly one. By Lemma 6.9, and since P does not have the same image as R or R' , the major lifts P , R , and R' are disjoint. See Figure 6.13 (right). Also, P does not have the same pair of limit points as R (or R'): for otherwise, by Lemma 5.3 and Lemma 5.9, P and R would project to closed curves freely homotopic in S (up to reversal), and thus freely homotopic in Σ by Proposition 6.2, but then P and R would project to the same geodesic closed curve, which is impossible since they are disjoint. Any homotopy of L induces a homotopy of the lifts P , R , and R' , preserving the limit points on $\partial\widetilde{S}$. Thus, even after a homotopy, one crossing between P and Q , R , or R' must remain (even if P shares one endpoint with R and/or one endpoint with R'). This contradicts the assumption that L can be untangled. \square

Let v be a vertex of L , and let e be a directed major edge of L based at v . We say that e is **pulled to the right** if there exists a minor edge based at v that leaves v and/or arrives at v to the right of e ; in other words, in counterclockwise order around v , we do not see consecutively the target of e and the source of e . We say that a directed major lift is *pulled to the right* if its projection is.

Lemma 6.12. *Let P and Q be two major lifts, projecting to different edges of L . Assume that they overlap; assume (up to reversing one of them) that they have the same direction. Then (1) at most one of P and Q is pulled to the right, and (2) none of them is pulled both to the left and to the right.*

Proof. We first prove (1); see Figure 6.14, left. Assume, for the sake of a contradiction, that both P and Q are pulled to the right. Let \bar{P} and \bar{Q} be these lifts after a homotopy that untangles L . (Generally, we use bars to denote lifts after this homotopy.) They must be disjoint (except at their limit points), so without loss of generality, up to exchanging P and Q , assume that \bar{P} lies to the left of \bar{Q} . Let R be the minor lift pulling P to the right; thus, P is part of the H-block of R ; let P' be the lift that forms the H-block of R together with P . Then, \bar{Q} intersects either \bar{R} , or \bar{P}' (twice), which is impossible.

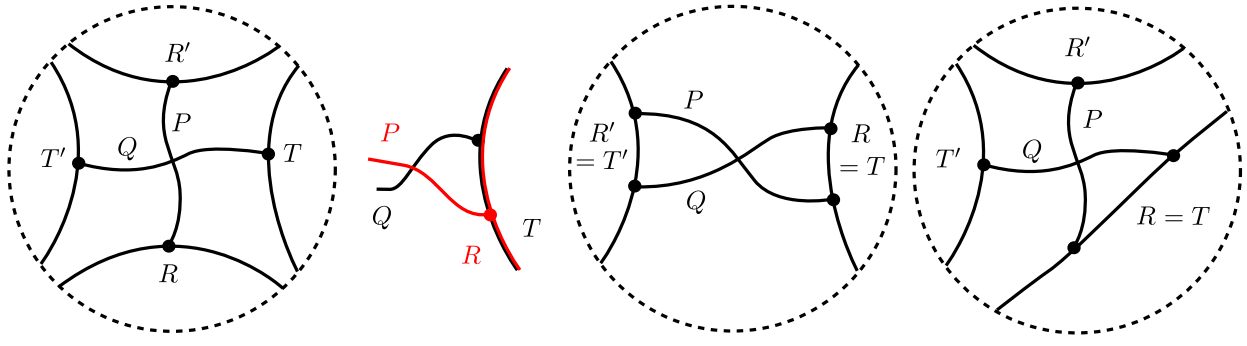


Figure 6.15: The four cases in the proof of Lemma 6.13.

We now prove (2); see Figure 6.14, right. Assume that P is pulled both to the left and to the right. After the homotopy, the lifts \bar{P} and \bar{Q} are disjoint, so without loss of generality, up to reversing the orientations of P and Q , assume that \bar{P} lies to the left of \bar{Q} . We are then in the same situation as the previous paragraph, and conclude similarly. \square

Lemma 6.13. *The relative interiors of any two distinct minor lifts are disjoint.*

Proof. If the relative interiors of two distinct minor lifts P and Q intersect without crossing, they overlap. Since P and Q are distinct they do not have the same pair of endpoints. Thus the relative interior of one of P and Q must intersect a major lift, a contradiction with Lemma 6.11.

If P and Q cross, they do so exactly once by Lemma 6.8. Let R and R' be the major lifts forming the H-block of P , and similarly let T and T' be the major lifts forming the H-block of Q . By Lemma 6.9, and up to exchanging notations, we distinguish between four cases, depicted in Figure 6.15:

- If R , R' , T , and T' are pairwise disjoint, the cyclic ordering of the limit points on $\partial\tilde{S}$ is necessarily $r_1r_2t_1t_2r'_1r'_2t'_1t'_2$, with obvious notations (R has limit points r_1 and r_2 , and so on), with possible identifications of two consecutive limit points in this cyclic order if they come from different lifts. Any homotopy of L induces a homotopy of the lifts P , Q , R , R' , T , and T' , preserving the limit points on $\partial\tilde{S}$. Thus, even after a homotopy, one crossing must remain. This contradicts the assumption that L can be untangled.
- If R is distinct from T but has the same image as T , these two lifts with the same image, when directed in the same way, are both pulled to the right, or both pulled to the left, which is impossible (Lemma 6.12(1)).
- If R is equal to T and R' is equal to T' , then any homotopy of L induces a homotopy of P , Q , R , R' , preserving the four limit points on $\partial\tilde{S}$ and the relative orders of the endpoints of P and Q on R and R' . Thus, even after a homotopy, one crossing must remain.
- If R is equal to T and R' is disjoint from T' , then, again, a crossing must remain after lifting a homotopy of L . \square

Proof of Proposition 6.8. By Lemmas 6.8, 6.11, and 6.13, the only reason why L may fail to be an embedding is because two distinct major lifts intersect, which implies that they have the same image by Lemma 6.9, and thus come from distinct major edges.

So now, consider an inclusionwise maximal set A of at least two overlapping, simple, major edges, directed in the same way. By Lemma 6.12 A contains at most one edge pulled to the left (and not to the right), at most one edge pulled to the right (and not to the left), and possibly several edges which are pulled neither to the left nor to the right. We can slightly perturb these edges to make them disjoint: from left to right, the edge pulled to the left (if it exists), then, the edges not pulled at all, and finally, the edge pulled to the right (if it exists). After this operation we have an embedding of L that approximates λ . \square

6.5 Untangling graphs

In this section we finally describe how to untangle general drawings of graphs (not just sparse drawings of loop graphs) on 8-reducing triangulations, by proving the main theorem of this chapter, Theorem 6.2, which we restate for convenience:

Theorem 6.2. *Let S be a surface of genus $g \geq 2$ without boundary. Let T be an 8-reducing triangulation of S . Let G be a graph, and let $f : G \rightarrow T$ be a drawing of size n . One can determine in $O(gn \log(gn))$ time whether f can be untangled in S . If so, one can construct in additional $O(n^2)$ time a weak embedding $f' : G \rightarrow H$, homotopic to f in S , of depth $O(n)$.*

The rest of this section is devoted to the proof of Theorem 6.2. Importantly, some of the definitions and lemmas of this section are stated on a generic surface S (with or without boundary). Here they are only applied to the case where S has no boundary and has genus at least two, but they will be applied to more general surfaces in Chapter 7, so we state them in full generality.

6.5.1 Factorization

The key step is to transform our initial drawing into a sparse drawing of a loop graph, in order to use the result of the previous section (Proposition 6.7 in Section 6.4). So consider a surface S , a graph G , and a map $f : G \rightarrow S$. One can transform f into a sparse drawing of a loop graph by contracting the image of a spanning forest of G , ignoring the resulting contractible loops, and identifying the resulting homotopic loops. We now describe this operation slightly more formally. First assume that G is connected, and let Y be a spanning tree of G . A **factorization** of f (with respect to Y) is obtained by the following process, see Figure 6.16. First, change f by contracting homotopically the image of the spanning tree Y to a single point $x \in S$. The non-tree edges of G are now drawn as loops under f . Move these loops that are contractible to the constant loop based at x . Now, whenever there are several loops in the same homotopy class (with basepoint x), select one of these loops, γ , arbitrarily, and redraw the other ones in the same way as γ . Let $f' : G \rightarrow S$ be the new drawing. Observe that, under f' , the graph G is first drawn onto a one-vertex graph L , which is itself sparsely drawn in S . The factorization of f is given by the one-vertex graph L , its sparse drawing $\lambda : L \rightarrow S$, and the drawing $\mu : G \rightarrow L$. By construction, f and $\lambda \circ \mu$ are homotopic; see Figure 6.16, left.

Equivalently, but we will not need this equivalence, a factorization of f (with respect to Y) is given by a one-vertex graph L , a *sparse* drawing $\lambda : L \rightarrow S$, and an *onto* drawing $\mu : G \rightarrow L$ that maps each edge of Y to the vertex of L , and that maps each edge of $G \setminus Y$ to either the vertex of L or a loop of L , in such a way that f and $\lambda \circ \mu$ are homotopic.

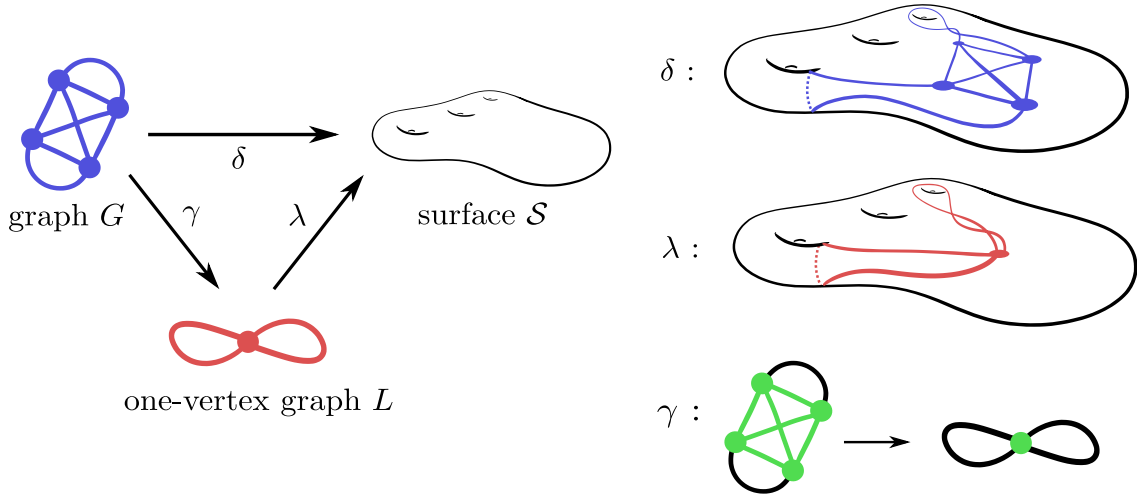


Figure 6.16: A factorization (L, λ, μ) of the drawing f of Figure 1.2.

A factorization of a drawing of a disconnected graph G is given by a factorization for each of the connected components of G . In the setting of 8-reducing triangulations, factorizing a drawing can be performed efficiently:

Proposition 6.9. *Let S be a surface of genus $g \geq 2$ without boundary. Let T be an 8-reducing triangulation of S . Let G be a graph, and let $f : G \rightarrow T$ be a drawing of size n . In $O(gn \log(gn))$ time, one can either correctly report that f cannot be untangled in S or compute a factorization (L, λ, μ) of f , such that L has $O(g)$ loops, and such that λ has depth $O(n)$.*

We will prove Proposition 6.9, but only in Section 6.6, as we prefer to first finish the details of our algorithm for untangling drawings of graphs. We just provide a first, rather naive, algorithm for Proposition 6.9 with worse running time and output size:

Proof of Proposition 6.9, with worse running time and output size. Assume without loss of generality that G is connected. We choose arbitrarily a vertex v and a spanning tree Y of G . We then contract the image of Y to the image point of v , thus transforming f into a drawing $f' : G \rightarrow H$ such that $f'(Y) = f'(v) = f(v)$. The length of f' is $O(n^2)$, because every non-tree edge is now drawn as a walk of length $O(n)$. We reduce all these walks in $O(n^2)$ total time with Proposition 6.2.3.

Afterward the contractible loops are shrunk to the basepoint and the homotopic loops overlap by Proposition 6.1. We remove the contractible ones, and aggregate the ones that overlap, using $O(n^2)$ pairwise comparisons, and thus in $O(n^3)$ total time. We retrieve the resulting loop graph L and its sparse drawing $\lambda : L \rightarrow T$, along with the drawing $\mu : G \rightarrow L$. Then L has $O(n)$ loops and λ has depth $O(n)$. \square

6.5.2 Key lemmas

We now present the two key lemmas that relate factorization to the untangling problem.

Lemma 6.14. *Let S be a surface. Let G be a graph, and let $f : G \rightarrow S$ be a map. Let (L, λ, μ) be a factorization of f . If f can be untangled, then λ can be untangled.*

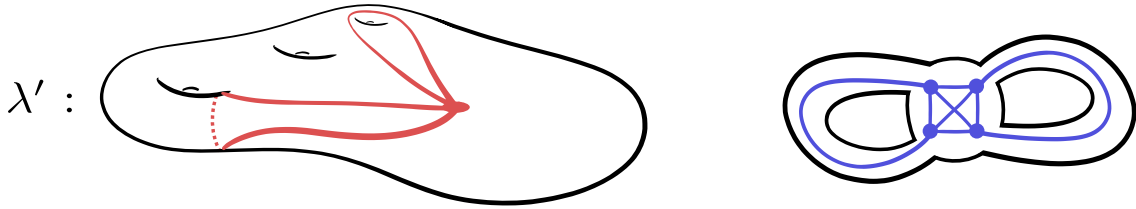


Figure 6.17: (Continuation of Figures 1.2 and 6.16) Although the map λ is homotopic to an embedding λ' (left), the map $\lambda' \circ \mu$ is not a weak embedding (right), which implies by Lemma 6.15 that f is not homotopic to an embedding.

Proof. Let $f' : G \rightarrow S$ be an embedding homotopic to f . Starting from f' , we contract the edges of G that are part of the spanning trees used to define the factorization, obtaining a loop graph embedded on S . We then remove contractible loops and keep only one loop whenever several loops are in the same homotopy class. In this way, we obtain an embedding $\lambda' : L \rightarrow S$ homotopic to λ . Thus λ can be untangled. \square

Lemma 6.15. *Let S be a surface. Let G be a graph, and let $f : G \rightarrow S$ be a map. Let (L, λ, μ) be a factorization of f . If f and λ are embeddings, then $\lambda \circ \mu$ is a weak embedding.*

See Figure 6.17 for an illustration of Lemma 6.15. The rest of this section is devoted to the proof of Lemma 6.15. It relies on the following, which might not be new, but we could not find a reference, so we provide a proof:

Lemma 6.16. *On a surface S , let each of $\Gamma = (\gamma_1, \dots, \gamma_k)$ and $\Gamma' = (\gamma'_1, \dots, \gamma'_k)$ be a set of simple, pairwise disjoint, pairwise non-homotopic, non-contractible loops with basepoint x . Assume that γ_i and γ'_i are homotopic with basepoint fixed for each i . Then Γ and Γ' are isotopic with basepoint fixed.*

Proof. Let \hat{S} be obtained from S by removing a small disk D around x . We can assume that all loops are piecewise linear with respect to a fixed triangulation of S [83, Appendix], and thus that no crossing occurs in D , and that each loop crosses the boundary of D exactly twice. We let $\hat{\gamma}_i$ and $\hat{\gamma}'_i$ be the arcs in \hat{S} that are the pieces of γ_i and γ'_i obtained after removing D , and $\hat{\Gamma}$ and $\hat{\Gamma}'$ be the corresponding sets of arcs.

For each i the loops γ_i and γ'_i are homotopic on S , so they are isotopic on S , by a result of Epstein [83, Theorem 4.1]. Thus $\hat{\gamma}_i$ and $\hat{\gamma}'_i$ are homotopic on \hat{S} , where the homotopy allows to slide the endpoints on $\partial\hat{S}$.

Because $\hat{\Gamma}$ and $\hat{\Gamma}'$ are simple, whenever there is an embedded bigon or an embedded “half-biggon” [91, Section 1.2.7] between $\hat{\Gamma}$ and $\hat{\Gamma}'$, there is an innermost embedded bigon or innermost embedded half-biggon, which we can remove using an isotopy of $\hat{\Gamma}$ (sliding endpoints on the boundary is allowed), decreasing the number of crossings. So without loss of generality we can assume that there is no embedded bigon or half-biggon between $\hat{\Gamma}$ and $\hat{\Gamma}'$.

In particular, for every i , the loops $\hat{\gamma}_i$ and $\hat{\gamma}'_i$ are in minimal position in their homotopy classes [91, Section 1.2.7], and since they are homotopic (allowing sliding on the boundary), they are disjoint. The corresponding loops γ_i and γ'_i bound a disk on S . Moreover, because the loops in Γ are pairwise non-homotopic, and because there is no embedded (half-)bigon between $\hat{\Gamma}$ and $\hat{\gamma}'_i$, the disk does not meet Γ . We can thus, for each i , push γ_i to γ'_i by an isotopy of Γ . \square

Corollary 6.1. *Let S be a surface. Let L be a loop graph and let $\lambda, \lambda' : L \rightarrow S$ be embeddings. If λ and λ' are sparse and homotopic, then they induce the same rotation system on L .*

Proof. Assume without loss of generality that L is connected, and thus has a single vertex v . Further assume without loss of generality that $\lambda(L)$ and $\lambda'(L')$ are disjoint from the boundary of S (if S has boundary), by slightly perturbing them otherwise. There is a homotopy transforming λ into λ' . In this homotopy the image point of v follows a (possibly non-simple) path p . Without loss of generality p is disjoint from the boundary of S , so there is also an ambient isotopy of S that displaces the initial point $\lambda(v)$ along the same path p . This ambient isotopy ultimately transforms λ into an embedding $\lambda'' : L \rightarrow S$, with the same rotation system than λ , that is also homotopic to λ' *relatively to v* (meaning that the image of v is fixed by the homotopy). Then λ'' and λ' are isotopic relatively to v by Lemma 6.16, which proves the result. \square

Proof of Lemma 6.15. First, we remark that, without loss of generality, we can assume that G is connected; this is because μ maps the connected components of G to those of L bijectively.

Then, we prove that we can isotope f so that its new image in S lies in the neighborhood of some sparsely embedded one-vertex graph. For this purpose, we almost-contract the image of the spanning tree Y used to define the factorization, keeping the fact that we have an embedding of G . The resulting loops fall into homotopy classes. The loops in the trivial homotopy class can be isotoped close to the basepoint; indeed, in an embedded one-vertex graph, any contractible simple loop bounds a disk with only (possibly) contractible loops inside it, this a result of Epstein [83, Theorem 1.7]. The loops in any other given homotopy class can be bundled together so that they are parallel; indeed, in an embedded one-vertex graph, any pair of homotopic loops bounds a disk with only (possibly) contractible or homotopic loops inside it. To summarize, we have an embedding f' of G , homotopic to f , whose image lies in a neighborhood of the image of some sparse embedding λ' of a loop graph L' .

Actually, there is a canonical isomorphism between L and L' , because each edge of L and L' corresponds to a particular set of non-tree edges of G ; so we can identify L and L' via this isomorphism. Also, for use at the end of the proof, we remark that λ and λ' are (freely) homotopic.

By construction, the embedding f' can be chosen to lie in any neighborhood of the map $\lambda' \circ \mu$ (for the compact-open topology of maps from G to S). Hence $\lambda' \circ \mu$ is a weak embedding. Alternatively, it would now be easy to build the patch system of $\lambda'(L')$ associated to λ' , so that f and this patch system indeed witness that $\lambda' \circ \mu$ is a weak embedding.

Now, we recall that λ and λ' are homotopic embeddings of L , so the rotation systems are the same in λ and λ' by Corollary 6.1. Also, the fact that $\lambda' \circ \mu$ is a weak embedding depends only on the rotation system induced on L by λ' , not on λ' itself. This implies that $\lambda \circ \mu$ is a weak embedding as well. \square

6.5.3 Algorithm

We are now finally in a position to prove Theorem 6.2 (assuming Proposition 6.9 for efficient factorization), by giving our algorithm for untangling graphs on 8-reducing triangulations:

Proof of Theorem 6.2, assuming Proposition 6.9. First we determine whether f can be untangled in S , in $O(gn \log(gn))$ time, as follows:

1. We apply Proposition 6.9 in $O(gn \log(gn))$ time and either determine that f cannot be untangled in S , in which case we abort, or compute a factorization (L, λ, μ) of f such that L has $O(g)$ loops, and such that λ has depth $O(n)$.
2. We apply Proposition 6.7 in $O(gn)$ time and compute a drawing $\lambda' : L \rightarrow T$, homotopic to λ in S , of depth $O(n)$, such that if λ can be untangled in S then λ' is a weak embedding.
3. We apply the result of Akitaya, Fulek, and Tóth [10], restated in Theorem 5.1, and determine in $O(gn \log(gn))$ time whether λ' is a weak embedding. If not, then λ cannot be untangled in S , and so f cannot be untangled in S by Lemma 6.14, so we abort. Otherwise, if λ' is a weak embedding, we use Theorem 5.1 to actually compute an embedding $\lambda'' : L \rightarrow \Sigma$ approximating λ' in the patch system Σ of T , in the same amount of time.
4. We equip L with the rotation system induced by λ'' , so that μ is a weak embedding (with respect to this rotation system of L) if and only if $\lambda'' \circ \mu$ is a weak embedding. We apply Theorem 5.1 again to determine whether μ , equivalently $\lambda'' \circ \mu$, is a weak embedding. This step takes $O(n \log n)$ time since μ has size $O(n)$. The result tells whether f can be untangled in S by Lemma 6.15.

Now if f can be untangled in S , equivalently if $f' := \lambda'' \circ \mu$ is a weak embedding, then f' has depth $O(n)$ and can be retrieved in additional $O(n^2)$ time. \square

6.6 Efficient factorization

In this section we implement the last detail of our algorithm, which is the efficient factorization promised in Proposition 6.9. Our main tool for this is a data structure on 8-reducing triangulations, the *compressed homotopy tree*, extending the *compressed homotopy sequence* from Section 6.2.3; while the compressed homotopy sequence is a linear list, the compressed homotopy tree is a tree-like structure. (We will also extend proof techniques from Section 6.2.3.) We first present compressed homotopy trees, then we prove Proposition 6.9.

6.6.1 Compressed homotopy trees

Consider a surface S of genus $g \geq 2$ without boundary, an 8-reducing triangulation T of S , and a vertex r of T . We need to support fast homotopy queries on an evolving set of walks starting at r . Intuitively, there is a map κ that associates a pointer to each walk starting at r , such that two walks W and W' are homotopic if and only if $\kappa(W) = \kappa(W')$. We call these $\kappa(W)$ **keys**. Our data structure, a **compressed homotopy tree**, provides efficient access to such a map κ in the following sense: If W' is the concatenation of W with a single edge, then we can compute $\kappa(W')$ from $\kappa(W)$ quickly (in time logarithmic in the number of operations already performed).

For this purpose, we use the fact that the homotopy class of a walk W is determined by the unique reduced walk $\rho(W)$ homotopic to W (Proposition 6.1). We store the reduced walks $\rho(W)$ in compressed form, by enhancing the data structure from Section 6.2.3 (compressed homotopy sequence) in a tree-like fashion, instead of a linear list (in a way similar to shortest path trees); for each walk W starting at r , we let $\kappa(W)$ be a pointer to the last elementary

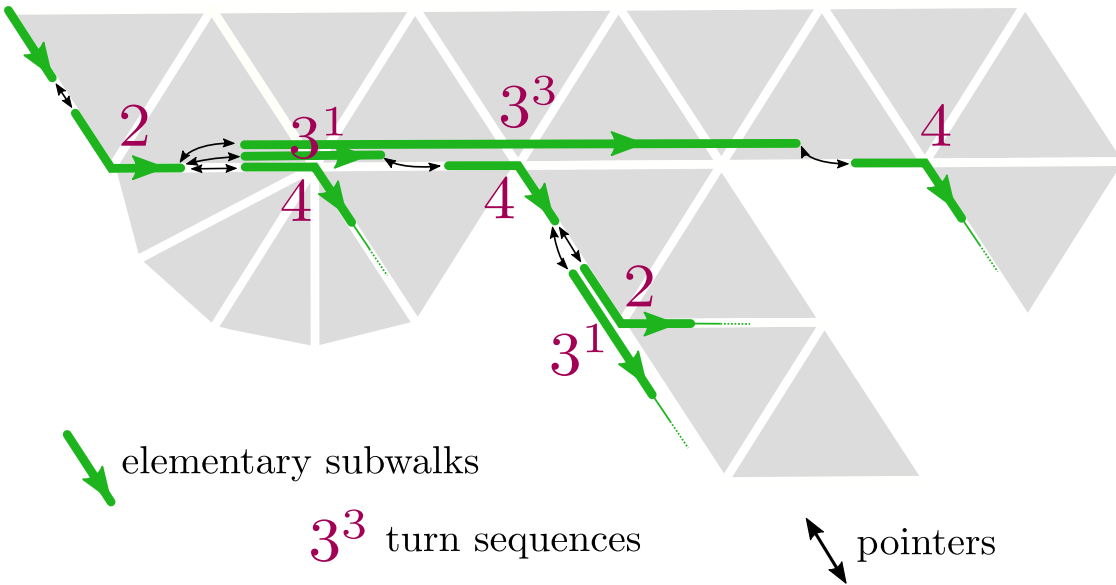


Figure 6.18: Homotopy classes of walks are represented by storing the elementary subwalks of their reduced walks in a tree-like fashion.

subwalk of W . Each node of the tree corresponds to an elementary subwalk, and stores (see Figure 6.18):

- the first and last directed edges of T of the elementary subwalk;
- the turn sequence of the elementary subwalk, in compressed form (as in Section 6.2.3: the elementary subwalk has a turn sequence of the form 3^k , $(-3)^k$, or another symbol a ; we store its form together with the integer k or the symbol a);
- a pointer to its parent;
- the elementary subwalks of its children, stored in appropriate search trees (see below).

We maintain the following invariants:

- the children of any given node in the tree correspond to pairwise distinct turn sequences;
- the first edge of an elementary subwalk equals the last edge of its parent.

By these invariants, and because reduced paths are unique, two walks starting at r are homotopic if and only if they have the same keys. Thus, once the keys of two walks have been computed, we can, in $O(1)$ time, decide whether they are homotopic.

We now list a few operations that can be handled by our data structure. Two of them are easy:

Lemma 6.17. *Compressed homotopy trees support the following operations:*

- **TRIVIALKEY:** return the key corresponding to the empty walk at r , in $O(1)$ time;
- **REDUCEDWALK:** given the key of a walk W , return the compressed turn sequence of the reduced walk homotopic to W , in time linear in its length.

Proof. The TRIVIALKEY operation is indeed trivial.

The REDUCEDWALK operation can be done by traversing the tree from $\kappa(W)$ up to the root, noting the labels of the nodes in order in which they are encountered, and then reading them in reverse order. \square

More interestingly, we can also extend the set of walks considered:

Lemma 6.18. *Compressed homotopy trees support (with additional data structures described in the proof) the operation EXTEND: Given the key of a walk W , finishing at vertex v , and given a directed edge e of T starting at v , return the key of the concatenation of W and e , in $O(\log p)$ time, where p is the number of EXTEND operations already performed.*

Proof. Because we must maintain the invariant that the children of any given node in the tree correspond to pairwise distinct turn sequences, we require one more ingredient to our data structure. Given an elementary subwalk W , we need to be able to find the child of W that has a given turn sequence in $O(\log p)$ time, or certify that such a child does not exist. For this purpose, recall that each elementary subwalk has the turn sequence 3^k or $(-3)^k$ for some $k \geq 1$, or a for some $a \notin \{-3, 3\}$. We split the children of W according to each of these three categories. In a given category, a child of W is encoded by the nonnegative integer k or a . We use three red-black trees [112] (one for each category, indexed by either k or a) to decide whether the child of W with a specified compressed turn sequence exists, or to insert it if it does not exist. Each of these operations takes $O(\log p)$ time, because each red-black tree contains $O(p)$ elements.

The rest of the proof reuses tools and arguments from Section 6.2.3. Let W be a reduced walk finishing at vertex v ; let e be a directed edge starting at v ; let $W.e$ be the concatenation of W and e ; and let W' be the reduced walk homotopic to $W.e$. We claim that the compressed homotopy sequences of W and W' each have at most 49 elementary subwalks after their longest common prefix. To prove the claim it is enough to prove that the compressed homotopy sequences of $W.e$ and W' each have at most 48 symbols after their longest common prefix; indeed the compressed homotopy sequences of W and $W.e$ do not differ by more than one final elementary subwalk. Now recall from Section 6.2.3 that, for any walk W'' , $\varphi(W'')$ equals three times the length of W'' plus the number of bad turns of W'' , and that φ strictly decreases when performing a reduction move. In the same spirit as the proof of Proposition 6.3, observe that $\varphi(W.e) \leq \varphi(W) + 4$. Observe also that $\varphi(W) \leq \varphi(W') + 4$, since W can be obtained from the concatenation of W' and the reversal of e by performing reduction moves, which decrease the value of φ . So $\varphi(W.e) \leq \varphi(W') + 8$. Since W' is the unique walk obtained by reducing $W.e$, we have that any sequence of reductions on $W.e$ has length at most eight. Initially, only the last elementary subwalks of $W.e$ can yield a reduction. Each reduction replaces at most six consecutive elementary subwalks by at most seven ones, and then backtracks by at most six elementary subwalks (see the proof of Proposition 6.3). Thus, only the last 48 elementary subwalks of $W.e$ can be changed using successive reductions, which implies that the remaining first elementary subwalks of $W.e$ are not affected when reducing to W' . This proves the claim.

Let W and e be as in the statement of the lemma; we can assume that W is reduced. The claim implies that we can compute $\kappa(W.e)$ from $\kappa(W)$ in $O(\log p)$ time, for example as follows. Starting at the elementary subwalk representing W , in $O(1)$ time we go up in the tree by 49 levels, reaching an elementary subwalk that represents a walk W_1 . We can then compute, again in $O(1)$ time, the compressed homotopy sequence of W_2 , the walk obtained

from W by removing its prefix W_1 and by concatenating e to the result. We reduce this compressed homotopy sequence in $O(1)$ time (see again the proof of Section 6.3); finally, using the first paragraph of this proof, we extend the elementary subwalk representing W with each elementary subwalk of this compressed homotopy sequence in the tree in turn, in $O(\log p)$ time, reaching eventually the elementary walk for W' . \square

Finally:

Lemma 6.19. *Compressed homotopy trees support (with additional data structures described in the proof) the operation PARTITION: Given a set X of instances of some data structure containing, in particular, a key, we can, in time linear in the size of X , compute the partition of X such that two elements in X belong to the same part if and only if they contain the same key.*

Proof. This operation relies on easy bookkeeping techniques; in detail: Slightly extend the data structure of elementary subwalks with a pointer, initially NULL; for each element x of X in turn, if its key refers to an elementary subwalk whose pointer is NULL, create a new part of the partition, initially containing only x , and make the elementary subwalk refer to that part; otherwise, the key of x refers to an elementary subwalk W that has already been visited, and x can be added to the part thanks to the pointer in W . After computing this partition, restore all pointers to NULL. \square

One final detail: The root of the tree of our data structure must be handled in a special way. By convention, it is a virtual elementary subwalk whose only directed edge e does not belong to the triangulation T but points towards the root r , so that by convention the turns from e to each edge starting at r are ∞ , with the obvious modifications on the algorithm to reduce walks. We omit the tedious and trivial details.

6.6.2 Algorithm

We are now in a position to prove Proposition 6.9. The proof relies on the following lemma, which is easy and folklore, but we could only find a proof in the case where the surface S has no boundary [35, Lemma 2.1] (the constants differ, but this is of no importance to us), so we provide a quick proof in the general case, for later use:

Lemma 6.20. *Let S be a surface of genus g with b boundary components. Let Γ be a set of simple pairwise disjoint loops based at the same point in S . Assume that the loops of Γ are non-contractible and pairwise non-homotopic. Then Γ has at most $9g + 6b$ loops.*

Proof. Assume without loss of generality that the loops in Γ do not intersect the boundary of S , by slightly perturbing them otherwise. We think of Γ has a graph with a single vertex, embedded on S , and we let n and m count respectively the edges and faces of Γ . The lemma clearly holds if $n \leq 1$ so we may assume $n \geq 2$ without loss of generality. Then every face of Γ either has positive genus, and there are at most g of them, contains a boundary component of S , and there are at most b of them, or is incident to at least three occurrences of loops of Γ (a single loop of Γ may occur twice). Double counting implies that at most $2n/3$ faces are of the latter kind. Altogether $m \leq g + b + 2n/3$. Euler's formula gives $1 - n + m = 2g + b - 2$. That proves $n \leq 9g + 6b$. \square

Proof of Proposition 6.9. By definition of a factorization, we can assume in the whole proof that G is connected. We fix arbitrarily a vertex r and a spanning tree Y of G , such that Y is obtained by a *depth-first search* from r . We direct each edge e of $G \setminus Y$ so that its target $t(e)$ is an ancestor of its source $s(e)$. We denote by ℓ_e the loop that is the concatenation of the (unique) path in Y from r to $s(e)$, edge e , and the (unique) path in Y from $t(e)$ to r . Given a vertex v on the path from $t(e)$ to r , we denote by ℓ_e^v the loop ℓ_e where the last segment from v to r is truncated (thus, v always appears in ℓ_e^v).

In a first step we compute, for every vertex v of G , the key of the image walk, in T , of the path from r to v in Y . This can be done in $O(n \log n)$ time by traversing Y in top-down order and using the EXTEND operation $O(n)$ times. Similarly, in the same amount of time, we compute, for each edge e of $G \setminus Y$, the key of the image walk of $\ell_e^{t(e)}$.

In a second step, using the keys already computed, we compute the keys of the image walks of the entire loops ℓ_e , but to get an efficient algorithm we eliminate duplicate keys as we encounter them, and halt whenever there are too many distinct keys (i.e., too many homotopy classes, so that f cannot be untangled). We do this in a bottom-up way in the tree Y . For each vertex v of G , we denote by $K(v)$ the set of keys $\kappa(f(\ell_e^v))$ over the edges e of $G \setminus Y$ for which v appears after e in ℓ_e .

Assume that we have computed the sets $K(v')$ for each child v' of a vertex v ; using the PARTITION operation, we can assume each $K(v')$ to be without duplicates. If one of them has size larger than $18g$, then the *directed* loops $f(\ell_e)$ fall into more than $18g$ distinct homotopy classes, which implies by Lemma 6.20 that G cannot be untangled, so we abort. Otherwise, for each child v' of v in Y and for each key $k \in K(v')$, we apply the EXTEND operation to k and edge $v'v$. Let $K(v', v)$ be the resulting set of keys. We now observe that $K(v)$ is obtained by removing the duplicates in the union of the following sets of keys:

- the sets $K(v', v)$, for each child v' of v , and
- the set of keys of the form $\kappa(f(\ell_e^v))$, for each edge e such that $t(e) = v$.

At the end of the recursion, unless the algorithm aborted, we have computed $K(r)$. At each vertex v , the number of times we apply EXTEND is $O(g \deg(v))$, where $\deg(v)$ is the degree of v in Y . So, in total, EXTEND has been applied $O(gn)$ times, and the entire algorithm takes $O(gn \log(gn))$ time.

When $K(r)$ has been computed, we can also compute the reduced walks corresponding to the keys in $K(r)$ using the REDUCEDWALK operation. This takes in $O(gn)$ total time, thus asymptotically without overhead in the running time, since $K(r)$ corresponds to $O(g)$ walks, each of length $O(n)$. We have thus computed the one-vertex graph L of the factorization, and its sparse drawing $\lambda : L \rightarrow H$.

Finally, remember that we also need to compute the drawing $\mu : G \rightarrow L$ of the factorization. In other words, we need to compute the mapping from each edge $e \in G \setminus Y$ to the loops of L (or to its vertex), or, equivalently, the key of $f(\ell_e)$ in $K(r)$. We now explain how to refine the second step above to achieve this. In this second step, every key considered is of the form $k = \kappa(f(\ell_e^v))$; whenever we encounter such a key k , we also store together with it a corresponding edge e such that $\kappa(f(\ell_e^v)) = k$. Whenever we detect redundancies in the current set of keys, we actually compute the set of edges $e_1, \dots, e_p \in G \setminus Y$, $p \geq 1$, whose keys share a common value k , which in particular implies $\kappa(f(\ell_{e_1})) = \dots = \kappa(f(\ell_{e_p}))$. In that case, we declare that the edge corresponding to the common key k is e_1 , we declare that the *leader* of e_2, \dots, e_p is e_1 , and then completely forget about the edges e_2, \dots, e_p . There is no

overhead in the running time of the algorithm. At the very end, once the keys in $K(r)$ have been computed (each of them coming with an associated edge in $G \setminus Y$), we need to recover, for each edge $e \in G \setminus Y$, the corresponding key $\kappa(f(\ell_e)) \in K(r)$. For this purpose, we remark that the set of edges in $G \setminus Y$ is implicitly organized as a forest, in which the “leader” relation is actually a “parent” relation. Thus, our problem boils down to this: Given a rooted forest, we need to compute, for each node, the root of its corresponding tree. This can easily be done in time linear in the size of the forest, and thus, in our case, in $O(n)$ time. \square

Chapter 7

Untangling Graphs on Surfaces

This chapter is almost entirely dedicated to the proofs of Theorems 3.3 and 3.2, which we recall for convenience:

Theorem 3.3. *Let S be a surface of genus smaller than s , with less than s boundary components. Let H be a graph of size m cellularly embedded on S . Let G be a graph, and let $f : G \rightarrow H$ be a drawing of size n . One can determine in $O(m + s^2n \log(sn))$ time whether f can be untangled in S . If so, one can construct in additional $O(s^2mn^2)$ time a weak embedding $f' : G \rightarrow H$, homotopic to f in S , of depth $O(s^2mn)$.*

The weak embedding f' returned by Theorem 3.3 can be given to the algorithm of Akitaya, Fulek, and Tóth [10] (restated in Chapter as Theorem 5.1) to construct an embedding approximating f' . This provides the very first polynomial time algorithm for untangling general drawings of graphs. This is one of the main contributions of the thesis.

Theorem 3.2. *Let S be a surface of genus smaller than s , with less than s boundary components. Let H be a graph of size m cellularly embedded on S . Let C be a collection of closed walks of total length n in H . One can compute $i_S(C)$ in $O(m + s^2 + sn \log(sn))$ time. One can construct in additional $O(s^2mn)$ time a collection of closed walks C' in H , freely homotopic to C in S , in minimal position.*

The collection of closed walks C' returned by Theorem 3.2 can be given to the algorithm of Fulek and Tóth [101] (restated in Chapter 5 as Theorem 5.1) to compute a perturbation of C' with $i_S(C)$ self-crossings. This improves upon the state of the art results of Despré and Lazarus [69] (restated in Chapter 4 as Theorems 4.2 and 4.3). Our result is more general since we can put an arbitrary number of closed curves in minimal position. Also, our algorithms are quasi-linear in n instead of quadratic and quartic. And our proofs are simpler and shorter.

Techniques and discussion. Theorems 3.3 and 3.2 extend the two main results of Chapter 6: Theorems 6.1 and 6.2. While the algorithms of Theorems 6.1 and 6.2 take as input graphs drawn in 8-reducing triangulations, on surfaces that have no boundary and genus at least two, Theorems 3.3 and 3.2 take as input drawings in *any* graph H cellularly embedded on *any* surface (and they return in H). In the case where the surface S has no boundary and genus at least two, we deduce Theorems 3.3 and 3.2 from their analogs on 8-reducing triangulations, basically by converting the input and output from one embedded graph to the other: we draw an 8-reducing triangulation T on S , we push the input in T , we untangle in

T , and we pull the output back into the initial embedded graph H . For the torus, and for the surfaces with boundary (the case of the sphere is trivial in this context), we adopt the same strategy of pushing the input into a particular model (embedded graph), untangling in this model, and pulling the output back. Only the models for these surfaces are not 8-reducing triangulations, but the *canonical system of loops* for the torus, and the *loop systems* for the surfaces with boundary (Chapter 3).

Note that for surfaces with boundary, an obvious strategy would also be to attach a handle to each boundary component to reduce to the case of surfaces without boundary. While this is certainly a valid approach, we prefer to show that the techniques developed in Chapter 6 on 8-reducing triangulations can be mimicked on loop systems to circumvent a large part of the technical machinery.

Note also that the time complexity and output size of the algorithms presented in Theorems 3.3 and 3.2 depend on the genus and the number of boundary components of the surface. When the surface has boundary, this dependency is slightly worse than in the paper versions [1, 5]. The main reason is that surfaces with boundary benefit from a slightly more efficient conversion of model than surfaces without boundary. Yet, in this thesis, we hide those differences by presenting unified statements for Theorems 3.3 and Theorem 3.2.

Application. At the very end of this chapter we apply our results to an alternative framework where the surface S is the Euclidean plane minus a finite set of obstacle points, and where the drawing f is piecewise-linear. The model of computation is the Real RAM. In this framework, we prove the following:

Theorem 7.1. *Let P be a set of p points of \mathbb{R}^2 . Let G be a graph, and let $\varphi : G \rightarrow \mathbb{R}^2 \setminus P$ be a piecewise linear drawing of size n . One can determine whether φ can be untangled in $\mathbb{R}^2 \setminus P$ in $O(p^{5/2}n \log(pn))$ time. If so, one can construct in additional $O(p^5 n^2 \log(pn))$ time a piecewise-linear embedding homotopic to φ in $\mathbb{R}^2 \setminus P$.*

The **size** of a piecewise linear drawing f of a graph G is the size of G plus the total number of segments comprising the edges of the images of G under f .

Organization of the sections. In Section 7.1 we provide algorithms for untangling graphs in the canonical system of loops of the torus. In Section 7.2 we provide algorithms for untangling graphs in the loop systems of the surfaces with boundary. In each case we basically mimick the algorithms for untangling graphs in the 8-reducing triangulations of the closed surfaces of genus at least two. At this point we have untangling algorithms in each one of our three specific models: 8-reducing triangulations for the closed surfaces of genus at least two, canonical system of loops for the torus, and loop systems for the surfaces with boundary. In Section 7.3 we describe the conversions between these specific models and the general model of a graph cellularly embedded on a surface. In Section 7.4 we use all our untangling algorithms, and all our model conversions, to prove our main results, Theorems 3.3 and 3.2. In Section 7.5 we prove our application result, Theorem 7.1.

7.1 Untangling graphs on the canonical system of loops of the torus

In this section, we provide algorithms that untangle graphs and curves drawn in a canonical system of loops of the torus.

7.1.1 Making closed curves cross minimally

In this section we solve the problem of making closed curves cross minimally on the canonical system of loops of the torus. More precisely, we prove the following, analogous to Theorem 6.1 on 8-reducing triangulations:

Theorem 7.2. *On the torus \mathbb{T} , let K a canonical system of loops. Let C be a collection of closed walks of total length n in K . One can compute in $O(n)$ time a collection C' of closed walks in K , freely homotopic to C in \mathbb{T} , such that there exists an approximation of C' with $i_{\mathbb{T}}(C)$ self-crossings.*

Given a collection C of closed curves on \mathbb{T} , there exist formulas for computing $i_{\mathbb{T}}(C)$, see e.g. [91, Section 1.2.3]. However, putting C in minimal position in our setting requires additional work. Recall that the canonical system of loops K consists in two pairwise disjoint simple loops with common basepoint that cross at the basepoint. The dual embedded graph K^* of K is also a canonical system of loops on \mathbb{T} . Endow \mathbb{T} with a flat metric for which the face of K^* is isometric to the interior of a flat square (or parallelogram). Let \mathbb{T}^\times be obtained from \mathbb{T} by removing the vertex of K^* . We say that a closed walk D in K is **quasi-geodesic** if D has no spur, and if D is homotopic to a (non-contractible) geodesic closed curve in \mathbb{T}^\times . We insist that both the geodesic closed curve and the homotopy are in \mathbb{T}^\times , not in \mathbb{T} . The following is analogous to Proposition 6.4 on 8-reducing triangulations:

Lemma 7.1. *On the torus \mathbb{T} , let K be a canonical system of loops. Let C be a non-contractible closed walk of length n in K . One can compute in $O(n)$ time a quasi-geodesic closed walk C' in K , freely homotopic to C in \mathbb{T} .*

Proof. See Figure 7.1. Let K^* be the canonical system of loops dual to K on \mathbb{T} . Let K_1, K_2 be the two loops of K , and let K_1^*, K_2^* be their respective dual loops. Identify \mathbb{T} with the quotient $\mathbb{R}^2/\mathbb{Z}^2$, such that K^* lifts to the following grid: the vertex of K^* lifts to \mathbb{Z}^2 , the loop K_1^* lifts to the vertical segments between (i, j) and $(i, j + 1)$ for $i, j \in \mathbb{Z}$, and the loop K_2^* lifts to the horizontal segments between (i, j) and $(i + 1, j)$ for $i, j \in \mathbb{Z}$. Orient K_1 and K_2 so that, in \mathbb{R}^2 , the lifts of K_1 cross the lifts of K_1^* from left to right, and the lifts of K_2 cross the lifts of K_2^* from bottom to top. Let \mathbb{T}^\times be the surface obtained from \mathbb{T} by removing the vertex of K^* . Let \tilde{K}^* and \tilde{K} be the lifts of K^* and K .

First, we define the quasi-geodesic closed walk C' , without actually computing it. For every $i \in \{1, 2\}$, let k_i record the number of times C takes the loop K_i in the positive direction, minus the number of times C takes K_i in the negative direction. Then $(k_1, k_2) \neq (0, 0)$ since C is non-contractible in \mathbb{T} . Consider any point $p = (p_1, p_2) \in \mathbb{R}^2$ for which the geodesic line $\tilde{\gamma}$ containing p and $p' := (p_1 + k_1, p_2 + k_2)$ does not intersect \mathbb{Z}^2 . Record the sequence of crossings of $\tilde{\gamma}$ with the edges of \tilde{K}^* between the points p and p' . Dually, record a walk \tilde{C}' in \tilde{K} . Then \tilde{C}' projects to a closed walk C' on K . This defines C' .

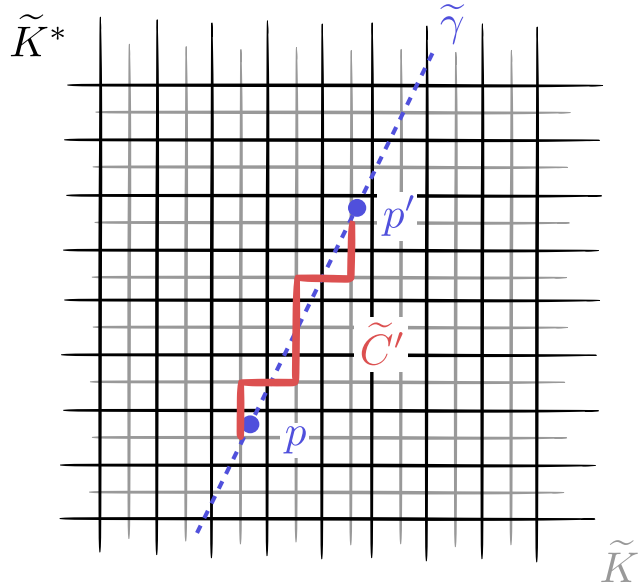


Figure 7.1: The situation in the proof of Lemma 7.1.

By definition C' is freely homotopic to C in \mathbb{T} , and C' has length $O(k_1 + k_2) = O(n)$. Moreover C' is a quasi-geodesic closed walk. Indeed C' has no spur, and in the punctured torus \mathbb{T}^\times there is a geodesic closed curve homotopic to C' , lifted by $\tilde{\gamma}$.

To compute C' , one must choose a point $(p_1, p_2) \in \mathbb{R}^2$ for which the geodesic segment between (p_1, p_2) and $(p_1 + k_1, p_2 + k_2)$ does not intersect \mathbb{Z}^2 , and then compute the sequence of crossings of this segment with the edges of the integral grid \tilde{K}^* . This can be done in $O(n)$ time, using integer arithmetic only, with the standard Bresenham's line algorithm [27]. \square

The following is analogous to Proposition 6.5 on 8-reducing triangulations:

Proposition 7.1. *On a torus \mathbb{T} , let K be a canonical system of loops. Let Σ be the surface obtained from \mathbb{T} by removing an open disk from the face of K . Let C be a collection of quasi-geodesic closed walks in K . Then $i_{\mathbb{T}}(C) = i_{\Sigma}(C)$.*

Proof. We shall construct a closed curve γ_c for every closed walk $c \in C$, homotopic to c in Σ , in such a way that the collection $\{\gamma_c \mid c \in C\}$ is in general position and admits $i_{\mathbb{T}}(C)$ crossings. First assume that every closed walk in C is primitive. Let K^* be the dual of K on \mathbb{T} . Endow \mathbb{T} with a flat metric for which the face of K^* is isometric to the interior of a flat square. Identify the interior of Σ with \mathbb{T} minus the vertex of K^* , such that the arcs of Σ correspond to the loops of K^* . For every $c \in C$, use the assumption that c is quasi-geodesic, and let γ_c be a geodesic closed curve homotopic to c in Σ . Every such γ_c is simple since in the universal cover of \mathbb{T} the lifts of γ_c are parallel geodesic lines, so they cannot intersect themselves nor other lifts of γ_c . Moreover, and without loss of generality, for every $c \neq d \in C$, the closed curves γ_c and γ_d do not overlap (otherwise, perturb them slightly). Also, they cross each other minimally among their homotopy classes in \mathbb{T} . For otherwise there would be a lift of γ_c and a lift of γ_d that cross twice, by Lemma 5.10. The portions of the two lifts in-between the two-crossings would form a bigon with geodesic sides, contradicting the Gauss–Bonnet formula.

For the general case, for every $c \in C$, let $n \geq 1$ be such that c is homotopic in \mathbb{T} to the n^{th} power of a primitive closed curve. Then, and since c is quasi-geodesic, c is actually equal to the n^{th} power of a primitive closed walk \hat{c} , where \hat{c} is quasi-geodesic. Let $\widehat{C} := \{\hat{c} \mid c \in C\}$. By the previous paragraph, put the closed walks in \widehat{C} in general position by homotopy in Σ , so that they intersect $i_{\mathbb{T}}(\widehat{C})$ many times. Then draw each $\gamma_c \in C$ in a neighborhood of \hat{c} as in Figure 5.1. The resulting collection $\{\gamma_c \mid c \in C\}$ is in general position and admits $i_{\mathbb{T}}(C)$ crossings by Lemma 5.9. \square

Proof of Theorem 7.2. Apply Lemma 7.1 to compute in $O(n)$ time a collection C' of quasi-geodesic closed walks in L , freely homotopic to C in \mathbb{T} . Then $i_{\mathbb{T}}(C) = i_{\mathbb{T}}(C') = i_{\Sigma}(C')$ by Proposition 7.1. And there exists an approximation of C' with $i_{\Sigma}(C')$ crossings by Proposition 6.6, since C' clearly has no spur. \square

7.1.2 Untangling loop graphs

In this section we attack the problem of untangling graphs on the canonical system of loops of the torus. We adopt the same strategy as on 8-reducing triangulations, that is, we start by untangling sparse drawings of loop graphs. More precisely, we prove the following, analogous to Proposition 6.7 on 8-reducing triangulations:

Proposition 7.2. *On the torus \mathbb{T} , let K be a canonical system of loops. Let L be a loop graph. Let $\lambda : L \rightarrow K$ be a drawing of size n and depth N . Assume that λ is sparse. One can compute in $O(n)$ time a drawing $\lambda' : L \rightarrow K$, homotopic to λ in \mathbb{T} , such that if λ can be untangled in \mathbb{T} then λ' is a weak embedding.*

Proof. If at some point in the algorithm we are sure that λ cannot be untangled, then we can return as λ' any drawing that clearly cannot be untangled. Now we claim that we can assume, without loss of generality, that L is connected and contains at most three loops. Indeed, if λ can be untangled, then each connected component of L has at most three loops (by Euler's formula) and if it has at least two loops, then by sparsity every embedding of that connected component cuts the torus into a disk. Thus, either the conclusion of the claim holds, or L has several connected components, each made of a single loop. These loops must be pairwise freely homotopic, because otherwise they cannot be untangled; but then λ can be untangled if and only if its restriction to a single connected component of L can be untangled, and a weak embedding of this single loop would immediately provide a weak embedding of L (and in that case the rotation systems are trivial). All this takes linear time. This proves the claim.

Let K^* be the canonical system of loops dual to K on the torus \mathbb{T} . Let k_1, k_2 be the two loops of K , and let k_1^*, k_2^* be their respective dual loops. We identify \mathbb{T} with the quotient $\mathbb{R}^2/\mathbb{Z}^2$, such that K^* lifts to the following grid: the vertex of K^* lifts to \mathbb{Z}^2 , the loop k_1^* lifts to the vertical segments between (i, j) and $(i, j+1)$ for $i, j \in \mathbb{Z}$, and the loop k_2^* lifts to the horizontal segments between (i, j) and $(i+1, j)$ for $i, j \in \mathbb{Z}$; the loops k_1 and k_2 are oriented so that, in \mathbb{R}^2 , the lifts of k_1 cross the lifts of k_1^* from left to right, and the lifts of k_2 cross the lifts of k_2^* from bottom to top. In this way, \mathbb{T} is endowed with a flat metric.

Now, we define a map $f : L \rightarrow \mathbb{T}$, homotopic to λ , by representing the loops of L as geodesics in this metric. For this purpose, we first select arbitrarily the image of the basepoint of L under f ; let p be one of its lifts in \mathbb{R}^2 . The images of any loop e of L under f are then uniquely determined: Indeed, if $\lambda(e)$ is homotopic to $k_1^{u_1} \cdot k_2^{u_2}$, then $f(e)$ must lift

to a line segment from p to $p + (u_1, u_2)$. Finally, we can ensure that f does not intersect the vertex of K^* , by slightly perturbing p if necessary. Note that f actually maps each edge of L to a geodesic closed curve (not only a geodesic path). Now for every edge e of L , the path $f(e)$ crosses $O(n)$ edges of K^* . We can compute the sequence of crossings of $f(e)$ with the edges of K^* in $O(n)$ time: Indeed, $f(e)$ lifts to a line segment in \mathbb{R}^2 that does not intersect the integer points, and given its endpoints, we can compute the sequence of horizontal and vertical edges of the grid crossed by the line segment, in order, with the standard Bresenham's line algorithm [27], which uses integer arithmetic only. This sequence of crossings of $f(e)$ with K^* gives, by duality, a walk in W_e in K . Let $\lambda' : L \rightarrow K$ be the drawing that maps each edge e of L to its walk W_e .

If λ (and thus f) can be untangled, we claim that f is an embedding. It is then immediate that λ' is a weak embedding, since f approximates λ' in the patch system of K , which is the surface obtained from \mathbb{T} by removing the vertex of K^* .

There remains to prove the claim. So assume that f can be untangled. If a non-contractible geodesic closed curve γ in \mathbb{T} is homotopic to a simple closed curve, then γ itself is simple. This is by Lemma 5.10, since the lifts of γ in the universal cover of \mathbb{T} are injective and do not cross each other, γ being primitive by Lemma 5.9. Similarly, any two non-contractible non-homotopic simple geodesic closed curves γ_0 and γ_1 cross minimally, up to (free) homotopy, by Lemma 5.10 and Lemma 5.9. Thus every loop e of L is mapped to a simple closed curve by f , by sparsity and since the image curve of e is simple in an embedding homotopic to f . Also for any two distinct loops e_1 and e_2 of L , the closed curves $f(e_1)$ and $f(e_2)$ cross only once (at the image of the vertex of L), by sparsity and since the image curves of e_1 and e_2 cross only once in an embedding homotopic to f . This proves that f is an embedding. \square

7.1.3 Untangling graphs, efficient factorization

In this section we solve the problem of untangling graphs on the canonical system of loops of the torus. More precisely, we prove the following, analogous to Theorem 6.2 on 8-reducing triangulations:

Theorem 7.3. *On the torus \mathbb{T} , let K a canonical system of loops. Let G be a graph, and let $f : G \rightarrow K$ be a drawing of size n . One can determine in $O(n \log n)$ time whether f can be untangled in \mathbb{T} . If so, one can construct in additional $O(n^2)$ time a weak embedding $f' : G \rightarrow K$, homotopic to f in \mathbb{T} , of depth $O(n)$.*

We adopt the same strategy as on 8-reducing triangulations, so that the proof of Theorem 7.5 is similar to the proof of Theorem 6.2 in Section 6.5. It relies on the notion of factorization defined in Section 6.5.1, and makes use of the key lemmas of Section 6.5.2 (Lemma 6.14 and Lemma 6.15). The efficient factorization stated in Proposition 6.9 for 8-reducing triangulations translates as follows:

Lemma 7.2. *On the torus \mathbb{T} , let K be a canonical system of loops. Let G be a graph, and let $f : G \rightarrow K$ be a drawing of size n . In $O(n \log n)$ time, one can either correctly report that f cannot be untangled in \mathbb{T} or compute a factorization (L, λ, μ) of f , such that L has $O(1)$ loops, and such that λ has depth $O(n)$.*

Proof of Lemma 7.2. The algorithm is an easy variation on the one described on 8-reducing triangulations (Section 6.6). The only change concerns the data structure that stores homotopy classes of walks in K . Here we replace the reduced walks in a 8-reducing triangulation by pairs of integers (u_1, u_2) uniquely representing the homotopy class of $k_1^{u_1} \cdot k_2^{u_2}$, where k_1 and k_2 are the two loops of K . The compressed homotopy tree structure is replaced by a two-level tree-like structure, the first level for the integer u_1 and the second level for the integer u_2 in the notations above. All the operations of the data structure easily extend to this context, as well as the contraction algorithm, since it only uses these four operations. \square

Proof of Theorem 7.3. The algorithm is the one proving Theorem 6.2 in Section 6.5.3, with the following modifications. The surface S , the 8-reducing triangulation T , and the genus g are replaced by the torus \mathbb{T} , the canonical system of loops K , and $O(1)$. Also Proposition 6.7 and Proposition 6.9 are replaced by their analogs, Proposition 7.2 and Lemma 7.2. \square

7.2 Untangling graphs on the loop systems of surfaces with boundary

In this section, we provide algorithms that untangle graphs and curves drawn in a loop system Y of a surface S with boundary.

To do that, we identify S with the surface of the patch system of Y , and we think of Y as embedded in its patch system, where the edges of Y are dual to the arcs of the patch system. In fact, the results of this section would hold more generally if we took Y to be any graph embedded in its patch system, but we will not need that.

7.2.1 Making closed curves cross minimally

In this section we observe that we already have all the tools to make closed curves cross minimally on loop systems. More precisely, we prove the following, analogous to Theorem 6.1 on 8-reducing triangulations, and to Theorem 7.2 on the canonical system of loops of the torus:

Theorem 7.4. *Let Y be a loop system in a surface S with boundary. Let C be a collection of closed walks of total length n in Y . One can compute in $O(n)$ time a collection C' of closed walks in Y , freely homotopic to C , such that there exists an approximation of C' with $i_S(C)$ self-crossings.*

Proof of Theorem 7.4. Greedily remove all spurs from C in $O(n)$ time, resulting in a collection C' of closed walks in Y . Then C' is as desired by Proposition 6.6. \square

7.2.2 Untangling loop graphs

In this section we attack the problem of untangling graphs on loop systems. We adopt the same strategy as on 8-reducing triangulations, and as on the canonical system of loops of the torus, that is we start by untangling sparse drawings of loop graphs. More precisely, we prove the following, analogous to Proposition 6.7 and Proposition 7.2:

Proposition 7.3. *Let Y be a loop system in a surface S with boundary. Let L be a loop graph. Let $\lambda : L \rightarrow Y$ be a drawing of size n and depth N . Assume that λ is sparse. One can compute in $O(n)$ time a drawing $\lambda' : L \rightarrow Y$, homotopic to λ , of depth $O(N)$, such that if λ can be untangled in S then λ' is a weak embedding.*

The proof of Proposition 7.3 resembles the proof of Proposition 6.7 in Section 6.4. Given a drawing $\lambda : L \rightarrow Y$, we choose an edge in each connected component of L and declare it to be a **major edge**; the other edges of L (if any) are **minor edges**. We say that λ is **straightened** if, under λ , (1) each major edge is mapped to a reduced closed walk, and (2) each minor edge is mapped to a reduced walk. The following is analogous to Lemma 6.7:

Lemma 7.3. *One can compute in $O(n)$ time a drawing $\lambda' : L \rightarrow Y$, homotopic to λ , straightened, of size $O(n)$, and of depth $O(N)$.*

Proof. The algorithm and its proof are similar to that of Lemma 6.7, to which we refer for details. Assuming without loss of generality that L is connected, one constructs λ' from λ by first choosing the major edge e_0 of L such that the image walk $\lambda(e_0)$ has minimal length, by removing all spurs from the closed walk $\lambda(e_0)$ by free homotopy, and finally by removing all spurs from the image walks of the minor edges while fixing their basepoint. \square

The following is analoguous to Proposition 6.8:

Lemma 7.4. *If a drawing $\lambda : L \rightarrow Y$ is sparse, straightened, and can be untangled in S , then λ is a weak embedding.*

Recall that we view S as the surface of the patch system of Y , where the arcs of the patch system are dual to the edges of Y . Also, the proof of Lemma 7.4 make use of the classical Nielsen–Schreier theorem, which we recall for convenience: this theorem states that every subgroup of a free group is itself free.

Proof. Assume that λ is sparse and straightened, and that there is an embedding $\lambda' : L \rightarrow S$ homotopic to λ (we view λ as a map $L \rightarrow S$ by composing it with the embedding $Y \rightarrow S$). We shall prove that λ is a weak embedding. In a first step, we modify λ' by an ambient isotopy (fixing the boundary of S) so that afterward λ' maps every major edge of L to a closed curve without spur in S (with respect to the arcs of S). For this purpose, we remark that λ' maps the major edges of L to a set of pairwise disjoint simple closed curves in S . Whenever there is a bigon between the image of a major edge and an arc of S , there is an innermost bigon, which we remove by ambient isotopy, thus decreasing the number of crossings between $\lambda'(L)$ and the arcs of S . We repeat this operation until there is no more bigon, at which point the image curves of the major edges are have no spur.

Now consider a connected component L_0 of L , the vertex v of L_0 , and the major edge e in L_0 . We can make the image walk of e cross the arcs of S with the same sequences in λ' and λ (not up to cyclic permutation, *exactly* the same sequence) simply by sliding the image of v along the image of e in λ' . We slide $\lambda'(v)$ by an ambient isotopy in the tubular neighborhood of $\lambda'(e)$. We can do so since the sequence of crossings of $\lambda'(e)$ with the arcs of S is a cyclic permutation of the one of $\lambda(e)$; here we make use of the fact that if two freely homotopic closed curves have no spur, then their sequences of crossings with the arcs of S are equal up to cyclic permutation. In λ' we slide the image of v along the image of e so that

the two sequences become equal; λ' is still an embedding. We do this for every connected component L_0 of L in turn.

Consider again some connected component L_0 of L , with vertex v , and major edge e . We claim that we can modify λ' by sliding the image of v some finite number of times around the image of e (each time, the image of v making one full loop around the image of e) so that, in the end, there is a free homotopy between $\lambda'|_{L_0}$ and $\lambda|_{L_0}$ in which the image of v does not leave its face of the patch system. To prove this claim first observe that it would be possible to do so, not by sliding along the image of e , but by some *free* homotopy of $\lambda'|_{L_0}$. During this homotopy the image of v makes a loop γ in S . The loop γ commutes, up to homotopy, with the loop $\lambda'(e)$ as $\lambda'(e) \simeq \lambda(e)$ by the previous paragraph and $\lambda(e) \simeq \gamma \cdot \lambda'(e) \cdot \gamma^{-1}$ by construction, where \simeq denotes homotopy of loops relatively to their basepoint. Moreover, the loop $\lambda'(e)$ is non-contractible since λ' is sparse, so it is also primitive by Lemma 5.9. Thus γ is a power (up to homotopy) of $\lambda'(e)$. Let us prove this. The fundamental group of S is a free group. It is known (and we prove) that in a free group if two elements x and y commute, then they are powers of some common element: indeed, the subgroup K generated by x and y is an Abelian subgroup, which is free by the Nielsen–Schreier theorem; but the only Abelian free group is \mathbb{Z} ; so K is cyclic. Now, as mentioned above, $\lambda'(e)$ is primitive.

Now in λ' any bigon between the image of a minor edge of L_0 and an arc of S does not contain any vertex of $\lambda'(L)$. Indeed, otherwise, the image walk of the major edge incident to that vertex would have a spur, a contradiction. So we can remove any innermost bigon by an ambient isotopy. When this is not possible anymore, by the preceding claim, the image loops of the minor edges intersect the arcs of S with the same sequence in λ' and λ . Here we make use of the fact that if two loops are homotopic relatively to their basepoint (or via a free homotopy in which the basepoint does not leave its face of S), and if they have no spur, then they intersect the arcs of S with the same sequence. \square

Proof of Proposition 7.3. Apply Lemma 7.3 to compute the drawing $\lambda' : L \rightarrow Y$. If λ can be untangled then λ' is a weak embedding by Lemma 7.4. \square

7.2.3 Untangling graphs, efficient factorization

In this section we solve the problem of untangling graphs on loop systems. More precisely, we prove the following, analogous to Theorem 6.2 on 8-reducing triangulations, and to Theorem 7.3 on the canonical system of loops of the torus:

Theorem 7.5. *Let Y be a loop system of size m in a surface S with boundary. Let G be a graph, and let $f : G \rightarrow Y$ be a drawing of size n . One can determine in $O(mn \log(mn))$ time whether f can be untangled in S . If so, one can construct in additional $O(n^2)$ time a weak embedding $f' : G \rightarrow Y$, homotopic to f , of depth $O(n)$.*

Again, we adopt the same strategy as on 8-reducing triangulations, so that the proof of Theorem 7.5 is similar to the proof of Theorem 6.2 in Section 6.5. The efficient factorization (Proposition 6.9) here translates as follows:

Lemma 7.5. *Let Y be a loop system of size m in a surface S with boundary. Let G be a graph, and let $f : G \rightarrow Y$ be a drawing of size n . In $O(mn \log(mn))$ time, one can either correctly report that f cannot be untangled in S or compute a factorization (L, λ, μ) of f , such that L has $O(m)$ loops, and such that λ has depth $O(n)$.*

Proof. The algorithm is an easy variation of the one for 8-reducing triangulations (Section 6.6.2, proof of Proposition 6.9). The only change concerns the data structure that stores homotopy classes of walks. Here we replace the reduced walks in a 8-reducing triangulation by walks without spur in H . That is, we store these walks as lists of directed edges of H in a tree-like fashion to implement the data-structure of Section 6.6.1. The operations introduced in Section 6.6.1 extend to this context, and Section 6.6.2 extends immediately, because it only uses these operations. \square

Proof of Theorem 7.5. The algorithm is the one proving Theorem 6.2 in Section 6.5.3, with the following modifications. The 8-reducing triangulation T and the genus g are replaced by the loop system Y and its size m . Also Proposition 6.7 and Proposition 6.9 are replaced by their analogs, Proposition 7.3 and Lemma 7.5. \square

7.3 Model conversions

Until now, our untangling algorithms operate on drawings of graphs in very specific models: reducing triangulations for surfaces without boundary of genus greater than or equal to two, canonical system of loops for the torus, and loop systems for the surfaces with boundary. In this section we describe the conversions between these specific models and the general model of an arbitrary graph cellularly embedded on the surface. This is in preparation for the proofs of the two main theorems of this chapter, Theorems 3.3 and 3.2.

We fix a surface S of genus g with b boundary components, and a graph H of size m cellularly embedded on S . We consider the case where S is closed genus at least two ($b = 0$ and $g \geq 2$) in Section 7.3.1, the case where S is a torus ($b = 0$ and $g = 1$) in Section 7.3.2, and the case where S has boundary ($b \geq 1$) in Section 7.3.3.

7.3.1 Closed surfaces of genus at least two

In this section we prove the following:

Lemma 7.6. *Assume $g \geq 2$ and $b = 0$. One can construct in $O(gm)$ time an 8-reducing triangulation T of S , and a drawing $\varphi : H \rightarrow T$, of depth $O(g)$, homotopic to the inclusion map $H \rightarrow S$. One can construct in additional $O(g^2m)$ time a weak embedding $\psi : T \rightarrow H$, of depth $O(gm)$, isotopic to the inclusion map $T \rightarrow S$.*

In the lemma 7.6, and in the other lemmas of this chapter, when we say that a weak embedding f is isotopic to an embedding g , we mean that there exist embeddings arbitrarily close to f that are all isotopic to g .

To prove Lemma 7.6 we use the following result of Pocchiola, Lazarus, Vegter, and Verroust [133]:

Lemma 7.7 (Pocchiola, Lazarus, Vegter, and Verroust, 2001). *Let S be a surface of genus g without boundary. Let H be a graph of size m cellularly embedded on S . One can compute in $O(gm)$ time the overlay of H and a canonical system of loops K , such that each loop of K crosses each edge of H at most four times*

Proof of Lemma 7.6. First, we construct from H a particular graph Q embedded on S , that we obtain by inserting a new vertex in every face, by adding an edge between this vertex

and every corner of the face, and by removing from H all its initial edges. Observe that Q is a quadrangulation of size $O(m)$ since H has size $O(m)$. We will use Q advantageously, and this is crucial to obtain the claimed $O(gm)$ time complexity. Let K be the canonical system of loops for the surface of genus g without boundary. With Lemma 7.7 we compute in $O(gm)$ time an embedding of K in general position with respect to Q , such that each loop of K crosses each edge of Q at most four times. Then we consider the 8-reducing triangulation T for the surface of genus g without boundary depicted in Figure 6.1. This triangulation T extends K , so the embedding of K extends to an embedding of T in general position with respect to Q , in which each edge of T crosses Q at most $O(gm)$ times, see Figure 7.2. While we already computed the overlay of K and Q , we do not compute the overlay of T and Q yet, as this overlay may have size $\Omega(g^2m)$.

Let us first explain how to compute the drawing $\varphi : H \rightarrow T$, in $O(gm)$ time. Our strategy is to push the 1-skeleton of H by homotopy into the 1-skeleton of T , and then to let φ be the resulting drawing of H on T . As a preliminary, we push every edge e of H to a walk of length 2 in Q . We shall now explain how to push Q into the 1-skeleton of T by homotopy, in a way that will send every edge of Q to a walk of length $O(g)$ in T . See Figure 7.3. Consider the overlay between K and Q . For each loop of K crossed k times by Q , we contract $k - 1$ such subedges, and then we contract some subedges of Q in order to bring every vertex of Q to the basepoint of K (Figure 7.3). Let Q' be the resulting contracted version of Q ; now, we have the overlay of Q' and of K , two one-vertex graphs sharing the same vertex. The effect is that each edge of Q' is transformed into an ordered set of $O(g)$ pairwise non-crossing arcs in the polygonal schema, each connecting two corners. We push each of those arcs into a path of length $O(1)$ in T .

Finally, let us explain how to construct the drawing $\psi : T \rightarrow H$, in $O(g^2m)$ time. Our strategy is to push the 1-skeleton of T arbitrarily close to H , and then to let ψ be the resulting weak embedding of T in H . To do so, we forget about the modifications of the previous paragraph, and we compute the overlay A of T and Q (Figure 7.2, Right) in $O(g^2m)$ time. Then, we modify A in two steps. See Figure 7.4. First, recall that by construction, every edge e of Q is between a vertex v of H and a dual vertex w that was inserted in a face of H when building Q . In the overlay A , we bring the k intersection points between e and T close to v , by contracting the $k - 1$ subedges of e that are not incident to w . Second, we contract some subedges of T in A to put every vertex of T close to a vertex of H . In the end, every edge e of T is close to a walk of length $O(gm)$ in H , so we can retrieve the desired weak embedding of the 1-skeleton of T into H . \square

7.3.2 Torus

The following is analogous to Lemma 7.6:

Lemma 7.8. *Assume $g = 1$ and $b = 0$. One can construct in $O(m)$ time a canonical system of loops K of S , a drawing $\varphi : H \rightarrow K$, of depth $O(1)$, homotopic to the inclusion map $H \rightarrow S$, and a weak embedding $\psi : K \rightarrow H$, of depth $O(m)$, isotopic to the inclusion map $K \rightarrow S$.*

Lemma 7.8 is easy, in fact almost immediate from Lemma 7.7, so the proof is omitted.

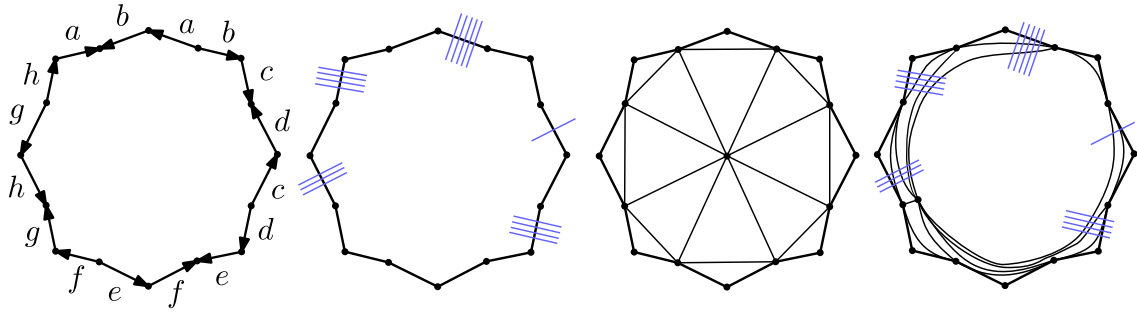


Figure 7.2: From left to right: (a) The canonical polygonal schema associated to the canonical system of loops K for the surface S of genus $g = 4$. (b) A blue graph Q on S , in general position with respect to K , that intersects every edge of K at most m times. (c) A reducing triangulation T whose 1-skeleton contains K . (d) An embedding of T on S such that each edge of T crosses Q at most $O(gm)$ times.

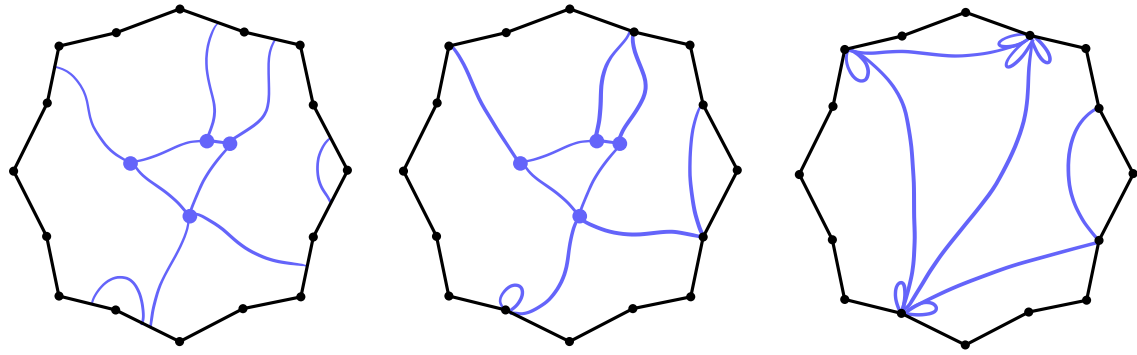


Figure 7.3: (Left) In the proof of Lemma 7.6, the graph Q is represented in blue in the face of K . (From Left to Middle) The intersection points between Q and K are slided along the edges of K . (From Middle to Right) Some subedges of Q are contracted to push the vertices of Q to the vertex of K .

7.3.3 Surfaces with boundary

In this section we prove the following, analogous to Lemma 7.6 and Lemma 7.8:

Lemma 7.9. *Assume $b \geq 1$. One can construct in $O((g+b)m)$ time a loop system Y of S , a drawing $\varphi : H \rightarrow Y$, of depth $O(g+b)$, homotopic to the inclusion map $H \rightarrow S$, and a weak embedding $\psi : Y \rightarrow H$, of depth $O(m)$, isotopic to the inclusion map $Y \rightarrow S$.*

(Lemma 7.9 is trivial when $g = 0$ and $b = 1$, equivalently when the surface S is a closed disk. In this case the loop system Y is a single vertex without any loop.)

Proof. Let us first explain how to construct the loop system Y from H . We close each boundary component of S with a disk, and we remove one point from the interior of each disk, obtaining a non-compact surface \hat{S} . We operate in \hat{S} instead of S . The graph H is embedded in \hat{S} . The faces of that graph that correspond to boundary components of S are punctured. We keep the invariant that, at every step, every face contains at most one puncture. See Figure 7.5. First, we contract an arbitrary spanning tree Z in H , so that the resulting H' has only one vertex. Second, as long as an edge of H' is incident to a face

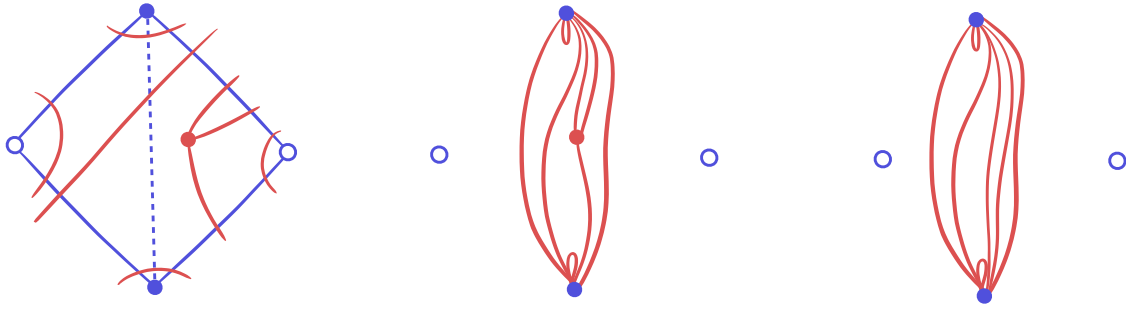


Figure 7.4: (Left) In the proof of Lemma 7.6, a portion of T is here represented in red in some face of Q . The two blue disk vertices belong to H . The two blue circle vertices were inserted in faces of H to build Q , they are dual vertices. The dashed edge was deleted from H to build Q . The plain edges belong to Q . (From Left to Middle) In the overlay A between T and Q , every edge of Q is detached from its incident dual vertex, then contracted. (From Middle to Right) Some subedge incident to the red disk vertex of T is contracted.

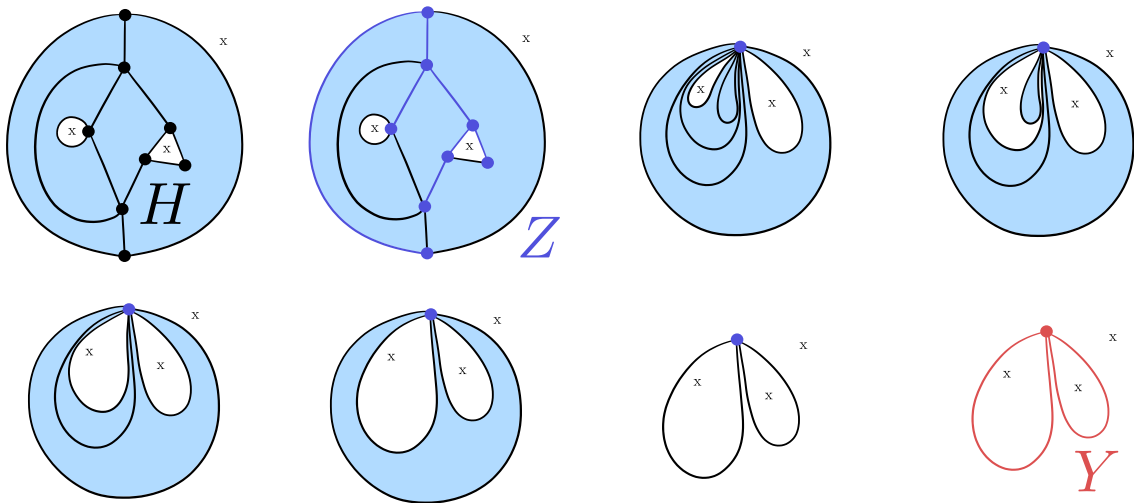


Figure 7.5: In the proof of Lemma 7.9 the loop system Y is constructed from the embedded graph H by contracting the spanning tree Z and then deleting some edges.

punctured *and* to a face not punctured, we remove it, thus merging the two faces into a single punctured face. In the end every face is punctured, so the resulting graph Y is indeed a loop system of S . It is easy to achieve this in linear time, e.g., by using a spanning forest of the faces of H' in which the ‘‘seeds’’ are the punctured faces.

Let us now explain how to compute the drawing $\psi : Y \rightarrow H$. See Figure 7.6. Consider an arbitrary root vertex r for Z . We constructed Y from H by contracting Z , and then by deleting some edges, so each loop of Y corresponds to an edge $uv \in H \setminus Z$, and is naturally mapped to the (undirected) walk W in H that is the concatenation of the path in Z between r and u , of the edge uv , and of the path in Z between v and r . We map e to W in ψ , and we map the basepoint of Y to r . Then ψ is as desired, and it can be constructed in $O((g+b)m)$ time since Y has $O(g+b)$ loops by Euler’s formula, each mapped to a walk of length $O(m)$.

Finally, let us explain how to compute the drawing $\varphi : H \rightarrow Y$. Our strategy is to push the 1-skeleton of H into the 1-skeleton of Y by homotopy, and then to let φ be the resulting

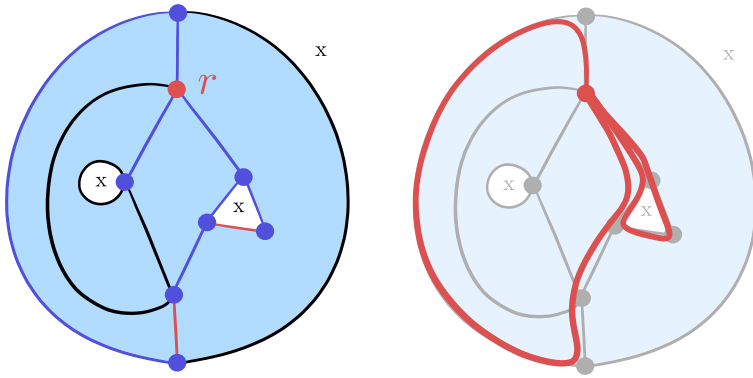


Figure 7.6: Following Figure 7.5. In the proof of Lemma 7.9, construction of the weak embedding $\psi : Y \rightarrow H$.

drawing of H on Y . First, as above, we contract the edges of the spanning tree Z , so that the contracted edges are now mapped to the basepoint of Y . Then we consider the other edges of H . Any such edge that is not in Y belongs to a unique face of Y , and can be rerouted homotopically in φ to a walk on the boundary of the face. By Euler's formula, Y contains $O(g + b)$ loops, so the boundary of the face is made of $O(g + b)$ edges. Thus, φ maps each edge of H to a walk of length $O(g + b)$ in Y . \square

7.4 Untangling graphs on surfaces

In this section, we finally wrap things up and prove the two main theorems of this chapter, Theorems 3.3 and 3.2. We start with Theorem 3.3, which we restate for convenience:

Theorem 3.3. *Let S be a surface of genus smaller than s , with less than s boundary components. Let H be a graph of size m cellularly embedded on S . Let G be a graph, and let $f : G \rightarrow H$ be a drawing of size n . One can determine in $O(m + s^2n \log(sn))$ time whether f can be untangled in S . If so, one can construct in additional $O(s^2mn^2)$ time a weak embedding $f' : G \rightarrow H$, homotopic to f in S , of depth $O(s^2mn)$.*

As a preliminary in proving Theorem 3.3, note that we can compute in $O(m)$ time the genus g of S (by using Euler's formula on H), and the number b of boundary components of S . Then the topological type of S is fully specified by g and b . If S is the sphere, then any drawing that maps G to a single vertex of H is a weak embedding whenever f can be untangled, so this case is solved by the algorithm of Akitaya, Fulek, and Tóth [10], restated in Theorem 5.1. There are three other cases, depending on whether S has boundary or not, and with a special case for the torus. The general strategy is the same for all cases: Roughly, we push the initial drawing f into the appropriate model (8-reducing triangulation, canonical system of loops, loop system), we untangle the drawing in this model (or correctly determine that the drawing cannot be untangled, in which case we abort), and we push the result back into the initial graph H for returning it. There is a subtlety though: If we are only interested in determining whether f can be untangled in S , and thus applying only the first part of the algorithm, then we can gain efficiency by contracting H (and transforming f accordingly) into a graph of size $O(s)$ as a preliminary step, before applying the algorithm. We now provide the details for each case.

Proof of Theorem 3.3 when $b = 0$ and $g \geq 2$. Consider the following algorithm, in two steps. As a first step, apply Lemma 7.6 to construct in $O(sm)$ time an 8-reducing triangulation T of S , and a drawing $\varphi : H \rightarrow T$, of depth $O(s)$, homotopic to the inclusion map $H \rightarrow S$. The composed map $\varphi \circ f$ is homotopic to f , and has size $O(sn)$. Apply Theorem 6.2 to determine in $O(s^2n \log(sn))$ time whether $\varphi \circ f$, equivalently f , can be untangled in S . This first step takes $O(sm + s^2n \log(sn))$ time in total.

As a second step, if f can be untangled, Theorem 6.2 provides in additional $O(s^2n^2)$ time a weak embedding $f' : G \rightarrow T$, homotopic to f , of depth $O(sn)$. And Lemma 7.6 provides in additional $O(s^2m)$ time a weak embedding $\psi : T \rightarrow H$, of depth $O(sm)$, isotopic to the inclusion map $T \rightarrow S$. The composed drawing $\psi \circ f'$ is then a weak embedding, homotopic to f , of depth $O(s^2mn)$, that can be retrieved in $O(s^2mn^2)$ time.

If we are just interested in determining whether f can be untangled in S , then we can just apply the first step. Moreover, we claim that in that case we can first contract H in $O(m)$ time into a graph of size $O(s)$ (and transform f accordingly), as a preliminary step, so even before applying the first step. This way, determining whether f can be untangled takes $O(m + s^2n \log(sn))$ time instead of $O(sm + s^2n \log(sn))$ time. Let us prove the claim. We can, in $O(m)$ time, contract an arbitrary spanning tree of H and transform the input drawing f homotopically into a drawing of G in that new graph. Then we can iteratively remove edges forming monogons in H , and merge together edges forming bigons, all in $O(m)$ time. Euler's formula then implies that H has $O(s)$ loops. This proves the claim, and the theorem in the case $b = 0$ and $g \geq 2$. \square

Proof of Theorem 3.3 when $b = 0$ and $g = 1$. The overall strategy is similar. For the first step, apply Lemma 7.8 to construct in $O(m)$ time a canonical system of loops K of S , and a drawing $\varphi : H \rightarrow K$, of depth $O(1)$, homotopic to the inclusion map $H \rightarrow S$. The composed map $\varphi \circ f$ is homotopic to f , and has size $O(n)$. Apply Theorem 7.3 to determine in $O(n \log n)$ time whether $\varphi \circ f$, equivalently f , can be untangled in S .

For the second step, if f can be untangled, Theorem 7.3 provides in additional $O(n^2)$ time a weak embedding $f' : G \rightarrow K$, homotopic to f , of depth $O(n)$. And Lemma 7.8 provides in additional $O(m)$ time a weak embedding $\psi : K \rightarrow H$, of depth $O(m)$, isotopic to the inclusion map $K \rightarrow S$. The composed drawing $\psi \circ f'$ is then a weak embedding, homotopic to f , of depth $O(mn)$, that can be retrieved in $O(mn^2)$ time.

Again, if we are just interested in determining whether f can be untangled, we can, as a preprocessing step, contract the graph H into a small graph, here of size $O(1)$. This proves the theorem in the case $b = 0$ and $g = 1$. \square

Proof of Theorem 3.3 when $b \geq 1$. Again, the overall strategy is similar. As a first step, apply Lemma 7.9 to construct in $O(sm)$ time a loop system Y of S , and a drawing $\varphi : H \rightarrow Y$, of depth $O(s)$, homotopic to the inclusion map $H \rightarrow S$. The composed map $\varphi \circ f$ is homotopic to f , and has size $O(sn)$. Also Y has size $O(s)$. Apply Theorem 7.5 to determine in $O(s^2n \log(sn))$ time whether $\varphi \circ f$, equivalently f , can be untangled in S .

For the second step, if f can be untangled in S , Theorem 7.5 provides in additional $O(s^2n^2)$ time a weak embedding $f' : G \rightarrow Y$, homotopic to f , of depth $O(sn)$. And Lemma 7.9 provides in additional $O(sm)$ time a weak embedding $\psi : Y \rightarrow H$, of depth $O(m)$, isotopic to the inclusion map $Y \rightarrow S$. The composed drawing $\psi \circ f'$ is then a weak embedding, homotopic to f , of depth $O(smn)$, and it can be retrieved in $O(smn^2)$ time. This second step takes $O(s^2n^2 + smn^2)$ time in total.

And again, if we are just interested in determining whether f can be untangled, we can, as a preprocessing step, contract the graph H into a graph of size $O(s)$. This proves the theorem. \square

Now we prove Theorem 3.2, which we restate for convenience:

Theorem 3.2. *Let S be a surface of genus smaller than s , with less than s boundary components. Let H be a graph of size m cellularly embedded on S . Let C be a collection of closed walks of total length n in H . One can compute $i_S(C)$ in $O(m + s^2 + sn \log(sn))$ time. One can construct in additional $O(s^2mn)$ time a collection of closed walks C' in H , freely homotopic to C in S , in minimal position.*

Proof of Theorem 3.2. As in the proof of Theorem 3.3 the case where S is the sphere (or the disk) is trivial, and there are three other cases depending on the topological type of the surface S , specified by its genus g and its number b of boundary components. Again, in each case we push the input (here a set of closed walks instead of a drawing of a graph) into the appropriate model, solve the problem in this model, and push the result back into the initial graph H . We only detail the case $b = 0$ and $g \geq 2$, since the other cases are similar and easier, and since we already provided details on conversions between models in the proof of Theorem 3.3.

So assume $b = 0$ and $g \geq 2$. Similarly to the algorithm untangling graphs (proof of Theorem 3.3), the algorithm putting the curves in C in minimal position has two steps: the first step only computes $i_S(C)$, while the second step actually produces curves in minimal position. For the first step, apply Lemma 7.6 to construct in $O(sm)$ time the 8-reducing triangulation T of S and the drawing $\varphi : H \rightarrow T$. The closed walks in C , once composed by φ , become a collection C' of closed walks in T , freely homotopic to C , of total length $O(sn)$. Apply Theorem 6.1 to compute in $O(sn)$ time a collection C' of closed walks in T , freely homotopic to C in S , in minimal position. At this point $i_S(C) = i_S(C')$ can be computed in $O(sn \log(sn))$ time by computing a minimal perturbation of C' with Theorem 5.2, and then counting its self crossings with Lemma 5.11. This first step takes $O(sm + sn \log(sn))$ time.

For the second step, Lemma 7.6 provides in additional $O(s^2m)$ time a weak embedding $\psi : T \rightarrow H$. The closed walks in C' , once composed by ψ , become a collection of closed walks C'' in H , of total length $O(s^2mn)$, freely homotopic to C , in minimal position. Retrieve C'' in $O(s^2mn)$ time, and return it. This second step takes $O(s^2mn)$ time.

Again, if we are just interested in computing $i_S(C)$, we can just apply the first step after preliminarily contracting the graph H into a graph of size $O(s)$. This preliminary contraction step allows us to compute $i_S(C)$ in $O(m + s^2 + sn \log(sn))$ time instead of $O(sm + sn \log(sn))$ time.

Finally, as already explained, the two other cases (torus and surfaces with boundary) are treated similarly. Lemma 7.6 and Theorem 6.1 are replaced by Lemma 7.9 and Theorem 7.4, and by Lemma 7.8 and Theorem 7.2, respectively. \square

7.5 Application to the punctured plane

In this section we prove our application result, Theorem 7.1, which we restate for convenience:

Theorem 7.1. *Let P be a set of p points of \mathbb{R}^2 . Let G be a graph, and let $\varphi : G \rightarrow \mathbb{R}^2 \setminus P$ be a piecewise linear drawing of size n . One can determine whether φ can be untangled in*

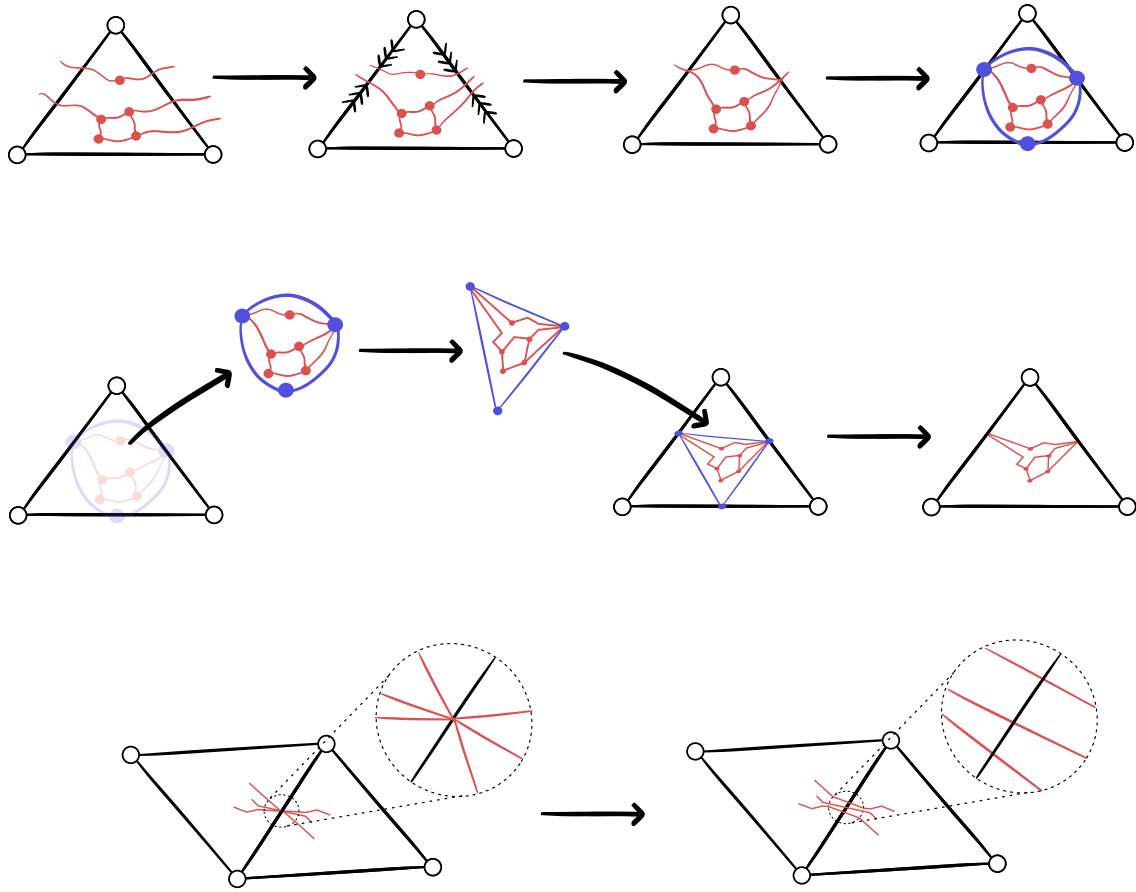


Figure 7.7: In the proof of Theorem 7.1, the topological embedding φ' (in red) is transformed into a piecewise-linear embedding. (Top) In a triangle Δ of T (in black), the crossings of φ' with the sides of Δ are packed at the middle points of those edges, then a cycle with three vertices (in blue) is attached to the image X of φ' in Δ . (Middle) $X \cup C$ is replaced by a piecewise-linear embedding ambient isotopic to it, then C is deleted. (Bottom) The resulting piecewise linear drawing ψ' of G is made an embedding again by unpacking its crossings the edges of T .

$\mathbb{R}^2 \setminus P$ in $O(p^{5/2}n \log(pn))$ time. If so, one can construct in additional $O(p^5 n^2 \log(pn))$ time a piecewise-linear embedding homotopic to φ in $\mathbb{R}^2 \setminus P$.

Proof of Theorem 7.1. First we reduce to the combinatorial map model in a way very similar to Cabello, Liu, Mantler, and Snoeyink [32, Lemma 12], in the same spirit as Colin de Verdière and de Mesmay [47, Section 5.2]. More precisely we do the following. We fix a closed box around each point of P that does not intersect the image of φ nor the other boxes, and we denote by B_P the resulting collection of boxes. We also fix a bounding box B that contains the image of φ and all the boxes in B_P in its interior. Then we construct in time almost linear in p a cellular decomposition T of $B \setminus B_P$, of size $O(p)$, whose edges are rectilinear. Without loss of generality T and φ are in general position. Finally, we consider the dual graph H of T , and the drawing $f : G \rightarrow H$ that (1) maps each vertex v of G to the vertex of H dual to the face of T containing $\varphi(v)$, and (2) maps each edge e of G to the walk in H encoding the crossings between the path $\varphi(e)$ and the edges of T . The drawing f has size

$O(\lambda n)$, where λ is the maximum number of times a segment of the drawing intersects edges of T . Also, f is computed in $O(\lambda n)$ time, and is homotopic to φ in $B \setminus P$.

First assume that we are just interested in determining if there exists an embedding homotopic to f . In this case we can ensure $\lambda = O(\sqrt{p})$ by constructing T in such a way that each line in the plane crosses at most $O(\sqrt{p})$ edges of T [32, Lemma 11]. We apply Theorem 3.3 to f and H to determine in $O(p^{5/2}n \log(pn))$ time if there exists an embedding homotopic to f , equivalently to φ , in $B \setminus P$.

Now assume that there exists an embedding homotopic to f , and that we want to compute a piecewise linear embedding homotopic to f . In this case we prefer to construct T so that it is a triangulation (for example, but not necessarily, a Delaunay triangulation), without caring about λ . We have $\lambda = O(p)$. Let us now explain how to compute the desired embedding in additional $O(p^5 n^2)$ time. Theorem 3.3 provides in $O(p^5 n^2)$ time a weak embedding $f' : G \rightarrow H$, of size $O(p^5 n^2)$. The algorithm of Akitaya, Fulek, and Tóth (Theorem 5.1) provides in $O(p^5 n^2 \log(pn))$ time an embedding φ' approximating f' in the patch system of H . Here the patch system of H corresponds to the triangulation T , and the overlay between T and the embedding φ' is given *topologically* by a an embedded graph of size $O(p^5 n^2)$ in which T and G are embedded.

We transform the topological embedding φ' into a piecewise-linear embedding in three steps. See Figure 7.7. As a first step we do the following for each edge e of T . We consider the crossings between e and $\varphi'(G)$, and we modify φ' by sliding those crossings along e to pack all of them at the middle point of e . We do so for every edge e of T , and we consider the resulting drawing ψ of G . The crossings between $\psi(G)$ and the edges of T are now packed at the middle points of those edges, but ψ is still an embedding everywhere else.

As a second step, we do the following in each triangle Δ of T . We consider the part X of $\psi(G)$ that lies inside Δ . We attach an outer-cycle C to X , whose vertices are the middle points of the edges of Δ ; this is the blue cycle in Figure 7.7. If X does not intersect every edge of Δ some of the vertices of C may not be attached to X : this is fine, and is for example the case of the bottom vertex of the blue cycle in Figure 7.7. We now construct an embedding isotopic to $X \cup C$ (in particular, C remains the outer-cycle of the embedding). Ideally, we would like such an embedding in which every edge is a linear segment, a Fáry embedding. But this is not always possible since $X \cup C$ may have loops and parallel edges. This is easily solved: we insert two vertices in each edge of X , consider the resulting graph X' , observe that $X' \cup C$ has no loops nor parallel edges, and compute a Fáry embedding isotopic to $X' \cup C$ instead, using classical algorithms [171, 60, 59], in linear time. Equivalently, a piecewise-linear embedding isotopic to $X \cup C$ in which every edge of C is a linear segment and every edge of X is a path of three linear segments. Up to applying an affine transformation to the embedding, we may assume without loss of generality that the three vertices of C are embedded at the corresponding middle points of the edges of Δ . In ψ , we replace X by its piecewise-linear embedding, and we forget C . We do so for every triangle Δ of T , and we consider the resulting piecewise-linear drawing ψ' of G .

As a third and final step, we make ψ' an embedding by unpacking the crossings of ψ' with each edge of T , while keeping ψ' piecewise linear, as in Figure 7.7 (Bottom). \square

Chapter 8

A Discrete Analog of Tutte Embeddings

In this chapter we focus on reducing triangulations, on which we translate the framework of Tutte embeddings. We consider drawings of graphs G in reducing triangulations T . Recall (Chapter 3) that such drawings map the vertices of G to vertices of T , and the edges of G to walks in T . Our first contribution is the definition of *harmonious drawings*, which are a natural discrete analog of Tutte drawings. We omit this definition for now. Our second contribution is a purely discrete analog of the theorems of Tutte (Theorem 4.1) and Y. Colin de Verdière (Theorem 4.4):

Theorem 3.4. *Let S be a surface of genus $g \geq 2$ without boundary. Let T be a reducing triangulation of S . Let G be a graph, and let $f : G \rightarrow T$ be a harmonious drawing. There is an embedding homotopic to f in S if and only if f is a weak embedding.*

Note that Theorem 3.4 handles reducing triangulations, not just 8-reducing triangulations, and reducing triangulations can be subdivided to obtain finer reducing triangulations (Section 6.1).

Our third contribution is a polynomial-time algorithm to make a drawing harmonious. Our algorithm proceeds by “local” moves, which never increase the length of any edge of the drawing. In this way, it allows to build many harmonious drawings. In detail:

Theorem 3.5. *Let S be a surface of genus $g \geq 2$ without boundary. Let T be a reducing triangulation of S , with m edges. Let G be a graph, and let $f : G \rightarrow T$ be a drawing of size n . We can compute in $O((m+n)^2 n^2)$ time a drawing $f' : G \rightarrow T$, harmonious, homotopic to f in S , such that for every edge e of G , the image of e under f' is not longer than under f .*

We emphasize surfaces without boundary as they constitute the hardest cases, but we obtain similar results on all the surfaces with boundary, by extending the notion of reducing triangulations to those surfaces, attaching or not vertices of the drawing to the boundary; this includes the case of the disk, similar to Tutte’s original result. In contrast, the case of the sphere is not relevant in this context. Moreover, our results are not valid on the torus; this case is also very particular, since it admits a flat metric, and a reducing triangulation, but it turns out that we need non-positive curvature and at least one point of negative curvature; see Lemma 6.5 below.

Discussion. The original theorem of Tutte assumes that the graph is 3-connected, and the generalization by Y. Colin de Verdière assumes that it is the 1-skeleton of a triangulation.

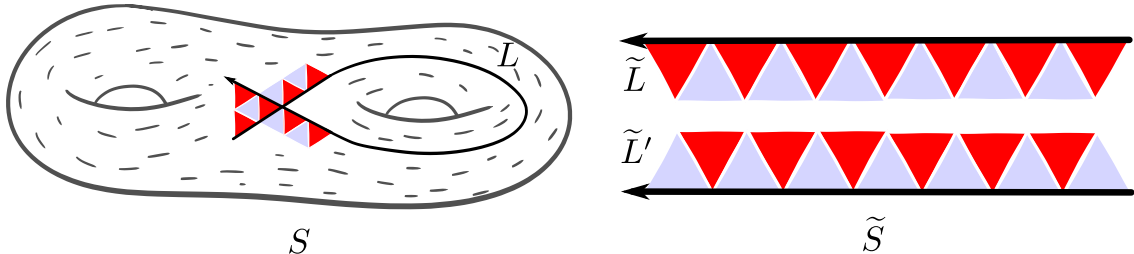


Figure 8.1: (Left) The surface S of genus two without boundary, equipped with a reducing triangulation T , and a left line L in T . (Top Right) The universal covering space \tilde{S} of S , i.e. the plane, and a left line \tilde{L} that lifts L in \tilde{S} . (Bottom Right) A right line \tilde{L}' in \tilde{S} .

Those assumptions are necessary to deduce that the drawing is an embedding. In our setting however, we are happy with a weak embedding, and this allows us to get rid of any assumption on the graph in Theorem 3.4.

In a sense Theorem 3.4 generalizes Proposition 6.8 from drawings of loop graphs to drawings of general graphs. Although formally Proposition 6.8 is not a particular case of Theorem 3.4 since a drawing of a loop graph can be straightened without being harmonious, and vice-versa.

Organization of the sections. We introduce harmonious drawings in Section 8.1. We prove Theorem 3.4 in Section 8.2. We prove Theorem 3.5 in Section 8.3. We discuss the extensions to surfaces with boundary in Section 8.4.

Preliminaries on drawings. In this chapter we need some additional definitions about drawings. A drawing $f : G \rightarrow H$ is **simplicial** if the depth (Chapter 3) of f is smaller than or equal to one, equivalently if f sends each edge of G to a vertex or an edge of H . Even more particular, a (graph) **homomorphism** is a drawing that sends every edge of G to an edge of H . Importantly, drawings can be turned into simplicial drawings, which can be turned into graph homomorphisms. Indeed every drawing $f : G \rightarrow H$ **factors** uniquely as a *simplicial* $\bar{f} : \bar{G} \rightarrow H$, where \bar{G} is a subdivision of G , where every edge e of G whose image walk $f \circ e$ has length $n \geq 2$ is subdivided into a path of length n in \bar{G} , and where e is not subdivided otherwise. Also a simplicial map f **factors** uniquely as a *homomorphism* $\hat{f} : \hat{G} \rightarrow H$ for some graph \hat{G} : the graph \hat{G} is obtained from \bar{G} by contracting the edges mapped to single vertices; then f corresponds naturally to a homomorphism from \hat{G} to H .

8.1 Harmonious drawings

In this section, we provide the key definition of *harmonious drawings* of graphs in a reducing triangulation, used in the statements of our theorems. We actually start with the notion of strongly harmonious drawings, which are the discrete analog of barycentric drawings, in which each inner vertex is drawn in *convex position*: every straight line I containing v sees edges incident to v on both sides, here understood in the *strong sense* that some edges incident to v enter the two *open* half-planes separated by I . Harmonious drawings are a slightly relaxed notion that is suitable for our results.

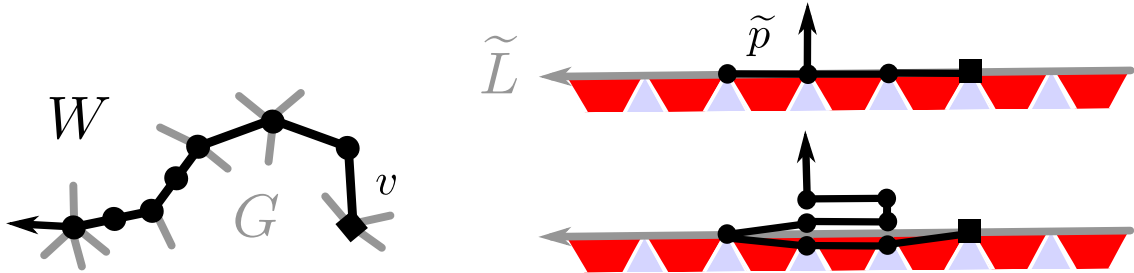


Figure 8.2: (Left) The vertex v and the walk W in the definition of strong harmony. (Top right) The lifts \tilde{L} and \tilde{p} , when L makes only 3_r -turns. (Bottom right) The path \tilde{p} slightly unpacked to illustrate that \tilde{p} can go back and forth, and stagnate.

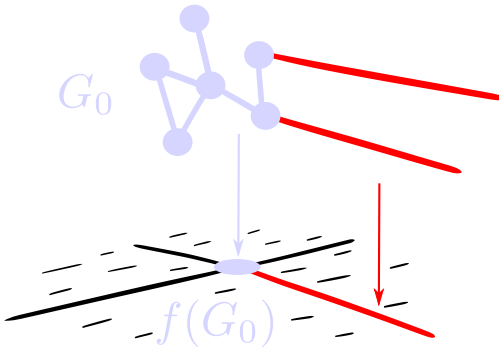


Figure 8.3: A spur.

8.1.1 Preliminary definitions

Let S be a surface without boundary not homeomorphic to the sphere, and let T be a reducing triangulation of S . Let \tilde{T} be the (infinite) reducing triangulation that lifts T in the universal cover \tilde{S} of S . In \tilde{T} , we consider a left (resp. right) **line** to be a bi-infinite walk \tilde{L} that makes only 3_r -turns (resp. -3_r -turns). See Figures 8.1 and 8.2. Note that \tilde{L} is reduced, and is thus simple by Proposition 6.1. Here L is directed, so that informally L has a *right* side and a *left* side. Also L has a **central vertex** v , separating L into two semi-infinite paths, both containing v . The part of L after v is the **non-negative part** of L , it contains v . A path \tilde{p} starting from the central vertex v of \tilde{L} **escapes** \tilde{L} if \tilde{p} enters the right (resp. left) side of \tilde{L} at some point, and if the prefix of \tilde{p} before this point is contained in the non-negative part of \tilde{L} .

On S , the **lines** are again the bi-infinite walks (not simple this time, since T is finite) that make only 3_r -turns or only -3_r -turns; note that the lines on S lift to the lines on \tilde{S} . On S , a path p **escapes** a line L if there are a lift \tilde{L} of L , and a lift \tilde{p} of p starting from the central vertex of \tilde{L} , such that \tilde{p} escapes \tilde{L} .

Now we generalize the notion of spurs from walks and closed walks to drawings of graphs. So let G and M be graphs, and let $f : G \rightarrow M$ be simplicial. A **cluster** of f is a connected subgraph G_0 of G whose edges are all mapped by f to a single vertex of M , maximal under this condition. A cluster G_0 of f is a **spur** if G_0 is not a connected component of G , and if the directed edges from G_0 to $G \setminus G_0$ are all mapped by f to the same directed edge of M ; see Figure 8.3. Note that the direction of the edges matters when M has loops.

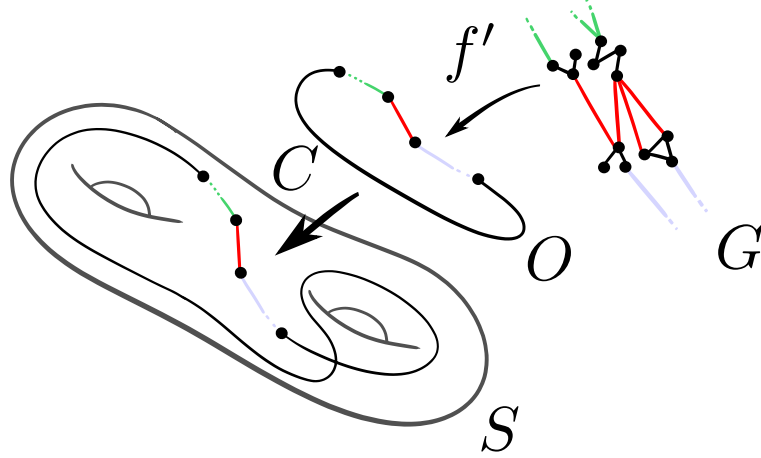


Figure 8.4: A graph G , a cycle graph O , and a surface S equipped with a reducing triangulation T (not represented). A simplicial map $f' : G \rightarrow O$ without spur, and a reduced closed walk $C : O \rightarrow T$. The composed drawing $C \circ f'$ is harmonious.

8.1.2 Strongly harmonious drawings

A simplicial map $f : G \rightarrow T$ is **strongly harmonious** if for every vertex v of G , and for every line (left or right) L whose central vertex is $f(v)$ in T , there is a walk W based at v in G whose image path $f \circ W$ escapes L . See Figure 8.2.

Intuitively, f is strongly harmonious if for every vertex v of G , and for every bi-infinite walk L in T starting at $f(v)$ making only 3_r -turns (resp. -3_r -turns), there is a walk W in G whose image by f may go “forward” on L , sometimes “backward” on L , but not to the point it goes before its central point, and then leaves L to its right (resp. left). But L is non-simple, and periodic since T is finite; W is allowed to wrap, say, 2.3 times forward along L , then 1.8 times backward, and then to leave L to its right (resp. left). Formalizing this phenomenon seems to be more easily captured using the universal covering space, as above.

8.1.3 Harmonious drawings

Harmony is a slightly relaxed version of strong harmony. On a connected graph G , a simplicial map $f : G \rightarrow T$ is **harmonious** if f is strongly harmonious, or if $f = C \circ f'$ for some cycle graph O , some reduced closed walk $C : O \rightarrow T$, and some simplicial map $f' : G \rightarrow O$, without spur. See Figure 8.4. We emphasize that C does not need to be strongly reduced, so that it is possible for C to make only 3_r -turns. In general, a simplicial map $f : G \rightarrow T$ is harmonious if f is harmonious on every connected component of G .

Finally, recall that every drawing $f : G \rightarrow T$ factors into a unique simplicial map $\bar{f} : \bar{G} \rightarrow T$. We say that f is harmonious (resp. strongly harmonious) if \bar{f} is.

8.1.4 Remarks

We conclude this section with two remarks. First we remark that one reason (among others) explaining why our results do not extend to the torus is given by Lemma 6.5, that there are a reducing triangulation T of the torus, and a closed walk C in T , such that every closed walk freely homotopic to C is not reduced. Second we illustrate why strong harmony is

not sufficient for our purposes. The reason is that some drawings of graphs in reducing triangulations cannot be made strongly harmonious by homotopy:

Lemma 8.1. *Let S be a surface without boundary, not the sphere nor the torus. There are a reducing triangulation T of S , and a closed walk C in T , such that every closed walk freely homotopic to C is not strongly harmonious.*

Proof. There is an 8-reducing triangulation T of S . There is a closed walk C_2 in T that makes only 3_r -turns; indeed every walk that makes only 3_r -turns will repeat itself since T is finite. Let C_1 be the closed walk obtained by pushing C_2 to the left in the way depicted in Figure 6.10: C_1 makes only -3_r -turns. Then C_1 and C_2 are not strongly harmonious. Let C' be a closed walk in T , freely homotopic to C_1 or C_2 . If C' is strongly harmonious, then C' is equal to C_1 or to C_2 (up to cyclic permutation and reversal). Indeed C' is reduced. If C' does not make only 3_r -turns, then C' is *strongly* reduced, so $C' = C_1$ by Proposition 6.2. If C' makes only 3_r -turns, then reversing the colors of T makes C' strongly reduced under the new coloring, and gives $C' = C_2$. \square

8.2 A Tutte theorem on reducing triangulations

In this section we prove our discrete analog of Tutte's theorem, Theorem 3.4, which we restate for convenience:

Theorem 3.4. *Let S be a surface of genus $g \geq 2$ without boundary. Let T be a reducing triangulation of S . Let G be a graph, and let $f : G \rightarrow T$ be a harmonious drawing. There is an embedding homotopic to f in S if and only if f is a weak embedding.*

In spirit, the proof of Theorem 3.4 follows some of the steps of previous proofs of Tutte's theorem [52, 79]: (1) we reduce to the case where f is homotopic to the embedding of the 1-skeleton of a triangulation of S . We then have a continuous map φ from a triangulated copy of S to S itself. (2) We prove that φ is orientation-preserving (or degenerate) on each triangle. (3) We deduce that f can be turned into an embedding f' by homotopy not only in S , but even in the neighborhood Σ of the 1-skeleton of the reducing triangulation. (4) In Σ , we transform f' by isotopy into an embedding arbitrarily close to f , thereby proving that f is a weak embedding.

We emphasize that, since our goal is to prove that f is a weak embedding, we do not have to worry about degenerate cases, which is one of the difficulties in the continuous case. Rather, we *allow* such degeneracies, which leads to challenges with a different flavor.

In order to ease the reading, we present steps (1)-(4) in a different order. We start with (4) in Section 8.2.1, then (3) in Section 8.2.2, (1) in Section 8.2.3, and (2) in Section 8.2.4. We finally wrap things up and prove Theorem 3.4 in Section 8.2.5.

8.2.1 A Tutte theorem on patch systems

In this section all graphs and drawings are finite, without further mention. We prove the following:

Proposition 8.1. *Let M be a graph embedded on a surface. Let G be a graph, and let $f : G \rightarrow M$ be simplicial and without spur. If there is an embedding homotopic to f in the patch system of M , then f is a weak embedding.*

Proposition 8.1 can be seen as an analog of Tutte's theorem for drawings in patch systems, in the sense that it asserts that if a drawing f can be untangled and is “straightened” (here, has no spur), then f is already untangled (here, is a weak embedding).

The rest of this section is devoted to the proof of Proposition 8.1. The strategy to prove Proposition 8.1 is to find a sequence of moves (swaps) between the drawing f and a weak embedding, and to prove that applying a move to a weak embedding results in a weak embedding.

In a graph M , we say that a (closed) walk W is **canonical** if W has no spur, that is if W does not use an edge of M and its reversal consecutively. We shall use the three following classical facts, see, e.g., Stillwell [177, Chapter 2]. (1) If two canonical walks are homotopic in M relatively to their end-vertices, then they are equal. (2) If two canonical closed walks are freely homotopic, then they differ by a cyclic permutation. (3) If two loops a and b based at the same point of M commute, i.e., if there is a loop c such that a is homotopic to $c \cdot b \cdot c^{-1}$ (where the homotopy fixes the basepoint), then a and b are homotopic to powers of a common loop.

Lemma 8.2. *Let G and M be graphs, and let $f : G \rightarrow M$ be simplicial. If G is connected, if f is contractible, and if f has no spur, then $f(G)$ is a single vertex of M .*

Proof. We may assume without loss of generality that f is a homomorphism by contracting the edges that belong to clusters of f . Assume by contradiction that $f(G)$ is not a single vertex of M . Since G is connected, some edge of G is mapped by f to an edge of M . Since f has no spur, there is a semi-infinite walk W in G such that $f \circ W$ is canonical. Since G is finite, there is a subwalk W' of W , not a single vertex, that starts and ends at the same vertex of G . And the loop $f \circ W'$ is non-contractible in M by (1), contradicting the assumption that f is contractible. \square

Until the end of this section, we need to consider general drawings (instead of simplicial ones). Recall from Chapter 3 that every drawing $f : G \rightarrow M$ factors uniquely as a simplicial map $\bar{f} : \bar{G} \rightarrow M$, where \bar{G} is a subdivision of G . The clusters and spurs of f are those of \bar{f} . The vertices of \bar{G} inserted in the edges of G are clusters of \bar{f} . All other clusters of \bar{f} are subgraphs of G .

Lemma 8.3. *Let M be a graph embedded on a surface. Let G be a graph, and let $f : G \rightarrow M$ be a drawing. If there is an embedding homotopic to f in the patch system of M , then there is a weak embedding $f' : G \rightarrow M$, homotopic to f , that has no spur.*

Proof. Let Σ be the patch system of M . We regard f as a map from G to Σ . There is by assumption an embedding $g : G \rightarrow \Sigma$ homotopic to f . We can assume that g crosses the arcs of Σ as few times as possible subject to the constraint that it is an embedding homotopic to f . Let $f' : G \rightarrow M$ be the drawing of which g is an approximation. Then f' is a weak embedding homotopic to f .

There remains to prove that f' has no spur. By contradiction, assume that it does. See Figure 8.5. Let G_0 be the cluster of the spur, and let a be the arc of Σ dual to the directed edge of the spur. Let $E \subset \Sigma$ contain, for every edge e directed from G_0 to $G \setminus G_0$, the prefix of the image path $g(e)$ that leaves $g(G_0)$ to reach its first crossing with a . Let a_1 be the subpath of a that starts just before its first crossing with E and ends just after its last crossing with E . Because g is an embedding, there exists a simple path a_2 in Σ with the

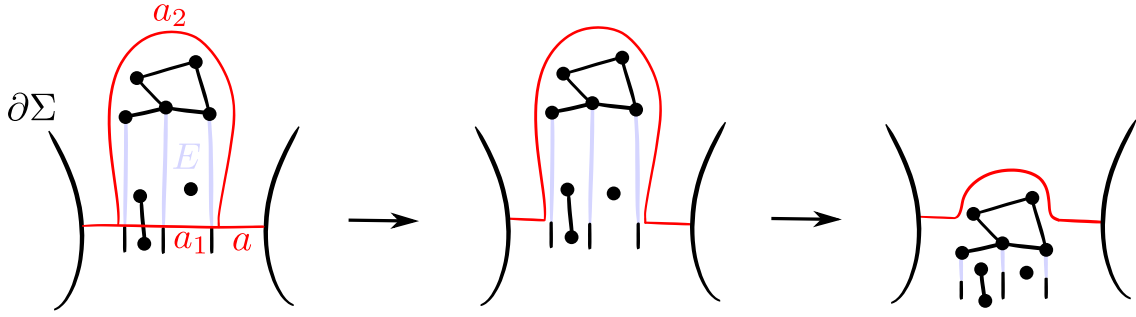


Figure 8.5: In the proof of Lemma 8.3, if f' had a spur, then the number of crossings of g with the arcs of Σ could be decreased.

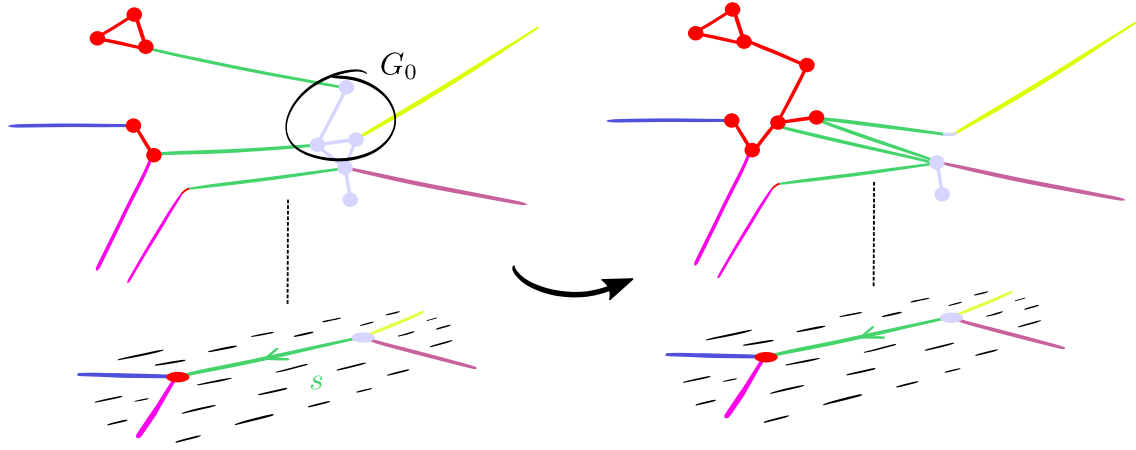


Figure 8.6: Swap of the subgraph G_0 along the directed edge s .

same endpoints as a_1 , otherwise disjoint from the arcs of Σ and from $g(G)$, such that the disk bounded by a_1 and a_2 contains $g(G_0)$. We consider a self-homeomorphism h of Σ that affects only a neighborhood of the disk bounded by a_1 and a_2 , and pushes a_2 to a_1 . Then $h \circ g$ is an embedding of G homotopic to g , with less crossings with the arcs of Σ , a contradiction. \square

A drawing $f : G \rightarrow M$ is **essential** if there is no connected component of G on which f is contractible. Let $f : G \rightarrow M$ be an essential drawing. Let G_0 be an induced subgraph of G , connected and mapped to a single vertex of T by f . Let s be a directed edge of T based at the vertex $f(G_0)$. Consider the following operation that transforms f homotopically into another essential drawing $f' : G \rightarrow M$ (Figure 8.6). First slide $f(G_0)$ along s . Then, among the image walks of the edges directed from G_0 to $G \setminus G_0$, those that initially admitted s as a prefix now start with the concatenation of s^{-1} and s : shorten those walks by removing this prefix. In the particular case where f and f' both have no spur (in addition of being essential), we call this operation a **swap**. A key but trivial observation is that, if f' results from a swap of f , then f results from a swap of f' .

Note that if f has no spur, if G_0 is a cluster of f , and if s is the image by f of some edge directed from G_0 to $G \setminus G_0$, then f' has no spur, so the operation is indeed a swap in this case. Every swap constructed in this section will either be such a swap, or the “inverse” of such a swap.

Lemma 8.4. *Let G and M be graphs, and let $f, f' : G \rightarrow M$ be drawings. If f and f' are essential and without spur, and if they are homotopic, then there is a sequence of swaps between f and f' .*

Proof. We shall perform swaps on f and f' so that in the end $f = f'$. Assume without loss of generality that G is connected, and fix a spanning tree Y of G . We claim that there is a sequence of swaps that modify f so that in the end $f(Y)$ is a single vertex of M . To prove the claim, we say that an edge e of Y is contracted if $f(e)$ is a single vertex of M . We choose an arbitrary root for Y , and given any edge e of Y , we refer to the edges of Y distinct from e and separated from the root by e as the descendants of e . We prove the claim by considering an edge e of Y , by assuming that e is not contracted and that every descendant of e is contracted, and by exhibiting a swap that shortens $f \circ e$ while keeping the descendants of e contracted. Direct e so that the tail vertex of e is the closest to the root of Y . Let G_0 be the cluster containing the head vertex of e . Since the descendants of e are all contracted, they all belong to G_0 . Since e is not contracted, we may consider the last directed edge s of the walk $f \circ e$. The swap of $f(G_0)$ along the reversal of s shortens $f \circ e$, and keeps the descendants of e contracted. This proves the claim.

We use the claim immediately on both f and f' , then contract the spanning tree Y in both drawings. Every edge e of G not in Y becomes a loop. The image loop $f \circ e$ is contractible if and only if $f' \circ e$ is contractible, and in that case $f(e) = f(Y)$ and $f'(e) = f'(Y)$ are single vertices of M by (1). Also given any two edges e_1 and e_2 of G not in Y , we have $f \circ e_1 \simeq f \circ e_2$ if and only if $f' \circ e_1 \simeq f' \circ e_2$, where \simeq denotes the homotopy of loops relatively to their basepoint. In that case $f \circ e_1 = f \circ e_2$ and $f' \circ e_1 = f' \circ e_2$ by (1). By contracting the contractible loops and identifying the homotopic loops in both f and f' , we may assume that every connected component of G has a single vertex (all its edges are loops), and that each of f and f' maps the edges of G to pairwise distinct non-trivial walks in M .

The end of the proof is similar to the proof of Lemma 7.4, to which we refer for details. Let v be the vertex of G . Since f and f' are essential, the graph G is not a single vertex, so G has a loop e . At this point, $f \circ e$ and $f' \circ e$ are canonical walks, but not necessarily canonical closed walks; however, by performing swaps on f and f' at v a few times if needed, we enforce that $f \circ e$ and $f' \circ e$ are canonical closed walks. Then by (2), and since $f \circ e$ and $f' \circ e$ are freely homotopic, $f \circ e$ is a cyclic permutation of $f' \circ e$. By performing swaps on f again a few times, we enforce that $f \circ e$ and $f' \circ e$ are actually equal (not up to cyclic permutation). At this point, we claim that we can slide $f(v)$ around $f \circ e$ by performing swaps on f , so that in the end f and f' are homotopic relatively to v . This claim implies $f = f'$ by (1), which proves the lemma. There remains to prove the claim. For this, consider the path followed by $f(v)$ during some free homotopy from f to f' . This path is a loop based at $f(v)$. Let W be the canonical walk homotopic to it. We prove the claim by showing that $f \circ e$ and W are equal to powers of the same walk. Indeed let C be a primitive canonical closed walk such that $f \circ e$ is freely homotopic to a power of C . Without loss of generality $f \circ e$ is equal to a power of C by (2). Also W commutes with $f \circ e$ since $f \circ e = f' \circ e$, and since $f \circ e$ is homotopic to the walk $W \cdot (f' \circ e) \cdot W^{-1}$. Thus the walk W is homotopic to a power of C by (3). And so W is equal to this power of C by (1). \square

Lemma 8.5. *Let M be a graph embedded on a surface. Let G be a graph, and let $f, f' : G \rightarrow M$ be drawings. If f and f' are essential, if f' results from a swap of f , and if f is a weak embedding, then f' is a weak embedding.*

Proof. Let Σ be the patch system of M , and let $F : G \rightarrow \Sigma$ be an embedding that approximates f in Σ . Let G_0 be the subgraph of the swap, and let a be the arc of Σ dual to the directed edge of the swap. Let $E \subset \Sigma$ contain, for every edge e directed from G_0 to $G \setminus G_0$, the prefix of the image path $F(e)$ that leaves $F(G_0)$ to reach either a vertex of $F(G \setminus G_0)$ in the same face of Σ , or its first crossing with an arc of Σ . Let $E_1 \subset E$ contain the paths that reach a . Then $E_1 \neq \emptyset$, for otherwise G_0 would either be a spur in f' , or it would be a cluster mapped to a single vertex in f' . Let a_1 be the subpath of a that starts just before its first crossing with E_1 and ends just after its last crossing with E_1 . Because F is an embedding, there exists a simple path a_2 with the same endpoints as a_1 , otherwise disjoint from the arcs of Σ , and disjoint from $F(G)$ except for each path in $E \setminus E_1$ that a_2 may cross at most once, such that the disk D bounded by a_1 and a_2 contains $F(G_0)$.

We claim that D does not contain any part of $F(G)$ other than $F(G_0)$ and E . By contradiction assume that it does. Then D contains the image $F(v)$ of a vertex v of $G \setminus G_0$, since G_0 is an induced subgraph of G , and since any edge of $F(G \setminus G_0)$ intersecting D must have an endpoint in D . If a path based at $F(v)$ in $F(G)$ does not intersect a_1 nor $F(G_0)$, then this path stays in the interior of D , and so it does not intersect any arc of Σ . Therefore, in f' , the cluster containing v is either mapped to a single vertex, or is a spur, which is a contradiction.

Now consider a self-homeomorphism h of Σ that affects only a neighborhood of D , and pushes a_2 to a_1 . Then $h \circ F$ is an embedding of G , that approximates f' by the preceding claim. \square

The following lemma is easy and might be folklore, but we could not find a reference, so we provide a proof for completeness:

Lemma 8.6. *Let S be a surface. Let G be a graph, and let $f : G \rightarrow S$ be a map. If f is contractible, and if there is an embedding homotopic to f , then G is planar.*

Proof. Without loss of generality G is connected. Fix a vertex r and a spanning tree T of G . There is an embedding $f' : G \rightarrow S$ homotopic to f . In f' , almost contract the image of T by isotopy, without changing the image of r , in order to push the image of T inside a small neighborhood N of $f(r)$. Every edge e of G not in T is mapped by f' to a simple contractible loop. Those loops can be pushed inside N by isotopy since each of them bounds a disk with only (possibly) contractible loops inside it, by a result of Epstein [83, Theorem 1.7]. \square

Finally, we prove Proposition 8.1:

Proof of Proposition 8.1. If G' is a connected component of G on which f is contractible, then $f(G')$ is a single vertex of M by Lemma 8.2, and $f|_{G'}$ can made an embedding in an arbitrarily small disk in the patch system of Σ by Lemma 8.6. So we can assume that f is essential. By Lemma 8.3, there is a weak embedding $g : G \rightarrow M$, homotopic to f , without spur. By Lemma 8.4, there is a sequence of swaps from g to f . By Lemma 8.5, all the maps from G to M in this sequence are weak embeddings, thus f is itself a weak embedding, as desired. \square

8.2.2 A property of the coherently oriented maps homotopic to the identity

In a surface S , let $Y \subset S$ be finite. A map $\varphi : S \rightarrow S$ is **coherently oriented** at Y if $\varphi^{-1}(Y)$ is finite and if φ is, locally, an orientation-preserving homeomorphism around every point of $\varphi^{-1}(Y)$, or an orientation-reversing homeomorphism around every point of $\varphi^{-1}(Y)$.

In this section we prove the following, that will be used in the case where Y contains one point per face of T , regarding $S \setminus Y$ as the patch system of T .

Proposition 8.2. *Let S be a surface without boundary. Let $\varphi : S \rightarrow S$ be a map, homotopic to the identity map of S . Let $Y \subset S$ be finite. If φ is coherently oriented at Y , then $\#\varphi^{-1}(Y) = \#Y$ and $\varphi|_{S \setminus \varphi^{-1}(Y)}^{S \setminus Y}$ is homotopic to a homeomorphism $S \setminus \varphi^{-1}(Y) \rightarrow S \setminus Y$.*

We prove Proposition 8.2 using the topological notion of the degree of a self-map $\varphi : S \rightarrow S$.

Proof. Let $y \in Y$. We claim that $\varphi^{-1}(y)$ contains only one point, and that φ is orientation-preserving around this point. To prove this claim, let n^+ and n^- denote the number of points of $\varphi^{-1}(y)$ around which φ is respectively orientation-preserving and orientation-reversing. The difference $n^+ - n^-$ does not depend on the choice of y (as long as y is chosen so that φ is locally a homeomorphism around every point of $\varphi^{-1}(y)$) and is known as the degree of φ .

The degree of a map is invariant by homotopy, and φ is homotopic to the identity of S , so $n^+ - n^- = 1$. We assumed $n^- = 0$ or $n^+ = 0$. Thus $n^- = 0$ and $n^+ = 1$.

Using our claim, for every $y \in Y$, there is a closed disk $B_y \subset S$ containing y in its interior, such that $\varphi^{-1}(B_y)$ is a closed disk A_y , and such that $\varphi|_{A_y}^{B_y}$ is an orientation-preserving homeomorphism. Without loss of generality, the disks $\{B_y\}_{y \in Y}$ are pairwise disjoint. Let N be the surface obtained from S by removing the interiors of the disks $\{B_y\}_{y \in Y}$, and M be obtained by removing the interiors of the disks $\{A_y\}_{y \in Y}$. The map $\varphi' := \varphi|_M^N$ is defined. Since φ is a degree one map, $\varphi' : M \rightarrow N$ is a degree one map. By construction, φ' maps the boundary of M to the boundary of N and the interior of M to the interior of N , and the restriction and corestriction of φ' to the boundaries of M and N is a homeomorphism. It follows from a result by Edmonds [80, Theorem 4.1] that φ' is homotopic to a homeomorphism $M \rightarrow N$, where the homotopy is relative to ∂M . (More precisely, this result follows from [80, Theorem 3.1] by noting that (1) each branch covering of degree ± 1 is a homeomorphism, and that (2) each pinch map from M to M is homotopic to the identity, because the simple closed curve defining the pinch must bound a disk.) \square

8.2.3 From graphs to triangulations

Let T be a reducing triangulation of a surface S , and let Z be a triangulation of S . A map $\varphi : S \rightarrow S$ is **simplicial for** (Z, T) if φ maps Z to T simplicially, and if φ sends every face of Z to a vertex, an edge, or a face of T . It is **strongly harmonious** if $\varphi|_Z^T$ is strongly harmonious.

In this section, we prove the following proposition, which (essentially) allows us to consider mappings from the entire surface to itself, instead of drawings of graphs:

Proposition 8.3. *Let S be a surface without boundary distinct from the sphere. Let T be a reducing triangulation of S . Let G be a finite graph embedded in S , and let $f : G \rightarrow T$ be*

simplicial. Assume that f is strongly harmonious, and that f is homotopic to the inclusion map $G \hookrightarrow S$. There are a triangulation Z of S whose 1-skeleton contains a subdivision of G as a subgraph, and a map $\varphi : S \rightarrow S$ simplicial for (Z, T) , with $\varphi|_G^T = f$, such that φ is strongly harmonious and homotopic to the identity map of S .

The proof of Proposition 8.3 relies on two lemmas:

Lemma 8.7. *Let S be a surface without boundary distinct from the sphere. Let T be a reducing triangulation of S . Let G be a graph obtained from another graph G' by inserting a path graph P between (possibly equal) vertices of G' . Let $f : G \rightarrow T$ be simplicial. If $f|_{G'}$ is strongly harmonious, and if f maps P to a reduced walk in T , then f is strongly harmonious.*

Proof. If P is a single edge, then it does not affect strong harmony. So assume that P has an interior vertex v , and let L be a left line (the right line case being similar) in T whose central vertex is $f(v)$. We will exhibit a walk based at v in G whose image path escapes L . This will prove the lemma. Consider the universal covering triangulation \tilde{T} of T , and a lift \tilde{L} of L in \tilde{T} . Consider also the reduced walk $X := f|_P$. There are a lift \tilde{P} of P , a lift \tilde{v} of v in \tilde{P} , and a lift $\tilde{X} : \tilde{P} \rightarrow \tilde{T}$ of X , such that $\tilde{X}(\tilde{v})$ is the central vertex of \tilde{L} . Let \tilde{w}_0 and \tilde{w}_1 be the two end-vertices of \tilde{P} , and let \tilde{P}_0 and \tilde{P}_1 be the two sub-walks of \tilde{P} that go from \tilde{v} to respectively \tilde{w}_0 and \tilde{w}_1 . Since \tilde{X} is a reduced walk, and since \tilde{L} makes only 3_r -turns, one of \tilde{P}_0 and \tilde{P}_1 , say \tilde{P}_0 without loss of generality, is such that $\tilde{X} \circ \tilde{P}_0$ either escapes \tilde{L} , or stays in the non-negative part of \tilde{L} . In the first case, considering the vertex w_0 of G lifted by \tilde{w}_0 , the portion P_0 of P from v to w_0 is such that $f \circ P_0$ escapes L . In the latter case, replace the central vertex of \tilde{L} by $\tilde{X}(\tilde{w}_0)$, and project the resulting line onto the surface, obtaining a line L' which is a shift of L . Since w_0 belongs to G' , and since $f|_{G'}$ is strongly harmonious, there is a walk Q based at w_0 in G such that $f \circ Q$ escapes L' . Then the concatenation P'_0 of P_0 and Q is such that $f \circ P'_0$ escapes L . \square

Lemma 8.8. *Let w, v_0, v_1 be pairwise distinct vertices of a plane reducing triangulation T . If v_0 and v_1 are adjacent in T , then there is $i \in \{0, 1\}$ such that, along the reduced walk from v_i to w , the vertex consecutive to v_i is adjacent to or equal to v_{1-i} .*

Proof. Let e be the edge of T between v_0 and v_1 ; direct e so that it sees blue at its left, and assume without loss of generality that it is directed from v_0 to v_1 . Let W_1 be the reduced walk from v_1 to w . Assume that the vertex consecutive to v_1 in W_1 is neither equal nor adjacent to v_0 , for otherwise there is nothing to do. Let W_0 be the concatenation of e with W_1 . By assumption, W_0 does not make a 0-turn, 1-turn, or -1 -turn at v_1 , and by our choice of direction of e , it also does not make a 2_r -turn, so it is reduced. And W_0 starts with edge e , as desired. \square

Proof of Proposition 8.3. In this proof, we will use the following standard topological fact: Every graph embedded on a surface can be extended to a triangulation by adding edges (not vertices). This can be done by repeatedly inserting an edge e inside a face F , where e “differs” from every edge e' on the boundary of F in the sense that the concatenation of e and e' does not bound a disk in F .

At any time we denote by G^\diamond the graph derived from G by removing its degree two vertices. The proof is in three steps; see Figure 8.7. In the first step, as long as some face of G^\diamond is not a triangle, we insert an edge e in this face, as described in the preceding paragraph.

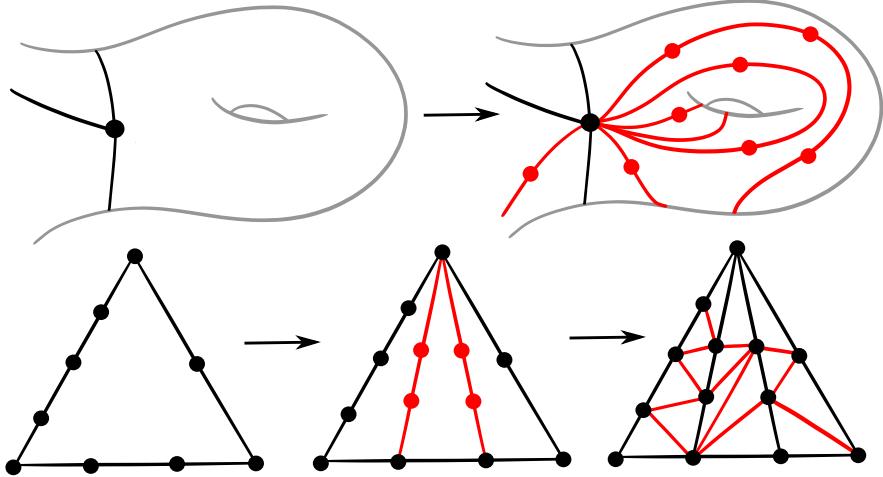


Figure 8.7: In the proof of Proposition 8.3, the embedded graph G is extended to a triangulation.

Doing so, we consider the homotopy from the inclusion map $G \hookrightarrow S$ to the map f , and apply this homotopy to the two end-vertices of e , thus extending e to a path e' between vertices of T . Let p be the unique reduced path homotopic to e' (Proposition 6.1). If the length n of p is greater than one, then we insert $n - 1$ vertices in G along e . We also extend f to e by mapping e to p . In this way, f remains homotopic to the inclusion map $G \hookrightarrow S$, and f remains strongly harmonious by Lemma 8.7. Now, every face of G^\diamond is a triangle.

In the second step (see Figure 8.7, bottom center), for every (triangular) face m of G^\diamond , we consider an edge e incident to m in G^\diamond . If e is subdivided in G , then we insert a path in m from each interior vertex of e to the vertex of m opposite to e . As in the previous paragraph, we map each of the new paths to a reduced path in T , so that f remains homotopic to the inclusion map $G \hookrightarrow S$, and so that f remains strongly harmonious. Now, every (triangular) face m of G^\diamond is incident to an edge that is not subdivided in G .

In the last step, Lemma 8.8 ensures that we can triangulate m by inserting new edges in m (see Figure 8.7, bottom right), and by mapping in f each such new edge to a vertex or an edge of T , keeping f strongly harmonious and homotopic to the inclusion map $G \hookrightarrow S$. Now G is the 1-skeleton of a triangulation Z , and f trivially extends to a map $\varphi : S \rightarrow S$ simplicial for (Z, T) . \square

8.2.4 A property of the maps homotopic to the identity and strongly harmonious

Here is another key step towards the proof of Theorem 3.4: we prove that our simplicial drawings of triangulations orient the (non-degenerate) triangles coherently. In detail:

Proposition 8.4. *Let S be a surface without boundary distinct from the sphere. Let T be a reducing triangulation of S . Let Z be a triangulation of S , and let $\varphi : S \rightarrow S$ be simplicial for (Z, T) . If φ is strongly harmonious, and if φ is homotopic to the identity map of S , then there cannot be two faces z_+ and z_- of Z for which $\varphi|_{z_+}$ is positive and $\varphi|_{z_-}$ is negative.*

The rest of this section is devoted to the proof of Proposition 8.4. In this section only, it is convenient to consider the plane P , and an (infinite) reducing triangulation T of P ;

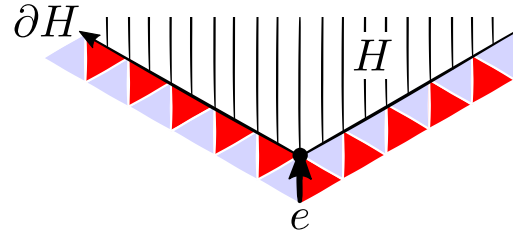


Figure 8.8: A cone.

the notion of strong harmony immediately extends to that setting. And again, if Z is a triangulation of P , a map $\varphi : P \rightarrow P$ simplicial for (Z, T) is strongly harmonious if $\varphi|_Z^T$ is strongly harmonious.

In T , the minimum number of edges of a path between two given vertices defines a distance on the vertex set of T . A map $\varphi : P \rightarrow P$ is **uniformly homotopic** to the identity map $1_{P \rightarrow P}$ if it is homotopic to the identity and there is $\kappa > 0$ such that every point $x \in P$ mapped to a vertex v of T by φ lies in a vertex, edge, or face of T whose incident vertices are at distance less than κ from v . We shall prove the following:

Proposition 8.5. *Let P be the plane. Let T be a reducing triangulation of P . Let Z be a triangulation of P , and let $\varphi : P \rightarrow P$ be simplicial for (Z, T) . If φ is strongly harmonious, and if φ is uniformly homotopic to the identity map of P , then there cannot be two faces z_+ and z_- of Z for which $\varphi|_{z_+}$ is positive and $\varphi|_{z_-}$ is negative.*

Proposition 8.4 (concerning surfaces) easily follows from Proposition 8.5 (concerning the plane) by lifting:

Proof of Proposition 8.4, assuming Proposition 8.5. The universal covering space \tilde{S} of S is the plane. Also T lifts to a reducing triangulation \tilde{T} of \tilde{S} , Z lifts to a triangulation \tilde{Z} of \tilde{S} , and φ lifts to a map $\tilde{\varphi} : \tilde{S} \rightarrow \tilde{S}$ simplicial for (\tilde{Z}, \tilde{T}) . Since φ is strongly harmonious, $\tilde{\varphi}$ is strongly harmonious. We claim that $\tilde{\varphi}$ is uniformly homotopic to the identity map of \tilde{S} . This claim implies by Proposition 8.5 that there cannot be two faces z_+ and z_- of \tilde{Z} for which $\tilde{\varphi}|_{z_+}$ is positive and $\tilde{\varphi}|_{z_-}$ is negative. Then the same holds for Z and φ , proving the proposition.

To prove the claim, we use the assumption that there is a homotopy H between φ and the identity map of S , and we lift H to a homotopy \tilde{H} between $\tilde{\varphi}$ and the identity map of \tilde{S} . For every lift $\tilde{x} \in \tilde{S}$ of a point $x \in S$, the path \tilde{p} followed by the image of \tilde{x} in \tilde{H} , and the path p followed by the image of x in H are such that the number of vertices, edges, and faces of \tilde{T} crossed by \tilde{p} is equal to the number of vertices, edges, and faces of T crossed by p . The latter is uniformly bounded since S is compact. \square

The rest of this section is devoted to the proof of Proposition 8.5. We need some definitions and lemmas. See Figure 8.8. Let T be a reducing triangulation of the plane. The part of T on a given side of a bi-infinite reduced path ∂H , and not on ∂H , is a **half-plane** H of T , and ∂H is the boundary of H . We emphasize that half-planes are open. A half-plane H is **nested** in another half-plane H' if $H \subset H'$ and $\partial H \cap \partial H' = \emptyset$. Let e be a directed edge e of T that sees blue on its left, and let L be the bi-infinite reduced walk in T that contains the head vertex v of e , and makes only 3_b - and 3_r -turns, except at v where it makes a 4_b -turn

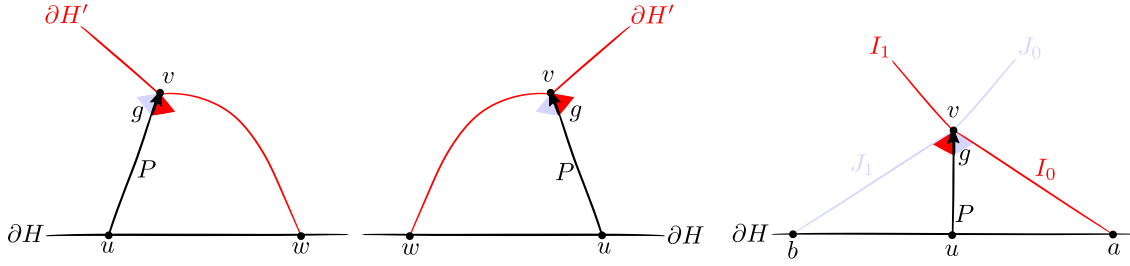


Figure 8.9: The impossible cases in the proof of Lemma 8.9.

whose middle edge is e . The **cone** of e is the half-plane H on the right of L , and v is the **tip** of H .

Lemma 8.9. *Let T be a reducing triangulation of the plane. If H is a half-plane of T , and if $v \in H$ is a vertex of T , then v is the tip of a cone H' nested in H .*

Proof. There is a reduced path P between v and a vertex u of ∂H , such that P is internally included in H . Let g be the edge of P incident to v , directed toward v . First assume that g sees blue on its left. We claim that the cone H' of g is nested in H . First we prove $\partial H' \cap \partial H = \emptyset$ by contradiction. See Figure 8.9. Assuming that ∂H and $\partial H'$ share a vertex w , let Q' be the concatenation of P and of the subpath of $\partial H'$ between v and w , and let Q be the subpath of ∂H between u and w . Then Q and Q' are distinct reduced paths with the same end-vertices in T , contradicting Proposition 6.1. It then easily follows that $H' \subset H$, and we now provide the details. We have $\partial H' \subset H$ since $\partial H' \cap H \neq \emptyset$ and $\partial H' \cap \partial H = \emptyset$. The reduced path P is internally disjoint from ∂H and $\partial H'$ by Proposition 6.1, and since ∂H and $\partial H'$ are reduced. So the relative interior of P lies in the open region R between ∂H and $\partial H'$. Also, the relative interior of g is disjoint from H' , and so is R .

Now assume that g sees red on its left. We claim that there is a rotation of one turn of g around its head vertex v (either clockwise or counter-clockwise) after which the cone H' of g satisfies $\partial H' \cap \partial H = \emptyset$. As above, this claim implies that H' is nested in H . Let I be the boundary of H' after a clockwise-rotation around v , and let J be the boundary after a counter-clockwise rotation around v . Assume by contradiction that I and J both intersect ∂H . See Figure 8.9. Cut I into two semi-infinite walks at v , the right part (with respect to g) denoted by I_0 , and the left part denoted by I_1 . Cut J into two parts at v , the right part J_0 , the left part J_1 . The concatenation of P and I_1 is a reduced walk, so I_1 is disjoint from ∂H by Proposition 6.1, and so I_0 intersects ∂H in a vertex a . The concatenation of P and J_0 is a reduced walk, so J_0 is disjoint from ∂H by Proposition 6.1, and so J_1 intersects ∂H in a vertex b . Let Q' be the concatenation of the subpath of I_0 between a and v , and of the subpath of J_1 between v and b . Let Q be the subpath of ∂H between a and b . Then Q and Q' are distinct reduced paths with the same end-vertices in T , contradicting Proposition 6.1. \square

Lemma 8.10. *Let T be a reducing triangulation of the plane. Let G be a graph, and let $f : G \rightarrow T$ be simplicial. Let H be a cone of T , and let v be a vertex of G . If f is strongly harmonious, and if $f(v)$ is the tip of H , then there is a walk W based at v in G that satisfies $f(W) \subset H \cup \partial H$ and $f(W) \not\subset \partial H$.*

Proof. Let $G_0 \subset G$ be the cluster of f containing v . Since f is strongly harmonious, there is a directed edge e from G_0 to $G \setminus G_0$ such that $f(e) \in H \cup \partial H$. If $f(e) \in H$, then we are

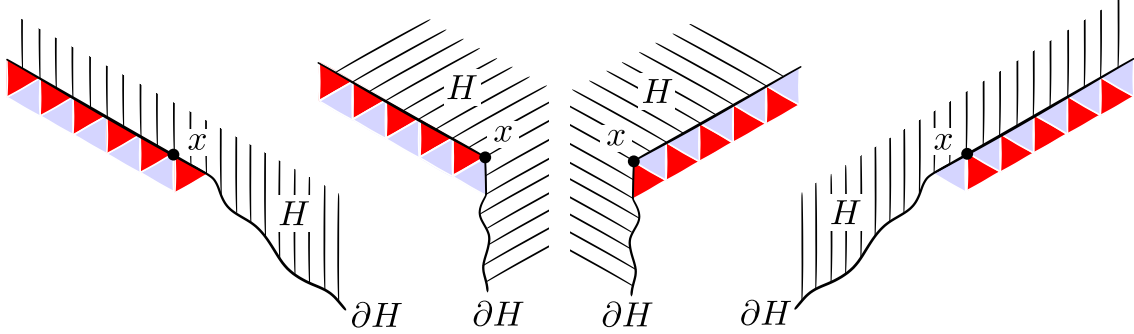


Figure 8.10: Combs.

done. So we assume $f(e) \in \partial H$. The boundary ∂H splits into two semi-infinite walks I_0 and I_1 based at $f(v)$, where H lies on the left of I_0 and on the right of I_1 . Assume $f(e) \in I_0$, the other case being similar. Let w be the head vertex of e . Let J be the suffix of I_0 obtained by removing its first edge ($f(w)$ is the first vertex of J). Let L be the bi-infinite walk that makes only 3_r -turns and contains J as a subwalk. Since f is strongly harmonious, there is a walk W based at w in G , such that $f \circ W$ may stay in J for a while, and then leaves J on its left. \square

In order to ease the reading of the proof of Proposition 8.5, we shall not use Lemma 8.9 and Lemma 8.10 as they are. Instead, we shall use two corollaries:

Corollary 8.1. *Let T be a reducing triangulation of the plane. Let G be a graph, and let $f : G \rightarrow T$ be simplicial. Let H be a half-plane of T , and let v be a vertex of G . Let $\kappa > 0$. If f is strongly harmonious, and if $f(v) \in H$, then there is a walk W from v to a vertex w in G , such that $f(W) \subset H$, and such that $f(w)$ is at distance greater than κ from ∂H .*

Proof. This follows immediately from repeated iterations of Lemmas 8.9 and 8.10. \square

The next corollary is easier to state with the following definition. See Figure 8.10. In a reducing triangulation T of the plane, a right (resp. left) **comb** is a pair (H, x) where H is a half-plane of T , and x is a vertex of ∂H , that satisfy the following: directing ∂H so that H lies on its right (resp. left), every turn of ∂H at x and after x is 3_r or 2_b (resp. -3_r or -2_b). The **glen** of (H, x) is the union of H and of the part of ∂H consecutive to x , including x .

Corollary 8.2. *Let T be a reducing triangulation of the plane. Let G be a graph, and let $f : G \rightarrow T$ be simplicial. Let (H, x) be a (left or right) comb of T , and let v be a vertex of G . Let $\kappa > 0$. If f is strongly harmonious, and if $f(v) = x$, then there is a walk W from v to a vertex w in G , such that $f(W)$ is included in the glen of (H, x) , and such that $f(w)$ is at distance greater than κ from ∂H .*

Proof. The vertex x is the tip of a cone H' such that $H' \cup \partial H'$ is included in the glen of (H, x) . Lemmas 8.9 and 8.10 conclude. \square

We need a few more technical lemmas.

Lemma 8.11. *Let T be a plane reducing triangulation, and let T' be subgraph of T . If T' is connected, finite, and not a single vertex, then T' admits at least two vertices x such that the edges of T' incident to x are all included in some bad turn of T .*

Proof. If T' has more than one vertex of degree one, then we are done. So assume that this is not the case. Then T' has at least three vertices since it has neither loops nor multiple edges (Section 6.1). First assume that T' has no degree one vertex. Then the outer closed walk W of T' has length greater than or equal to three, and never uses an edge of T and its reversal consecutively. Orient W so that the outer-face of T' lies on the right of W . Walk along W until some vertex x_0 is visited for the second time, then cut the portion of W from x_0 to itself, thus obtaining a closed walk C based at x_0 . Then C is a simple closed walk, not a single vertex. Thus, since T has no loop nor multiple edges, C has length greater than or equal to three. Also, every vertex $x \neq x_0$ of C is such that all the edges of T' incident to x either lie on C , or on the left of C . Lemma 6.3 ensures that at least three of the left turns of C are bad, and at least two of them do not occur at x_0 , proving the lemma in this case.

Now assume that T' has exactly one vertex of degree one. Removing degree one vertices from T' as long as there is one immediately gives the following: T' is the union of a path P , not single vertex, and of a connected graph Q , not a single vertex, such that the intersection of P and Q is one of the two end-vertices x of P , and such that Q has no degree one vertex. By the preceding, Q has a vertex distinct from x that suits our need. And the end-vertex of P distinct from x also suits our needs. \square

In the following, we denote by T^0 the set of vertices of a triangulation T .

Lemma 8.12. *Let P be the plane. Let T be a reducing triangulation of P . Let Z be a triangulation of P , and let $\varphi : P \rightarrow P$ be simplicial for (Z, T) . If φ is strongly harmonious, and if φ is uniformly homotopic to the identity map of P , then $\varphi^{-1}(T^0)$ does not disconnect P .*

Proof. By contradiction, assume that it does. There is no simple bi-infinite walk W in T that belongs entirely to $\varphi^{-1}(T^0)$, for otherwise $\varphi(W)$ would be a single vertex of T (being a connected subset of T^0), contradicting the assumption that φ is uniformly homotopic to the identity map. Therefore, and since φ is simplicial for (Z, T) , there are a simple cycle C in Z , a vertex $v \in Z^0$ in the interior of the bounded side of C , and a vertex x of T , such that $\varphi(C) = x$ and $\varphi(v) \neq x$. Let G be the subgraph of Z that contains C and the part of Z lying in the bounded side of C . Then $\varphi(G)$ is a finite connected subgraph of T , not a single vertex. So by Lemma 8.11 there is a vertex $y \neq x$ in $\varphi(G)$ such that the set B of edges of $\varphi(G)$ incident to y is included in a bad turn of T . There is a cluster $G_0 \subset Z$ such that $\varphi(G_0) = y$, and such that the edges between G_0 and $Z \setminus G_0$ all belong to G . Those edges are mapped to B by φ , contradicting the assumption that φ is strongly harmonious. \square

In the following, we say that 1-turns and 2_r -turns are **bad left turns**.

Lemma 8.13. *In a plane reducing triangulation T , let I be a simple bi-infinite walk that does not make any bad left turn. The vertices of T on the left of I at distance one from I are the vertices of a simple bi-infinite walk I' that does not make any bad left turn.*

Proof. Consider the sequence E of directed edges of T emanating from vertices of I to the left side of I . If e_1 and e_2 are consecutive in E , then either e_1 and e_2 have the same target vertex, or their they have the same source vertex. In the first case, e_2 is the counter-clockwise rotation of e_1 around their target vertex, in the second case e_2 is the clockwise-rotation of e_1 around their source vertex. Let I' be the bi-infinite walk corresponding to the target vertices

of the directed edges in E . The vertices of I' are those on the left of I at distance one from I .

Then I' does not make any 0-turn, nor any bad left turn. For otherwise there are three consecutive $e_1, e_2, e_3 \in E$ that all have the same target vertex (at which I' makes a bad left turn), such that e_2 sees red on its left. But then I makes a 2_r -turn at the source vertex of e_2 , a contradiction.

Moreover I' is simple. For otherwise some portion W of I' is a non-trivial simple closed walk, and the bounded side of W lies on its right by Lemma 6.3, and since W makes at most one bad left turn. But then I is contained in the bounded side of W , a contradiction. \square

Proof of Proposition 8.5. The overall proof is illustrated in Figure 8.11. By contradiction, assume that there are two faces z_0 and z_- of Z such that $\varphi|_{z_+}$ is positive and $\varphi|_{z_-}$ is negative. By Lemma 8.12, there is a simple path p from z_+ to z_- in the dual of Z , that is disjoint from $\varphi^{-1}(T^0)$. Up to replacing z_+ and z_- by other faces of Z , we may assume that φ is null on every face of Z intermediately visited by p . Extend p to the respective vertices of z_+ and z_- not incident to the first and last edges crossed by p . Because φ is null on every face visited by p except the first and last ones, and because p is disjoint from $\varphi^{-1}(T^0)$, there is an edge $s \in T$ such that the image, by φ , of all the edges of Z crossed by p is exactly s . Moreover, one can direct s in such a way that all the edges of Z crossed by p from left to right are mapped to s . Consider the left-most bi-infinite reduced walk of T that contains s , and let H be the half-plane on its left. Because $\varphi|_{z_+}$ is positive and $\varphi|_{z_-}$ is negative, the interiors \dot{z}_+ and \dot{z}_- of triangles z_+ and z_- are mapped inside H .

Using the assumption that φ is uniformly homotopic to the identity, there is $\kappa > 0$ such that each vertex of T is at distance smaller than κ from its pre-images under φ . Let p' be any of the directed edges crossed by p from left to right. By Corollary 8.1 there is, in Z , a walk U_0 (resp. U_1) based at the source (resp. target) end-vertex of p such that, for $i = 1, 2$, $\varphi(U_i) \subset H$, and such that $\varphi(U_i)$ contains a point at distance greater than 3κ from ∂H . Cut p into two parts p_0 and p_1 at its intersection with p' , and reverse p_0 . Let q_i be the concatenation of p_i and U_i . Make q_i a simple path by shortening it if necessary. Then q_0 and q_1 are disjoint from p' except for their basepoint, since $\varphi(U_0), \varphi(U_1) \subset H$, $\varphi(p') = s$, and $\varphi(\dot{z}_+), \varphi(\dot{z}_-) \subset H$. We prove by contradiction that q_0 and q_1 are disjoint except for their basepoint. If not, then $q_0 \cup q_1$ contains a simple closed curve whose bounded side contains an endpoint y of p' . By Corollary 8.2 there is a walk X based at y in Z such that $\varphi(X)$ is disjoint from $\dot{s} \cup H$, and such that X intersects $q_0 \cup q_1$. That contradicts the fact that $\varphi(q_0 \cup q_1) \subset \dot{s} \cup H$.

Now cut p' into two parts p'_0 and p'_1 at its intersection with p . Reverse p'_0 . By Corollary 8.2 there is a simple walk U'_0 (resp. U'_1) based at the source (resp. target) end-vertex of p' in Z , such that $\varphi(U'_i)$ is disjoint from $\dot{s} \cup H$, and such that $\varphi(U'_i)$ contains a point at distance greater than 3κ from ∂H . Let q'_i be the concatenation of p'_i and U'_i . Since $\varphi(U'_0)$ and $\varphi(U'_1)$ are disjoint from $\dot{s} \cup H$, the paths q'_0 and q'_1 are simple, and each of them is disjoint from q_0 and q_1 except for their basepoint. An argument by contradiction similar to the one of the previous paragraph shows that q'_0 and q'_1 are disjoint except for their basepoint.

Let Q be the concatenation of q_0 and q_1 , and Q' be the concatenation of q'_0 and q'_1 . By construction, Q and Q' are simple, and cross exactly once. Until now, we have considered separately the situation in Z (before applying φ) and in T (after applying φ). But recall that Z and T are both triangulations of the plane, and that each vertex of T is at distance smaller than κ from its pre-images under φ . Because of this, and by the properties of $\varphi(Q)$

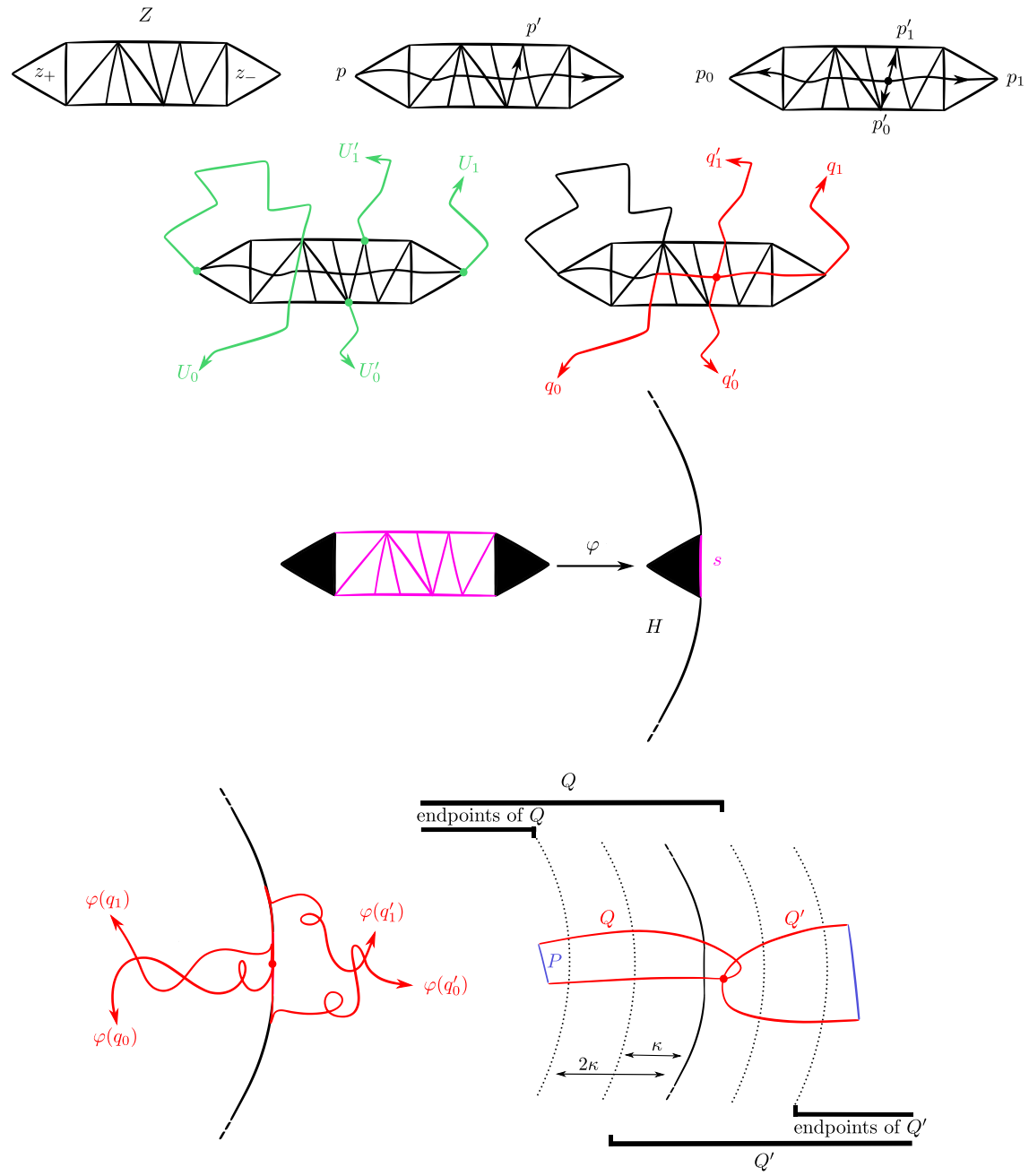


Figure 8.11: The construction in the proof of Proposition 8.5.

and $\varphi(Q')$, we have that Q has its endpoints inside H , at distance at least 2κ from ∂H , and may enter the complement of H , but only by a distance of at most κ . Similarly, Q' has its endpoints outside H , at distance at least 2κ from ∂H , and may enter H but only by a distance of at most κ . By (repeated applications of) Lemma 8.13, the vertices of T inside H at distance 2κ from ∂H are the vertices of a simple bi-infinite walk I . Then I separates the endpoints of Q from every point of Q' . Join the endpoints of Q by a path P , where P is separated from Q' by I , thus turning Q into a (not necessarily simple) closed curve C . Because Q and Q' cross exactly once, and because P and Q' are disjoint, then C and Q' cross exactly once. Similarly, there is a simple bi-infinite walk that separates the endpoints of Q' from C , so Q' can be extended to a closed curve C' such that C and C' cross exactly once. But this is impossible, since any two closed curves in the plane cross an even number of times. \square

8.2.5 Proof of Theorem 3.4

We now have almost all the material to prove Theorem 3.4. We first prove the theorem for strongly harmonious drawings, in the following proposition.

Proposition 8.6. *Let S be a surface without boundary distinct from the sphere. Let T be a reducing triangulation of S . Let G be a finite graph embedded in S , and let $f : G \rightarrow T$ be simplicial. If f is strongly harmonious, and if f is homotopic to the inclusion map $G \hookrightarrow S$, then f is a weak embedding.*

(As a side note, observe that Proposition 8.6 considers also the torus.)

Proof. By Proposition 8.3 there are a triangulation Z of S whose 1-skeleton contains a subdivision of G as a subgraph, and a map $\varphi : S \rightarrow S$ simplicial for (Z, T) with $\varphi|_G^T = f$, such that φ is strongly harmonious and homotopic to the identity map of S . By Proposition 8.4 there cannot be two faces z_+ and z_- of Z for which $\varphi|_{z_+}$ is positive and $\varphi|_{z_-}$ is negative. Thus, letting $Y \subset S$ contain one point in the interior of each face of T , φ is coherently oriented at Y . By Proposition 8.2 the map $\varphi|_{S \setminus \varphi^{-1}(Y)}^{S \setminus Y}$ is homotopic to a homeomorphism $S \setminus \varphi^{-1}(Y) \rightarrow S \setminus Y$. In particular, and since $G \cap \varphi^{-1}(Y) = \emptyset$, the map $f|_{S \setminus Y}^{S \setminus Y}$ is homotopic to an embedding $G \rightarrow S \setminus Y$. Also $S \setminus Y$ is the patch system of T , and f has no spur since f is strongly harmonious. So f is a weak embedding by Proposition 8.1. \square

The proof of Theorem 3.4 relies on a few additional lemmas. Firstly, the following is an immediate corollary of Lemma 6.6 from Section 6.3:

Corollary 8.3. *Let S be a surface without boundary distinct from the sphere and the torus. Let T be a reducing triangulation of S . Let C be a collection of closed walks in T . If the walks in C are reduced, and if C is homotopic to an embedding in S , then C is a weak embedding.*

Proof. Every closed curve $c \in C$ is primitive in S by Lemma 5.9, since $i_S(c) = 0$. So Lemma 6.6 applies. \square

Preparing for the next lemma, observe that if M is a finite graph embedded on a surface, then the universal cover of M is a tree \widetilde{M} naturally equipped with a rotation system. Moreover, if C_0 is a closed walk without spur in M , then every lift \widetilde{C}_0 of C_0 partitions \widetilde{M} into three parts: the left of \widetilde{C}_0 , the right of \widetilde{C}_0 , and the image of \widetilde{C}_0 .

Lemma 8.14. *Let M be a finite graph embedded on a surface. Let G be a finite graph simplicially mapped to M , and let C be a collection of closed walks in M . Assume that G and C are weak embeddings without spur, and that their union is not a weak embedding. Then in the universal cover of M there is a lift of G that has vertices on both sides of a lift of a walk C_0 from C .*

Proof. Without loss of generality every edge of G is mapped to an edge of M (contract the clusters of G otherwise). Let Σ be the patch system of M , and let G' and C' be embeddings approximating G and C in Σ . Without loss of generality G' , C' , and the arcs of Σ are in general position. Also, G' and C' cross minimally. By assumption they cross at a point x in the interior of some face of Σ . Let $\tilde{\Sigma}$ be the universal covering space of Σ , and let \tilde{x} be a lift of x in $\tilde{\Sigma}$. Let \tilde{C}'_0 be the lift of a walk C'_0 from C' that contains \tilde{x} . Cut the lifts of G' at every intersection with \tilde{C}'_0 , and let \tilde{G}' be one of the two cuts that meet \tilde{x} . Since the number of crossings between G' and C' is minimal, \tilde{G}' is not contained in the union of the faces and arcs of $\tilde{\Sigma}$ used by \tilde{C}'_0 . \square

The following is analogous to Lemma 8.6.

Lemma 8.15. *Let S be a surface. Let G be a graph, and let $f : G \rightarrow S$ be a map. If $f(G)$ is a simple circle $S_0 \subset S$, if S_0 does not bound a disk in S , and if f is homotopic to an embedding in S , then f is homotopic to an embedding in a tubular neighborhood of S_0 .*

Proof. Without loss of generality G is connected. Fix a vertex r of G and a spanning tree T of G rooted at r . Let ℓ be the simple loop on S based at $x := f(r)$ whose image is S_0 . We first claim that we can assume without loss of generality that each edge of T is mapped to x by f , and that each edge not in T is mapped, under f , to a power of ℓ . To see this, contract, in S_0 , the edges in T ; each remaining edge is homotopic to some power of ℓ in S_0 . Actually, each edge of T is actually mapped to either ℓ , to ℓ^{-1} , or to the constant loop in S_0 . This is by Lemma 5.9, since the edges not in T are mapped to loops that can be made simple by homotopy in S .

On the other hand, there is an embedding $f' : G \rightarrow S$ homotopic, in S , to f . Without loss of generality, we can assume that this homotopy between f and f' holds the image of r fixed. Indeed consider a homotopy H from f to f' , and the path $p : [0, 1] \rightarrow S$ followed by the image of r under H . There is an ambient isotopy H' of S that “counteracts” H in the sense that it maps $p(t)$ to x for all $t \in [0, 1]$. Composing the maps in H by the maps in H' gives a homotopy from f to an embedding (not f') that holds the image of r fixed.

We contract the edges of T in f' to a small neighborhood of x , this time preserving the fact that we have an embedding. The remaining edges are loops that, under f' , are homotopic to their counterparts under f (if T would be really contracted to x). The contractible ones can be pushed by isotopy into a small neighborhood of x , as each of them bounds a disk with only (possibly) contractible loops inside it [83, Theorem 1.7]. The other loops can be bundled together parallel, since any pair of them bounds a disk with only (possibly) contractible or homotopic loops inside it. Then they can be pushed altogether in a neighborhood of ℓ . \square

Proof of Theorem 3.4. Clearly if f is a weak embedding, then there is an embedding homotopic to f in S . For the other direction assume that there is an embedding homotopic to f in S . We shall prove that f is a weak embedding.

Partition G into two subgraphs A and B such that $f|_B$ is strongly harmonious, and f is not strongly harmonious on any of the connected components of A . Then $f|_A = C \circ f'$ for

some disjoint union O of cycle graphs, mapped to reduced closed walks by $C : O \rightarrow T$, and some simplicial map $f' : A \rightarrow O$, without spur.

Our first claim is that the collection of closed walks C is homotopic to an embedding in S . Indeed C can be realized as the restriction of f to a collection of disjoint cycles in A , as follows. For every cycle O_0 in O , since f' has no spur, there is a simple closed walk W in A mapped by f' to a non-trivial power of O_0 . Then W is mapped by f to a non-trivial power of the closed walk $C_0 := C|_{O_0}$, homotopic to an embedding (since f is), and so it is actually mapped to $C|_0$ or its reversal (Lemma 5.9).

Thus C is a weak embedding by Corollary 8.3, and since the walks in C are reduced. Now f' is a weak embedding by Lemma 8.15 and Proposition 8.1. Our second claim is that $f|_B \cup C$ is a weak embedding. This claim proves the theorem as $f|_{A \cup B}$ is then a weak embedding. We prove the claim by contradiction so assume that $f|_B \cup C$ is not a weak embedding. Let U_T be the universal cover of the 1-skeleton of T . There is by Lemma 8.14 some lift of $f|_B$ in U_T that contains vertices on both sides of some lift of a walk C_0 from C . Now let \tilde{S} be the universal cover of S . In \tilde{S} , there are lifts \tilde{B} and \tilde{C}_0 of $f|_B$ and C_0 such that \tilde{B} contains vertices on both sides of \tilde{C}_0 . Then \tilde{C}_0 is a semi-infinite reduced walk in the lift of T , and $\tilde{B} \cup \tilde{C}_0$ is uniformly homotopic to an embedding. That contradicts Corollary 8.1. \square

8.3 Harmonizing a drawing monotonically

In this section we prove Theorem 3.5, which we restate for convenience:

Theorem 3.5. *Let S be a surface of genus $g \geq 2$ without boundary. Let T be a reducing triangulation of S , with m edges. Let G be a graph, and let $f : G \rightarrow T$ be a drawing of size n . We can compute in $O((m+n)^2 n^2)$ time a drawing $f' : G \rightarrow T$, harmonious, homotopic to f in S , such that for every edge e of G , the image of e under f' is not longer than under f .*

The strategy is to transform a drawing f iteratively by some “local” moves satisfying the property that, if no move can be applied, then the current drawing is harmonious. Two of these moves, the shortening and balancing moves, decrease strictly the length of the drawing. On the other hand, the flip move does not affect the length of the drawing. Roughly but not exactly, the algorithm performs moves iteratively, giving priority to the shortening and balancing moves over the flip moves. To bound the complexity of the algorithm, it then suffices to bound the length of a flip sequence, assuming that at each step of this sequence, no shortening or balancing move is possible. The details are actually more complicated; in particular, the flip sequence is chosen carefully.

8.3.1 Reduction to simplicial maps

We have the following preliminary observation:

Lemma 8.16. *To prove Theorem 3.5, we can assume that f is simplicial.*

Proof. Let $f : G \rightarrow T$ be as in the statement of Theorem 3.5. Let $\bar{f} : \bar{G} \rightarrow T$ be the associated simplicial map that factorizes f . If Theorem 3.5 holds for simplicial maps, then we obtain a map $\bar{f}' : \bar{G} \rightarrow T$ that is harmonious, is homotopic to \bar{f} , and does not increase the length of the edges (compared to f'). In particular, \bar{f}' is simplicial. It naturally corresponds to a drawing f' of G on T that satisfies the desired properties. \square

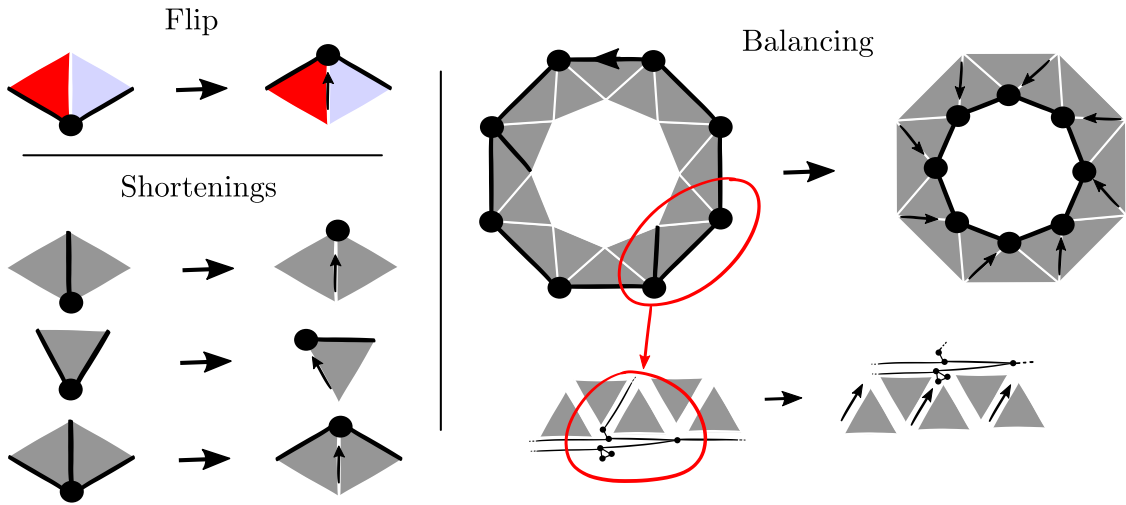


Figure 8.12: The moves. (Left) Each disk represents a single cluster. (Right) Each disk may represent several clusters. The balancing is slightly counter-clockwise (clockwise would not decrease any edge length here).

8.3.2 Flips, shortenings, and balancings

Throughout this section, T is a reducing triangulation of a surface S distinct from the sphere and the torus, G is a graph, and $f : G \rightarrow T$ is a *simplicial* map. Recall that f factors uniquely into a homomorphism $\hat{f} : \hat{G} \rightarrow T$. We now define the three moves bringing \hat{f} (and thus f) closer to harmony; see Figure 8.12.

- First, if the edges of \hat{G} incident with v leave v via two edges around $\hat{f}(v)$, which together form a 2_r -turn around $\hat{f}(v)$, then we can perform a **flip move** to \hat{f} , which transforms \hat{f} into a homotopic map $\hat{f}' : \hat{G} \rightarrow T$ (Figure 8.12, top left), which is actually also a homomorphism. From \hat{f}' , we immediately deduce a simplicial map $f' : G \rightarrow T$. Since $\hat{f}, \hat{f}' : \hat{G} \rightarrow T$ are both homomorphisms, we can also view a flip as a specific operation that turns a homomorphism into another one (we will use this point of view later).
- Second, let v be a vertex of \hat{G} . If the edges of \hat{G} incident with v leave v via one, two, or three consecutive edges of T around $\hat{f}(v)$, then we can perform a **shortening move** to \hat{f} , which transforms \hat{f} into a homotopic, simplicial map \hat{f}' of \hat{G} in which no edge of \hat{G} is longer than in \hat{f} (Figure 8.12, bottom left). From \hat{f}' , we immediately deduce a simplicial map $f' : G \rightarrow T$.
- Third, consider a simple directed cycle C in \hat{G} that makes only 3-turns under f . We say that a walk of \hat{G} , identified by its sequence of directed edges (e_0, \dots, e_k) , *follows* C if there is a walk on C , its *following walk*, (which may go back and forth on C), identified by its directed edges (c_0, \dots, c_k) such that $f(e_i) = f(c_i)$ for each i . A walk $(e_0, \dots, e_k, e_{k+1})$ of \hat{G} *pulls C to the left* if (e_0, \dots, e_k) follows C , with following walk (c_0, c_1, \dots, c_k) , and if moreover edge $f(e_{k+1})$ leaves the image of the directed cycle C , at the end-vertex of c_k , to its left. The notion of being pulled to the right is defined analogously.

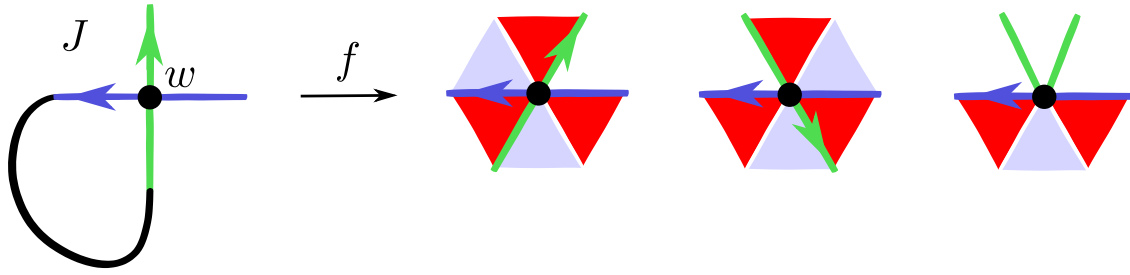


Figure 8.13: In the proof of Lemma 8.17, the first two and the last two edges of J cannot be mapped to two edge-disjoint walks.

If C makes only 3-turns under f , is pulled left, and is not pulled right, we can define a **balancing move** as follows (Figure 8.12, right). We consider all the vertices of \hat{G} that are parts of walks following C (including the vertices of C themselves) and move them to the left of C , in such a way that we still have a homomorphism when restricted to the vertices following C . There are exactly two possibilities to do this, depending on whether the cycle is rotated “slightly clockwise” or “slightly counterclockwise” (as in Figure 8.12). In any case, the length of the image of an edge of \hat{G} does not increase, and we choose a possibility that strictly decreases the length of the image of at least one edge, based on how a walk pulls C to the left. As before, from \hat{f}' , we immediately deduce a simplicial map $f' : G \rightarrow T$.

These three moves are useful in the following sense:

Lemma 8.17. *If f cannot be flipped, shortened, or balanced, then f is harmonious.*

Proof. Without loss of generality G is connected. Also f is a homomorphism (for otherwise f factors into a homomorphism $\hat{f} : \hat{G} \rightarrow T$ such that no move applies to \hat{f} by definition, and such that if \hat{f} is harmonious, then f also). If f is strongly harmonious, we are done, so we can assume that f is not strongly harmonious. So let v be a vertex of G , and let L be a (left or right) line in T whose central vertex is $f(v)$ such that, for each walk W in G based at v , the image of W under f does not escape L . In the universal cover, this means the following. There are a vertex \tilde{x} of \tilde{T} , projecting to $f(v)$, and a (left or right) line \tilde{L} in \tilde{T} whose central vertex is \tilde{x} , such that, for each walk W in G based at v , the lift of $f \circ W$ based at \tilde{x} does not escape \tilde{L} . We assume that \tilde{L} is a left line (equivalently, that it makes only 3_r -turns), the other case being similar. We claim that, for each walk W in G based at v , the lift of $f \circ W$ based at \tilde{x} is actually *contained* in \tilde{L} .

First, we explain why the claim implies the lemma. Because T is finite, there are a cycle graph O and a reduced closed walk $C : O \rightarrow T$ such that \tilde{L} is a lift of C . Using the claim, and since \tilde{L} is simple by Proposition 6.1, there is a simplicial map $f' : G \rightarrow O$ such that $f = C \circ f'$. Moreover, f' has no spur since f cannot be shortened. So f is harmonious, proving the lemma. There remains to prove the claim, which we do in the remaining part of the proof.

Recall that \tilde{L} makes only 3_r -turns. In G , one can build a semi-infinite walk I based at v such that the lift of $f \circ I$ based at \tilde{x} is equal to the non-negative part of \tilde{L} . (Indeed, at a given step on \tilde{L} , there is no edge that goes strictly to the right of \tilde{L} since no walk based at v can

escape L under f ; if all edges go strictly to the left of \tilde{L} or backward on \tilde{L} , a shortening or a flip could be applied to f .) Since I is a semi-infinite walk in G , it contains a subwalk J that, after removing its first and last edge, becomes a simple loop Q in G , based at some vertex w of G . Let P be the prefix of I leading to Q . The lift of $f \circ P$ based at \tilde{x} is a portion of the non-negative part of \tilde{L} , ending at a vertex \tilde{y} of \tilde{T} . Also $f \circ Q$, regarded as a closed walk by concatenating it with itself, makes a 3_r -turn also at the middle occurrence of w ; Otherwise, the first two and the last two edges of J would map, under f , to two edge-disjoint walks of length two making 3_r -turns at $f(w)$ (Figure 8.13), and so one could stop I at this point and escape from \tilde{L} , a contradiction. In particular the lift of $f \circ Q$ based at \tilde{y} is (a translate of) \tilde{L} .

We conclude in two steps. First we prove that for every walk W based at v in G , the lift of $f \circ W$ based at \tilde{x} cannot enter the right side of \tilde{L} , even after staying in \tilde{L} for a while. By contradiction, assume that it does. For every $n \geq 1$ the walk $P \cdot Q^n \cdot P^{-1} \cdot W$ is based at v in G , and is such that the lift of $f \circ (P \cdot Q^n \cdot P^{-1} \cdot W)$ based at \tilde{x} enters the right side of \tilde{L} after staying in \tilde{L} . There is n such that this lift does not intersect \tilde{L} outside of its non-negative part. We obtained a walk based at v that escapes L under f , a contradiction.

Now we prove that the lift of $f \circ W$ based at \tilde{x} cannot enter the left side of \tilde{L} , even after staying in \tilde{L} for a while. By contradiction, assume that it does. Without loss of generality, removing the last edge from W gives a walk W' such that the lift of $f \circ W'$ based at \tilde{x} is contained in \tilde{L} . Then the lift of $f \circ (P^{-1} \cdot W')$ based at \tilde{y} is contained in \tilde{L} , which lifts $f \circ Q$, and so $P^{-1} \cdot W'$ follows Q . Then $P^{-1} \cdot W$ pulls Q to the left. Since Q is pulled to the left, and since no balancing applies, Q is pulled to the right. So there is a walk U based at w in G such that the lift of $f \circ U$ based at \tilde{y} is contained in \tilde{L} , except for its last edge that enters the right side of \tilde{L} . Then the walk $P \cdot U$, based at v , is such that the lift of $f \circ (P \cdot U)$ based at \tilde{x} enters the right side of \tilde{L} after staying in \tilde{L} for a while. That contradicts the previous paragraph. \square

8.3.3 Preliminaries on flip sequences

By the preceding lemma, a natural strategy is to apply flips, shortenings, and balancings as much as possible until it is not possible any more. Shortenings and balancings strictly decrease the length of the map, so only finitely many such moves can be applied. Most of the argument thus focuses on sequences of flips in which no shortening or balancing can be applied at any step. Recall that flips transform a homomorphism into another one, and thus *henceforth we consider maps from G to T that are homomorphisms*.

Formally, a **flip sequence** is a sequence of *homomorphisms* $f_0, \dots, f_p : G \rightarrow T$ such that f_{i+1} results from a flip of f_i for every $0 \leq i < p$, and no shortening or balancing can be applied to any of f_0, \dots, f_{p-1} . We use the following conventions. Given $0 \leq i < p$ we call flip i and abusively denote by i the flip from f_i to f_{i+1} . Given $0 \leq i \leq j \leq p$, we denote by $F_{i \rightarrow j}$ the flip sequence f_i, \dots, f_j . Given a vertex v of G , we denote by $F|v$ the walk performed in T by the image of v through the flips of v in F .

The map f induces a **left-blue direction** of G , obtained by directing each edge e of G in such a way that $f(e)$ has a blue triangle on its left. Thus G becomes a digraph. A **source** in a digraph is a vertex that has no incoming edge. We will use the following trivial observation repeatedly, without mentioning it explicitly: Each flippable vertex v is a source of its left-blue direction, and each flip reverses the direction of the edges incident to v . We need a series of easy lemmas.

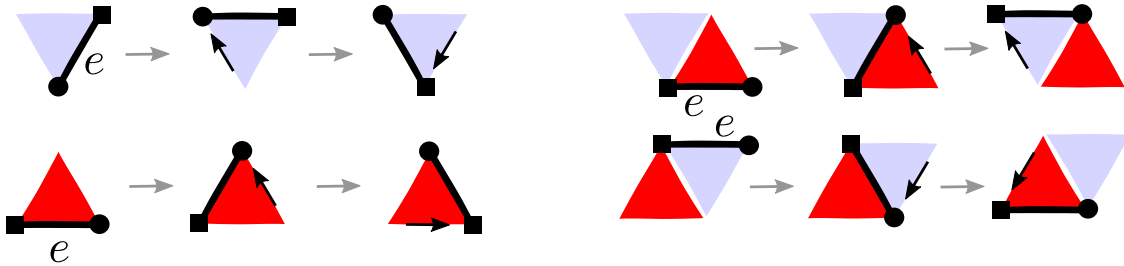


Figure 8.14: (Left) The second flip of the edge e does not counteract the first flip of e . (Right) The second flip of e counteracts the first one.

Lemma 8.18. *Let F be a flip sequence. If v and w are two adjacent vertices in G , then v is flipped in F in-between any two flips of w .*

Proof. When w is flipped, it is a source in its left-blue direction, and it can only become a source again after v is flipped. \square

Lemma 8.19. *Let F be a flip sequence. If, before the first flip of F , vertex v is a source in its left-blue direction, and v cannot be flipped, then v is not flipped in F .*

Proof. Vertex v cannot be flipped before at least one of its neighbors is flipped, but no neighbor w of v can be flipped before v is flipped, because w is not a source. \square

Lemma 8.20. *Let F be a flip sequence. If C is a cycle in G (not reduced to a single vertex) that is a directed cycle in its left-blue direction, then no vertex of C is flipped in F .*

Proof. The first vertex of C that would be flipped would not be a source (in its left-blue direction) before the flip. \square

Let e be an edge of G . In a flip sequence, assume that flip i flips an end-vertex of e , that flip j flips the other end-vertex of e , and that the end-vertices of e are not flipped between i and j . We say that flip j **counteracts** flip i if the image of e is rotated clockwise by i and counter-clockwise by j , or if it is rotated counter-clockwise by i and clockwise by j . See Figure 8.14.

Lemma 8.21. *Let F be a flip sequence, and let $i < j$ be two flips of the same vertex v of G , such that no flip of v appears between i and j . Then we have the following properties:*

- Every neighbor of v is flipped exactly once between i and j ;
- if every such flip counteracts flip i , then $F_{i \rightarrow j+1}|v$ is a 3_r -turn; otherwise, it is either a 1_r -turn or a -1_r -turn.

Proof. By Lemma 8.18, every neighbor of v is flipped exactly once between i and j , so there are three cases depicted in Figure 8.15. \square

Lemma 8.22. *Let f_0, \dots, f_p be a flip sequence. If $i < j$ are flips of distinct adjacent vertices v and w respectively, and if no flip between i and j flips a neighbor of w , then flip j counteracts flip i .*

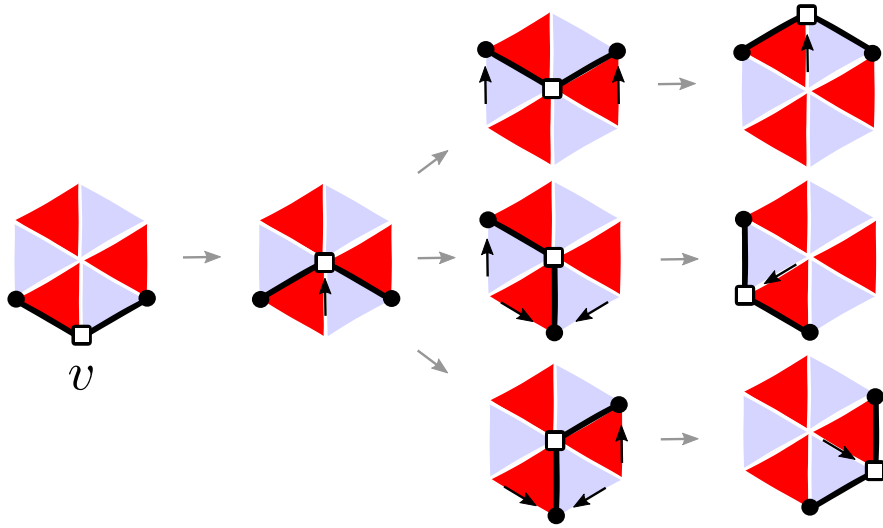


Figure 8.15: In a flip sequence, between two contiguous flips of a vertex v , the neighbors of v are flipped once.

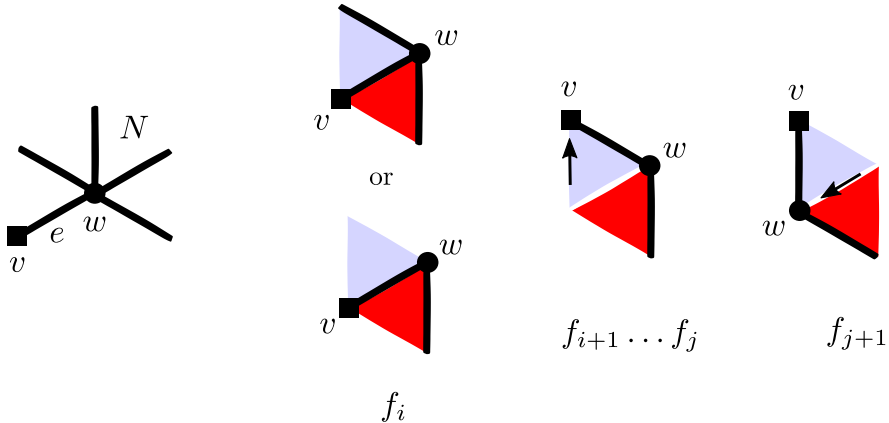


Figure 8.16: (Left) In the proof of Lemma 8.22, the vertices v and w , the edge e , and the set N of edges incident to w . (Right) If flips i and j both rotate the image of e clockwise, then f_i can be shortened.

Proof. Assume, for the sake of a contradiction, that flip j does not counteract flip i . See Figure 8.16. Let e be the edge of G between v and w , directed from v to w . Assume that flips i and j rotate the image of e clockwise, the other case being similar. Let N be the directed edges of G with source w .

We look at the situation in f_j , and thus just before flip j . We have that f_j maps N to two directed edges a and b of T such that the reversal of a , followed by b , make a 2_r -turn in T . Since j rotates e clockwise, $f_j(e)$ is the reversal of b .

Note that w is not flipped between flips i and j (because otherwise v , a neighbor of w , would also be flipped between flips i and j , by Lemma 8.18). Since also no neighbor of w is flipped between flips i and j , we have $f_{i+1}(N) = f_j(N) = \{a, b\}$. Since i rotates the image of e clockwise, $f_i(e)$ is the edge in the middle of the 2_r -turn formed by a and b (directed towards the image of w). Thus $f_i(N)$ is included in a set of three consecutive directed edges with source $f_i(w)$, and contains the middle directed edge, and so f_i can be shortened, contradicting

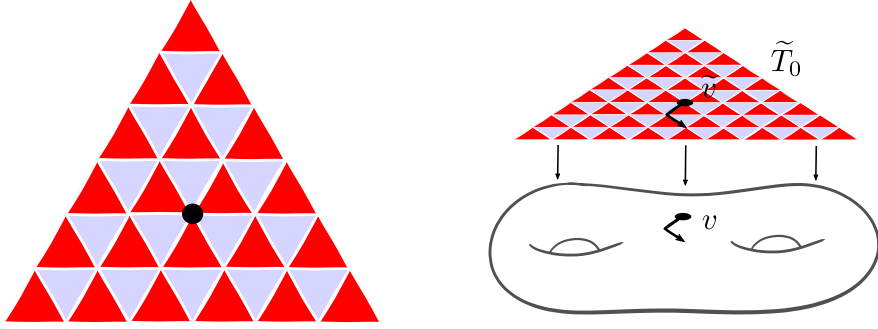


Figure 8.17: (Left) Flat zone of size six, and its central vertex. (Right) In the proof of Lemma 8.24, if there is a flat zone \tilde{T}_0 of size nine in the universal covering triangulation of T , then the central vertex \tilde{v} of \tilde{T}_0 projects to a vertex v on T such that every vertex of T at distance two or less from v has degree six.

the fact that we have a flip sequence. \square

8.3.4 Proof of Theorem 3.5

In this section we prove Theorem 3.5. The proof follows from a few definitions and lemmas.

Lemma 8.23. *Assume that G is connected and has q vertices. Let r be a vertex of G , and let F be a flip sequence of G that never flips r . Then F is composed of $O(q^2)$ flips.*

Proof. In G every vertex is at distance less than q from r . By Lemma 8.18 every vertex at distance $i \geq 0$ from r is flipped at most i times. \square

In a reducing triangulation T , a **flat zone** of size $m' \geq 1$ is a subtriangulation T_0 of T isomorphic to the subdivision of a triangle depicted in Figure 8.17, in which the sides of T_0 have length m' .

Lemma 8.24. *Every flat zone of the universal covering triangulation of T has size less than $3(m + 1)$, where m is the number of edges of T .*

The key property used in the proof is that, as we have assumed, S is not a torus. This is actually the only place where this assumption is used. (Since T is a reducing triangulation, S cannot be a sphere anyway.)

Proof. Assume the existence of a flat zone \tilde{T}_0 of size $3(m + 1)$ in the universal covering triangulation of T . See Figure 8.17. The central vertex of \tilde{T}_0 is at distance $m + 1$ from the boundary of \tilde{T}_0 . So every vertex of T admits a lift in the interior of \tilde{T}_0 . Then every vertex of T has degree six, so S is a torus by Euler's formula, contradicting our assumption. \square

A flip sequence F is **k -forward**, $k \geq 1$, if some vertex v of G is such that $F|v$ contains a subwalk of length k that makes only 3_r -turns.

Lemma 8.25. *Let F be a flip sequence of homomorphisms $G \rightarrow T$. If F is k -forward for some $k \geq 1$, then the universal covering triangulation of T has a flat zone of size k .*

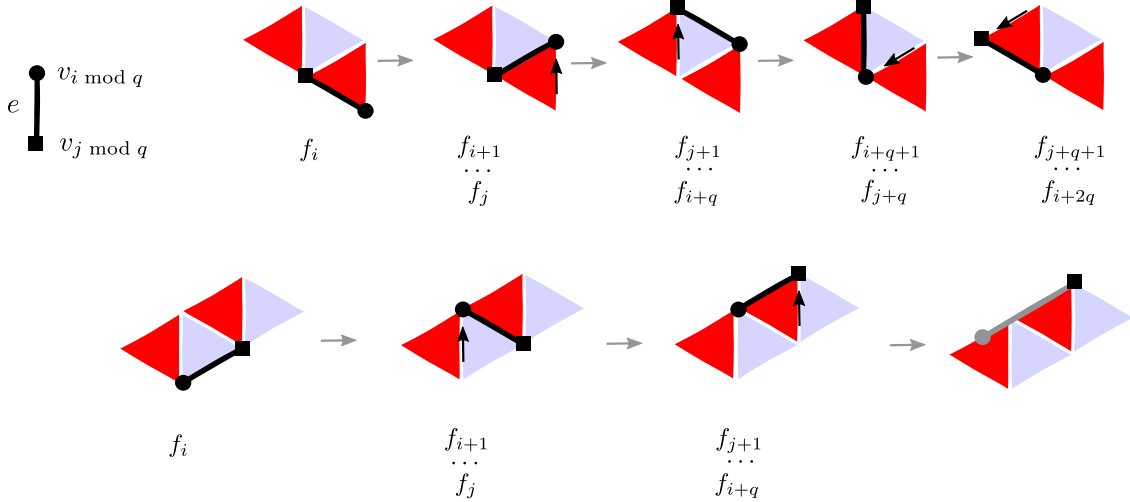


Figure 8.18: In the proof of Lemma 8.26, if W_i makes a 1_r -turn, then W_j makes a 1_r -turn.

Proof. Let \tilde{T} be the universal covering triangulation of T . Lift F to a sequence \tilde{F} of homomorphisms $\tilde{G} \rightarrow \tilde{T}$, where \tilde{G} is a covering space of G . Assume without loss of generality (up to restricting to a smaller flip sequence) that some vertex v of \tilde{G} is such that $\tilde{F}|v$ has length k and makes only 3_r -turns, and that the first and last flips of \tilde{F} are flips of v . We shall prove by induction that $\tilde{F}|v$ is a side of a flat zone in \tilde{T} lying to the left of $\tilde{F}|v$. The case $k = 1$ is clear since a flat zone of size one is just a triangle of \tilde{T} . So assume $k \geq 2$. Consider the first flip of v in \tilde{F} , and let $f : \tilde{G} \rightarrow \tilde{T}$ be the first map in \tilde{F} . Let e be the directed edge of \tilde{T} along which the flip is performed (e is the first directed edge of $\tilde{F}|v$). Consider the triangle t of \tilde{T} on the left of e , and the vertex x of t that is not incident to e .

There is a neighbor w of v in \tilde{G} such that $\tilde{f}(w) = x$. By Lemma 8.18 there is in \tilde{F} a flip of w in-between any two flips of v . Recall that v makes only 3_r -turns; by Lemma 8.21, this implies that every flip of w counteracts the previous flip of v . It follows that $\tilde{F}|w$ is a walk of length $k - 1$ that makes only -3_r -turns, running parallel to $\tilde{F}|v$; by Lemma 8.21 again, these walks can only be 3_r , 1_r , or -1_r -turns, and because the degree of each vertex of T is at least six, the only possibility is that $\tilde{F}|w$ makes only 3_r -turns. By induction, there is a flat zone of size $k - 1$ on the left of $\tilde{F}|w$, so there is a flat zone of side k on the left of $\tilde{F}|v$. \square

We now need some definitions. Consider an ordering v_0, \dots, v_{q-1} of the vertices of a graph. We say that v_i is a **lowpoint** if every neighbor of v_i , except perhaps v_0 , is higher than v_i in the ordering. The ordering is **proper** if (1) each vertex but v_0 is adjacent to a lower vertex, and (2) the set of lowpoints has the form $\{0, \dots, k\}$ for some k . A flip sequence f_0, \dots, f_p is **proper** if there is a proper ordering v_0, \dots, v_{q-1} of the vertices of G such that for every $0 \leq i < p$ the vertex flipped from f_i to f_{i+1} is $v_{i \bmod q}$.

Lemma 8.26. *Assume that G is connected and has q vertices. Let F be a proper flip sequence of $kq + 2$ homomorphisms $G \rightarrow T$, for some integer k . Then F is k -forward.*

Proof. Let v_0, \dots, v_{q-1} be the corresponding proper ordering of the vertices of G . Since F is composed of $kq + 1$ flips, the lowest vertex v_0 is both the first and the last vertex flipped in F , and v_0 is flipped $k + 1$ times in F , so $F|v_0$ has length $k + 1$. Let w_0 be the highest

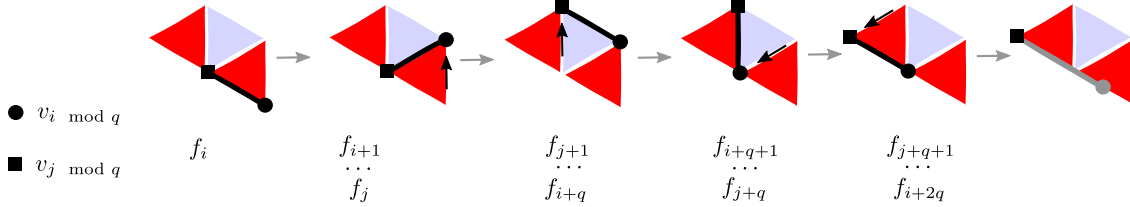


Figure 8.19: In the proof of Lemma 8.26, W_i cannot make a 1_r -turn.

neighbor of v_0 . There are two cases. First assume that w_0 is a lowpoint. Then, consider any neighbor x of v_0 . Because w_0 is a lowpoint, x is a lowpoint as well. Thus v_0 is the last neighbor of x to be flipped in F before a flip of x , and so every flip of x counteracts the last flip of v_0 by Lemma 8.22. That being true for every neighbor x of v_0 , Lemma 8.21 implies that $F|v_0$ makes only 3_r -turns, and thus that F is $(k+1)$ -forward.

Now assume that there is a neighbor of w_0 distinct from v_0 that is lower than w_0 in L . Among the neighbors of w_0 lower than w_0 , let w_1 be the highest. Among the neighbors of w_1 lower than w_1 , let w_2 be the highest \dots , and so on until $w_{m-1} = v_0$ for some $m \geq 3$. Then w_{m-1}, \dots, w_0 are the vertices of a directed cycle C in G , in order, such that for every i the vertex w_{i+1} is both the last neighbor of w_i flipped before w_i , and the last vertex of C flipped before w_i , indices being taken modulo m .

Let I contain the flips $i \in \{0, \dots, (k-1)q\}$ whose vertex flipped, here $v_i \bmod q$, belongs to C . For every $i \in I$, the image of $v_i \bmod q$ makes a walk W_i of length two between f_i and f_{i+q+1} . Indeed $v_i \bmod q$ is here flipped twice: in flips i and $i+q$.

We claim that for every two consecutive $i < j \in I$, if W_i makes a 1_r -turn, then W_j also makes a 1_r -turn. See Figure 8.18. Consider the edge e between $v_i \bmod q$ and $v_j \bmod q$, and consider the flips $i, j, i+q$, and $j+q$. By definition no neighbour of $v_j \bmod q$ is flipped between i and j , nor between $i+q$ and $j+q$, so by Lemma 8.22 flip j counteracts flip i , and flip $j+q$ counteracts flip $i+q$. Then flip i cannot rotate the image of e clockwise (as in the bottom part of Figure 8.18), for otherwise flip j would rotate the image of e counter-clockwise since it counteracts flip i , and then flip $i+q$ could not be such that W_i makes a 1_r -turn. So flip i rotates the image of e counter-clockwise (as in the top part of Figure 8.18). Then flip j rotates the image of e clockwise, since it counteracts flip i . Flip $i+q$ is also clockwise since W_i makes a 1_r -turn, and flip $j+q$ is counter-clockwise since it counteracts flip $i+q$. We proved that W_j makes a 1_r -turn.

We use the claim immediately to prove by contradiction that for every $i \in I$, if $i \leq (k-2)q$, then W_i does not make a 1_r -turn. For otherwise, by our claim, every $l > i \in I$ is such that W_l makes a 1_r -turn. In particular, the smallest $j > i \in I$ is such that W_j makes a 1_r -turn, so the flips $i, j, i+q$, and $j+q$ are such as depicted in Figure 8.19. But then flip $i+2q$ cannot be such that W_{i+q} makes a 1_r -turn, which is a contradiction.

The same arguments show that for every $i \in I$, if $i \leq (k-2)q$, then W_i does not make a -1_r -turn. So W_i makes a 3_r -turn by Lemma 8.21. In particular $F_{0 \rightarrow (k-1)q+1}|v_0$ makes only 3_r -turns, so F is k -forward. \square

An ordering v_0, v_1, \dots of the vertices of a digraph D is **monotonic** if every edge of D is directed from a vertex v_i to a vertex v_j such that $i < j$.

Lemma 8.27. *Let D be a digraph of size n . If D has no directed cycle and has a single source, then we can compute in $O(n)$ time an ordering of the vertices of D that is both proper and monotonic.*

Proof. Without loss of generality, D has at least two vertices. Let v_0 be the unique source of D . Since D has no directed cycle, the vertex set of D can be partitioned into sets I_0, \dots, I_m , $m \geq 1$, where $I_0 := \{v_0\}$, and where I_k contains the sources of $D \setminus \bigcup_{i < k} I_i$ for every $1 \leq k \leq m$. Order arbitrarily each of the sets I_0, \dots, I_m , and concatenate them into an ordering L of the vertices of D . Then L is monotonic. Moreover, each vertex but v_0 is adjacent to a lower vertex, and $I_0 \cup I_1$ is the set of lowpoints of L , so L is proper. \square

Before proving Theorem 3.5 we detail how to detect, given a *homomorphism* f , if a balancing move applies to f :

Lemma 8.28. *Let T be a reducing triangulation of size m . Let G be a graph of size n , and let $f : G \rightarrow T$ be a homomorphism. In $O(m + n)$ time we can determine if there is a simple closed walk C in G such that $f \circ C$ makes only 3-turns, is pulled left, and not right. In that case, both C and the subgraph G_0 of G spanned by the walks that follow C are computed at the same time.*

Proof. Without loss of generality, assume that we look for C such that $f \circ C$ makes only 3_r -turns (the 3_b -turns case being symmetric). Consider the following algorithm. As a preliminary, build a graph G' from G by detaching every vertex v of G from its incident edges, and by re-attaching those edges to copies of v as follows. Let N contain the directed edges emanating from v in G , whose basepoints have thus been detached from v . For every two directed edges a and b based at $f(v)$ in T such that (a^{-1}, b) makes a 3_r -turn, consider all the directed edges in N that are mapped to a or b (if any), and attach all their basepoints to a common copy v' of v . Mark v' with red if $f(N)$ contains a directed edge of T on the right of (a^{-1}, b) . Mark v' green if $f(N)$ does not contain any such directed edge, and if it contains a directed edge on the left of (a^{-1}, b) .

The graph G' *projects* to G in the sense that the edges of G' are those of G , and every vertex of G' corresponds to a vertex of G (though not in a one-to-one manner). We say that a vertex v' of G' *lifts* a vertex v of G if v is the projection of v' .

Build the graph G' in $O(m + n)$ time. Direct every edge e' of G' so that $f(e')$ sees red on its left. Then determine in $O(n)$ time if there is a connected component G'_0 of G' that does not contain any red vertex, that contains a green vertex, and that contains a simple directed cycle C' . If there is none, then return that nothing was found. Otherwise, return the closed walk C in G to which C' projects, and the subgraph G_0 of G' to which G'_0 projects.

Let us now prove that this algorithm is correct. Every closed walk C in G whose image walk makes only 3_r -turns is lifted by a directed cycle C' in G' , and if C is simple, then C' is simple. Conversely, every simple directed cycle C' in G' projects to a closed walk C that makes only 3_r -turns. And if the connected component G'_0 of C' contains no red vertex, then C is simple; indeed any self-intersection vertex of C would either correspond to a self-intersection vertex of C' , which is impossible since C' is simple, or otherwise it would correspond to red vertices in C' . We conclude with the claim that G_0 is the subgraph of G spanned by the walks following C , and that C is pulled left (resp. right) if and only if G'_0 contains a green (resp. red) vertex. Indeed every walk W that follows C in G lifts to a walk W' based at some vertex of C' in G'_0 . Also, if W can be extended by one edge into a walk

that pulls C to the left (resp. right), then the end-vertex w' of W' is marked green (resp. red). Reciprocally, any walk in G'_0 from C' to a vertex w' projects to a walk W in G that follows C . And if w' is green (resp. red), then W can be extended by one edge to pull C to the left (resp. right). \square

Proof of Theorem 3.5. By Lemma 8.16, we can assume that f is simplicial. Without loss of generality, we assume that G is connected, for otherwise we could apply the algorithm to each connected component separately. Making f harmonious is done using balancings, shortenings, and flips. Since balancings and shortenings decrease the length of the drawing, we give them priority over flips. More precisely, the algorithm consists in applying the routine given below, which only performs flips, with the following important twist, left implicit in the description: *whenever a balancing or a shortening is possible, we apply it and resume the routine from scratch.* Recall that the simplicial map $f : G \rightarrow T$ factors as a homomorphism $\hat{f} : \hat{G} \rightarrow T$; it is convenient to express the routine in terms of \hat{f} , since flips can be described at the homomorphism level. Here is the routine:

1. Choose an arbitrary vertex r of \hat{G} , and flip any vertex of \hat{G} other than r , in any order, as long as possible.
2. Direct \hat{G} with the left-blue direction. If \hat{G} has no directed cycle and has a single source, then do the following: apply Lemma 8.27 to build in $O(n)$ time a proper and monotonic ordering v_0, \dots, v_{q-1} of the $q \geq 1$ vertices of \hat{G} ; initialize $i := 0$. Then, while it is possible to flip $v_{i \bmod q}$, flip it and increment i . (Some precisions: (a) we go to Step 3 as soon as $v_{i \bmod q}$ is not flippable; (b) The ordering is fixed during this entire step; if, after a flip, we update the direction of the edges to preserve the left-blue direction, it ceases to be monotonic.)
3. Flip any vertex of \hat{G} (even possibly r), in any order, as long as possible.

If the algorithm terminates, then f is harmonious by Lemma 8.17. We now bound the number of flips of the routine, assuming that it is not interrupted by a balancing or a shortening. Step 1 does not flip r , so it consists of $O(n^2)$ flips by Lemma 8.23. Also the flip sequence of Step 2 is proper, so it has length $O(mn)$ by Lemmas 8.24, 8.25, and 8.26. Let F be the flip sequence of Step 3. For the sake of the analysis, we preserve the left-blue direction of the edges of \hat{G} after each flip (equivalently, at each flip of a vertex v , we reverse the direction of the edges incident to v). We now prove that in all cases, some vertex of \hat{G} is not flipped in F :

- If Step 2 was skipped because \hat{G} has a directed cycle, then this cycle remains fixed by Lemma 8.20;
- if Step 2 was skipped because \hat{G} has a source v distinct from r , then v is a source that cannot be flipped, so v is not flipped in Step 3 by Lemma 8.19;
- if Step 2 was executed, we claim that in Step 2, every attempt to flip a vertex v happens when v is a source. Indeed, at the first round of flips, the neighbours of v that have already been flipped correspond precisely to the edges that were directed towards v in the initial monotonic ordering, which have thus been reversed by the flips, making v a source.

After each vertex of \hat{G} has been flipped, the directed graph is again monotonic. This proves the claim. It follows that v cannot be flipped in Step 3 by Lemma 8.19.

This implies that the flip sequence F of Step 3 has length $O(n^2)$ by Lemma 8.23, as desired. Thus, overall, if not interrupted, the routine terminates after $O((m+n)n)$ flips if not interrupted. Since there are $O(n)$ balancings or shortenings, the total number of flips, balancings, and shortenings is $O((m+n)n^2)$.

To prove the claimed running time of $O((m+n)^2n^2)$ time, it remains to note that finding and applying the next move, or correctly asserting that no move can be applied anymore, takes $O(m+n)$ time. Indeed, \hat{G} and \hat{f} can be computed in $O(n)$ time by constructing the clusters of f . On \hat{G} finding a flip, or correctly asserting that there is none, takes $O(m+n)$ time. Same for the shortenings. Concerning the balancings, an application of Lemma 8.28 determines in $O(m+n)$ time if there is a simple closed walk C in \hat{G} such that $\hat{f} \circ C$ makes only 3-turns, is pulled left, and is not pulled right. If there is none, then no balancing is available. Otherwise C can be balanced, and Lemma 8.28 computes both C and the subgraph \hat{G}_0 of \hat{G} that will move with C during the balancing. The modification brought to f by the balancing then takes $O(m+n)$ time. \square

8.4 Extensions to reducing triangulations with boundary

Until now we only defined reducing triangulations on closed surfaces, but they can also be defined on surfaces with boundary. On those surfaces a triangulation T whose dual is bipartite is **reducing** if each vertex in the interior of T has degree at least six. There is no constraint on the degrees of the boundary vertices. In this section we extend the results of Sections 8.2 and 8.3 to reducing triangulations with boundary. To mimic the classical setting of Tutte's theorem, we consider the constraint of attaching vertices to the boundary of the surface. We formalize this constraint in the following definitions. Let S be a surface with non-empty boundary (such as the disk). Let G be a graph, and let $f : G \rightarrow S$ be a map. We use the following conventions: the boundary ∂S of S is directed so that the interior of S lies on its right, and the rotation system of a graph embedded on S records, for every vertex v embedded on S , the *clockwise* order of the edges meeting v .

Anchor. An **anchor** is a (possibly empty) set A of vertices of G mapped to ∂S by f , together with linear orderings of those vertices mapped to the same point of ∂S . Note that some vertices of G can be mapped to ∂S without belonging to A .

Untangling relatively to an anchor. Let $f' : G \rightarrow S$ be obtained from f by sliding infinitesimally along ∂S the images of the vertices in A , so as to separate them in the orders prescribed by A . We say that f can be **untangled relatively to A** if there is an embedding homotopic to f' , where the homotopy fixes the image of every vertex in A .

Weak embeddings relative to an anchor. Informally, we say that f is a weak embedding *relative to A* if there exist embeddings arbitrarily close to f in which the vertices in A are embedded along ∂S , and in the orders prescribed by A . We shall not use this definition as is, and instead we consider an equivalent formulation in the case where f is a drawing in the 1-skeleton T of a reducing triangulation T of S . This formulation better suits our needs. In

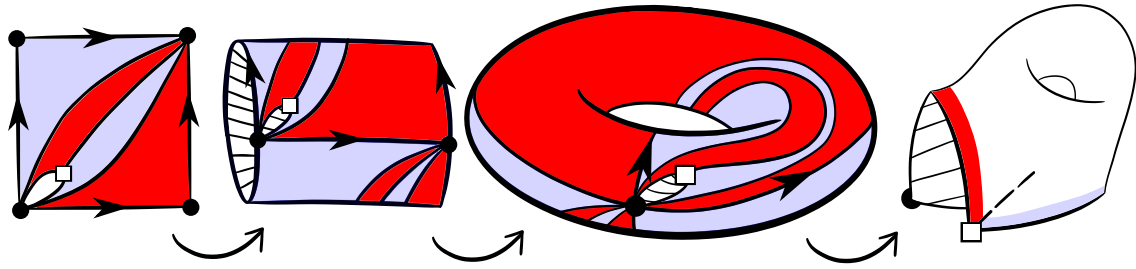


Figure 8.20: Construction of the 1-gadget.

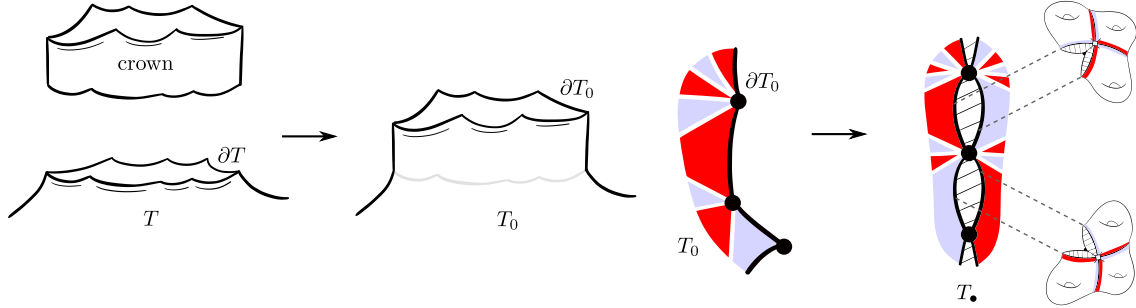


Figure 8.21: Construction of the triangulation T_* in the proof of Theorem 8.1.

detail, we extend T to a graph M^* equipped with a rotation system, we extend G and f to a graph G^* and a drawing $f^* : G^* \rightarrow M^*$ as follows. Consider every two consecutive edges e and f along the boundary of T , and let x be the vertex of T between e and f . Let v_1, \dots, v_k be the $k \geq 0$ vertices in A that are mapped to x by f , in the order prescribed by A . In M^* , create k degree one vertices attached to x by edges s_1, \dots, s_k : place them in the rotation system of M^* so that e, s_1, \dots, s_k, f are consecutive around x . Then for every $1 \leq i \leq k$, create an edge incident to v_i in G^* , and map this edge to s_i in f^* . We say that f is a **weak embedding relative to A** if f^* is a weak embedding.

Our result is the following :

Theorem 8.1. *Let S be a surface with boundary. Let T be a reducing triangulation of S , with m edges. Let G be a graph of size n , and let $f : G \rightarrow T$ be simplicial. Let A be an anchor for f . If f can be untangled rel. A , then we can compute in $O((m+n)^2 n^2)$ time a simplicial map $f' : G \rightarrow T$, homotopic to f relatively to A , weak embedding relative to A , not longer than f .*

The proof of Theorem 8.1 goes by extending T to a reducing triangulation without boundary (in order to apply Theorem 3.5). This extension step uses ad-hoc gadgets that we now define. Let S be the surface of genus one with one boundary component. The **1-gadget** is the reducing triangulation T of S depicted in Figure 8.20. The boundary of S is the union of two edges of T : one edge is incident to a blue face of T , and the other to a red face. The **3-gadget** is then the reducing triangulation T' obtained from disjoint 1-gadgets T_1, T_2, T_3 by identifying the blue-incident edge of T_i with the red-incident edge of T_{i+1} for every $i \in \{1, 2\}$. The boundary of T' is the union of the red-incident edge of T_1 and the blue-incident edge of T_3 .

We call **crown** any reducing triangulation T of the annulus obtained from a circular list of $k \geq 2$ triangles t_0, \dots, t_{k-1} by identifying some side of t_i with some side of t_{i+1} for every i , where indices are modulo k .

Proof of Theorem 8.1. We shall extend T to a reducing triangulation *without boundary* T_\bullet , and then extend f to a drawing on T_\bullet . The construction of T_\bullet is as follows. First extend T to a reducing triangulation T_0 by attaching a crown to each boundary component of T . Choose the crowns so that if x is a vertex of the boundary of T , and if $k \geq 0$ vertices of A are mapped to x by f , then x is incident to at least $k + 6$ edges in the interior of its crown; crucially, we make the observation (O) that the first three, and the last three edges incident to x in the interior of the crown will not be used by the extended drawing. Now build T_\bullet from T_0 as follows. See Figure 8.21. Consider a copy T_1 of T_0 . Reverse the direction of T_1 , and exchange the colors of its faces. Identify every edge of the boundary of T_0 with its copy in T_1 . At this point the faces of T_\bullet are properly colored, but T_\bullet may not be a reducing triangulation since vertices on the boundary of T_0 may have low degree. This is fixed by cutting open in T_\bullet every edge of the boundary of T_0 , and by identifying the two cut paths with the two boundary paths of a 3-gadget (keeping the coloring of the faces proper).

Now extend G and f to a graph G_\bullet , and a simplicial map $f_\bullet : G_\bullet \rightarrow T_\bullet$; first extend G and f to some G_0 and $f_0 : G_0 \rightarrow T_0$, as follows. Consider every vertex x of the boundary of T . Let v_1, \dots, v_k for some $k \geq 0$ be the vertices of A mapped to x by f , in order. Let e_1, \dots, e_{k+6} be consecutive edges around x in the interior of the crown incident to x . For every $1 \leq i \leq k$, add in G_0 an edge s_i incident to v_i , and let $f_0(s_i) := e_{i+3}$. We say that the newly created end-vertex of s_i is a tip vertex of G_0 , and that s_i is a tip edge of G . Build G_\bullet and f_\bullet from G_0 and f_0 by considering a copy G_1 of G_0 , and the mirror map $f_1 : G_1 \rightarrow T_1^1$, and by identifying in $G_0 \cup G_1$ and $f_0 \cup f_1$ every tip vertex of G_0 with its mirror vertex in G_1 .

To conclude, transform f_\bullet to a map $f'_\bullet : G_\bullet \rightarrow T_\bullet$ with the algorithm of Theorem 3.5, and return $f' := f'_\bullet|_G$. Let us show why this is correct. Let T^\flat be the sub-triangulation of T_\bullet that is the union of T and the mirror of T . Let G^\flat be the subgraph of G_\bullet that is the union of the two copies of G . By the above observation (O), applying the moves described in Section 8.3 to f_\bullet does not modify the images of the stem edges, and preserves the fact that $f_\bullet(G^\flat) \subset T^\flat$. In particular f' is homotopic to f rel. A . Moreover f_\bullet is homotopic to an embedding in T_\bullet since f can be untangled relatively to A in T . Thus f'_\bullet is a weak embedding by Theorem 3.4, and f'_\bullet is not longer than f_\bullet . And so f' is a weak embedding relative to A , not longer than f . \square

Part II

Computing Delaunay Triangulations of Surfaces

In this part of the thesis

In this second part of the thesis we consider computing a Delaunay triangulation (or tessellation) of a surface from an arbitrary triangulation of the surface. The review of the background and related works is postponed to Chapter 9. In particular we refer to Chapter 9 for the definitions of Delaunay tessellations, Delaunay triangulations, and Delaunay flips. Here we present some important concepts, provide an informal account of our contributions, and describe the organization of the chapters.

Computing the Delaunay tessellation. First we consider, on a closed piecewise-flat surface S , a particular Delaunay tessellation \mathcal{D} of S . It is the unique Delaunay tessellation of S whose vertices are exactly the singularities of S (the points of S that lie in the interior of S and are surrounded by an angle different from 2π or lie on the boundary of S and are surrounded by an angle different from π , see Chapter 3), with a single exception: if S has no singularity, then S is a flat torus and we let \mathcal{D} be any of the Delaunay tessellations of S that have exactly one vertex, for one can be mapped to the other via an orientation-preserving isometry of S anyway. In any case, we say that \mathcal{D} is **the Delaunay tessellation of S** , in a slight abuse. We consider computing \mathcal{D} from an arbitrary triangulation of S .

More precisely, recall from Chapter 3 that a portalgon is a disjoint collection of oriented flat polygons together with a partial matching of the sides of the polygons. We are given a triangular portalgon T whose surface $\mathcal{S}(T)$ is closed, and we consider computing the portalgon of the Delaunay tessellation of $\mathcal{S}(T)$. The **aspect ratio** of T is the maximum side length of a triangle of T divided by the smallest height of a triangle of T (possibly another triangle). Note that the aspect ratio is always greater than $\sqrt{3}/2 > 1$, for it is easily seen that the maximum side length of a triangle is always greater than or equal to $\sqrt{3}/2$ times its smallest height. We prove that the portalgon of the Delaunay tessellation of $\mathcal{S}(T)$ can be computed from T in time polynomial in the number of triangles of T and in the *logarithm* of the aspect ratio of T :

Theorem 8.2. *Let T be a portalgon of n triangles, of aspect ratio r , whose surface $\mathcal{S}(T)$ is closed. One can compute the portalgon of the Delaunay tessellation of $\mathcal{S}(T)$ in $O(n^3 \log^2(n) \cdot \log^4(r))$ time.*

The only two methods we are aware of for computing a Delaunay triangulation from an *arbitrary* triangulation (not issued of a mesh) are greedily performing Delaunay flips and computing the dual Voronoi diagram by adapting shortest path algorithms. The time complexities of these algorithms are not bounded by any polynomial in n and $\log(r)$, contrarily to the algorithm of Theorem 8.2. This follows from Theorem 8.3 below, and from the algorithm of Proposition 10.3 in Chapter 10.

As we shall see at the beginning of Chapter 10, our result has interesting applications. In particular, the time complexity of computing shortest paths on the surface of a portalgon depends on a geometric parameter, the *happiness* of the portalgon. As the portalgons of Delaunay triangulations have bounded happiness, Theorem 8.2 enables to pre-process a portalgon before computing shortest paths on its surface. Moreover, the Delaunay tessellation of a closed piecewise-flat surface being unique by definition, Theorem 8.2 enables to test whether the surfaces of two given portalgons are isometric, simply by computing and comparing the portalgons of the associated Delaunay tessellations.

Bounding Delaunay flip sequences. For our second contribution, we depart from looking for an efficient algorithm, and we consider instead the classical algorithm that greedily performs Delaunay flips on the edges of an input triangulation. On general piecewise-flat surfaces, the complexity of this algorithm is vastly open. We focus on the particular case where the surface is a flat torus. We call **sequence of Delaunay flips** any sequence T_0, \dots, T_m of triangulations, for some $m \geq 0$, such that for every $k \in \{1, \dots, m\}$ the triangulation T_k results from the Delaunay flip of an edge in the triangulation T_{k-1} . We say that m is the **length** of the sequence, and that the sequence **starts** from the triangulation T_0 . We prove:

Theorem 8.3. *Let \mathbb{T} be a flat torus. Let T be a triangulation of \mathbb{T} , with n vertices, of maximum edge length L . Every sequence of Delaunay flips starting from T has length at most $C \cdot n^2 \cdot L$, where $C > 0$ depends only on \mathbb{T} . This bound is tight up to a constant factor.*

An upper bound was already proved by Despré, Schlenker, and Teillaud [70, Theorem 16], as a particular (easy) case of a more general result on triangulations of hyperbolic surfaces:

$$C \cdot n^2 \cdot \Delta^2$$

where Δ is a parameter measuring in some sense how “stretched” T is. The definition of Δ is not used in this chapter. We just mention that to obtain their bound the authors showed that the edges flipped in a sequence of Delaunay flips cannot be longer than 2Δ [70, Lemma 10]. The upper bound follows from the observation that the number of segments no longer than $L > 0$ between two given points of \mathbb{T} is at most quadratic in L . Our first (small) improvement is to replace the parameter Δ by the maximum length L of an edge in T . The inequality $L \leq \Delta$ is easily observed to be true. Moreover the definition of Δ is more intricate than the definition of L and it is not obvious how to compute Δ while computing L is immediate. Our second (main) improvement is to replace the quadratic dependency by a linear dependency in L , obtaining a bound that is tight up to a constant factor.

Implementing Delaunay flips. Our final contribution is an implementation of the flip algorithm on triangulations of closed *hyperbolic* surfaces, a fundamental building block for computing with such surfaces. Our implementation is collected in a package of a standard library of computational geometry, along with convenient generation and visualization tools. In this setting, it is important and challenging to perform the arithmetic operations exactly and efficiently. To do so, we implemented a generation of triangulations of surfaces of genus two that are described entirely by rational numbers. This generation process is also a contribution of us.

Organization of the chapters. We review the background and the related works in Chapter 9. We prove Theorem 8.2 in Chapter 10. We prove Theorem 8.3 in Chapter 11. We discuss our package in Chapter 12.

Chapter 9

Background and Related Works

In this chapter we briefly review the background and works related to portalgons and Delaunay tessellations.

9.1 Portalgons versus meshes

We defined piecewise-flat surfaces and their tessellations from portalgons, polygons in \mathbb{R}^2 with matched sides (Chapter 3). These are more commonly obtained from *meshes*, polygons in \mathbb{R}^3 glued along their edges. Every (compact, orientable) piecewise-flat surface is isometric to the surface of a mesh, as proved by Burago and Zalgaller [29], see also the discussion of Lazarus and Talleire [135, Introduction]. Moreover, cutting the edges of a mesh and placing its polygons in the plane provides a portagon. However portalgons are more general than meshes as portalgons cannot in general be obtained from a mesh this way. To see that, observe that every edge e of a mesh is a shortest path in the surface of the mesh, since e is already a shortest path in \mathbb{R}^3 . On the other hand, given a portagon T , the edges of the tessellation T^1 (Chapter 3) are in general not shortest paths in the surface $\mathcal{S}(T)$. Strikingly, flat tori have portalgons with few polygons but their simplest meshes we are aware of have 80 polygons [157].

There is a recent development of algorithms that advantageously operate on triangulations of piecewise-flat surfaces (equivalently, triangular portalgons) that are not issued of a mesh. In this context the adjective “intrinsic” is sometimes placed before the name “triangulation” to make the distinction with the particular triangulations issued of a mesh. For example Sharp and Crane [172] find geodesics of a piecewise-flat surface quite simply by flipping edges of an intrinsic triangulation. The exact complexity of their algorithm is currently open. Another algorithm of Takayama [179] constructs a low distortion homeomorphism between two surfaces, and represents the homeomorphism by a correspondence between intrinsic triangulations. Also Liu et al [138] re-triangulate a surface to solve equations on it. Considering intrinsic triangulations gives them freedom to re-triangulate the surface without modifying it, an advantage over many mesh simplification techniques that commonly modify the surface [116].

9.2 Measuring distances, and tracing shortest paths

A fundamental problem on piecewise-flat surfaces is compute the distance between two points, or even to trace a shortest path between the two points. While there exist algorithm to compute shortest paths insides a given planar polygon [148, 111, 188], other algorithms are designed specifically for meshes. Recall that every edge of a mesh M is a shortest path on the surface of M . Of course on M not every pair of points are the endpoints of an edge, but no shortest path can cross an edge twice, for otherwise it could be shortened. And the number of geodesic paths crossing at most once each edge of M is bounded by a function of the number n of edges of M . So shortest paths on the surface of M can be computed by exhaustive search in time that depends only in n . In fact Mitchel, Mount, and Papadimitriou [149] obtained the following result. They are given as input a source point s in the surface of a mesh M and perform a preliminary computation in time $O(n^2 \log n)$ and space $O(n^2)$. Then they can answer the following queries. Given a point x in the surface of M they compute the distance between s and x in $O(\log n)$ time, and they report a shortest path between s and x in $O(k + \log n)$ time, where k is the number of faces visited by the path. Roughly, their algorithm propagates waves along the surface, starting from the source, in a discrete manner. Their result has since been improved by Chen and Han [41, 42] who proved, using a different technique, that shortest paths can be computed in $O(n^2)$ time and $\Theta(n)$ space.

On a portalgon however, the number of times a shortest path in the surface visits the image of a polygon is not bounded by any function of the number of polygons. This fact is folklore, it was for example noted almost 20 years ago in a popular blog post by Erickson [85]. Recently, Löffler, Ophelders, Staals, and Silveira [141, Section 3] coined the term **happiness** of a portalgon T , for the maximum number of times a shortest path in $\mathcal{S}(T)$ visits the image of a polygon of T . They adapted the single-source shortest paths algorithm from meshes to portalgons [141, Section 3], whose running time now depends on the happiness of the portalgon. They did not handle the case of multiple sources. We emphasize that their algorithm is more efficient on the portalgons of *low* happiness.

The fact that portalgons with low happiness are more suited to computations raises the question of replacing a portalgon T by another portalgon T' of the same surface whose happiness is “low”. Löffler, Ophelders, Staals, and Silveira [141, Section 5] provided a solution to this problem, but only for a restricted class of inputs whose surfaces are all homeomorphic to an annulus. Importantly, they also proved [141, Section 4.2] that the portalgons of Delaunay triangulations have bounded happiness. So, as they observed, providing an efficient algorithm for replacing T by the portalgon of a Delaunay triangulation would solve the problem. This will be our main contribution in Chapter 10.

9.3 Voronoi diagrams and Delaunay tessellations

In this section we review Voronoi diagrams and Delaunay tessellations, in the Euclidean plane and on closed piecewise-flat surfaces. These classical objects have been extensively studied, so we detail only the few definitions and results relevant to us, referring to textbooks [57, 99] for details.

9.3.1 Voronoi diagrams

Voronoi diagrams are mostly known in the Euclidean plane \mathbb{R}^2 . In this particular setting, the Voronoi diagram of a finite non-empty $V \subset \mathbb{R}^2$ contains the points $y \in \mathbb{R}^2$ whose distance to V is realized by at least two distinct points of V . In other words there exist at least two distinct points of V whose distance to y is the minimum among V . Informally, the Voronoi diagram of V decomposes \mathbb{R}^2 according to which points of V they are closer to.

Voronoi diagrams are defined one more spaces than the Euclidean plane. On a closed piecewise-flat surface S , one further assumes that V contains all the singularities of S . In this setting, the **Voronoi diagram** of (S, V) contains the points $x \in S$ such that the distance between x and V is realized by at least two distinct *paths* in S . Note that, contrarily to the Euclidean plane setting, it is possible for the Voronoi diagram of (S, V) to contain a point x such that all the shortest paths between x and V end at the same point of V . This is for example the case if S is a flat torus and V contains exactly one point of S .

9.3.2 Delaunay tessellations

Similarly to Voronoi diagrams, Delaunay tessellations are mostly known in the Euclidean plane \mathbb{R}^2 , and for a finite $V \subset \mathbb{R}^2$. In this setting, they can be defined using the notion of *empty disk*. Given $x \in \mathbb{R}^2$ and $r > 0$, consider the points of \mathbb{R}^2 whose Euclidean distance to x is smaller than r . This subset of \mathbb{R}^2 is an empty disk if it contains no point of V . Note that, importantly, it is possible for the boundary circle ∂D of an empty disk D to contain points of V . As it turns out, there is a unique tessellation \mathcal{D} of the convex hull of V that satisfies the following: for every empty disk D if $\partial D \cap V$ is not empty then the convex hull of $\partial D \cap V$ is either a vertex, an edge, or the closure of a face of \mathcal{D} , and every vertex, edge, and face of \mathcal{D} can be obtained this way. This tessellation \mathcal{D} is called the Delaunay tessellation of V .

This “empty disk” definition of the Delaunay tessellation has been generalized from the Euclidean plane \mathbb{R}^2 to closed piecewise-flat surfaces S by Bobenko and Springborn [22]. Empty disks are generalized by immersed empty disks. An **immersed empty disk** is a pair (D, φ) where D is an open metric disk of \mathbb{R}^2 , and $\varphi : \overline{D} \rightarrow S$ is a map defined on the closure \overline{D} of D that satisfies the following: the restriction of φ to D is an isometric immersion, and $\varphi(D) \cap V = \emptyset$. Note that φ is not necessarily injective. Bobenko and Springborn [22, Proposition 4] proved:

Lemma 9.1 (Bobenko and Springborn). *There is a unique tessellation \mathcal{D} of S such that for every immersed disk (D, φ) , if $\varphi^{-1}(V)$ is not empty, then the convex hull of $\varphi^{-1}(V)$ projects via φ to either a vertex, an edge, or the closure of a face of \mathcal{D} , and such that every vertex, edge, and face of \mathcal{D} can be obtained this way.*

The tessellation \mathcal{D} given by Lemma 9.1 is the **Delaunay tessellation** of (S, V) . It is “in general” a triangulation, but not always. A **Delaunay triangulation** is any triangulation obtained by triangulating the faces of a Delaunay tessellation along vertex-to-vertex arcs.

Delaunay tessellations are classically related to Voronoi diagrams. In the flat plane \mathbb{R}^2 for example, given a finite $V \subset \mathbb{R}^2$ of at least three points, any two $v \neq v' \in V$ are the endpoints of an edge in the Delaunay tessellation of V if and only if the Voronoi cells of v and v' share a side. In this sense the Delaunay tessellation of V is dual to the Voronoi diagram of V . This duality is folklore even on closed piecewise-flat surfaces, and has been

explored for algorithmic purposes [77, 120]. However we could not find a detailed depiction of it, so we provide details in the appendix of Chapter 10.

9.4 Computing Voronoi diagrams and Delaunay tessellations

In this section we review algorithms computing Voronoi diagrams and Delaunay tessellations. In the Euclidean plane there exist many algorithms to do so, but we do not review these algorithms. Instead we review the only two approaches we are aware of that generalize to closed piecewise-flat surfaces.

9.4.1 Approach by shortest paths

One approach computes a Voronoi diagram with a suitably adapted multiple-source shortest path algorithm, and then derives from it a Delaunay tessellation. On meshes, the single-source shortest path algorithm of Mitchel, Mount, and Papadimitriou [149] was adapted to compute Voronoi diagrams by Mount [151], and by Liu, Chen, and Tang [139]. This was used by Liu, Xu, Fan, and He [140] to compute Delaunay tessellations. To our knowledge, prior to this thesis, this approach has not been extended from meshes to portalgons beyond the recent single-source shortest path algorithm of Löffler, Ophelders, Staals, and Silveira [141].

9.4.2 Approach by flips

Another approach starts from an initial triangulation and flips its edges. This approach is mostly known in the Euclidean plane \mathbb{R}^2 . In this setting, given a triangulation T , consider two triangles t and t' adjacent to a common edge e , and the two end-vertices v and v' of respectively t and t' that do not belong to e . If v lies in the interior of the circumdisk of t' then v' lies in the interior of the circumdisk of t , and the edge e is said **Delaunay flippable** in T . In this case e can be replaced in T by the geodesic segment between v and v' . This operation is called a **Delaunay flip**. Spectacularly, a triangulation is Delaunay if and only if none of its edges are Delaunay flippable. Moreover, on triangulations with n vertices, every sequence of Delaunay flips has length $O(n^2)$. This provides a simple $O(n^2)$ time algorithm to compute a Delaunay triangulation of a set V of n points in \mathbb{R}^2 : construct an arbitrary triangulation of V , then perform Delaunay flips on it, greedily, as long as possible.

The notions of Delaunay flips and Delaunay flippable edges immediately extend to triangulations of closed piecewise-flat surfaces. Bobenko and Springborn [22] proved that with their definition a triangulation is Delaunay if and only if none of its edges are Delaunay flippable. Termination of the flip algorithm was proved by Indermitte, Liebling, Troyanov, and Clémenton [120]. The number of flips is not anymore bounded by any function depending only on the number of vertices. The only upper bound we are aware of is by Despré, Schlenker, and Teillaud [70, Theorem 16]. In the particular case where the surface is a flat torus, they proved that every sequence of Delaunay flips has length $O(n^2 \cdot \Delta^2)$, where n is the number of vertices, Δ is a geometric parameter of the initial triangulation T that we do not detail here, and the $O()$ notation depends on the (geometry of) flat torus.

The notions of Delaunay triangulations and Delaunay flips also extend to triangulations of closed *hyperbolic* surfaces [70, Definitions 4-5]. In this setting Despré, Schlenker, and

Teillaud [70, Theorem 19] proved that every sequence of Delaunay flips is finite, and provided an upper bound on the number of flips.

Chapter 10

Computing the Delaunay Tessellation of a Closed Piecewise-Flat Surface

10.1 Introduction

In this chapter we prove Theorem 8.2, which we restate for convenience:

Theorem 8.2. *Let T be a portalgon of n triangles, of aspect ratio r , whose surface $\mathcal{S}(T)$ is closed. One can compute the portalgon of the Delaunay tessellation of $\mathcal{S}(T)$ in $O(n^3 \log^2(n) \cdot \log^4(r))$ time.*

Throughout the chapter logarithms are in base two if not explicitly written otherwise. We analyze all our results in the Real RAM model of computation. We denote by $\ell(p)$ the length of a geodesic path p . We use the terminology and notations introduced in Chapter 3. For example, we denote by T^1 the 1-skeleton of a portalgon T .

10.1.1 Discussion of the aspect ratio

We briefly discuss the choice of the aspect ratio as parameter of the triangular portalgon T in Theorem 8.2. First observe that the aspect ratio of T is a natural parameter that can be read off the triangles of T . On the other hand there is no known algorithm to compute the happiness of T for example. Also, if the surface $\mathcal{S}(T)$ is connected the algorithm of Theorem 8.2 remains polynomial in n and $\log(r)$ when r is the *local* aspect ratio of T : the maximum, over the triangles Δ of T , of the maximum side length of Δ divided by the smallest height of *the same* triangle Δ . Indeed the aspect ratio and the local aspect ratio are related by the following:

Lemma 10.1. *Let T be a portalgon of n triangles, of local aspect ratio r , and of aspect ratio r' . If the surface $\mathcal{S}(T)$ is connected then $r \leq r' \leq r^n$.*

Proof. Clearly $r \leq r'$. For the other inequality let e be a side of a triangle of T whose length is the maximum possible over all the triangles of T and all their sides. And let Δ be a triangle such that the smallest height of Δ is the minimum d over all the triangles of T and all their heights. By definition $r' = \ell(e)/d$. Since $\mathcal{S}(T)$ is connected there is a sequence of sides of triangles e_0, \dots, e_{2k} for some $0 \leq k < n$ such that e_0 belongs to Δ , $e_{2k} = e$, for every $0 \leq i < n$ the side e_{2i} is matched with the side e_{2i+1} , and the sides e_{2i+1} and e_{2i+2} belong to the same triangle. Then $\ell(e_{2i+2}) \leq r \cdot \ell(e_{2i+1})$ and $\ell(e_{2i+1}) = \ell(e_{2i})$. So $\ell(e)/d \leq \ell(e_0)r^{n-1}/d \leq r^n$. \square

We will not use Lemma 10.1 ever again.

10.1.2 Corollaries of Theorem 8.2

Our result, Theorem 8.2, has two interesting corollaries. First, Löffler, Ophelders, Silveira, and Staals proved that the portalgons of Delaunay triangulations have bounded happiness [141, Section 4]. Combined with Theorem 8.2, we obtain:

Corollary 10.1. *Let T be a portalgon of n triangles, of aspect ratio r , whose surface $\mathcal{S}(T)$ is closed. One can compute in $O(n^3 \log^2(n) \cdot \log^4(r))$ time a portalgon T' of $O(n)$ triangles, whose surface is $\mathcal{S}(T)$, and whose happiness is $O(1)$.*

Proof. Apply Theorem 8.2 to compute the portalgon T' of the Delaunay tessellation of $\mathcal{S}(T)$ in $O(n^3 \log^2(n) \cdot \log^4(r))$ time. Some polygons of T' may not be triangles. Cut the polygons of T' that are not triangles (if any) along vertex-to-vertex arcs to obtain a triangular portalgon T'' . Then T'' is the portalgon of a Delaunay triangulation of $\mathcal{S}(T)$, so T'' has bounded happiness by the result of Löffler, Ophelders, Silveira, and Staals [141, Section 4]. Moreover the vertex set of its 1-skeleton T''^1 is exactly the set of singularities of $\mathcal{S}(T)$, except if $\mathcal{S}(T)$ is a flat torus in which case T''^1 has exactly one vertex, so in any case T'' has $O(n)$ triangles. \square

On the portalgon T' returned by Corollary 10.1 the single-source shortest path algorithm of Löffler, Ophelders, Silveira, and Staals [141, Section 3] would run in time quasi-quadratic in n , in particular:

Observation 10.1. *On T' one can compute a shortest path between two given points in time quasi-quadratic in n .*

Second, the Delaunay tessellation of a closed piecewise-flat surface being unique by definition, Theorem 8.2 enables to test whether the surfaces of two given portalgons are isometric, simply by computing and comparing the portalgons of the associated Delaunay tessellations:

Corollary 10.2. *Let T and T' be portalgons of less than n triangles, whose aspect ratios are smaller than r , and whose surfaces $\mathcal{S}(T)$ and $\mathcal{S}(T')$ are closed. One can determine whether $\mathcal{S}(T)$ and $\mathcal{S}(T')$ are isometric in $O(n^3 \log^2(n) \cdot \log^4(r))$ time.*

Proof. Theorem 8.2 computes the portalgons \mathcal{T} and \mathcal{T}' of the Delaunay tessellations of respectively $\mathcal{S}(T)$ and $\mathcal{S}(T')$ in $O(n^3 \log^2(n) \cdot \log^4(r))$ time. We claim that we can determine whether \mathcal{T} and \mathcal{T}' are equal in $O(n^2)$ time. The claim immediately implies the corollary.

Let us prove the claim. We consider the sides of the polygons of \mathcal{T} and \mathcal{T}' . There are $O(n)$ such sides. Fix a side s of a polygon of \mathcal{T} . For every side s' of a polygon of \mathcal{T}' , determine in $O(n)$ time whether there exists a one-to-one correspondence φ from the sides of the polygons of \mathcal{T} to the sides of the polygons of \mathcal{T}' that maps s to s' , the boundary closed walks of the polygons of \mathcal{T} to the boundary closed walks of the polygons of \mathcal{T}' , and the matching of \mathcal{T} to the matching of \mathcal{T}' . If φ exists then φ is unique since $\mathcal{S}(\mathcal{T})$ and $\mathcal{S}(\mathcal{T}')$ are connected: construct φ in $O(n)$ time. Then determine in $O(n)$ time if for every polygon P of \mathcal{T} there is an orientation-preserving isometry $\tau_P : \mathbb{R}^2 \rightarrow \mathbb{R}^2$ such that $\varphi(s) = \tau_P(s)$ for every side s of P . In which case return correctly that \mathcal{T} and \mathcal{T}' are equal. In the end, if every polygon side s' of \mathcal{T}' has been looped upon, and if no equality has been found, return correctly that \mathcal{T} and \mathcal{T}' are distinct. This proves the claim, and the corollary. \square

10.1.3 Overview and techniques for the proof of Theorem 8.2

Recall from Chapter 9 that Löffler, Ophelders, Silveira, and Staals [141] defined the **happiness** of a portalgon T as the maximum number of times a shortest path in the surface $\mathcal{S}(T)$ visits the image of a polygon of T . We introduce a slight variation, more suitable to our needs. On a piecewise-flat surface S , we define the **segment-happiness** of a segment e of S , denoted $h_S(e)$, as the maximum number of intersections between e and a shortest path of S , maximized over all the shortest paths of S . The segment-happiness of a portalgon T is then the maximum segment-happiness $h_{\mathcal{S}(T)}(e)$, maximized over the edges e of its 1-skeleton T^1 . A priori the segment-happiness of T differs from the happiness of T . Indeed a path in $\mathcal{S}(T)$ may visit many times a face of T^1 without intersecting any edge of T^1 more than once, if the face has high degree. However, if T is triangular, then the happiness and the segment-happiness of T do not differ by more than a constant factor.

To prove Theorem 8.2, the crux of the matter is to replace the input triangular portalgon by another triangular portalgon of the same surface, whose segment-happiness is “low”.

For that our approach is to focus on portalgons T whose surface $\mathcal{S}(T)$ is **flat**: the interior of $\mathcal{S}(T)$ contains no singularity (as defined in Chapter 3). Note that here we allow $\mathcal{S}(T)$ to be disconnected, and to have boundary. Also the boundary of $\mathcal{S}(T)$ may have singularities. The **systole** of $\mathcal{S}(T)$ is the smallest length of a non-contractible geodesic closed curve in $\mathcal{S}(T)$, except in the particular case where every closed curve in $\mathcal{S}(T)$ is contractible, in which case the systole is ∞ . The important thing is that for every positive real s smaller than the systole of $\mathcal{S}(T)$, any non-contractible closed curve in $\mathcal{S}(T)$ is longer than s . Our key technical result is:

Proposition 10.1. *Let T be a portalgon of n triangles, whose sides are all smaller than $L > 0$. Assume that $\mathcal{S}(T)$ is flat. Let $s > 0$ be smaller than the systole of $\mathcal{S}(T)$. One can compute in $O(n \log^2(n) \cdot \log^2(2 + L/s))$ time a portalgon of $O(n \cdot \log(2 + L/s))$ triangles, whose surface is isometric to that of T , and whose segment-happiness is $O(\log(n) \cdot \log^2(2 + L/s))$.*

Note that in Proposition 10.1 it is possible that $L < s$, which is why we write $\log(2 + L/s)$ instead of $\log(L/s)$.

Sections 10.2, 10.3, 10.4, 10.5, 10.6 are devoted to the proof of Proposition 10.1. In Section 10.2 we focus on particular triangular portalgons, whose surfaces are all homeomorphic to an annulus; the definitions and results of this section are used by the algorithm of Proposition 10.1. In Section 10.3 we describe the algorithm for Proposition 10.1. It is a finely tuned combination of elementary operations such as inserting and deleting edges and vertices in graphs. While the algorithm itself is relatively simple, its analysis is more involved, and occupies Sections 10.4, 10.5, 10.6. In Section 10.4 we provide a combinatorial analysis, doing only things such as counting polygons, not measuring the lengths of their sides. In Section 10.5 we prepare for the geometric analysis. For that we introduce a new parameter on the segments of a flat surface, *enclosure*, possibly of independent interest. Informally, in a surface S , a segment e is enclosed when a short non-contractible loop can be attached to a point of e not too close to the endpoints of e . In Section 10.6 we finally use enclosure to analyze the algorithm from a geometric point of view, proving Proposition 10.1.

In Section 10.7 we extend Proposition 10.1 from flat surfaces to surfaces having singularities in their interior, essentially by cutting out caps around those singularities. Also, in order to get a cleaner result, we replace $2 + L/s$ by the aspect ratio of T , and we replace segment-happiness by happiness. We obtain:

Proposition 10.2. *Let T be a portalgon of n triangles, of aspect ratio r . One can compute in $O(n \log^2(n) \cdot \log^2(r))$ time a portalgon of $O(n \cdot \log(r))$ triangles, whose surface is $\mathcal{S}(T)$, and whose happiness is $O(n \log(n) \cdot \log^2(r))$.*

We have not discussed Delaunay tessellations yet. Still, we are almost ready to prove the main result of the this chapter, Theorem 8.2, on computing the portalgon of the Delaunay tessellation of the surface. Indeed once we have a portalgon of low happiness, we can compute shortest paths on the surface. And shortest path algorithms classically extend to construct Voronoi diagrams and then Delaunay tessellations. Formally:

Proposition 10.3. *Let T be a portalgon of n triangles, of happiness h , whose surface $\mathcal{S}(T)$ is closed. One can compute the portalgon of the Delaunay tessellation of $\mathcal{S}(T)$ in $O(n^2 h \log(nh))$ time.*

Constructing the Delaunay tessellation this way is folklore on meshes, and a single-source shortest path algorithm has been brought from meshes to portalgons by Löffler, Ophelders, Silveira, and Staals [141] (Chapter 9), with the same linear dependency in the happiness. However we could not find a statement equivalent to Proposition 10.3 in the literature, so we provide a proof of Proposition 10.3 in Appendix 10.10 for completeness. We insist that the proof of Proposition 10.3 is incidental to us, and Proposition 10.3 is not surprising at all. Our contribution is really the proof of Proposition 10.2.

Theorem 8.2 is immediate from Proposition 10.2 and Proposition 10.3:

Proof of Theorem 8.2. Proposition 10.2 computes in $O(n \log^2(n) \cdot \log^2(r))$ time a portalgon T' of $O(n \cdot \log(r))$ triangles, whose surface is that of T , and whose happiness is $O(n \log(n) \cdot \log^2(r))$. Proposition 10.3 then computes the portalgon of the Delaunay tessellation from T' in $O(n^3 \log^2(n) \cdot \log^4(r))$ time. \square

10.2 Tubes and bifaces

In this section we focus on particular triangular portalgons. This is similar to but different from [141, Section 5]. See Figure 10.1. First we provide a few definitions.

A **tube** is a triangular portalgon X whose surface $\mathcal{S}(X)$ is homeomorphic to an annulus and has no singularity in its interior, and whose 1-skeleton X^1 has exactly one vertex on each boundary component of $\mathcal{S}(X)$.

Among tubes, a **biface** is a portalgon B of two triangles whose respective sides s_0, s_1, s_2 and s'_0, s'_1, s'_2 , in order (clockwise say, but counter-clockwise would do to), are such that s_0 is matched with s'_0 and s_1 is matched with s'_1 . Its 1-skeleton B^1 has four edges: two loop edges forming the two boundary components of $\mathcal{S}(B)$, which we call **boundary edges**, and two edges relatively included in the interior of $\mathcal{S}(B)$, which we call **interior edges**.

We say that a biface B is **good** if the two interior edges e and f of B^1 satisfy both of the following up to possibly exchanging e and f . First, e is a shortest path in $\mathcal{S}(B)$. Second, cut $\mathcal{S}(B)$ along e , and consider the resulting quadrilateron. If this quadrilateron has two diagonals then f is smallest among the two diagonals: replacing f by the other diagonal would not shorten f . We will distinguish good bifaces. A good biface B is **thin** if every interior edge of B^1 is longer than every boundary edge of B^1 . Otherwise B is **thick**.

While tubes and bifaces have unbounded happiness and segment-happiness, good bifaces on the other hand are designed to satisfy the following:

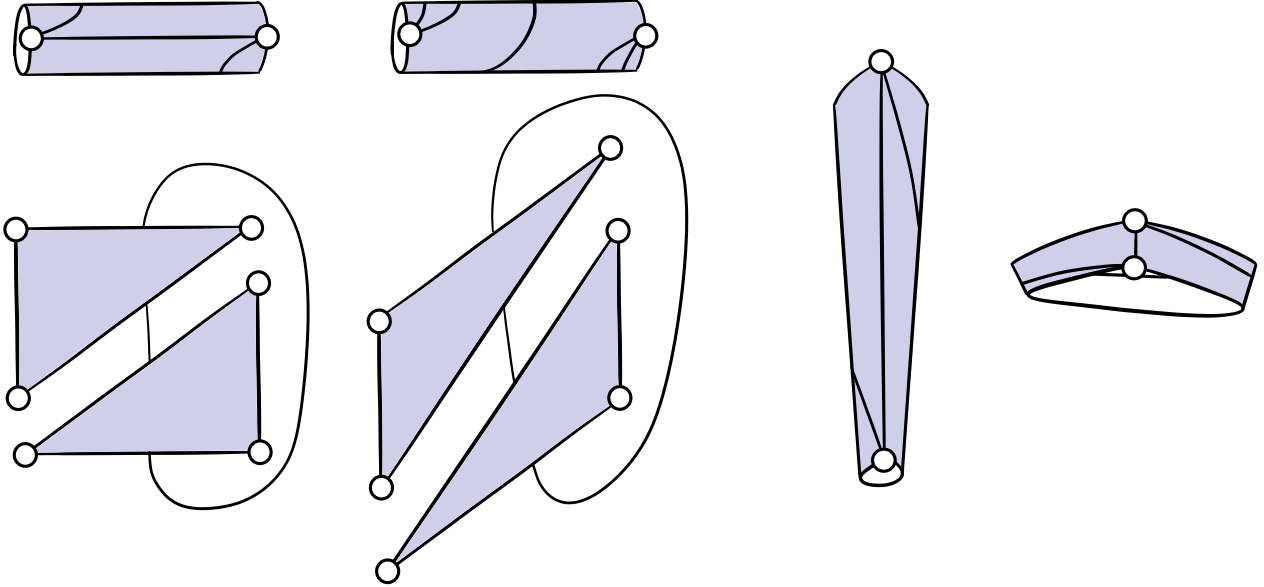


Figure 10.1: (From left to right) A good biface, a biface not good, a thin biface, a thick biface.

Lemma 10.2. *Given a good biface B , let e be an interior edge of B^1 . Then $h_{\mathcal{S}(B)}(e) \leq 6$.*

Proof. Among the two interior edges of B^1 , let f be a shortest one. Let $g \neq f$ be the other interior edge of B^1 . Let p be a shortest path in $\mathcal{S}(B)$. The relative interior $\overset{\circ}{p}$ of p cannot intersect the relative interior of f twice for those intersections would be crossings and p and f are both shortest paths since B is good. So $\overset{\circ}{p}$ intersects f less than four times. Then $\overset{\circ}{p}$ cannot intersect the relative interior of g five times, for those intersections would be crossings, and $\overset{\circ}{p}$ would intersect f in-between any two consecutive crossings with the relative interior of g . Altogether p intersects f and g at most six times each. \square

We will use the elementary operation of replacing a tube by a good biface:

Proposition 10.4. *Let X be a tube with n triangles, whose sides are smaller than $L > 0$. Let $s > 0$ be smaller than the systole of $\mathcal{S}(X)$. One can compute a good biface whose surface is $\mathcal{S}(X)$ in $O(n \log n \cdot \log(2 + L/s))$ time.*

Proposition 10.4 is similar to a result of Löffler, Ophelders, Silveira, and Staals [141, Theorem 45] (building upon a ray shooting algorithm of Erickson and Nayyeri [86]), so the proof is deferred to Appendix 10.8.

10.3 Algorithm

In this section we describe the algorithm for Proposition 10.1. We first describe the elementary operations and the data structure, before giving the algorithm itself. Along the way, we provide informal explanations of our choices, we do not prove anything yet.

10.3.1 Inserting vertices and edges

Informally, our goal is to improve the geometry of a triangular portalgon T , and the issue is that the edges of T^1 that lie in the interior of $\mathcal{S}(T)$ can be arbitrarily long. A naive way of shortening an edge is to cut the edge in two at its middle point. Formally:

INSERTVERTICES: Given a triangular portalgon T , consider every edge e of T^1 that lies in the interior of $\mathcal{S}(T)$, and insert the middle point of e as a vertex in T^1 .

To perform INSERTVERTICES, recall that T is given as a disjoint collection of triangles in the plane, together with a partial matching of their sides: we consider every triangle P of T , and every side s of P that is matched in T , and we make the middle point of s a new vertex of P .

The problem is that applying INSERTVERTICES to a *triangular* portalgon T produces a portalgon T' whose polygons are usually not triangles (they have more than three vertices). We now consider transforming T' into a triangular portalgon. To do that we repeatedly cut the polygons of T' . We need a definition.

In the plane consider a polygon P , two distinct vertices u and v of P , and the geodesic segment a between u and v . If the relative interior of a is included in the interior of P then a is called a vertex-to-vertex arc of P . It is easily seen that if P has at least four vertices (is not a triangle) then P admits at least one vertex-to-vertex arc. Among the vertex-to-vertex arcs of P , the shortest ones are the **shortcuts** of P . We emphasize that we consider the shortest ones among all the vertex-to-vertex arcs, without fixing the endpoints, but the endpoints are chosen among the vertices of P . For example the shortcuts of a square are its two diagonals, but every other kite (a quadrilateral in which there are two incident sides of the same length) has only one shortcut. In a portalgon T every polygon P corresponds to a face F of T^1 , and every shortcut of P corresponds to a path relatively included in F : we say of this path that it is a shortcut of F .

INSERTEDGES: Given a portalgon T , as long as there is a face of T^1 that is not a triangle, insert a shortcut of this face as an edge in T^1 .

We perform INSERTEDGES as follows: as long as there is a polygon P of T that is not a triangle, we cut P into two polygons along a shortcut. This creates two new polygon sides, which we match in T .

We shall apply INSERTVERTICES followed by INSERTEDGES to a triangular portalgon T in order to produce another triangular portalgon T' , hopefully with a nicer geometry. The problem is now that T'^1 has more vertices than T^1 . All the other operations of the algorithm are devoted to keeping the number of vertices low.

10.3.2 Deleting vertices

From now on it is important that every surface considered is flat, there is no singularity in its interior. Given a triangular portalgon T , assuming that the surface $\mathcal{S}(T)$ is flat, we consider decreasing the number of vertices of T^1 . To do that we naturally consider deleting some vertices. Not all vertices can be deleted. For example a vertex incident to a loop edge cannot be deleted. Also we will not delete vertices that lie on the boundary of the surface $\mathcal{S}(T)$. A

vertex of T^1 is **weak** if it lies in the interior of $\mathcal{S}(T)$ and is not incident to any loop edge in T^1 . It is **strong** otherwise.

DELETEVERTICES: Given a triangular portalgon T whose surface $\mathcal{S}(T)$ is flat, construct a maximal independent set V of weak vertices of T^1 that have degree smaller than or equal to six. For every vertex $v \in V$ delete v and its incident edges from T^1 .

We perform DELETEVERTICES as follows. To delete a vertex v of T^1 , we consider the vertices of the triangles of T that correspond to v . No two of them belong to the same triangle for otherwise there would be a loop of T^1 based at v , contradicting the assumption that v is weak. We move their triangles in the plane so that these vertices are now placed at the same point of the plane, and so that the triangles are placed in the correct cyclic order around this point, without overlapping. This is possible since v lies in the interior of $\mathcal{S}(T)$, and since we assumed that every point in the interior of $\mathcal{S}(T)$ is flat: it is surrounded by an angle of 2π . Now the union of the triangles is a polygon. In T , we replace all the triangles by this single polygon.

Afterward the polygons of T are usually not triangles anymore, but this will be solved by applying INSERTEDGES after each application of DELETEVERTICES.

Observe that in DELETEVERTICES we delete only vertices of degree smaller than or equal to six. Informally, the reason is that deleting a weak vertex of degree $d \geq 3$ creates a face of degree d around it. We then insert $d - 3$ edges in this face when applying INSERTEDGES. The problem is that only a constant number of edges can be inserted in each face without risking to destroy our improvements on the geometry of the tessellation. This is why we make sure that $d = O(1)$ beforehand. The exact bound on d is not really important (although changing it would change some constants of the algorithm), but it must be at least six so that we can still remove a fraction of the excess vertices this way, at least when most of them are strong. We will see that in due time. Similar ideas can be found in the literature, see for example Kirkpatrick [128, Lemma 3.2].

10.3.3 Simplifying tubes

The operation DELETEVERTICES cannot delete strong vertices. Among them the vertices that lie the interior of the surface and are incident to a loop edge. In this section we describe an operation for deleting such vertices.

In order to grasp the intuition observe informally that it is possible that almost all the vertices of T^1 lie in the interior of $\mathcal{S}(T)$ and are incident to a loop edge. Fortunately, we will see that in this case there must be a sub-portalgon X of T such that X is a tube and such that the interior of $\mathcal{S}(X)$ contains loop edges of X^1 . The solution is to delete those loop edges by replacing X by a good biface with Proposition 10.4. There is one subtlety though: we must choose the tube X carefully, so that we replace any concatenation of tubes by a single biface whenever possible, in order to delete the loops in-between the tubes, instead of replacing each one of the tubes individually. Taking that into consideration leads to the following:

SIMPLIFYTUBES: In a triangular portalgon T whose surface $\mathcal{S}(T)$ is flat, do the following:

1. In T^1 build a set J of loop edges that lie in the interior of $\mathcal{S}(T)$ and are pairwise disjoint, as follows. There are two cases:

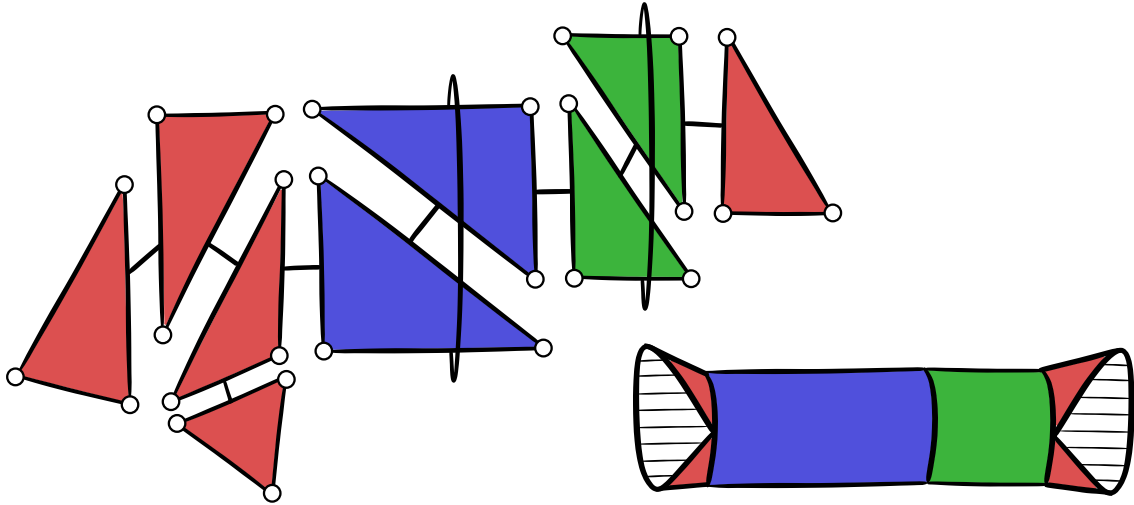


Figure 10.2: (Top) Data structure for ALGORITHM: a portalgon R whose polygons are partitioned, here by color, inducing sub-portalgons of R called regions, and one region singularized as being active, here in red. (Bottom) The surface $S(T)$ is here homeomorphic to an annulus.

- a) If $S(T)$ is homeomorphic to a torus, do the following. Let J contain two disjoint loop edges of T^1 if there exist two such edges, otherwise let $J = \emptyset$.
 - b) Otherwise, if $S(T)$ is not homeomorphic to a torus, do the following. First construct a set J' of loop edges by considering every vertex v of T^1 that lies in the interior of $S(T)$ and is incident to a loop edge, and by putting one (and only one!) of the loop edges incident to v in J' . Then build a subset $J \subseteq J'$ by removing from J' every $e \in J'$ that satisfies each of the following. First, cutting $S(T)$ along the loops in J' , and considering the resulting connected components, two such components are adjacent to e (instead of only one). Second, letting S_0 and S_1 be those two components, and considering the two sub-portalgons of T whose surfaces are S_0 and S_1 , each of these two portalgons is a tube.
2. Cut the surface $S(T)$ along the loops in J , and consider the resulting connected components. Each such component is the surface of a sub-portalgon X of T . If X is a tube replace X by a good biface B .

The idea behind step 1b is to remove loops from J' so that step 2 replaces a concatenation of tubes by a single good biface when possible, instead of replacing the tubes individually.

10.3.4 Data structure for marking bifaces as inactive

We are almost ready to give the algorithm, but there is still one important thing to understand. For geometric reasons that we will detail in Section 10.6, in step 2 of SIMPLIFYTUBES, if the good biface B is *thin* we will not just replace X by B , but we will also make sure to not modify B ever again. In this sense B becomes inactive. Doing so requires a data structure remembering which parts of the portalgon are inactive, which we now describe.

See Figure 10.2. The data structure maintains a portalgon R together with a partition of the polygons of R . Each set X of polygons in the partition defines a sub-portalgon of R

that we call **region**. One region is singularized as the **active** region R_A . The other regions are **inactive**. Note that the surface of the active region may be disconnected, and that the surfaces of distinct inactive regions may be adjacent.

Let us now describe what the algorithm will do to the data structure. The data structure will be initialized by setting $R_A = R$, without inactive region. Then the algorithm will use the data structure like the reader imagines: it will apply the routines `INSERTVERTICES`, `INSERTEDGES`, `DELETEVERTICES`, and `SIMPLIFYTUBES` to the active region R_A , and mark as inactive every thin biface encountered in step 2 of `SIMPLIFYTUBES`. Observe that $\mathcal{S}(R_A)$, the surface of R_A , will diminish over time as more and more regions are marked inactive. This may increase the topological complexity of $\mathcal{S}(R_A)$ (the numbers of connected components and boundary components), ruining our efforts to keep the combinatorial complexity of R_A bounded. To counteract this, we introduce a small gardening routine:

GARDENING: Consider every connected component of $\mathcal{S}(R_A)$. Each such component is the surface of a sub-portalgon X of R_A . If X is a tube replace X by a good biface B , and mark B as inactive.

We emphasize that in GARDENING the good biface B is always marked as inactive, even if B is thick.

We described everything that the algorithm can do to the data structure. This immediately implies three invariants maintained by the algorithm, that we give now in order to ease the reading. The first two invariants are:

- Every polygon of the active region has degree at most six.
- Every inactive region is a good biface.

For the last invariant we need a definition. Recall that in R if two sides s and s' of polygons are matched then s and s' correspond to an edge e of R^1 . If moreover s and s' belong to different polygons, and if their respective polygons belong to different regions, we say that e is **separating**. Then e is a loop, for it is a boundary edge of a biface by the first invariant, and e belongs to the interior of $\mathcal{S}(R)$. Then the third invariant maintained by the algorithm is:

- The separating loops are pairwise disjoint. Equivalently, no two of them are based at the same vertex of R^1 .

10.3.5 Algorithm

Finally, we give the algorithm. The algorithm consists in repeatedly applying two parts. In a first part, we improve the geometry by applying `INSERTVERTICES` and then `INSERTEDGES`. However this increases the number of vertices. So in a second part we apply `SIMPLIFYTUBES`, `DELETEVERTICES`, and `INSERTEDGES`, in combination with GARDENING. The problem is that this second part can only remove a fraction of the vertices at once, so it needs to be repeated several times in order to counteract the increase of vertices in the first part. It turns out that 350 repetitions suffice, as we shall see.

ALGORITHM: Given a triangular portalgon T whose surface $\mathcal{S}(T)$ is flat, and a positive integer N , do the following. Initialize the data structure by letting R be the input portalgon T , and the active region R_A be R itself, without inactive region. Then repeat N times the following:

- Apply INSERTVERTICES to R_A . Then apply INSERTEDGES to R_A .
- Repeat 350 times the following:
 - Apply GARDENING.
 - Apply SIMPLIFYTUBES to R_A but in step 2 whenever the good biface B is thin mark B as inactive.
 - Apply GARDENING.
 - Apply DELETEVERTICES to R_A . Then apply INSERTEDGES to R_A .

In the end return R .

Note that perhaps the algorithm would work too if it applied GARDENING only once, but applying GARDENING twice will simplify our analysis. When proving Proposition 10.1, we will apply the algorithm with $N = \lceil \log(2 + L/s) \rceil$, but we will see that in due time.

10.4 Combinatorial analysis of the algorithm: proof of Proposition 10.5

In this section we provide the combinatorial analysis of ALGORITHM, by proving the following:

Proposition 10.5. *Apply ALGORITHM to a portalgon T of n triangles, whose surface $\mathcal{S}(T)$ is flat. During the execution the number of polygons of the active region R_A is $O(n)$.*

We analyze each operation independently before proving Proposition 10.5. Our analysis is on the number vertices of R_A^1 , not the number of polygons of R_A , but bounding one immediately bounds the other, as we shall see, and we find more convenient to argue on the vertices of R_A^1 .

10.4.1 Analysis of INSERTVERTICES

We start by bounding the increase in vertices of INSERTVERTICES:

Lemma 10.3. *Let T be a triangular portalgon. Let g be the genus of $\mathcal{S}(T)$. Let m be the number of vertices of T^1 . Apply INSERTVERTICES to T and consider the resulting portalgon T' . Then T'^1 has less than $7(g + m)$ vertices.*

Lemma 10.3 relies on the following classical consequence of Euler's formula:

Lemma 10.4. *There are less than $6(g + m)$ edges in T^1 .*

Proof. Let m_1 and m_2 count respectively the edges and the faces of T^1 , and let b count the boundary components of $\mathcal{S}(T)$. Double counting gives $3m_2 \leq 2m_1$. Euler's formula gives $m_1 - m_2 = m + 2g + b - 2$. And we have $b \leq m$. Therefore $m_1 \leq 3m_1 - 3m_2 < 6(m + g)$. \square

Proof of Lemma 10.3. There are no more vertices inserted than there are edges in T^1 , and there are less than $6(g + m)$ edges in T^1 by Lemma 10.4. \square

10.4.2 Analysis of DELETEVERTICES

For DELETEVERTICES to remove a fraction of the vertices, it suffices that the number of vertices exceeds the topology of the surface, and that almost all of the vertices are strong:

Lemma 10.5. *Let T be triangular portalgon whose surface $\mathcal{S}(T)$ is flat. Let m be the number of vertices of T^1 . Let g be the genus of $\mathcal{S}(T)$, and let \bar{m} be the number of strong vertices of T^1 . Apply DELETEVERTICES to T and consider the resulting portalgon T' . If $m > 24(g + \bar{m})$ then T'^1 has less than $167m/168$ vertices.*

Lemma 10.5 relies on the following simple consequence of Euler's formula:

Lemma 10.6. *Let S a topological surface of genus g with b boundary components. Let Y be a topological triangulation of S with m vertices. If $m > 24(g + b)$ then at least $m/12$ vertices of Y have degree smaller than or equal to 6.*

Proof. Let m_1 and m_2 count respectively the edges and the faces of Y . Euler's formula gives $6m - 6m_1 + 6m_2 = 12 - 12g - 6b$. Double counting gives $3m_2 \leq 2m_1 - b$ and $2m_1 = \sum_v \deg v$, where the sum is over the vertices, and where $\deg v$ denotes the degree of a vertex v . Then $\sum_v 6 - \deg v = 6m - 2m_1 \geq 6m - 6m_1 + 6m_2 + 2b \geq 12 - 12g - 4b > -m/2$. Let a and b count the number of vertices whose degree is respectively smaller than or equal to six, and greater than six. Then $b < 5a + m/2$. Assuming $a < m/12$, we get $b < 11m/12$, and so $a + b < m$. This is a contradiction. This proves the lemma. \square

Proof of Lemma 10.5. Let b be the number of boundary components of $\mathcal{S}(T)$. We have $m > 24(g + b)$. Indeed we assumed $m > 24(g + \bar{m})$, and we have $\bar{m} \geq b$ as every boundary component of $\mathcal{S}(T)$ contains a strong vertex of T^1 . So by Lemma 10.6 at least $m/12$ vertices of T^1 have degree smaller than or equal to six. Moreover less than $m/24$ vertices of T^1 are strong by assumption. So more than $m/24$ vertices of T^1 are weak and have degree smaller than or equal to six. Any maximal independent set of such vertices contains more than $m/(24 \times 7) = m/168$ vertices, so DELETEVERTICES deletes more than $m/168$ vertices. \square

10.4.3 Analysis of SIMPLIFYTUBES

Right after applying SIMPLIFYTUBES the number of vertices that lie in the interior of the surface and are incident to a loop is bounded by the topology of the surface:

Lemma 10.7. *Let T be a triangular portalgon whose surface $\mathcal{S}(T)$ is flat. Let g and b be the genus and the number of boundary components of $\mathcal{S}(T)$. Apply SIMPLIFYTUBES to T , and consider the resulting portalgon T' . At most $9(g + b)$ vertices of T'^1 lie in the interior of $\mathcal{S}(T')$ and are incident to a loop in T'^1 .*

Lemma 10.7 relies on the following:

Lemma 10.8. *Let I be a set of loop edges of T^1 that lie in the interior of $\mathcal{S}(T)$ and are pairwise disjoint. In I all but at most $9(g+b)$ loops e satisfy the following: there are two connected components of $\mathcal{S}(T) \setminus I$ incident to e , and each of them is the surface of a sub-triangulation of T that is a tube.*

Proof. Cut $\mathcal{S}(T)$ along I , and consider the resulting connected components. Those components are the surfaces of sub-portalgons of T . Let Z contain those sub-portalgons of T . Let $Z' \subseteq Z$ contain the sub-portalgons that are not tubes. Without loss of generality $I \neq \emptyset$. Then every $T_0 \in Z$ is such that $\partial\mathcal{S}(T_0) \neq \emptyset$ since $\mathcal{S}(T)$ is connected. Let $\chi(T_0)$ and $d(T_0)$ be respectively the Euler characteristic of $\mathcal{S}(T_0)$ and the number of boundary components of $\mathcal{S}(T)$ that belong to $\mathcal{S}(T_0)$. Let $\lambda(T_0) = 2d(T_0) - \chi(T_0)$.

We claim that every $T_0 \in Z$ satisfies $\lambda(T_0) \geq 0$, and that if $T_0 \in Z'$ then $\lambda(T_0) > 0$. Indeed we have $\chi(T_0) \leq 1$ since $\mathcal{S}(T_0)$ is not homeomorphic to a sphere. So assuming $\lambda(T_0) \leq 0$, we get $d(T_0) = 0$. Then $\chi(T_0) \neq 1$ for otherwise $\mathcal{S}(T_0)$ would be homeomorphic to a disk, would have no curved point in its interior, and would be bounded by a single geodesic loop issued of I , contradicting the formula of Gauss–Bonnet. So $\chi(T_0) = 0$. Then T_0 is a tube since $\mathcal{S}(T_0)$ is not homeomorphic to a torus. This proves the claim.

Now for every $T_0 \in Z'$ let $b(T_0)$ be the number of boundary components of $\mathcal{S}(T_0)$. The claim implies $b(T_0) \leq 2 - \chi(T_0) \leq 2 + \lambda(T_0) \leq 3\lambda(T_0)$. So $\sum_{T_0 \in Z'} b(T_0) \leq 3 \sum_{T_0 \in Z'} \lambda(T_0) \leq 3 \sum_{T_0 \in Z} \lambda(T_0) \leq 9(g+b)$. Therefore at most $9(g+b)$ loops in I are incident to the surface of some $T_0 \in Z'$. If every other loop in I is incident to the surfaces of two distinct $T_0, T_1 \in Z$ then we are done. Otherwise there is a loop $e \in I$ incident to the surface of only one $T_0 \in Z$. Since T_0 is a tube, $\mathcal{S}(T)$ is a homeomorphic to a torus, and e is the only loop in I , so we are done. This proves the lemma. \square

Proof of Lemma 10.7. We claim that in the application of SIMPLIFYTUBES the set J contains at most $9(g+b)$ loops. This is true if step 1a is applied, for in this case $g = 1$ and J contains either zero or two loops. And if step 1b is applied all but $9(g+b)$ loops in J' are incident to two distinct connected component of $\mathcal{S}(T) \setminus J'$ whose corresponding sub-triangulations of T are tubes, by Lemma 10.8. Those loops are not retained in J . This proves the claim.

In the particular case where the surface $\mathcal{S}(T)$ is homeomorphic to a torus, and where T^1 contains exactly one vertex incident to a loop edge, the application of SIMPLIFYTUBES does nothing and $T = T'$. In this case the lemma is proved. In all other cases if a vertex v of T'^1 lies in the interior of $\mathcal{S}(T')$ and is incident to a loop edge in T'^1 , then v is the base vertex of some loop in J . Indeed v would otherwise have been deleted by SIMPLIFYTUBES when replacing a tube by a biface. There are at most $9(g+b)$ such vertices by our claim. This proves the lemma. \square

10.4.4 Analysis of GARDENING

Right after applying GARDENING the topology of $\mathcal{S}(R_A)$, the surface of the active region, is bounded by the topology of $\mathcal{S}(R)$, the whole surface:

Lemma 10.9. *Let g and b be the genus and the number of boundary components of $\mathcal{S}(R)$. The genus of $\mathcal{S}(R_A)$ is smaller than or equal to g . And right after applying GARDENING $\mathcal{S}(R_A)$ has at most $10(g+b)$ boundary components.*

Proof. Of course the genus of $\mathcal{S}(R_A)$ is smaller than or equal to g . It is the number of boundary components that we must handle. Each boundary component of $\mathcal{S}(R_A)$ is either a

boundary component of $\mathcal{S}(R)$, and there are b of them, or it is a separating loop. We bound the number of separating loops adjacent to $\mathcal{S}(R_A)$, so let I contain those loops. Each $e \in I$ is incident to two connected components of $\mathcal{S}(R) \setminus I$: one of them is in $\mathcal{S}(R_A)$, the other is not. The component in $\mathcal{S}(R_A)$ is not the surface of a tube since GARDENING was just applied. So I contains at most $9(g + b)$ loops by Lemma 10.8. We proved that $\mathcal{S}(R_A)$ has at most $10(g + b)$ boundary components. \square

10.4.5 Proof of Proposition 10.5

Proof of Proposition 10.5. We will prove that the number of vertices of R_A^1 is $O(n)$ throughout the execution. This will prove the lemma for then the number of edges of R_A^1 is also $O(n)$ by Lemma 10.4, since the genus of $\mathcal{S}(R_A)$ is $O(n)$, and so the number of polygons of R_A is also $O(n)$.

Consider the input triangular portalgon T . Let m be the number of vertices of T^1 . Let g and b be the genus and the number of boundary components of $\mathcal{S}(T)$. Observe that $m \leq 3n$, $g \leq n$, and $b \leq n$. We will argue using m , g , and b instead of n . There are two loops in the algorithm: the main loop, which repeats N times, and the interior loop, which repeats 350 times within each iteration of the main loop.

First we consider a single iteration of the interior loop. Let m_A be the number of vertices of R_A^1 at the begining of this iteration. Observe that the iteration does not insert any new vertex in R_A^1 . We claim that if $m_A > 3000(g + b + m)$ then less than $167m_A/168$ vertices are in R_A^1 at the end of the loop. To prove the claim first observe that after each application of GARDENING $\mathcal{S}(R_A)$ has at most $10(g + b)$ boundary components by Lemma 10.9. And the genus of $\mathcal{S}(R_A)$ is smaller than or equal to g . Now after the application of SIMPLIFYTUBES at most $9(g + 10(g + b)) \leq 99(g + b)$ vertices of R_A^1 lie in the interior of $\mathcal{S}(R_A)$ and are incident to a loop by Lemma 10.7. This is still the case just before the application of DELETEVERTICES. Moreover, at this point, at most $m + 10(g + b)$ vertices of R_A^1 lie on the boundary of $\mathcal{S}(R_A)$; indeed every such vertex is either a vertex of T^1 , and there are at most m , or it is the base vertex of a separating loop, in which case it is the unique vertex in its boundary component of $\mathcal{S}(R_A)$, and there are at most $10(g + b)$. Altogether, just before the application of DeleteVertices, the number \bar{m}_A of strong vertices of R_A^1 satisfies $\bar{m}_A \leq m + 109(g + b)$. If at this point R_A^1 has at most $24(g + \bar{m}_A)$ vertices then it already has less than $167m_A/168$ vertices since we assumed $m_A > 3000(g + b + m)$. Otherwise less than $167m_A/168$ vertices remain after DELETEVERTICES by Lemma 10.5. In any case the claim is proved.

Now we prove the lemma by considering a single iteration of the main loop. Assuming that R_A^1 has more than $3000(g + b + m)$ vertices at the beginning of the iteration, we shall prove that in the end of the iteration the number of vertices of R_A^1 has decreased. To do so first observe that the iteration starts with INSERTVERTICES, and this is the only moment where vertices are inserted. At this point the number of vertices of R_A^1 is multiplied by less than 8 by Lemma 10.3. And by our claim, as long as the number of vertices exceeds $3000(g + b + m)$ it is divided by more $168/167$ by each iteration of the interior loop. There are 348 iterations of the interior loop, and $8 < (168/167)^{350}$. This proves the lemma. \square

10.5 Enclosure

In this section we fix a flat surface S . We introduce a parameter on the segments of S that we call *enclosure*. Then we relate enclosure to segment-happiness and length, and we show what the elementary operations used by ALGORITHM do to the enclosure and the length of the edges involved, preparing for the geometric analysis of ALGORITHM.

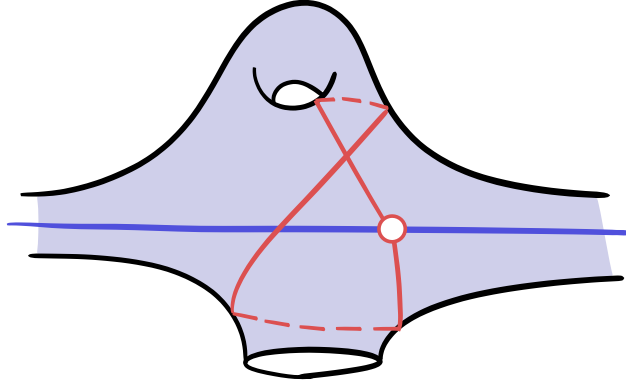


Figure 10.3: The red loop encloses the blue segment in the surface.

First we define enclosure. See Figure 10.3. Consider a segment e of S . Informally, e is enclosed in S when a short non-contractible loop can be attached to a point of e not too close to the endpoints of e . Formally, consider a point x in the relative interior of e . We denote by $\langle x \rangle_e$ the minimum length of the two sub-segments of e separated by x . Assume that there exists a loop γ based at x in S , such that γ is geodesic except possibly at its basepoint. Further assume that $\ell(\gamma) < \langle x \rangle_e$. In this case γ and e are necessarily in *general position*: Informally, they do not overlap, more formally, every sufficiently short sub-path of γ is either disjoint from e or its intersection with e is a single point. There are two cases: either γ crosses e at x , or γ meets x on only one side of e . If γ crosses e at x , then we say that γ **encloses e in S** . Also we say that γ encloses e **by a factor of $\langle x \rangle_e / \ell(\gamma)$** in S . The **enclosure** $c_S(e) \geq 1$ is the supremum of the ratios $\langle x \rangle_e / \ell(\gamma)$ over the loops γ enclosing e in S , conventionally set to one if there is no loop enclosing e in S .

10.5.1 Enclosure of a sub-segment

Recall that, given an edge e of a tessellation of S , the operation INSERTVERTICES may insert the middle point of e as a vertex in the tessellation. The following ensures that the two resulting edges are not more enclosed in S than the initial edge. It is straightforward:

Lemma 10.10. *Let e be a segment in S , and let f be a segment included in e . Then $c_S(e) \geq c_S(f)$.*

Proof of Lemma 10.10. Let $t > 1$. Assume that there is a loop γ , based at a point x , that encloses f by a factor of t . Then γ encloses e by a factor of t since $\langle x \rangle_f \leq \langle x \rangle_e$. \square

10.5.2 Enclosure and length of a shortcut

Recall that, given a face F of a tessellation of S , the operation INSERTEDGES may insert a shortcut of F as an edge in the tessellation. The following ensures that if the shortcut

inserted is “very enclosed” in S , then it is “not much more enclosed” in S and “not much longer” than the edges initially in the tessellation:

Proposition 10.6. *Let F be a face of a tessellation of S . Assume that F has a shortcut e such that $c_S(e) > 6$. Then F has a side f such that $c_S(f) \geq c_S(e) - 4$ and $\ell(f) \geq (1 - 4/c_S(e)) \cdot \ell(e)$.*

In this section we prove Proposition 10.6. First we need a lemma:

Lemma 10.11. *In S , let e and f be two relatively disjoint segments, and let γ be a geodesic loop. Assume that γ encloses e by a factor of $t > 2$, and that γ intersects f at a point y such that $\langle y \rangle_f > \ell(\gamma)$. Rebase γ at y , and let γ' be the geodesic loop homotopic to it. Then γ' meets y on both sides of f .*

Proof. We have $\ell(\gamma') \leq \ell(\gamma)$ so $\ell(\gamma') < \langle y \rangle_f$, and so γ' is in general position with f . We prove the lemma by contradiction, so assume that γ' meets y only on the right side of f , for some direction of f . In the universal covering space \tilde{S} of S , consider a lift \tilde{f} of f . Let \tilde{y} be the lift of y that belongs to \tilde{f} . Since the interior of \tilde{S} is flat, there is a geodesic \tilde{L} , containing \tilde{f} , such that on both ends \tilde{L} is either infinite or reaches the boundary of \tilde{S} . Then \tilde{L} separates \tilde{S} in two connected components. The two lifts of γ' incident to \tilde{y} meet \tilde{y} on the right side of \tilde{f} by assumption, and they are otherwise disjoint from \tilde{L} . In particular, their other endpoints lie on the right side of \tilde{L} .

We have $\ell(\gamma) < \langle y \rangle_f$ so γ is in general position with f . Direct γ so that γ crosses f from right to left at y , and write γ as the concatenation of two paths γ_0 and γ_1 respectively before and after its crossing at y . There is a lift $\tilde{\gamma}_1$ of γ_1 that leaves \tilde{y} on the left of \tilde{f} . And $\tilde{\gamma}_1$ is otherwise disjoint from \tilde{L} , since the interior of \tilde{S} is flat. Thus the endpoint \tilde{x} of $\tilde{\gamma}_1$ lies on the left of \tilde{L} . There is a lift $\tilde{\gamma}_0$ of γ_0 that starts at \tilde{x} . And $\tilde{\gamma}_0$ is otherwise disjoint from $\tilde{\gamma}_1$ since γ meets x on both sides of e , and since the interior of \tilde{S} is flat. By the previous paragraph, the endpoint of $\tilde{\gamma}_0$ lies on the right side of \tilde{L} , so $\tilde{\gamma}_0$ intersects \tilde{L} . Cut $\tilde{\gamma}_0$ at its first intersection point \tilde{z} with \tilde{L} . Let \tilde{I} be the sub-segment of \tilde{L} between \tilde{y} and \tilde{z} . The concatenation of the prefix of $\tilde{\gamma}_0$ ending at \tilde{z} , of \tilde{I} , and of $\tilde{\gamma}_1$ is a simple closed curve \tilde{C} . At \tilde{x} , there is a portion of \tilde{e} that enters the bounded side of \tilde{C} , since γ meets x on both sides of e . This portion of \tilde{e} can be extended into a geodesic \tilde{p} that meets \tilde{C} at some point \tilde{v} , since the interior of \tilde{S} is flat. Then \tilde{v} belongs to the relative interior of \tilde{I} . We claim that \tilde{v} belongs to the relative interiors of both \tilde{e} and \tilde{f} , which is a contradiction since e and f are relatively disjoint. To prove the claim, first observe that the distance between \tilde{y} and \tilde{z} in \tilde{S} is at most $\ell(\gamma)$, and this distance is equal to the length of \tilde{I} , since the interior of \tilde{S} is flat. So the sub-segment of \tilde{I} between \tilde{y} and \tilde{v} is no longer than $\ell(\gamma) < \langle y \rangle_f$, and is thus included in the relative interior of \tilde{f} . Also, the distance between \tilde{v} and \tilde{x} is smaller than or equal to $2\ell(\gamma) \leq 2\langle x \rangle_e/t < \langle x \rangle_e$, so \tilde{p} is included in the relative interior of \tilde{e} . \square

The proof of Proposition 10.6 also relies on the following construction. See Figure 10.4. In the Euclidean plane \mathbb{R}^2 let Q be a polygon with more than three vertices. Let e be a shortcut of Q . Let f and f' be sides of Q separated by e along the boundary of Q . Let x be a point in the relative interior of e . Let y and y' be points that lie on respectively f and f' (possibly vertices of Q), and do not lie on e . Assume that the segments p and p' between x and respectively y and y' are relatively included in the interior of Q . Then:

Lemma 10.12. *Let $t > 6$. If $\ell(p) \leq \langle x \rangle_e/t$ and $\ell(p') \leq \langle x \rangle_e/t$, then at least one of f and f' , say f , is such that $\langle y \rangle_f \geq (1 - 4/t) \cdot \langle x \rangle_e$ and $\ell(f) \geq (1 - 4/t) \cdot \ell(e)$.*

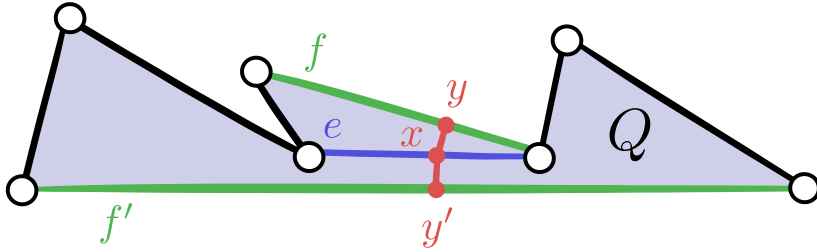


Figure 10.4: The setting of Lemma 10.12.

Proof. Assume without loss of generality that e is horizontal, that f lies above e , and that x is the origin $(0, 0) \in \mathbb{R}^2$. Then x cuts e into two segments e_0 and e_1 , respectively the right and left one. Let v_0 and v_1 be respectively the right and left endpoints of e . Consider the following algorithm in three phases. In the first phase consider the point $z = x$ and move z along p . Doing so, consider the segments from z to v_0 and v_1 . If moving z makes the relative interior of one of those two segments intersect ∂Q , then stop: this is a break condition. Also break if z reached y and y is a vertex of Q . Otherwise the algorithm enters its second phase. Then y cuts f in two segments f_0 and f_1 , where f_0 is on the right of y as seen from the path p directed from x to y . In phase two move z along f_0 or f_1 , choosing carefully which segment to move along so that the second coordinate of z does not increase. We assume without loss of generality that z moves along f_0 , by flipping the figure horizontally otherwise. Move along f_0 by a distance of $(1 - 4/t)\ell(e_0)$, but break if z reaches the right end-vertex of f , or if the relative interior of the segment between z and v_0 intersects ∂Q . If the algorithm did not break, it enters its third and final phase. In this phase put z back on y , and move it along the other sub-segment of f , here f_1 , by a distance of $(1 - 4/t)\ell(e_1)$, breaking if z reaches the left end-vertex of f , or if the relative interior of the segment between z and v_1 intersects ∂Q .

If the algorithm did not break then $\ell(f) \geq (1 - 4/t)\ell(e)$ and $\langle y \rangle_f \geq (1 - 4/t)\langle x \rangle_e$ and we are done. Otherwise, if the algorithm broke, consider the triangle Δ between v_0 , v_1 , and z . The break conditions ensure that the interior of Δ is included in the interior of Q , and that there is a vertex w of Q that lies on $\partial\Delta$ and not on e . We claim that the inner-angles of Δ at v_0 and v_1 are both strictly smaller than $\pi/4$. We prove this claim by considering the coordinates $(\alpha, \beta) \in \mathbb{R} \times [0, +\infty[$ of z , and the coordinates $(\ell(e_0), 0)$ and $(-\ell(e_1), 0)$ of v_0 and v_1 respectively, and by proving that the invariants $\ell(e_0) - \alpha > \beta$ and $\alpha + \ell(e_1) > \beta$ hold at any time during the algorithm. Let $m = \min(\ell(e_0), \ell(e_1)) = \langle x \rangle_e$. In the first phase $|\alpha| \leq m/t$ and $0 \leq \beta \leq m/t$, so the invariants hold since $t > 2$. In the second phase β does not increase and α does not decrease. Moreover α does not increase by more than $\ell(e_0)(1 - 4/t)$ so the invariants hold. If the second phase ends without breaking then the absolute slope λ of the line supporting f is smaller than or equal to $1/(t - 5)$. Indeed during the second phase β decreased by at most m/t while z moved a distance $\ell(e_0)(1 - 4/t)$, so α increased by at least $\ell(e_0)(1 - 4/t) - m/t$, and so $1/\lambda \geq \ell(e_0)(1 - 4/t)t/m - 1 \geq t - 5$. In the third phase $\alpha \geq -m/t - \ell(e_1)(1 - 4/t)$ and $\beta \leq m/t + \lambda\ell(e_1)(1 - 4/t)$ so $\alpha + \ell(e_1) \geq 3\ell(e_1)/t > \beta$ since $t > 6$. Also β increases less than α decreases since $\lambda < 1/2$, so $\ell(e_0) - \alpha > \beta$ remains true. This proves the claim.

Applying the algorithm to p' and f' on the other side of e , either the algorithm does not break in which case $\ell(f') \geq (1 - 4/t)\ell(e)$, $\langle y' \rangle_{f'} \geq (1 - 4/t)\langle x \rangle_e$, and we are done. Or the algorithm breaks and we get similarly a triangle Δ' and a vertex w' of P . The inner angles of Δ' at v_0 and v_1 are also both strictly smaller than $\pi/4$, so the segment between

w and w' is relatively included in the interior of the quadrilateron formed by Δ and Δ' , and is strictly shorter than e . This segment is a vertex-to-vertex arc of Q shorter than e , a contradiction. \square

Proof of Proposition 10.6. Let $t > 6$. Assume that there is a geodesic loop γ that encloses e by a factor of t . Let x be the basepoint of γ . In the Euclidean plane, consider the polygon Q corresponding to F . Let \widehat{e} and \widehat{x} be the pre-images of e and x in Q . Consider the prefix and the suffix of γ that leave x on both sides of e to meet ∂F , and their pre-image paths in Q that meet two boundary edges \widehat{f} and \widehat{f}' of Q , at respective points \widehat{y} and \widehat{y}' . By Lemma 10.12, one of those two points, say \widehat{y} without loss of generality, is such that $\langle \widehat{y} \rangle_{\widehat{f}} \geq (1 - 4/t) \langle \widehat{x} \rangle_{\widehat{e}}$ and $\ell(\widehat{f}) \geq (1 - 4/t) \ell(\widehat{e})$. Also \widehat{f} projects to a boundary edge f of F , and \widehat{y} projects to a point y in the relative interior of f . Now rebase γ at y , and consider the geodesic loop γ' homotopic to it (where the basepoint at y is fixed by the homotopy). Then $\ell(\gamma') \leq \ell(\gamma) = \langle x \rangle_e / t < \langle y \rangle_f / (t - 4)$. In particular $\ell(\gamma') < \langle y \rangle_f$ since $t > 5$. And γ' meets y on both sides of f by Lemma 10.11, since $t > 2$. \square

10.5.3 Interior of a thick biface

Recall that, given a portalgon R whose surface is S , ALGORITHM may replace a sub-portalgon of R by a good biface B . The following ensures that if B is thick, and if an interior edge of B^1 is “very enclosed” in the surface S , then it is “not much more enclosed” in S and “not much longer” than the edges initially in R^1 , similarly to Proposition 10.6:

Proposition 10.7. *Assume that S contains the surface of a thick biface B , and let e be one of the two interior edges of B^1 . Assume that $c_S(e) > 6$. Then there is a boundary edge f of B^1 such that $c_S(f) \geq c_S(e) - 5$ and $\ell(f) \geq (1 - 4/c_S(e)) \cdot \ell(e)$.*

In this section we prove Proposition 10.7. First we need a lemma:

Lemma 10.13. *Let B be a good biface. Among the two interior edges of B^1 let f be a longest one. Let F be the face of B^1 adjacent to f . Each corner of F incident to f has angle smaller than or equal to $\pi/2$.*

Proof. Among the two interior edges of B^1 let e be a shortest one, and let $g \neq e$ be the other one. Then e , g , and f are the sides of F . The angle at the corner of F between f and g is smaller than $\pi/2$ since $\ell(e) \leq \ell(g)$. Now consider the corner c between f and e . Cut $\mathcal{S}(B)$ open along e and consider the resulting quadrilateron Q in the plane. The edge f of B^1 corresponds to a side \widehat{f} of Q , the edge e corresponds to two opposite sides \widehat{e} and \widehat{e}' , and the edge g corresponds to a vertex-to-vertex arc \widehat{g} of Q . Also the other boundary edge $f' \neq f$ of B^1 corresponds to the side \widehat{f}' of Q opposite to \widehat{f} . And the corner c corresponds to the corner \widehat{c} of Q between \widehat{e} and \widehat{f} . Let \widehat{d} be the corner of Q opposite to \widehat{c} , between \widehat{e}' and \widehat{f}' . Assume by contradiction that the angle at \widehat{c} is greater than $\pi/2$. We have $\ell(\widehat{e}) = \ell(\widehat{e}')$ and $\ell(\widehat{f}) \geq \ell(\widehat{f}')$ so the angle at \widehat{d} is greater than or equal to the angle at \widehat{c} , and in particular is also greater than $\pi/2$. The two other angles of Q are smaller than π , so Q is convex and admits a diagonal $p \neq \widehat{g}$. Consider the unique circle C that admits \widehat{g} as a diameter. Then the two endpoints of p lie in the interior of C . So p is shorter than \widehat{g} . This contradicts the assumption that B is good. \square

Proof of Proposition 10.7. Among the two interior edges of B^1 let g be a shortest one. Among the two boundary edges of B^1 let g' be a longest one. Then $\ell(g) \leq \ell(g')$ since B is thick. We claim that if $c_S(g) > 2$, then $c_S(g') \geq c_S(g) - 1$. To prove the claim let $t > 2$ and assume that there is a loop γ that encloses g by a factor of t in S . Let x be the basepoint of γ . Let F be the face of B^1 adjacent to g' . Around x there is a portion of γ that enters F . This portion of γ must leave F by a point y of g' since the angle of F between g and g' is smaller than or equal to $\pi/2$ by Lemma 10.13, since $\ell(g) \leq \ell(g')$, and since $\ell(\gamma) = \langle x \rangle_g / t < \langle x \rangle_g / \sqrt{2}$. Then $\langle y \rangle_{g'} \geq \langle x \rangle_g - \ell(\gamma) = (1 - 1/t) \langle x \rangle_g$ by triangular inequality and since $\ell(g) \leq \ell(g')$. Rebase γ at y , and consider the geodesic loop γ' homotopic to it (where the homotopy fixes the basepoint at y). Then $\ell(\gamma') \leq \ell(\gamma) = \langle x \rangle_g / t \leq \langle y \rangle_{g'}/(t - 1)$. And γ' encloses g' by Lemma 10.11, since $t > 2$. This proves the claim.

If $e = g$ we are done by our claim, so assume that e is a longest interior edge of B^1 . Deleting e merges the two faces of B^1 into a single face F' of which e is a shortcut, since B is good. So Proposition 10.6 applies since $c_S(e) > 6$: there is a boundary edge f of F' such that $c_S(f) \geq c_S(e) - 4$ and $\ell(f) \geq (1 - 4/c_S(e))\ell(e)$. If f is a boundary edge of B^1 we are done. Otherwise $f = g$ so $\ell(g') \geq \ell(f) \geq (1 - 4/c_S(e))\ell(e)$ and $c_S(g') \geq c_S(f) - 1 \geq c_S(e) - 5$ by our claim since $c_S(e) > 6$. This proves the proposition. \square

10.5.4 Boundary of a thin biface

Recall that ALGORITHM keeps some thin bifaces in the output portalgon by marking them as inactive. The following enforces that their boundary edges are “not very enclosed” in S , which is not surprising:

Proposition 10.8. *Assume that S contains the surface of a thin biface B , and let e be one of the two boundary edges of B^1 . Then $c_S(e) \leq 2$.*

In this section we prove Proposition 10.8. First we need two lemmas:

Lemma 10.14. *Let B be a thin biface. Among the two interior edges of B^1 let e be a shortest one. Each of the four corners between e and the boundary of $\mathcal{S}(B)$ has angle greater than $\pi/4$.*

Proof. Assume by contradiction that there is a corner c between e and a boundary edge f of B^1 whose angle is smaller than or equal to $\pi/4$. Cut $\mathcal{S}(B)$ open along e and embed the resulting quadrilateron Q in the plane, isometrically. The edge e corresponds to two opposite sides \widehat{e} and \widehat{e}' of Q . The edge f corresponds to one of the other two sides of Q , that we call \widehat{f} . The vertex v of the corner c corresponds to the two end-vertices of \widehat{f} : let \widehat{v} be the one incident to \widehat{e} , and let \widehat{v}' be the one incident to \widehat{e}' . Without loss of generality the corner c corresponds to the corner of Q at \widehat{v} , whose angle is thus smaller than or equal to $\pi/4$. Consider the orthogonal projection x of \widehat{v}' on the line containing \widehat{e} . Then x belongs to \widehat{e} since \widehat{e} is longer than \widehat{f} , as B is thin. The segment p between x and \widehat{v}' is shorter than the portion of \widehat{e} between x and \widehat{v} . Also p is included in Q since \widehat{e} and \widehat{e}' are longer than \widehat{f} . Thus p projects to a path that shortcuts e , contradicting the fact that B is a good biface. \square

Lemma 10.15. *In $\mathcal{S}(B)$ every path p between the two boundary components of $\mathcal{S}(B)$ is such that $\ell(p) \geq \ell(e)/2$.*

Proof. Without loss of generality one of the two endpoints of p (at least) is a vertex v of B^1 . Consider the other endpoint x of p , and the vertex $w \neq v$ of B^1 . There is a path q from x to w in the boundary of $\mathcal{S}(B)$. Without loss of generality $\ell(q) \leq \ell(e)/2$ since B is thin. Also e is a shortest path since B is good. So $\ell(p) + \ell(q) \geq \ell(e)$. We proved $\ell(p) \geq \ell(e)/2$. \square

Proof of Proposition 10.8. Among the two interior edges of B^1 let e be a shortest one. Let f be any one of the two boundary edges of B^1 . We have $\ell(e) \geq \ell(f)$ since B is thin. Assume by contradiction that there is in S a loop γ that encloses f by a factor of $t > 2$. Let x be the basepoint of γ . There is a portion of γ that leaves x and enters the interior of $\mathcal{S}(B)$. This portion of γ cannot leave $\mathcal{S}(B)$ via the other boundary edge of $\mathcal{S}(B)$, for otherwise $\ell(\gamma) \geq \ell(e)/2$ by Lemma 10.15, so $\ell(\gamma) > \langle x \rangle_f / t$, a contradiction. Then γ intersects e . And f and e have a corner whose angle is smaller than $\pi/4$ since $\ell(\gamma) < \langle x \rangle_f / 2$. This contradicts Lemma 10.14. \square

10.5.5 Upper bound on segment-happiness and length

In this section, given a segment e of S , we bound from above the segment-happiness and the length of e by the enclosure of e . Our bounds depend on the surface S . More precisely, on the systole of S and the diameter of S . But instead of the diameter of S , we consider an arbitrary triangulation of S , and we use its number n of triangles together with the maximum length L of its edges (it is easily seen that the diameter of S is smaller than or equal to nL). This will be more convenient to us when analyzing ALGORITHM in Section 10.6, for then S will be given by a triangular portalgon, whose 1-skeleton is a triangulation of S . We prove:

Proposition 10.9. *Let e be a segment of S . Let $s > 0$ be smaller than the systole of S . Assume that there is a triangulation of S with $n \geq 1$ triangles, whose edges are all smaller than $L > 0$. Then $h_S(e) = O(c_S(e) \cdot (1 + \log c_S(e) + \log n + \log \lceil L/s \rceil))$ and $\ell(e)/s = O(c_S(e) \cdot n \cdot \lceil L/s \rceil^2)$.*

In Proposition 10.9 the $O()$ notation does not depend on S , it involves a universal constant. In the second inequality of Proposition 10.9 the exact powers above $\lceil L/s \rceil$ and n , here 2 and 1, do not matter to us. We need only a polynomial in $\lceil L/s \rceil$ and n . The rest of this section is devoted to the proof of Proposition 10.9. First we need a few lemmas.

Lemma 10.16. *Let $t > 1$. Assume that there is a shortest path whose relative interior crosses the relative interior of e twice in the same direction, at points x and y . If the sub-segment of e between x and y is shorter than $\langle x \rangle_e / 2t$ then $c_S(e) > t$.*

Proof. Consider the portion p of the shortest path that starts just before its crossing at x , and ends just before its crossing at y . Consider also the geodesic path q that runs parallel to the sub-segment of e from y to x , such that the concatenation of p and q forms a loop γ . Base γ at x . There is a unique geodesic loop γ' homotopic to γ (where the base-point at x is fixed in the homotopy) since the interior of S is flat. We have that γ' is not the constant loop based at x ; for otherwise γ would be contractible, so p would be homotopic to the reversal of q , and so p would actually be equal to the reversal of q since the interior of S is flat, a contradiction. Moreover γ' is shorter than $\langle x \rangle_e / t$; indeed γ' is not longer than γ , q is shorter than $\langle x \rangle_e / 2t$ by assumption, and p is not longer than q since p is a shortest path. Then γ' is in general position with e . We shall prove that γ' meets x on both sides of e . This will prove the lemma for then γ' will enclose e by a factor of $\langle x \rangle_e / \ell(\gamma') > t$.

Let us prove that. Orient e so that γ crosses e from right to left. Consider the universal covering space \tilde{S} of S , and a lift \tilde{e} of e in \tilde{S} . The interior of \tilde{S} being flat, there is a geodesic \tilde{L} , containing \tilde{e} , such that on both ends \tilde{L} is either infinite or reaches the boundary of \tilde{S} . And \tilde{L} separates \tilde{S} in two connected components. Now let \tilde{x} be the lift of x in \tilde{e} . There are two lifts of γ' incident to \tilde{x} : one lift $\tilde{\gamma}'_0$ starts at \tilde{x} , the other lift $\tilde{\gamma}'_1$ ends at \tilde{x} . Let \tilde{a}_0 be the endpoint of $\tilde{\gamma}'_0$, and let \tilde{a}_1 be the startpoint of $\tilde{\gamma}'_1$. We claim that \tilde{a}_0 lies strictly to the left of \tilde{L} , and that \tilde{a}_1 lies strictly to the right of \tilde{L} . This claim implies that $\tilde{\gamma}'_0$ meets \tilde{x} on the left of \tilde{e} , and that $\tilde{\gamma}'_1$ meets \tilde{x} on the right of \tilde{e} , which implies that γ' meets x on both sides of e .

Let us prove the claim. First we prove that \tilde{a}_0 lies strictly to the left of \tilde{L} . To do so consider also the lift \tilde{p} of p that starts at \tilde{x} , and the lift \tilde{q} of q that starts at the endpoint of \tilde{p} . The endpoint of \tilde{q} is \tilde{a}_0 since the concatenation of \tilde{p} and \tilde{q} is a lift of γ , and since γ is homotopic to γ' . By definition \tilde{p} leaves \tilde{x} on the left of \tilde{L} . Also \tilde{p} is disjoint from \tilde{L} except for its startpoint at \tilde{x} , the interior of S being flat. Moreover \tilde{q} is disjoint from \tilde{L} . For otherwise \tilde{q} would intersect \tilde{L} at a point \tilde{z} whose distance to \tilde{x} would be smaller than $\langle x \rangle_e / t$. But then the sub-segment of \tilde{L} between \tilde{z} and \tilde{x} would be no longer, and so would be included in \tilde{e} . In particular \tilde{q} and \tilde{e} would intersect, a contradiction. This proves that \tilde{a}_0 lies strictly to the left of \tilde{L} .

To prove that \tilde{a}_1 lies strictly to the right of \tilde{L} , consider the lift \tilde{y} of y in \tilde{e} , and the lift \tilde{p}_1 of p that ends at \tilde{y} . Then the startpoint of \tilde{p}_1 is \tilde{a}_1 , and it lies strictly to the right of \tilde{L} since \tilde{p}_1 meets \tilde{y} on the right of \tilde{L} , and since \tilde{p}_1 is otherwise disjoint from \tilde{L} . This proves the claim, and the lemma. \square

Lemma 10.17. *We have $h_S(e) = O(c_S(e) \cdot (1 + \log \lceil \ell(e)/s \rceil))$.*

Proof. Let $t > 1$. Assume $h_S(e) > 12t \cdot (3 + \log \lceil \ell(e)/s \rceil)$. We will prove $c_S(e) \geq t$, and this will prove the lemma. In S there is a shortest path p that intersects e more than $12t \cdot (3 + \log \lceil \ell(e)/s \rceil)$ times. Cut e at its middle point. One of the two resulting sub-segments of e , say f , intersects p more than $6t \cdot (3 + \log \lceil \ell(e)/s \rceil)$ times. Partition f into sub-segments f_0, f_1, \dots, f_n with $n \leq 2 + \log \lceil \ell(e)/s \rceil$, where the sub-segment f_0 contains the points $x \in f$ such that $\langle x \rangle_e \leq s/4$, and where for every $1 \leq i \leq n$ the sub-segment f_i contains the points $x \in f$ such that $2^{i-3}s \leq \langle x \rangle_e \leq 2^{i-2}s$. There is $0 \leq i \leq n$ such that p intersects f_i more than $6t$ times. Then the relative interior of p crosses f_i twice (at least) in the same direction at points x and y , such that the sub-segment of f_i between x and y is shorter than $2^{i-4}s/t$, since $\ell(f_i) \leq 2^{i-3}s$. Also $i \geq 1$ as no shortest path crosses f_0 twice, since $\ell(f_0) < s/2$, and since the interior of S is flat. In particular $\langle x \rangle_e \geq 2^{i-3}s$. Then $c_S(e) \geq t$ by Lemma 10.16. \square

Lemma 10.18. *We have $\ell(e) = O(c_S(e) \cdot n \lceil L/s \rceil L)$.*

Proof. Let $t > 1$. Assume $\ell(e) \geq 600t \cdot n \lceil L/s \rceil L$. We will prove that $c_S(e) \geq t$, and this will prove the proposition. To do so let $d = 120n \lceil L/s \rceil L$. Cut e into three segments, a middle segment e_0 of length d , and two peripheral segments each longer than $2t \cdot d$. We claim that there is in S a shortest path crossing the relative interior of e_0 twice in the same direction. This claim implies $c_S(e) \geq t$ by Lemma 10.16, which proves the proposition.

Let us prove the claim. Consider a triangulation T of S with n triangles, whose edges are all smaller than $L > 0$. Cut each edge of T into $2 \lceil L/s \rceil$ equal-length segments, that we shall call *doors*. Each door is smaller than or equal to half the systole of S so it is a shortest path. There are at most $6n \lceil L/s \rceil$ doors since T has at most $3n$ edges. Each sub-segment e_1 of length $4L$ of e_0 contains in its relative interior three points x_0, x_1, x_2 in this order such

that $x_0 \notin p$, $x_1 \in p$, and $x_2 \notin p$ for some door p . The relative interior of e_0 intersects at least $30n\lceil L/s \rceil$ times doors this way, so there is a door p intersected at least 5 times by the relative interior of e_0 . Then each intersection is a single point (p and e_0 do not overlap). Two of those intersection points may be endpoints of p , but otherwise the relative interior of p crosses the relative interior of e_0 at least three times. So p crosses e_0 twice in the same direction, which proves the claim, and the proposition. \square

Proof of Proposition 10.9. We have $h_S(e) = O(c_S(e) \cdot (1 + \log\lceil \ell(e)/s \rceil))$ by Lemma 10.17. Also $\ell(e)/s = O(c_S(e) \cdot n \cdot \lceil L/s \rceil^2)$ by Lemma 10.18. So $\log(\lceil \ell(e)/s \rceil) = O(1 + \log c_S(e) + \log(n) + \log\lceil L/s \rceil)$. This proves the proposition. \square

10.6 Geometric analysis of the algorithm: proof of Proposition 10.1

In this section we complete the analysis of ALGORITHM to prove Proposition 10.1, which we restate for convenience:

Proposition 10.1. *Let T be a portalgon of n triangles, whose sides are all smaller than $L > 0$. Assume that $\mathcal{S}(T)$ is flat. Let $s > 0$ be smaller than the systole of $\mathcal{S}(T)$. One can compute in $O(n \log^2(n) \cdot \log^2(2+L/s))$ time a portalgon of $O(n \cdot \log(2+L/s))$ triangles, whose surface is isometric to that of T , and whose segment-happiness is $O(\log(n) \cdot \log^2(2+L/s))$.*

We consider the setting of Proposition 10.1: we fix a portalgon T of n triangles, whose sides are smaller than $L > 0$, and whose surface $\mathcal{S}(T)$ is flat. Then we apply ALGORITHM to T , and we analyze the execution using the notion of enclosure introduced in Section 10.5. In order to ease the reading, in the whole section we denote by $S = \mathcal{S}(T)$ the surface of T .

10.6.1 The inactive loops are not very enclosed

First we prove that any time during the execution the separating loops are “not very enclosed” in S :

Lemma 10.19. *Any time during the execution every separating loop e satisfies $c_S(e) \leq 2$.*

Proof. Only step 2 of SIMPLIFYTUBES may create a separating loop, by marking a *thin* biface B as inactive. Then B is never touched again by the algorithm. So the algorithm maintains the invariant that every separating loop e is adjacent to the surface of at least one inactive region that is a *thin* biface. So $c_S(e) \leq 2$ by Proposition 10.8. \square

10.6.2 The geometry of the active region is simplified

In this section we show that running the algorithm simplifies the geometry of the active region. More precisely the maximum length of the edges “very enclosed” in S (if any) scales down exponentially:

Proposition 10.10. *After $i \geq 1$ iterations of the main loop, let e be an edge of R_A^1 . If $c_S(e) > 22000 \cdot i$ then $\ell(e) < 2^{1-i}L$.*

Before proving Proposition 10.10 we analyze the operations performed independently with three lemmas. Each application of INSERTVERTICES improves the geometry of the active region:

Lemma 10.20. *Consider the active regions R_A and R'_A respectively before and after some application of INSERTVERTICES. Assume that there is an edge e' of R'_A such that $c_S(e') > 2$. Then there is an edge e of R_A^1 such that $c_S(e) \geq c_S(e')$ and $\ell(e) \geq 2\ell(e')$.*

Proof. First observe that e' is not included in the boundary of $S(R'_A)$ since e' is enclosed and thus not included in the boundary of S , and since e' is not a separating loop by Lemma 10.19. So there is an edge e of R_A^1 such that e' is one of the two half-segments obtained after the insertion of the middle point of e as a vertex. Then $\ell(e) = 2\ell(e')$. And $c_S(e) \geq c_S(e')$ by Lemma 10.10. \square

The rest of the algorithm may deteriorate the geometry of the active region, but not too much:

Lemma 10.21. *Consider the active regions R_A and R'_A respectively before and after some application of INSERTEDGES. Assume that there is an edge e' of R'_A such that $c_S(e') > 14$. Then there is an edge e of R_A^1 such that $c_S(e) \geq c_S(e') - 12$ and $\ell(e) \geq (1 - 12/c_S(e')) \cdot \ell(e')$.*

Proof. Here we crucially use the fact that every polygon of R_A has degree at most six, so that at most three edges are inserted within the polygon. Indeed either e' was already an edge of R_A^1 and there is nothing to do, or e' has been inserted in some face F of R_A^1 . At most three edges were inserted in F , and Proposition 10.6 applied at most three times gives a boundary edge e of F such that $c_S(e) \geq c_S(e') - 12$ and $\ell(e) \geq (1 - 12/c_S(e'))\ell(e')$. \square

Lemma 10.22. *Consider the active regions R_A and R'_A respectively before and after some application of SIMPLIFYTUBES. Assume that there is an edge e' of R'_A such that $c_S(e') > 6$. Then there is an edge e of R_A^1 such that $c_S(e) \geq c_S(e') - 5$ and $\ell(e) \geq (1 - 4/c_S(e')) \cdot \ell(e')$.*

Proof. Assume that e' was not already an edge of R_A^1 for otherwise there is nothing to do. Then there is a good biface B computed by step 2 of SIMPLIFYTUBES such that e is one of the two interior edges of B^1 . Also B is thick, for B has not been marked as inactive. So by Proposition 10.7 there is a boundary edge e of B^1 such that $c_S(e) \geq c_S(e') - 5$ and $\ell(e) \geq (1 - 4/c_S(e'))\ell(e')$. \square

Proof of Proposition 10.10. Consider the active regions R_A and R'_A respectively at the very beginning of the algorithm, and after i iterations of the main loop. Assume that there is an edge e' in R'_A such that $c_S(e') > 22000 \cdot i$. During those i iterations there has been i applications of INSERTVERTICES, $351i$ applications of INSERTEDGES, and $350i$ applications of SIMPLIFYTUBES. Also $12 \cdot 351i + 5 \cdot 350i < 11000i$. So Lemma 10.20, Lemma 10.21, and Lemma 10.22 imply that there is an edge e in R_A^1 such that $\ell(e) \geq 2^i(1 - 11000i/c_S(e'))\ell(e') > 2^{i-1}\ell(e')$. And $\ell(e) \leq L$ since e belongs to the input triangulation T^1 . \square

10.6.3 Proof of Proposition 10.1

Finally, we complete the analysis of ALGORITHM and prove Proposition 10.1. We need a last preliminary lemma:

Lemma 10.23. *Assume that S contains the surface of a tube X . Then the systole of $\mathcal{S}(X)$ is greater than or equal to systole of S .*

Proof. Otherwise one of the two loops of X^1 that constitute the boundary of $\mathcal{S}(X)$ is contractible in S . So this loop bounds a topological disk in S by a result of Epstein [83, Theorem 1.7]. The interior of the disk is flat, and its boundary is geodesic except possibly at the basepoint of the loop. This contradicts the formula of Gauss–Bonnet. \square

Proof of Proposition 10.1. Apply ALGORITHM to T with $N = \lceil \log(2 + L/s) \rceil$, and return the resulting triangular portalgon R . By Proposition 10.5 the number of polygons of the active region is $O(n)$ throughout the execution. So in the end R has $O(n \cdot \log(2 + L/s))$ triangles, since each iteration of the main loop marks $O(n)$ triangles as inactive, and since there are $\lceil \log(2 + L/s) \rceil$ iterations of the main loop. We have two claims that immediately imply the proposition.

Our first claim is that the algorithm takes $O(n \log^2(n) \cdot \log^2(2 + L/s))$ time. Let us prove this first claim. Each application of INSERTVERTICES or INSERTEDGES takes $O(n)$ time. And each application of SIMPLIFYTUBES or GARDENING takes $O(n \log(n) \cdot \log(2 + \Lambda/s))$ time by Proposition 10.4 and Lemma 10.23, where Λ is the maximum length reached by an edge of the 1-skeleton of the active region during the execution. Now let us bound Λ . If at some point an edge e of the 1-skeleton of the active region is longer than L then $c_S(e) = O(\log(2 + L/s))$ by Proposition 10.10. Moreover $\ell(e)/s = O(c_S(e) \cdot n \lceil L/s \rceil^2)$ by Proposition 10.9. This proves $\log(2 + \Lambda/s) = O(\log(n) + \log(2 + L/s))$, which proves the claim.

Our second claim is that in the end every edge e of R^1 satisfies $h_S(e) = O(\log(n) \cdot \log^2(2 + L/s))$. Let us prove this second claim. First observe that if e is in R_A^1 then $c_S(e) < 22000 \log(2 + L/s)$, for otherwise Proposition 10.10 would imply $\ell(e) < 2s$, implying that no loop encloses e in S , a contradiction. In this case $h_S(e) = O(\log(2 + L/s) \cdot (\log(n) + \log(2 + L/s)))$ by Proposition 10.9, and we are done. Every other edge of R^1 belongs to the 1-skeleton of an inactive good biface B . Every boundary edge e of B^1 is either a boundary component of S or a separating loop, so $c_S(e) \leq 2$ by Lemma 10.19, and so $h_S(e) = O(\log(n) + \log(2 + L/s))$ by Proposition 10.9. Every interior edge f of B^1 then satisfies $h_S(f) = O(\log(n) + \log(2 + L/s))$ by Lemma 10.2. This proves the second claim, and the proposition. \square

10.7 Extension to non-flat surfaces: proof of Proposition 10.2

In this section we finally prove Proposition 10.2, which we restate for convenience:

Proposition 10.2. *Let T be a portalgon of n triangles, of aspect ratio r . One can compute in $O(n \log^2(n) \cdot \log^2(r))$ time a portalgon of $O(n \cdot \log(r))$ triangles, whose surface is $\mathcal{S}(T)$, and whose happiness is $O(n \log(n) \cdot \log^2(r))$.*

We deduce Proposition 10.2 from Proposition 10.1, essentially by cutting out caps around the singularities in the interior of the surface, by applying Proposition 10.1 to the truncated surface, and by putting the caps back afterward. See Figure 10.5.

Proof of Proposition 10.2. Let $S := \mathcal{S}(T)$ be the surface of T . Let d be the minimum height of the triangles of T . Given a vertex v of T^1 in the interior of S , we define a region around

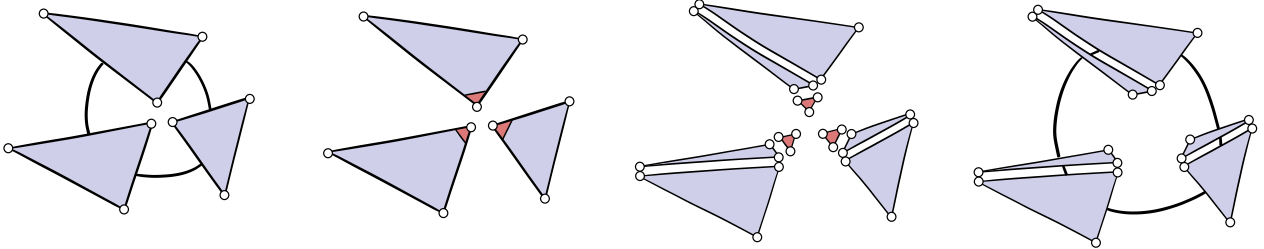


Figure 10.5: Cutting out a cap in the proof of Proposition 10.2.

v in S , as follows. On every directed edge e of T^1 whose tail is v , place a point at distance $d/6$ from the tail of e along e . Link those $k \geq 1$ points in order around v , using geodesic segments within the faces of T^1 incident to v . In each corner of T^1 incident to v there is a newly created triangle incident to v . Those k triangles define a region C around v , which we call *cap* of v . Importantly, every point in the cap of v is at distance smaller than or equal to $d/6$ from v in S . Also every segment p tracing the boundary of C satisfies $\ell(p) \geq d/6r$. To see that consider the face F of T^1 containing p , and the two sides e_0 and e_1 of F incident to v . For each i consider the point on e_i at distance $m := \min(\ell(e_0), \ell(e_1))$ from v along e_i . Join those two points by a geodesic segment q in F . Then q is at least as long as the minimum height of the triangle corresponding to F , so $\ell(q) \geq m/r$. Moreover $\ell(p)/\ell(q) = d/(6m)$ by the theorem of Thales. This proves $\ell(p) \geq d/6r$.

For the sake of analysis, given an arbitrary vertex v of T^1 (possibly on the boundary of S), we define another kind of region around v . Link the middle points of the edges around v in order around v . The resulting triangles around v constitute the *protected region* of v . Importantly, every path smaller than $d/2$ starting from v must lie in the protected region of v . Indeed every geodesic path p smaller than d starting from v is relatively included in a single face or edge of T^1 . Then every prefix of p smaller than $\ell(p)/2$ lies in the protected region of v .

First construct in $O(n)$ time a triangular portalgon T_0 whose surface is S , as follows. Consider every singularity in the interior of S (if any). This singularity is a vertex v of T^1 . Trace the boundary of the cap around v in the faces of T^1 . Then cut those faces along the trace, as in Figure 10.5. Afterward some polygons of T_0 may not be triangles, so cut each polygon of T_0 into triangles along shortcuts. Now remove the triangles corresponding to the caps from T_0 , and let T_1 be the resulting triangular portalgon. The surface $S(T_1)$ is flat.

Our first claim is that the systole of $S(T_1)$ is greater than or equal to $d/6r$. By contradiction assume that there is a non-contractible closed curve γ in $S(T_1)$ smaller than $d/6r$. Without loss of generality γ intersects a vertex w of T_1 ; indeed if such a γ has minimum length and does not intersect any vertex of T_1 then it can be slid along the surface, without changing its length, until it intersects a vertex of T_1 . If w is a vertex of T^1 , then γ lies in the protected region around w , and so γ is contractible in $S(T_1)$, a contradiction. If w is a vertex on the boundary of some cap C removed, then γ lies in the protected region around the central vertex of C . In that case γ is at least as long as any edge of the boundary of C , so $\ell(\gamma) \geq d/6r$. This proves the first claim.

The number of triangles and the maximum side length of a triangle of T_1 may be greater than those of T , but only by a constant factor. Using the first claim and Proposition 10.1, replace T_1 by a portalgon of $O(n \log(r))$ triangles, whose surface is that of T_1 , and whose segment-happiness is $O(\log(n) \log^2(r))$, all in $O(n \log^2(n) \log^2(r))$ time. Place back the caps

on $\mathcal{S}(T_1)$, and return the resulting triangular portalgon T' .

The segment-happiness of T' and the happiness of T' do not differ by more than a constant factor since the polygons of T' are all triangles. Our second claim is that the segment-happiness of T' , and thus the happiness of T' , is bounded by $O(n \log(n) \log^2(r))$. To prove the second claim, we call *cap path* any shortest path in S that lies in the closure of some cap. We call *rogue path* any shortest path in S whose relative interior is disjoint from the closures of the caps. Every rogue path intersects every edge of T'^1 at most $O(\log(n) \log^2(r))$ times, since the segment-happiness of T_1 is $O(\log(n) \log^2(r))$. Also every cap path intersects every edge of T'^1 at most once. Now consider a shortest path p in S . Then p uniquely writes as a sequence X of alternatively cap paths and rogue paths. Also, there cannot be two distinct cap paths q_0 and q_1 in X that both lie in the same cap C . For otherwise any point of q_0 would be at distance at most $d/3$ from any point of q_1 . Also the subpath of p between q_0 and q_1 contains a rogue path that must leave the protected region around the central vertex of C , and is thus longer than $d/2 - d/6 = d/3$. That contradicts the fact that p is a shortest path. We proved that there are at most $O(n)$ paths in X , each intersecting at most $O(\log(n) \log^2(r))$ times any given edge of T'^1 . This proves the second claim, and the proposition. \square

10.8 Appendix: proof of Proposition 10.4

In this section we prove Proposition 10.4, which we restate for convenience:

Proposition 10.4. *Let X be a tube with n triangles, whose sides are smaller than $L > 0$. Let $s > 0$ be smaller than the systole of $\mathcal{S}(X)$. One can compute a good biface whose surface is $\mathcal{S}(X)$ in $O(n \log n \cdot \log(2 + L/s))$ time.*

Proposition 10.4 is similar to but different from a result of Löffler, Ophelders, Silveira, and Staals [141, Theorem 45] (building upon a ray shooting algorithm of Erickson and Nayyeri [86]), in which the authors provide an algorithm to transform a biface into a portalgon of bounded happiness, and of bounded combinatorial complexity. They extend their result from bifaces to portalgons X such that the dual graph of X^1 in $\mathcal{S}(X)$ has at most one simple cycle, but unfortunately this does not include tubes. We extend their result to tubes to prove Proposition 10.4, reusing some of ideas developed in the core of the paper.

We need a few lemmas. The following is a corollary of [141, Theorem 45]:

Lemma 10.24. *Let B be a biface of happiness h . One can compute in $O(1 + \log h)$ time a good biface whose surface is that of B .*

Proof. By the result of Löffler, Ophelders, Silveira, and Staals [141, Theorem 45] we can compute in $O(1 + \log h)$ time a portalgon T , whose surface is $\mathcal{S}(B)$, whose happiness is $O(1)$, and whose 1-skeleton T^1 has $O(1)$ edges. Without loss of generality the two vertices b_0 and b_1 of B^1 are also vertices of T^1 , and we know which vertices of the polygons of T correspond to b_0 and b_1 .

We now describe how to compute, in constant time, from T , a good biface of $\mathcal{S}(T)$. The key thing is that we can exploit the fact that T has $O(1)$ combinatorial complexity and happiness to compute by exhaustive search. First compute, in constant time, by exhaustive search, a shortest path q between b_0 and b_1 in $\mathcal{S}(T)$: represent q by its pre-image in the polygons of T . Then cut the polygons of T along the pre-image of q : every time a polygon

is cut in two along a segment a , the two edges issued of a are not matched in the resulting portalgon (the goal is to cut the surface of T , not just changing T). Consider the resulting portalgon D . Then $\mathcal{S}(D)$ is homeomorphic to a closed disk. The two endpoints b_0 and b_1 of q become a set V of four vertices of D^1 that lie on the boundary of $\mathcal{S}(D)$. Every singularity of $\mathcal{S}(D)$ lies on the boundary of $\mathcal{S}(D)$ and belongs to V . Now replace D by a triangular portalgon D' , of the same surface, and such that the vertex set of D'^1 is exactly V . This can be done for example by iteratively inserting vertex-to-vertex arcs in the faces of D^1 to make D^1 a triangulation, and by deleting a vertex v of D^1 and its incident edges. When v lies on the boundary of $\mathcal{S}(D)$, only the edges relatively included in the interior of $\mathcal{S}(D)$ are deleted. In the end, identify back the occurrences of q on the boundary of $\mathcal{S}(D')$, by matching the two corresponding sides of polygons in D' , thereby obtaining a biface B' of $\mathcal{S}(B)$ such that q is an interior edge of B' . Change the other interior edge of B' if necessary so that B' is good. \square

Consider $k \geq 1$ bifaces B_1, \dots, B_k . For every $1 \leq i \leq k$ let e_i and f_i be the two sides of triangles of B_i that correspond to the boundary of $\mathcal{S}(B_i)$. If $i < k$, assume $\ell(e_i) = \ell(f_{i+1})$, and match e_i with f_{i+1} . The resulting triangular portalgon T is a **concatenation** of the bifaces B_1, \dots, B_k . Note that T is not necessarily a tube, for the vertices of T^1 in the interior of $\mathcal{S}(T)$ may be singularities.

Lemma 10.25. *Let T be the concatenation of two good bifaces. If T is a tube, then one can compute in constant time a good biface whose surface is that of T .*

Proof. Consider a shortest path p in $\mathcal{S}(T)$, and the loop edge e of T^1 that lies in the interior of $\mathcal{S}(T)$, in-between the surfaces of the two bifaces. We claim that the relative interior of p does not cross the relative interior of e more than twice. By contradiction assume that p crosses the relative interior of e three times. There is a connected component S_0 of $\mathcal{S}(T) \setminus e$ whose angle at the base vertex of e is greater than or equal to π . Some portion p' of p enters S_0 and then leaves S_0 by two of the three crossings between p and e . One of the two connected components of $S_0 \setminus p'$, say S_1 , is homeomorphic to an open disk. By construction S_1 has at most three angles distinct from π : at the two points where p crosses e , and possibly at the base vertex of e . By the Gauss-Bonnet theorem, there are exactly three such angles, not less, and they are all smaller than π . One of them is the incidence of S_0 and the base vertex of e . This is a contradiction. This proves the claim.

Using the claim immediately the intersection of p and e has $O(1)$ connected components, so p writes as a concatenation of $k = O(1)$ paths p_1, \dots, p_k such that for every $1 \leq i \leq k$ the path p_i is either included in e or relatively disjoint from e . Every edge $f \neq e$ of T^1 intersects p_i less than 7 times: if f is included in the boundary of $\mathcal{S}(T)$ then f intersects p_i at most once, otherwise Lemma 10.2 applies. So f intersects p less than $O(1)$ times. We proved that the segment-happiness of T is $O(1)$. Then the happiness of T is also $O(1)$ since the polygons of T are all triangles. So we can compute a good biface whose surface is that of T in constant time, exactly as in the proof of Lemma 10.24. \square

We will use the following simple consequence of Euler's formula, similar to Lemma 10.6:

Lemma 10.26. *Let S be the topological annulus. Let Y be a topological triangulation of S that has only one vertex on each boundary component of S . Among the vertices of Y that lie in the interior of S and are not incident to any loop edge, at least half have degree smaller than or equal to ten.*

Proof. We may assume without loss of generality that no vertex of Y in the interior of S is incident to a loop edge, by cutting S open at an interior loop edge and recursing on the resulting two triangulations otherwise. Euler's formula gives $m - m_1 + m_2 = 0$, where m , m_1 , and m_2 count respectively the vertices, edges, and faces of Y^1 . Double counting gives $3m_2 = 2m_1 - 2$ and $\sum_v \deg v = 2m_1$, where the sum is over the vertices v of Y . Then $\sum_v (6 - \deg v) = 4$. The two vertices of Y on the boundary of S have degree greater than or equal to four. So in the interior of S every vertex of degree greater than ten must be compensated by a vertex of degree smaller than or equal to ten. \square

Now we start proving Proposition 10.4. In particular we fix a tube X with n triangles, whose sides are all smaller than some $L > 0$.

Lemma 10.27. *One can compute in $O(n \log n)$ time a concatenation of less than $3n$ biforms, whose surface is that of X , whose edges are all shorter than $(3n)^c L$ with $c = \log_{14/13}(3) < 15$.*

Proof. Let us first describe the algorithm before analyzing it. As long as there are vertices of X^1 in the interior of $\mathcal{S}(X)$ that are not incident to any loop edge and have degree smaller than or equal to ten, we consider a maximal independent set V of such vertices, and we do the following. First we delete all the vertices in V along with their incident edges. Then we insert arbitrary vertex-to-vertex arcs in the faces of X^1 to make X^1 a triangulation again.

The algorithm terminates since the number of vertices of X^1 decreases at each iteration. In the end every vertex in the interior of $\mathcal{S}(X)$ is incident to a loop edge by Lemma 10.26, so X is a concatenation of less than m biforms, where $m \leq 3n$ is the initial number of vertices of X^1 . Each iteration can be performed in $O(n)$ time by maintaining a bucket with the vertices of degree smaller than or equal to ten. And we claim that there are less than $\log_{14/13} m$ iterations. Before proving the claim, observe that it implies the lemma. Indeed the algorithm then terminates in $O(n \log n)$ time. Also no edge can get longer than $3^{\log_{14/13} m} L = m^c L$ since the maximum edge length of X^1 cannot be multiplied by more than 3 at each iteration.

Let us now prove the claim. Consider the number m' of vertices of X^1 not incident to any loop edge that lie in the interior of $\mathcal{S}(X)$. By Lemma 10.26, if $m' > 0$ before an iteration of the algorithm, then at least $m'/2$ such vertices have degree smaller than or equal to ten. So V contains at least $m'/14$ vertices, which are deleted. Every non-deleted vertex that was incident to a loop edge before the iteration remains incident to a loop edge after the iteration. We proved that m' is divided by at least $14/13$ during the iteration, which proves the claim. \square

Proof of Proposition 10.4. Apply Lemma 10.27, and replace X in $O(n \log n)$ time by a concatenation of less than $3n$ biforms whose edges are smaller than $(3n)^c L$ for some constant $c > 0$. Each biform B has segment-happiness $O(1 + (3n)^c L/s)$; indeed the systole of $\mathcal{S}(B)$ is greater than or equal to the systole of X , so every segment e in $\mathcal{S}(B)$ satisfies $h_{\mathcal{S}(B)}(e) = O(1 + \ell(e)/s)$. Replace B by a good biform whose surface is that of B in $O(\log(n) + \log(2 + L/s))$ time with Lemma 10.24. Doing so for all biforms takes $O(n \cdot (\log(n) + \log(2 + L/s)))$ time in total. We crudely bound this running time from above by $O(n \log(n) \cdot \log(2 + L/s))$. In the end apply Lemma 10.25 repeatedly to merge those $O(n)$ good biforms into a single good biform, in $O(n)$ total time. \square

10.9 Appendix: Voronoi diagram and Delaunay tessellation

In this section we provide elementary properties of Voronoi diagrams and Delaunay tessellations, for use in Appendix 10.10. This is all folklore, but we could not find the exact statements in the literature, so we provide proofs for completeness.

Given a closed piecewise-flat surface S , and a finite non-empty $V \subset S$ containing all singularities of S , recall that the *Voronoi diagram* of (S, V) contains the points of S whose distance to V is realized by at least two distinct paths in S (see Chapter 9). Moreover, we use the definition of Bobenko and Springborn [22] of the *Delaunay tessellation* of (S, V) , based on *immersed disks* (Chapter 9).

Additionally, we will use the following definition. For every point $x \in S$ there is an immersed empty disk (D, φ) such that φ maps the center of D to x , and such that $\varphi^{-1}(V) \neq \emptyset$. And (D, φ) is unique to x in the sense that if (D', φ') is another such immersed empty disk then there is a plane isometry $\psi : \mathbb{R}^2 \rightarrow \mathbb{R}^2$ satisfying $D' = \psi(D)$ and $\varphi = \varphi' \circ \psi$. We say that (D, φ) is the **maxi-disk** of the point x .

10.9.1 Voronoi diagram

In this section we prove the following:

Lemma 10.28. *Let S be a closed piecewise-flat surface. Let $V \subset S$ be finite, non-empty, and containing all singularities of S . The Voronoi diagram of (S, V) is a graph with finitely many vertices in which every vertex has degree greater than or equal to three, every edge is geodesic, every face is homeomorphic to an open disk and contains exactly one point of V , and every angle at a corner of a face is smaller than or equal to π .*

Note that in Lemma 10.28, without the assumption that V contains all the singularities of S , it would be possible for the Voronoi diagram of (S, V) to not be a graph with geodesic edges.

Proof of Lemma 10.28. Consider the Voronoi diagram \mathcal{V} of (S, V) . We have three claims that immediately imply the lemma. Our first claim is that \mathcal{V} is a graph with finitely many vertices, in which every vertex has degree greater than or equal to three, and in which every edge is geodesic. To prove the first claim consider a point $x \in S$, and the maxi-disk (D, φ) of x . Let x^* be the center of D . The geodesic paths between x^* and $\varphi^{-1}(V)$ in \mathbb{R}^2 correspond via φ to the shortest paths between x and V in S . So x belongs to \mathcal{V} if and only if $\varphi^{-1}(V)$ contains several points. Assume that x belongs to \mathcal{V} , and let $m \geq 2$ be the number of points in $\varphi^{-1}(V)$. Consider, in \mathbb{R}^2 , the Voronoi diagram of $\varphi^{-1}(V)$, which we denote by X . Then X consists in m geodesic rays emanating from x^* . There is an open ball $O \subset D$ on which φ is injective, containing x^* , and such that $\varphi(X \cap O) = \mathcal{V} \cap \varphi(O)$. There are two cases. If $m = 2$ then \mathcal{V} is locally a geodesic path around x . If $m \geq 3$ then \mathcal{V} is locally a geodesic star whose central vertex is x . In particular \mathcal{V} is a graph whose minimum degree is greater than or equal to three, and whose edges are geodesic segments. And \mathcal{V} has finitely many vertices since S is compact. That proves the first claim.

Now consider a face F of \mathcal{V} . Our second claim is that F is simply connected, and that F contains exactly one point of V . This implies that F is homeomorphic to an open disk since

F is not homeomorphic to a sphere. To prove the second claim first consider a point $x \in F$. There is a unique shortest path p from x to V . Then p is disjoint from \mathcal{V} . So the endpoint of p belongs to F . That proves $F \cap V \neq \emptyset$. Now consider the universal covering space \tilde{F} of F . Then \tilde{F} does not contain two distinct lifts of points of V . For otherwise let \tilde{V} contain the lifts of the points of V in \tilde{F} . There is a point $\tilde{x} \in \tilde{F}$ whose distance to \tilde{V} is realized by two distinct paths. And \tilde{x} lifts a point of \mathcal{V} , a contradiction. That proves the second claim.

Finally, consider a vertex v of \mathcal{V} . Our third claim is that around v the angles between consecutive edges of \mathcal{V} are all smaller than or equal to π . To prove the claim consider the maxi-disk (D, φ) of v . Let v^* be the center of D . Let X be the Voronoi diagram of $\varphi^{-1}(V)$ in the plane. The faces of X are all convex, being intersections of half-planes. So the angles between consecutive rays of X around v^* are all smaller than or equal to π . There is an open disk O on which φ is injective, containing v^* , such that $\varphi(X \cap O) = \mathcal{V} \cap \varphi(O)$. That proves the third claim, and the lemma. \square

10.9.2 Voronoi diagram and Delaunay tessellation

In this section, given a closed surface S , and given two graphs G and H cellularly embedded on S , we say that G and H are **isomorphic** if there is a graph isomorphism between G and H that respects the rotation systems induced on G and H by a common orientation of S . This does not depend on the orientation of S . Also, note that G and H are isomorphic if and only if there is an orientation-preserving homeomorphism of S that maps G to H . We prove the following:

Lemma 10.29. *Let S be a closed piecewise-flat surface. Let $V \subset S$ be finite, non-empty, and containing all singularities of S . The Voronoi diagram of (S, V) is isomorphic to the dual of the Delaunay tessellation of (S, V) .*

(Recall that in Lemma 10.29 the Voronoi diagram of (S, V) is a graph cellularly embedded on S by Lemma 10.28.)

Proof of Lemma 10.29. Consider the Voronoi diagram \mathcal{V} of (S, V) , and the Delaunay tessellation \mathcal{D} of (S, V) . Consider a point x of S , and its maxi-disk (D, φ) . We already proved that x is a vertex of \mathcal{V} if and only if $\varphi^{-1}(V)$ contains at least three points. This is the case if and only if the convex hull of $\varphi^{-1}(V)$ projects via φ to the closure of a face f of \mathcal{D} (Lemma 9.1). Every face of \mathcal{D} can be obtained this way (Lemma 9.1), and distinct vertices of \mathcal{V} are clearly mapped to distinct faces of \mathcal{D} . So this defines a one-to-one correspondence between the vertices of \mathcal{V} and the faces of \mathcal{D} . When a vertex v of \mathcal{V} corresponds to a face f of \mathcal{D} this way we say that v is **dual** to f .

Now fix a vertex v of \mathcal{V} , and its dual face f of \mathcal{D} . We call **side** of f any directed edge of \mathcal{D} that sees f on its left. We now relate the directed edges based at v in \mathcal{V} to the sides of f . Again, let (D, φ) be the maxi-disk of v . Let v^* be the center of D , and let y_0, \dots, y_{m-1} be the $m \geq 3$ points of $\varphi^{-1}(V)$. In \mathbb{R}^2 the Voronoi diagram of $\varphi^{-1}(V)$ consists in m geodesic rays r_0, \dots, r_{m-1} emanating from v^* , so that $r_0, y_0, \dots, r_{m-1}, y_{m-1}$ are in clockwise order around v^* . There is an open ball $O \subset D$ on which φ is injective, containing v^* , such that within O the rays r_0, \dots, r_{m-1} correspond via φ to the directed edges e_0, \dots, e_{m-1} emanating from v in \mathcal{V} . For every i the geodesic path from y_i to y_{i+1} corresponds via φ to a side e'_i of f , indices are modulo m . We say that e_i and e'_i are **dual**. This duality is a one-to-one correspondence between the directed edges based at v and the sides of f . The former are

cyclically ordered around v , the latter are cyclically ordered along the boundary of f , and the duality correspondence respects these cyclic orders.

We claim that if a directed edge e_0 of \mathcal{V} is dual to a directed edge e'_0 of \mathcal{D} , then the reversal of e_0 is dual to the reversal of e'_0 . The claim immediately implies the lemma, for then the duality correspondences define the desired graph isomorphism between V and \mathcal{D} . Let us prove the claim. Let e'_1 be the reversal of e'_0 , and let e_1 be the dual of e'_1 . We shall prove that e_1 is the reversal of e_0 . Consider the maxi-disks (D_0, φ_0) and (D_1, φ_1) of the base vertices of e_0 and e_1 , and realize them so that they agree on the geodesic segment p that is the pre-image of the common edge of e'_0 and e'_1 . Then φ_0 and φ_1 agree on $\overline{D}_0 \cap \overline{D}_1$, so they agree with a common map $\varphi_0 \cup \varphi_1 : \overline{D}_0 \cup \overline{D}_1 \rightarrow S$. Let q be the geodesic segment between the centers of D_0 and D_1 . Then q is contained in $\overline{D}_0 \cup \overline{D}_1$, and projects via $\varphi_0 \cup \varphi_1$ to the common edge of e_0 and e_1 in \mathcal{V} . Indeed for every point x^* in the relative interior of q the maxi-disk (D, φ) of $\varphi(x^*)$ can be realized so that x^* is the center of D , and so that φ agrees with $\varphi_0 \cup \varphi_1$ on $\overline{D} \cap (\overline{D}_0 \cup \overline{D}_1)$. Then $\varphi^{-1}(V)$ contains exactly the two endpoints of p , and so $\varphi(x^*)$ belongs to the relative interior of an edge of \mathcal{V} . This proves the claim, and the lemma. \square

10.10 Appendix: Computing the Delaunay tessellation

In this section we prove Proposition 10.3, which we restate for convenience:

Proposition 10.3. *Let T be a portalgon of n triangles, of happiness h , whose surface $\mathcal{S}(T)$ is closed. One can compute the portalgon of the Delaunay tessellation of $\mathcal{S}(T)$ in $O(n^2h \log(nh))$ time.*

Proposition 10.3 slightly extends known results, and is not surprising at all, but we provide proofs for completeness. Our strategy for computing the Delaunay tessellation is, classically, to first compute the Voronoi diagram:

Proposition 10.11. *Let T be a portalgon of n triangles, of happiness h . Let V be a set of vertices of T^1 . Assume that V is not empty and contains all singularities of $\mathcal{S}(T)$. We can compute in $O(n^2h \log(nh))$ time a portalgon T' of $O(n^2h)$ triangles, whose surface is $\mathcal{S}(T)$, and a subgraph \mathcal{V} of T'^1 , such that \mathcal{V} is the Voronoi diagram of $(\mathcal{S}(T), V)$.*

We will then derive the Delaunay tessellation of from the Voronoi diagram:

Proposition 10.12. *Let T be a portalgon of n triangles. Let V be a set of vertices of T^1 . Let \mathcal{V} be a subgraph of T^1 . Assume that V is not empty and contains all singularities of $\mathcal{S}(T)$, and that \mathcal{V} is the Voronoi diagram of $(\mathcal{S}(T), V)$. We can compute the portalgon of the Delaunay tessellation of $(\mathcal{S}(T), V)$ in $O(n)$ time.*

Proposition 10.11 and Proposition 10.12 will immediately imply Proposition 10.3:

Proof of Proposition 10.3, assuming Propositions 10.11 and 10.12. Let V contain the singularities of $\mathcal{S}(T)$, except if $\mathcal{S}(T)$ is a flat torus in which case let V contain a single arbitrary vertex of T^1 . Apply Proposition 10.11 to replace T by a portalgon T' of $O(n^2h)$ triangles, and to compute a subgraph \mathcal{V} of T'^1 that is also the Voronoi diagram of $(\mathcal{S}(T), V)$, all in $O(n^2h \log(nh))$ time. Apply Proposition 10.12 to derive from T' and \mathcal{V} the portalgon of the Delaunay tessellation of $(\mathcal{S}(T), V)$ in $O(n^2h)$ time. \square

All there remains to do is to prove Proposition 10.11 and Proposition 10.12. We prove Proposition 10.12 in Section 10.10.1, and we prove Proposition 10.11 in Section 10.10.2.

10.10.1 Computing the Delaunay tessellation from the Voronoi diagram

In this section we prove Proposition 10.12, which we restate for convenience:

Proposition 10.12. *Let T be a portalgon of n triangles. Let V be a set of vertices of T^1 . Let \mathcal{V} be a subgraph of T^1 . Assume that V is not empty and contains all singularities of $\mathcal{S}(T)$, and that \mathcal{V} is the Voronoi diagram of $(\mathcal{S}(T), V)$. We can compute the portalgon of the Delaunay tessellation of $(\mathcal{S}(T), V)$ in $O(n)$ time.*

In the setting of Proposition 10.12, our goal is to compute the portalgon of the Delaunay tessellation \mathcal{D} of $(\mathcal{S}(T), V)$. If we do not care about the shapes of the polygons in the portalgon, then we can easily compute this portalgon from the embedded graph \mathcal{V} , due to the duality between \mathcal{D} and \mathcal{V} (Lemma 10.29). All there remains to do is to compute the shape of each polygon in the portalgon. First we need a definition and a lemma. Consider a walk W in the dual of T^1 . To ease the reading assume that every edge of T^1 is incident to two distinct faces of T^1 ; the following definition extends in a straightforward manner to general triangulations. In the plane \mathbb{R}^2 realize the $k \geq 1$ faces visited by W isometrically, and respecting their orientation, by respective triangles $\Delta_1, \dots, \Delta_k$. Make sure that for every $1 \leq i < k$ the triangles Δ_i and Δ_{i+1} agree on the placement of the i -th edge of T^1 crossed by W . The resulting sequence $\Delta = (\Delta_1, \dots, \Delta_k)$ is an **unfolding** of W . In general a vertex w of T^1 may occur several times among the vertices of the triangles in Δ , and those occurrences may be at distinct points in the plane. Nevertheless:

Lemma 10.30. *If the faces of T^1 visited by W are all included in the same face of \mathcal{V} , and if $w \in V$, then all the occurrences of w in Δ are at the same point of \mathbb{R}^2 .*

Proof. Let F be the face of \mathcal{V} containing the faces of T^1 visited by W . By Lemma 10.28 the face F is homeomorphic to an open disk, and w is the unique point of $V \cap F$. Let \widehat{F} be the surface homeomorphic to a closed disk obtained by cutting the closure of F along the boundary of F . The angles at the corners of \widehat{F} are smaller than or equal to π by Lemma 10.28. So the shortest paths between those corners and w are, together with the boundary edges of \widehat{F} , the edges of a triangulation Y of \widehat{F} . The dual of Y is a cycle, and w is the central vertex of Y . If Δ is an unfolding of a walk in the dual of Y , then all occurrences of w in Δ are at the same point in the plane. This easily extends to every other triangulation Y' of \widehat{F} , by considering a triangulation of \widehat{F} that contains both Y and Y' . \square

In the portalgon of \mathcal{D} , consider a polygon P . We describe how to compute the positions of the vertices of P . Note that these positions are only defined up to translating and rotating P in the plane. As a preliminary, consider the vertex v of the Voronoi diagram \mathcal{V} that is dual to P . Embed a neighborhood of v in the plane \mathbb{R}^2 , isometrically and respecting the orientation, by embedding the faces of T^1 incident to v . This is possible since v is flat.

Assign to each vertex x of P a point $\pi_P(x) \in \mathbb{R}^2$ as follows. The vertex x of P is dual to an incidence c between the vertex v of \mathcal{V} and some face F of \mathcal{V} . In this incidence c , consider one of the faces W_0 of T^1 that we embedded in the plane, and its embedding W_0^* . Consider

the unique point $w \in V \cap F$ (Lemma 10.28). Consider a walk W in the dual of T^1 that starts with W_0 , remains in F , and visits at least one face of T^1 incident to w . Unfold the faces visited by W in the plane, starting from W_0^* . Let $\pi_P(x)$ be any occurrence of w in the unfolding.

Lemma 10.31. *Up to translating and rotating P , the assignment π_P maps each vertex of P to its position.*

Proof of Lemma 10.31. Consider the maxi-disk (D, φ) of v . Without loss of generality φ agrees with the embedding of the neighborhood of v that we fixed as a preliminary. Recall from the definition of the Delaunay tessellation that P is the convex hull of $\varphi^{-1}(V)$. Let v^* be the middle point of D (the embedding of v). The points in $\varphi^{-1}(V)$ correspond to the incidences between v and the faces of \mathcal{V} around v . Consider such an incidence c , and its corresponding point $y \in \varphi^{-1}(V)$. Consider also the face F of \mathcal{V} that contains c . The geodesic path p from v^* to y projects via φ to a shortest path $\varphi \circ p$ from v to V . And $\varphi \circ p$ immediately enters F after leaving v . So $\varphi \circ p$ is relatively included in F , and thus ends at the unique point $w \in V \cap F$. By slightly perturbing p without changing its endpoints we may ensure that $\varphi \circ p$ corresponds to a walk in the dual of T^1 . Then $y = \pi_P(x)$ by Lemma 10.30. This proves the lemma. \square

Proof of Proposition 10.12. We must compute the portalgon of the Delaunay tessellation \mathcal{D} of (S, V) . We immediately compute the combinatorics of the portalgon from \mathcal{V} , since \mathcal{V} is isomorphic to the dual of \mathcal{D} by Lemma 10.29.

Now, by Lemma 10.31, all there remains to do is to compute, for each polygon P of the portalgon, the assignment π_P of positions for the vertices of P . Achieving the claimed linear running time when doing so requires a slight technicality. Consider a face F of \mathcal{V} , and the point $w \in V \cap F$. Recall that for some faces W_0 of T^1 included in F we need to construct a walk W from W_0 to w in the dual of T^1 , unfold W , and retain the relative positions of some occurrences of W_0 and w in the unfolding. Doing so independently for every face W_0 may take too long as we would visit faces of T^1 several times. Instead we consider a single spanning tree Y in the dual of T^1 within F , we unfold the faces of T^1 that are included in F along Y , and we retrieve all the required information from this unfolding. Note that the choice of Y does not matter, and that the unfolding may overlap. Doing so for all faces F of \mathcal{V} takes linear time. \square

10.10.2 Computing the Voronoi diagram

In this section we prove Proposition 10.11, which we restate for convenience:

Proposition 10.11. *Let T be a portalgon of n triangles, of happiness h . Let V be a set of vertices of T^1 . Assume that V is not empty and contains all singularities of $\mathcal{S}(T)$. We can compute in $O(n^2 h \log(nh))$ time a portalgon T' of $O(n^2 h)$ triangles, whose surface is $\mathcal{S}(T)$, and a subgraph \mathcal{V} of T'^1 , such that \mathcal{V} is the Voronoi diagram of $(\mathcal{S}(T), V)$.*

To prove Proposition 10.11 we revisit the single source shortest path algorithm described by Löffler, Ophelders, Silveira, and Staals [141]. In particular we extend their algorithm to multiple sources. The authors consider a triangulated surface, and compute the shortest paths emanating from a point x_0 on the surface by decomposing the surface according to how those paths visit the faces of the triangulation. They describe a discrete process that

simulates the propagation of some waves on the surface. Their waves all start from the point x_0 . In the setting of Proposition 10.11, we adapt this strategy to simulate waves on $\mathcal{S}(T)$ that start from all the points in V , so that the waves meet along the Voronoi diagram \mathcal{V} of $(\mathcal{S}(T), V)$. That simplifies the algorithm since waves now meet along a graph with geodesic edges (Lemma 10.28) and do not go through singularities. We now provide a formalization of this *wave algorithm*. The continuous propagation of waves is discretized by a propagation of *events*. A crucial feature of our formalization of the algorithm is that it operates on triangles, point sets, and Voronoi diagrams *in the plane* \mathbb{R}^2 , never in the surface $\mathcal{S}(T)$. Only the proofs of correctness will argue on the surface $\mathcal{S}(T)$. We will insist on that.

Recall that the triangles of the input portalgon T lie in the Euclidean plane \mathbb{R}^2 , and they are disjoint. The reader can think of them as being very far away from each other if this helps the reading. The data structure maintains, for every triangle Δ of T , a set X_Δ of points in \mathbb{R}^2 . We insist, again, that all these objects lie *in the plane* \mathbb{R}^2 , not in the surface $\mathcal{S}(T)$.

We need a definition. Given $X \subset \mathbb{R}^2$ finite and $x \in X$ we denote by $\text{Vor}(x, X)$ the closed cell of x in the Voronoi diagram of X in \mathbb{R}^2 . Formally, $\text{Vor}(x, X)$ contains the points $y \in \mathbb{R}^2$ such that the distance between x and y is smaller than or equal to the distance between x' and y for every $x' \in X$.

Central to the wave algorithm is the notion of candidate event that we now define. Consider a triangle Δ of T , a side s of Δ , a point $x \in \mathbb{R}^2$, and some $t > 0$. The surface $\mathcal{S}(T)$ being closed, there are a triangle Δ' of T and a side s' of Δ' such that s is matched to s' . Consider the orientation-preserving isometry of \mathbb{R}^2 that maps s to s' and puts Δ side-by-side with Δ' , apply this isometry to x , and consider the resulting point $x' \in \mathbb{R}^2$. The tuple (t, Δ, s, x) is a **candidate event** if it satisfies each of the following. First, $x \notin X_\Delta$ and $x' \in X_{\Delta'}$. Second, the intersection between $\text{Vor}(x', X_{\Delta'})$ and s' is not empty, and its distance to x' is equal to t . In other words, t is equal to the smallest distance between x' and a point of $\text{Vor}(x', X_{\Delta'}) \cap s'$. We say that t is the **date** of the candidate event (t, Δ, s, x) .

The data structure additionally maintains a list of the candidate events sorted by date.

WAVE ALGORITHM: Initialize for each triangle Δ of T the set X_Δ with the vertices of Δ that correspond to points in V , if any. Then, as long as possible, consider any candidate event (t, Δ, s, x) of smallest date t , add x to X_Δ , and repeat. In the end return the sets $(X_\Delta)_\Delta$.

Again, we insist that the wave algorithm operates *in the plane* \mathbb{R}^2 . In particular the sets X_Δ are subsets of \mathbb{R}^2 . Nevertheless, their Voronoi diagrams are related to the Voronoi diagram of V on the surface $\mathcal{S}(T)$, and more strongly:

Proposition 10.13. *The wave algorithm terminates after $O(n^2 h)$ iterations. In the end, for every triangle Δ of T , the intersection with Δ of the Voronoi diagram of X_Δ in \mathbb{R}^2 is the pre-image in Δ of the Voronoi diagram of V in $\mathcal{S}(T)$.*

It is easy to compute the list of the candidate events from the sets $(X_\Delta)_\Delta$ in polynomial time. More strongly:

Proposition 10.14. *We can maintain the list of candidate events sorted by date through k insertions of points in the sets $(X_\Delta)_\Delta$ in $O(k \log k)$ total time.*

Proposition 10.11 is immediate from Proposition 10.13 and Proposition 10.14:

Proof of Proposition 10.11. Proposition 10.13 and Proposition 10.14 imply that the wave algorithm can be performed in $O(n^2 \cdot h \cdot \log(nh))$ time. Consider the returned sets $(X_\Delta)_\Delta$. The sum of the cardinalities of the sets X_Δ , summed over all the triangles Δ of T , is $O(n^2h)$ by Proposition 10.13. Also, for every triangle Δ , the intersection with Δ of the Voronoi diagram of X_Δ in \mathbb{R}^2 is the pre-image in Δ of the Voronoi diagram of V in $\mathcal{S}(T)$, by Proposition 10.13. Cutting each triangle Δ along the Voronoi diagram of X_Δ , and cutting the resulting polygons into triangles along vertex-to-vertex arcs, provides the desired triangular portalgon T' , along with \mathcal{V} . \square

The rest of this section is dedicated to the proofs of Proposition 10.13 and Proposition 10.14.

10.10.2.1 Proof of Proposition 10.13

In this section we prove Proposition 10.13. Recall that the triangles of the portalgon T are realized dis-jointly in the Euclidean plane \mathbb{R}^2 , and that we think of these triangles as being very far away from each other, this will help the reading. It is now convenient to introduce a notation for the projection of this disjoint union of triangles onto the surface $\mathcal{S}(T)$, so we let ρ be this projection.

Given a triangle Δ of T , we consider the immersed disks (D, φ) such that the center of D belongs to Δ , and such that φ agrees with ρ on $\overline{D} \cap \Delta$. We say that (D, φ) is an immersed disk **attached to** Δ . We further consider the union of the sets $\varphi^{-1}(V)$ over the immersed disks (D, φ) attached to Δ . We call this union the **constellation** of Δ , and we denote it by V_Δ . We will show that the sets X_Δ computed by the wave algorithm are exactly the constellations V_Δ . Before that, we have two preliminary lemmas on constellations.

First, the constellations, while lying *in the plane* \mathbb{R}^2 , are related to the Voronoi diagram of V *in the surface* $\mathcal{S}(T)$:

Lemma 10.32. *For every triangle Δ of T the intersection with Δ of the Voronoi diagram of the constellation V_Δ is the pre-image in Δ of the Voronoi diagram of V in $\mathcal{S}(T)$.*

The proof of Lemma 10.32 relies on the following, which will be used again:

Lemma 10.33. *Let (D, φ) be an immersed disk attached to a triangle Δ of T . Then $V_\Delta \cap \overline{D} = \varphi^{-1}(V)$. In particular $V_\Delta \cap D = \emptyset$.*

Proof. We have $V_\Delta \cap \overline{D} \supseteq \varphi^{-1}(V)$ by definition of the constellation V_Δ . The other inclusion is immediate from the fact that if two immersed disks (D, φ) and (D', φ') are attached to Δ then φ and φ' agree on $\overline{D} \cap \overline{D'}$. Finally $\varphi^{-1}(V) \cap D = \emptyset$ by definition of an immersed disk (recall that D is open). \square

Proof of Lemma 10.32. Consider a point $x \in \Delta$. There is a unique immersed disk (D, φ) attached to Δ such that the center of D is x , and such that the radius of D is maximum. Then $\varphi^{-1}(V) \neq \emptyset$ since the radius of D is maximum. And $\varphi^{-1}(V) = V_\Delta \cap \overline{D}$ by Lemma 10.33. The geodesic path(s) between x and the point(s) in $\varphi^{-1}(V)$ corresponds via φ to the shortest path(s) between $\rho(x)$ and V . So $\rho(x)$ belongs to the Voronoi diagram of V in $\mathcal{S}(T)$ if and only if $\varphi^{-1}(V)$ contains several points, equivalently $V_\Delta \cap \overline{D}$, which is the case if and only if x belongs to the Voronoi diagram of V_Δ in \mathbb{R}^2 . \square

Second, the cardinalities of the constellations are bounded by the number n of triangles and the happiness h of the portalgon T :

Lemma 10.34. *For every triangle Δ of T the constellation V_Δ has cardinality $O(nh)$.*

Proof. Given a triangle Δ of T , and a point x in the constellation V_Δ , there is by definition an immersed disk (D, φ) attached to Δ such that $x \in \varphi^{-1}(V)$. And the center y of D belongs to Δ . Then the geodesic segment between y and x projects via ρ to a path between $\rho(y)$ and $\rho(x)$, and the length of this path is the smallest possible among all the paths between $\rho(y)$ and a point of V (possibly another point of V than $\rho(x)$). We will argue on such shortest paths between a point of $\mathcal{S}(T)$ and the set V .

We call regions the following subsets of $\mathcal{S}(T)$: a vertex of T^1 , the relative interior of an edge of T^1 , and a face of T^1 . The regions partition $\mathcal{S}(T)$. For every shortest path p between a point $x \in \mathcal{S}(T)$ and the set V , record the sequence of regions intersected by p when directed from V to x . If two such paths p and p' end in $\rho(\Delta)$ and have the same sequence then they correspond to the same point in the constellation V_Δ . We claim that for every region R there are $O(nh)$ sequences ending with R . This claim implies the lemma. Let us prove the claim. We say that a sequence is maximal if it is not a strict prefix of another sequence. And we say that a sequence is critical if it is the maximal common prefix of two distinct maximal sequences. Every critical sequence ends with a face of T^1 . For every face R' of T^1 there is at most one critical sequence ending with R' . Indeed every critical sequence is realized by two distinct paths. If two distinct critical sequences were to end with R' , then at least two of the four associated paths would cross, and thus could be shortened, a contradiction. We proved that there are $O(n)$ critical sequences. So there are $O(n)$ maximal sequences. And every sequence contains $O(h)$ occurrences of R since the happiness of T is equal to h . This proves the claim, and the lemma. \square

We will now show that the wave algorithm computes the constellations. To do so, we introduce an invariant. We need a definition. Fix a point $x \in V_\Delta$, and consider all the immersed disks (D, φ) attached to Δ such that $x \in \varphi^{-1}(V)$. Among all these immersed disks (D, φ) , the smallest radius of D is the **depth** of x in V_Δ .

INVARIANT: There is $\tau > 0$ such that both of the following hold for every triangle Δ of T . Every point of X_Δ belongs to the constellation V_Δ . And every point of $V_\Delta \setminus X_\Delta$ has depth greater than or equal to τ in V_Δ .

It is not clear a priori that the invariant is maintained by the wave algorithm, and this will be proved only at the very end, when proving Proposition 10.13. Before that we need some lemmas.

Lemma 10.35. *Assume that the invariant holds for some $\tau > 0$, and that there is a candidate event (t, Δ, s, x) such that $t \leq \tau$. Then $t = \tau$, x belongs to V_Δ , and the depth of x in V_Δ is equal to τ .*

Proof. We claim that $x \in V_\Delta$, and that the depth of x in V_Δ is smaller than or equal to t . The claim implies the lemma. Indeed we assumed $t \leq \tau$. And, if $x \in V_\Delta$, then the depth of x in V_Δ cannot be smaller than τ , for otherwise the invariant would imply $x \in X_\Delta$, contradicting the fact that (t, Δ, s, x) is a candidate event. All there remains to do is to prove the claim.

To do so consider the triangle Δ' of T and the side s' of Δ' such that s is matched to s' . Consider the orientation-preserving isometry of \mathbb{R}^2 that maps s to s' and puts Δ side-by-side with Δ' , apply this isometry to x , and consider the resulting point $x' \in \mathbb{R}^2$. Using the assumption that (t, Δ, s, x) is a candidate event, the point x' belongs to $X_{\Delta'}$, while x does not belong to X_Δ . Moreover there is a point z' along s' such that x' is at distance t from z' , and such that no point of $X_{\Delta'}$ is closer to z' than x' . Consider the immersed disk (D', φ') attached to Δ' such that the center of D' is z' , and such that the radius of D' is maximum.

By contradiction, assume that the radius of D' is smaller than t . There is a point $v \in \varphi'^{-1}(V)$ since the radius of D' is maximum. We have $v \in V_{\Delta'}$, and the depth of v in $V_{\Delta'}$ is smaller than or equal to the radius of D' , which is smaller than τ . So v belongs to $X_{\Delta'}$ by the invariant. But then v is a point of $X_{\Delta'}$ closer to z' than x' , a contradiction.

We proved that the radius of D' is greater than or equal to t . Then x' belongs to \overline{D} . Moreover x' belongs to $X_{\Delta'}$, and thus to $V_{\Delta'}$ by the invariant. Therefore x' belongs to $\varphi'^{-1}(V)$ by Lemma 10.33. In particular the radius of D' is *equal* to t .

It is now convenient to name the orientation-preserving isometry of \mathbb{R}^2 that maps s to s' and puts Δ side-by-side with Δ' , so let $\lambda : \mathbb{R}^2 \rightarrow \mathbb{R}^2$ be this isometry. Consider the point $z = \lambda^{-1}(z')$, and the immersed disk (D, φ) attached to Δ such that the center of D is z , and such that the radius of D is maximum. Observe that $\lambda(D) = D'$, and that $\varphi' \circ \lambda = \varphi$. In particular the radius of D is also t . And, crucially, $x \in \varphi^{-1}(V)$, since we already proved $x' \in \varphi'^{-1}(V)$. This proves that $x \in V_\Delta$. And the depth of x in V_Δ is smaller than or equal to the radius of D , which is t . The claim is proved, along with the lemma. \square

Lemma 10.36. *Assume that the invariant holds for some $\tau > 0$. Further assume that there is a triangle Δ of T such that $V_\Delta \setminus X_\Delta$ contains a point whose depth in V_Δ is τ . Then there is a candidate event whose date is smaller than or equal to τ .*

The proof of Lemma 10.36 relies on the following:

Lemma 10.37. *Let (D, φ) be an immersed disk attached to a triangle Δ of T . Assume that there is $x \in \varphi^{-1}(V)$, and let y be the center of D . If the geodesic segment between x and y intersect Δ in any other point than y then the depth of x in V_Δ is smaller than the radius of D .*

Proof. Assuming that the geodesic segment between x and y intersects Δ in a point $y' \neq y$ (at least), consider the open disk D' whose center is y' and whose boundary circle contains x' . Then $D' \subset D$. Let φ' be the restriction of φ to \overline{D}' . Then (D', φ') is an immersed disk, φ' agrees with ρ on $\Delta \cap \overline{D}'$, and $x \in \varphi'^{-1}(V)$. So the depth of x in V_Δ is smaller than or equal to the radius of D' , which is smaller than the radius of D . \square

Proof of Lemma 10.36. Consider a point $x \in V_\Delta \setminus X_\Delta$ that has depth τ in V_Δ . There is an immersed disk (D, φ) that satisfies each of the following. Let y be the center of D . Then y belongs to Δ , the radius of D is τ , φ agrees with ρ on $\overline{D} \cap \Delta$, and $x \in \varphi^{-1}(V)$. In top of that we can add that y belongs to the boundary of Δ , for otherwise the depth of x in V_Δ would be smaller than τ by Lemma 10.37, a contradiction. There are two cases: either y lies in the relative interior of a side of Δ , or y is a vertex of Δ .

First case First consider the case where y lies in the relative interior of a side s of Δ . In this case we shall prove that there is $t \leq \tau$ such that (t, Δ, s, x) is a candidate event. The

surface $\mathcal{S}(T)$ being closed, there are a triangle Δ' of T , and a side s' of Δ' , such that s is matched to s' . Consider the orientation-preserving isometry $\lambda : \mathbb{R}^2 \rightarrow \mathbb{R}^2$ that maps s to s' and puts Δ side-by-side with Δ' . We consider the points $x' = \lambda(x)$ and $y' = \lambda(y)$, the open disk $D' = \lambda(D)$, and the map $\varphi' = \varphi \circ \lambda^{-1}$. Observe that (D', φ') is an immersed disk attached to Δ' , that the center of D' is y' , and that x' belongs to the boundary circle of D' . Informally, x' , y' , and (D', φ') correspond to x , y , and (D, φ) , but in the reference frame of Δ' .

We claim that x' belongs to $X_{\Delta'}$. To prove the claim consider the geodesic line L supported by s , and direct L so that Δ is on the *right* of L . Similarly, consider the geodesic line $L' = \lambda(L)$. Then L' is supported by s' , and Δ' is on the *left* of L' . We have that x lies strictly on the left of L , for otherwise the depth of x in V_Δ would be smaller than τ by Lemma 10.37, a contradiction. So x' lies (strictly) on the left of L' . And so the depth of x' in $V_{\Delta'}$ is smaller than τ by Lemma 10.37. Therefore $x' \in X_{\Delta'}$ by the invariant. The claim is proved.

We use the claim immediately, x' belongs to $X_{\Delta'}$. No point of $X_{\Delta'}$ is closer to y' than x' , since $X_{\Delta'} \subseteq V_{\Delta'}$ by the invariant, and since $D' \cap V_{\Delta'} = \emptyset$ by Lemma 10.33. So $\text{Vor}(x', X_{\Delta'})$ intersects s' (at least in y'), and its intersection with s' is at distance a distance $t \leq \tau$ from x' (since the distance between y' and x' is τ). The tuple (t, Δ, s, x) is a candidate event. We are done in this case.

Second case. Now consider the case where y is a vertex of Δ . Then $\rho(y)$ is a vertex of the graph T^1 embedded on $\mathcal{S}(T)$. Note also that $\rho(y)$ lies in the interior of $\mathcal{S}(T)$ since $\mathcal{S}(T)$ has no boundary. And $\rho(y)$ is flat as it does not belong to V . We assume that no face of T^1 appears twice around y , for this eases the reading, and the proof trivially extends to the general case. Consider the $k \geq 3$ faces of T^1 incident to $\rho(y)$, in order around $\rho(y)$ (clockwise say, but counter-clockwise would do too), and the corresponding triangles $\Delta_0, \dots, \Delta_{k-1}$ of T , with $\Delta_0 = \Delta$. We fix Δ_0 , and we place copies of the triangles $\Delta_1, \dots, \Delta_{k-1}$ around y , in order. This is possibly since $\rho(y)$ is flat. For each i we record the orientation-preserving isometry $\lambda_i : \mathbb{R}^2 \rightarrow \mathbb{R}^2$ that maps the copy of Δ_i around y to the original triangle Δ_i . We consider the points $x_i = \lambda_i(x)$ and $y_i = \lambda_i(y)$. Also we consider the open disk $D_i = \lambda_i(D)$ and the map $\varphi_i = \varphi \circ \lambda_i^{-1}$. Observe that (D_i, φ_i) is an immersed disk attached to Δ_i , that the center of D_i is y_i , and that x_i belongs to the boundary circle of D_i . Informally, x_i , y_i , and (D_i, φ_i) correspond to x , y , and (D, φ) , but in the reference frame of Δ_i .

We claim that there is i such that $x_i \in X_{\Delta_i}$. Indeed there is i such that the geodesic segment between y and x intersects the copied triangle $\lambda_i^{-1}(\Delta_i)$ in another point than y . Then the geodesic segment between y_i and x_i intersects Δ_i in another point than y . So x_i belongs to V_{Δ_i} and has depth smaller than τ in V_{Δ_i} , by Lemma 10.37 applied to Δ_i , (D_i, φ_i) , x_i , and y_i . And so $x_i \in X_{\Delta_i}$ by the invariant. The claim is proved.

Using the claim immediately, and since $x_0 \notin X_{\Delta_0}$, there is i such that $x_i \in X_{\Delta_i}$ and $x_{i+1} \notin X_{\Delta_{i+1}}$, indices are modulo k . Consider the side s_i of Δ_i that is matched to a side of Δ_{i+1} . We shall prove that there is $t \leq \tau$ such that $(\tau, \Delta_i, s_i, x_i)$ is a candidate event. To do so first observe that no point of X_{Δ_i} is closer to y_i than x_i since $X_{\Delta_i} \subseteq V_{\Delta_i}$ by the invariant, and since $D_i \cap V_{\Delta_i} = \emptyset$ by Lemma 10.33. So $\text{Vor}(x_i, X_{\Delta_i})$ intersects s_i (at least in y_i), and its intersection with s_i is at a distance $t \leq \tau$ from x_i (since the distance between y_i and x_i is τ). The tuple (t, Δ_i, s_i, x) is a candidate event. We are done in this case. The lemma is proved. \square

Proposition 10.13. First we prove that the invariant holds throughout the execution of the wave algorithm. To prove the claim first observe that the invariant holds after the initialization phase. Now assume that it holds at the beginning of an iteration of the loop, for some $\tau > 0$, and that there is a candidate event (t, Δ, s, x) , of smallest date t . If every triangle Δ of T satisfies $X_\Delta = V_\Delta$ then the invariant holds for every $\tau > 0$ anyway. Otherwise there are without loss of generality a triangle Δ and a point in $V_\Delta \setminus X_\Delta$ whose depth in V_Δ is τ , so there is a candidate event whose date is smaller than or equal to τ by Lemma 10.36. In any case $t \leq \tau$ holds without loss of generality. Then $t = \tau$, x belongs to V_Δ , and the depth of x in V_Δ is equal to τ by Lemma 10.35. So, after adding x to X_Δ , the invariant still holds. This proves that the invariant holds throughout the execution of the wave algorithm.

The wave algorithm never adds twice the same point in a set X_Δ of a triangle Δ of T . Moreover $X_\Delta \subseteq V_\Delta$ by the invariant. And the cardinality of V_Δ is $O(nh)$ by Lemma 10.34. So the wave algorithm terminates after $O(n^2h)$ iterations. The algorithm does not stop until $X_\Delta = V_\Delta$ for every triangle Δ of T , by Lemma 10.36. And the sets $(V_\Delta)_\Delta$ are as desired by Lemma 10.32. The lemma is proved. \square

10.10.2.2 Proof of Proposition 10.14

In this section we prove Proposition 10.14, that during the wave algorithm the list of the candidate events sorted by date can be maintained in amortized $O(\log(nh))$ time per insertion of a point in the set X_Δ of a triangle Δ .

The crux of the matter is to maintain the intersection of a Voronoi diagram in \mathbb{R}^2 with a closed segment of \mathbb{R}^2 in a dynamic manner while adding the sources one-by-one to the Voronoi diagram. To do that we consider a game that we play with Alice. Informally, Alice sends us the sources of the Voronoi diagram one-by-one, and we tell her what is changed after each insertion of a source. Formally, Alice initially sends us a closed segment I of \mathbb{R}^2 . Then Alice sends us $k \geq 1$ pairwise distinct points $z_1, \dots, z_k \in \mathbb{R}^2$ in this order. We do not know the points before they are sent to us by Alice, nor the number of points to be sent. For each $i \in [k]$, after the i -th point z_i is sent to us by Alice, and before $i+1$ -th point z_{i+1} is sent to us, we must send two things to Alice. First, we must send the set $U_i \subseteq [i]$ containing the index i together with the indices $j \in [i-1]$ such that $\text{Vor}(z_j, Z_i) \cap I \neq \text{Vor}(z_j, Z_{i-1}) \cap I$. Second, for each index $j \in U_i$, we must send the (possibly empty) set $\text{Vor}(z_j, Z_i) \cap I$. Note that each set $\text{Vor}(z_j, Z_i) \cap I$ is a closed segment of \mathbb{R}^2 , so it is either empty, a single point, or has two distinct endpoints by which it is uniquely determined. We have two lemmas:

Lemma 10.38. *The sum over $1 \leq i \leq k$ of the cardinality of the set U_i is smaller than or equal to $5k$.*

Proof. Consider $i \in [k]$. We claim that at most four indices $j \in U_i$ are such that $\text{Vor}(z_j, Z_i)$ intersects I . The claim immediately implies the lemma.

To prove the claim we consider the subset Y of I that contains the points that are strictly closer to z_i than to any point of Z_{i-1} . And we consider the closure X of Y . Then X is a closed segment of \mathbb{R}^2 and, assuming that U_i is not empty, we have that Y is not empty, so X is not empty, and X is not a single point either. Informally, we now consider the two “ends” of X . Formally, we consider the two endpoints x_0 and x_1 of X , and for each $\varepsilon \in \{0, 1\}$, we consider an arbitrarily short closed segment $X_\varepsilon \subset X$, not a single point, that contains x_ε . Provided X_ε is short enough, there are no more than two indices $j \in U_i$ such that the relative interior of X_ε is included in $\text{Vor}(z_j, Z_{i-1})$.

On the other hand if $j \in U_i$ is such that $\text{Vor}(z_j, Z_i)$ intersects I , then not only $\text{Vor}(z_j, Z_{i-1})$ also intersects I , but $\text{Vor}(z_j, Z_{i-1}) \cap I$ contains a point in Y and a point not in Y , so it contains the relative interior of X_ε for some $\varepsilon \in \{0, 1\}$. This proves the claim, and the lemma. \square

Lemma 10.39. *There is an algorithm that receives I and z_1, \dots, z_k in this order, and that, after receiving z_i , $i \in [k]$, returns U_i together with the closed segments $\text{Vor}(z_j, Z_i) \cap I$ for all $j \in U_i$, and runs in $O(k \log k)$ total time.*

Proof. Consider $i \in [k]$, and assume that the point z_i has just been sent by Alice. We must return to Alice. The crux of the matter is to have maintained at this point the list of tuples $(j, \text{Vor}(z_j, Z_{i-1}) \cap I)$ over $j \in [i - 1]$, ordered by the position of $\text{Vor}(z_j, Z_{i-1}) \cap I$ along I (for some direction of I , and resolving any ambiguity arbitrarily). Now we can use the list to answer Alice, and update the list, as follows. Given a tuple $(j, \text{Vor}(z_j, Z_{i-1}) \cap I)$ we can determine in constant time whether $j \in U_i$ by checking whether there is a point of $\text{Vor}(j, Z_{i-1}) \cap I$ that is strictly closer to z_i than to z_j . If $j \notin U_i$, then either all the tuples $(j', \text{Vor}(z_{j'}, Z_{i-1}) \cap I)$ before $(j, \text{Vor}(z_j, Z_{i-1}) \cap I)$ in the list are such that $j' \notin U_i$, or all the tuples after $(j, \text{Vor}(z_j, Z_{i-1}) \cap I)$ are like that, and we can find out which case it is in constant time. So we can list by dichotomy the $k' \geq 0$ tuples $(j, \text{Vor}(z_j, Z_{i-1}) \cap I)$ such that $j \in U_i$ in $O(k' + \log k)$ time. For each such tuple $(j, \text{Vor}(z_j, Z_{i-1}) \cap I)$, we derive $\text{Vor}(z_j, Z_i) \cap I$ from $\text{Vor}(z_j, Z_{i-1})$, z_j , and z_i in constant time. In the end we compute $\text{Vor}(z_i, Z_i) \cap I$ in $O(\log k)$ time by finding by dichotomy the first and last tuples $(j, \text{Vor}(z_j, Z_{i-1}) \cap I)$ such that $\text{Vor}(z_j, Z_{i-1}) \cap I$ contains a point that is at least as close to z_i than to z_j , if any. This way we can return to Alice, and update the list of tuples, in $O(k' + \log k)$ total time. Lemma 10.38 concludes. \square

In the following, when maintaining the list of candidate events, we also maintain appropriate search trees in which we store the candidate events, so that the candidate events can be accessed by date or position in logarithmic time.

Proof of Proposition 10.14. When inserting a point x in the set X_Δ of a triangle Δ , we maintain the list of candidate events sorted by date as follows. First, we find the candidate events of the form $(\cdot, \Delta, \cdot, x)$, and we remove these candidate events from the list. All but $O(\log k)$ of the time spent here is amortized by the fact that every event deleted here was created earlier in the execution of the algorithm.

Second, for every side s of Δ , we consider the triangle Δ' and the side s' of Δ' such that s is matched to s , along with the orientation-preserving isometry $\lambda : \mathbb{R}^2 \rightarrow \mathbb{R}^2$ that maps s to s' and puts $\lambda(\Delta)$ and Δ' side by side. Among the candidate events of the form $(\cdot, \Delta', s', \lambda(y))$, $y \in X_\Delta$, those for which $\text{Vor}(y, X_\Delta \cup \{x\}) \cap s \neq \text{Vor}(y, X_\Delta) \cap s$ may have to be updated. If $\text{Vor}(y, X_\Delta \cup \{x\}) \cap s = \emptyset$, then the event must be deleted. Otherwise, only the date of the event may change. This is done in amortized $O(\log k)$ time using Lemma 10.39.

Finally, Lemma 10.39 also provides us with the set $\text{Vor}(x, X_\Delta \cup \{x\}) \cap s$. If this set is not empty, and if $\lambda(x) \notin X_{\Delta'}$, then we consider the distance t between x and $\text{Vor}(x, X_\Delta \cup \{x\}) \cap s$, and we create the event $(t, s', \Delta', \lambda(x))$, in $O(\log k)$ time. \square

Chapter 11

Bounds for Delaunay Flips on Flat Tori

In this chapter we prove Theorem 8.3, which we restate for convenience:

Theorem 8.3. *Let \mathbb{T} be a flat torus. Let T be a triangulation of \mathbb{T} , with n vertices, of maximum edge length L . Every sequence of Delaunay flips starting from T has length at most $C \cdot n^2 \cdot L$, where $C > 0$ depends only on \mathbb{T} . This bound is tight up to a constant factor.*

We provide some background in Section 11.1, prove the lower bound in Section 11.2, and prove the upper bound in Section 11.3, thereby obtaining Theorem 8.3.

11.1 Background: stereographic projection

In this chapter we denote by $\ell(p)$ the length of a geodesic path p . Given $d \geq 1$, we denote by \mathbb{R}^d the usual d -dimensional Euclidean space. We will use the following classical construction. We identify \mathbb{R}^2 with the plane of \mathbb{R}^3 containing the points whose third coordinate is 1. In \mathbb{R}^3 we consider the 2-dimensional sphere \mathbb{S}_2 of radius 1 centered at $(0, 0, 0)$. The point $P = (0, 0, -1)$ belongs to \mathbb{S}_2 . Given $\tilde{p} \in \mathbb{R}^2$ we denote by $I_{\tilde{p}}$ the unique geodesic line of \mathbb{R}^3 containing the points \tilde{p} and P (Figure 11.2). The correspondence $\pi : \mathbb{R}^2 \rightarrow \mathbb{S}_2 \setminus \{P\}$ that maps every point $\tilde{p} \in \mathbb{R}^2$ to the unique intersection of the line $I_{\tilde{p}}$ with $\mathbb{S}_2 \setminus \{P\}$ is called the **stereographic projection**, it is one-to-one.

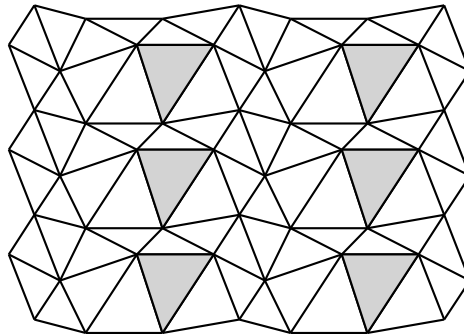


Figure 11.1: A portion of the lift of a Delaunay triangulation of a flat torus in the Euclidean plane \mathbb{R}^2 . (Gray) Six lifts of a single face.

We identify every flat torus with a quotient \mathbb{T}_Γ of \mathbb{R}^2 by the action of a group Γ generated by two linearly independent translations. We associate to every triangulation T of \mathbb{T}_Γ a

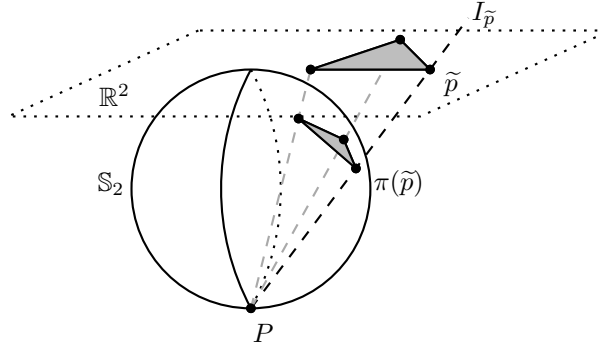


Figure 11.2: Mapping a triangulation of a flat torus to a stereographic surface.

surface $S \subset \mathbb{R}^3$ as follows. We consider the infinite triangulation \tilde{T} that lifts T in \mathbb{R}^2 . For every triangle \tilde{t} of \tilde{T} , we consider the three vertices \tilde{v}_1, \tilde{v}_2 and \tilde{v}_3 of \tilde{t} , and the convex hull in \mathbb{R}^3 of their image points $\pi(\tilde{v}_1), \pi(\tilde{v}_2)$, and $\pi(\tilde{v}_3)$. The union of those convex hulls, over all the triangles of \tilde{T} , is the surface S . We say that S is the **stereographic surface** associated to T . We emphasize that S shares no point with \mathbb{S}_2 other than the image points of the vertices of \tilde{T} . There is a one-to-one correspondence $\pi_S : \mathbb{R}^2 \rightarrow S$ sending every $\tilde{p} \in \mathbb{R}^2$ to the unique intersection with S of the line $I_{\tilde{p}}$. Given two stereographic surfaces S and S' (possibly with $S = S'$) we say that S is **above** S' if for every $\tilde{p} \in \mathbb{R}^2$ the point $\pi_{S'}(\tilde{p})$ lies on the closed segment $[P, \pi_S(\tilde{p})]$ of \mathbb{R}^3 , on the line $I_{\tilde{p}}$. The above-below relation is a partial order on the set of stereographic surfaces. We will use the following:

Lemma 11.1. *Assume that a triangulation T of a flat torus \mathbb{T}_Γ results from the Delaunay flip of an edge e' in a triangulation T' of \mathbb{T}_Γ and let e be the edge of T resulting from the flip. Let S and S' be the stereographic surfaces associated to T and T' , respectively. Then S is above S' . Let also $p \in \mathbb{T}_\Gamma$ be the intersection point of the relative interiors of e and e' and $\tilde{p} \in \mathbb{R}^2$ be any lift of p . Then $\pi_S(\tilde{p}) \neq \pi_{S'}(\tilde{p})$.*

Lemma 11.1 is folklore and follows from the fact that every circle on \mathbb{R}^2 is mapped under the stereographic projection to a circle on $\mathbb{S}_2 \setminus P$: the intersection of $\mathbb{S}_2 \setminus P$ and a plane of \mathbb{R}^3 .

11.2 Lower bound

In this section we provide our lower bound. Beforehand, observe that on a flat torus \mathbb{T}_Γ the length of a sequence of Delaunay flips ending at a Delaunay triangulation cannot be bounded from above by a function depending only on the number of vertices of the starting triangulation. This fact follows from two observations. The first observation is that it is easy to construct an infinite set of triangulations of \mathbb{T}_Γ all having a single common vertex, say v , as their vertex set (Figure 11.3). The second observation is that there can only be a finite number of Delaunay triangulations of \mathbb{T}_Γ having v as their unique vertex¹.

¹The theorem of Pick [156] implies the existence of $D > 0$ depending only on \mathbb{T}_Γ such that in \mathbb{R}^2 every disk of diameter D intersects a lift of v . It follows that the edges of any Delaunay triangulation of \mathbb{T}_Γ with vertex set $\{v\}$ are not longer than D . There can only be a finite number of such edges.

To understand this phenomenon more precisely, we consider a second parameter of the starting triangulation T : the maximum length L of an edge in T . We will exhibit a particular family of starting triangulations T and prove a lower bound on the length of every sequence of Delaunay flips starting from T and ending at a Delaunay triangulation.

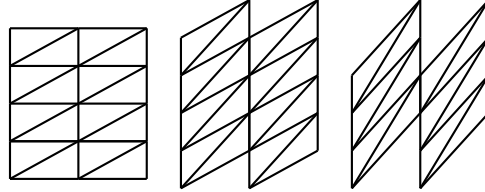


Figure 11.3: On a flat torus, three portions of the lifts of three triangulations with a single common vertex.

We are interested in a particular flat torus. Consider the two linearly independent translations by the vectors $(1, 0)$ and $(0, 1)$ respectively. We are interested in the flat torus \mathbb{T}_\square that is the quotient of \mathbb{R}^2 under the action of the group generated by those two translations. We denote by ρ_\square the projection map $\mathbb{R}^2 \rightarrow \mathbb{T}_\square$. We say that \mathbb{T}_\square is the **unit flat torus**. Then:

Proposition 11.1. *For every $n \geq 1$ and every $L_0 > 0$ there is a triangulation T of the unit flat torus \mathbb{T}_\square such that every sequence of Delaunay flips starting from T and ending at a Delaunay triangulation is longer than*

$$c \cdot n^2 \cdot L$$

where $L > L_0$ is the maximum length of an edge in T , n is the number of vertices of T , and $c > 0$ is a constant.

The quadratic dependency in the number of vertices is also a consequence of a more general fact about flips (not necessarily Delaunay flips) of triangulated polygons in the plane [119, Theorem 3.8]. Our construction is inspired from one previously known in that setting [119].

Proof. We fix $n \geq 1$ and $L_0 > 0$. See Figure 11.4.

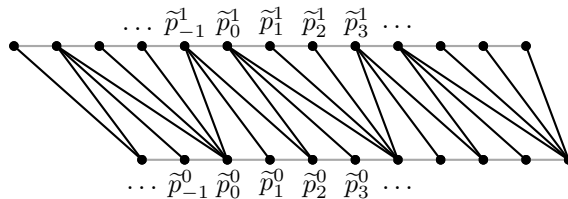


Figure 11.4: A portion of the lift of a triangulation belonging to \mathcal{F} in the proof of Proposition 11.1. The fixed edges are in gray.

For every $z \in \mathbb{Z}$ and every $\epsilon \in \{0, 1\}$ we define the point $\tilde{p}_z^\epsilon = (\frac{z}{n}, \epsilon)$ in \mathbb{R}^2 and the point p_z of \mathbb{T}_\square by $p_z = \rho_\square(\tilde{p}_z^0)$. Observe that if $z, z' \in \mathbb{Z}$ are such that $z \equiv z' \pmod{n}$ then $p_z = p_{z'}$ and the points $\tilde{p}_z^0, \tilde{p}_z^1, \tilde{p}_{z'}^0$, and $\tilde{p}_{z'}^1$ are all lifts of p_z . For every $z, z' \in \mathbb{Z}$, we define the segment $s_{z,z'}$ of \mathbb{T}_\square as $\rho_\square([\tilde{p}_z^0, \tilde{p}_{z'}^1])$.

We are interested in the set \mathcal{F} of the triangulations of \mathbb{T}_\square satisfying the following. The vertices of every triangulation $T \in \mathcal{F}$ are p_1, \dots, p_n and the edges of T are partitioned as follows: T contains n edges that we call **fixed** and $2n$ edges that we call **free**. For $k \in \{1, \dots, n\}$ the k^{th} fixed edge of T is $\rho_\square([\tilde{p}_{k-1}^0, \tilde{p}_k^0])$. The only restriction on the free edges of T is that they must belong to $\{s_{z,z'} : z, z' \in \mathbb{Z}\}$.

Claim 1. For every $T \in \mathcal{F}$ the following holds:

- (a) The fixed edges of T are not Delaunay-flippable.
- (b) The Delaunay flip of a free edge e in T results in a triangulation $T' \in \mathcal{F}$.
- (c) Such a Delaunay flip replaces the edge e in T by an edge e' in T' such that $l(e') \geq l(e) - 2/n$.
- (d) The lengths of two free edges of T cannot differ by more than 2.

Claim 2. There is a triangulation in \mathcal{F} having a free edge longer than L_0 .

Claim 3. There is a constant $L_1 > 0$ such that the edges of every Delaunay triangulation in \mathcal{F} are not longer than L_1 .

Claims 2 and 3 are straightforward. We will prove Claim 1 in the end. We first show that those claims imply the result. By Claim 2 there is a triangulation $T_0 \in \mathcal{F}$ having a free edge longer than L_0 . Let L denote the maximum length of an edge in T_0 ; L is the length of a free edge of T_0 . Indeed the free edges of T_0 have length at least 1 while the fixed edges of T_0 have length $1/n$.

We assign to every triangulation $T \in \mathcal{F}$ a weight $\omega(T)$ that is the sum of the lengths of its edges. By Claim 1.d, $\omega(T_0) \geq 1 + 2n(L - 2)$. Indeed T_0 has n fixed edges of length $1/n$ and $2n$ free edges of length at least $L - 2$.

Consider a sequence T_0, \dots, T_m of Delaunay flips for some $m \geq 0$ that starts from T_0 and ends at a Delaunay triangulation T_m . By Claims 1.a and 1.b all the triangulations T_0, \dots, T_m belong to \mathcal{F} . By Claim 1.c, holds $\omega(T_m) \geq \omega(T_0) - 2m/n$. By Claim 3 there is a constant $L_1 > 0$ such that $\omega(T_m) \leq 3nL_1$. Thus

$$2m \geq n(\omega(T_0) - \omega(T_m)) \geq n + (2L - 3L_1 - 4)n^2.$$

That proves the result. Now we prove Claim 1.

Proof of Claim 1. To prove (a) consider a fixed edge e of the triangulation T . There is some $k \in \{1, \dots, n\}$ such that the segment \tilde{e} of \mathbb{R}^2 between $\tilde{p}_{k-1}^0 = (\frac{k-1}{n}, 0)$ and $\tilde{p}_k^0 = (\frac{k}{n}, 0)$ is a lift of e . Consider the two faces \tilde{t}_1 and \tilde{t}_2 of the lift \tilde{T} of T that are incident to \tilde{e} . Let \tilde{v}_1 be the vertex of \tilde{t}_1 that is not a vertex of \tilde{t}_2 and let \tilde{v}_2 be the vertex of \tilde{t}_2 that is not a vertex of \tilde{t}_1 . Up to renaming \tilde{v}_1 and \tilde{v}_2 there are $z, z' \in \mathbb{Z}$ such that $\tilde{v}_1 = \tilde{p}_z^1 = (\frac{z}{n}, 1)$ and $\tilde{v}_2 = (\frac{z'}{n}, -1)$. It is straightforward to check that the open disk whose boundary contains $\tilde{p}_{k-1}^0, \tilde{p}_k^0$, and \tilde{v}_1 does not contain \tilde{v}_2 .

To prove (b) and (c) consider a free edge e of the triangulation T and assume that e is Delaunay-flippable. There are $z, z' \in \mathbb{Z}$ such that $e = s_{z,z'}$. The segment $\tilde{e} = [\tilde{p}_z^0, \tilde{p}_{z'}^1]$ is a lift of e so it is incident to two faces \tilde{t}_1 and \tilde{t}_2 of the lift \tilde{T} of T . Let \tilde{v}_1 be the vertex of \tilde{t}_1 that is not a vertex of \tilde{t}_2 and let \tilde{v}_2 be the vertex of \tilde{t}_2 that is not a vertex of \tilde{t}_1 . Up to renaming \tilde{v}_1 and \tilde{v}_2 there is $\epsilon \in \{1, -1\}$ such that $\tilde{v}_1 = \tilde{p}_{z-\epsilon}^0$ and $\tilde{v}_2 = \tilde{p}_{z'+\epsilon}^1$: every other case would

contradict the fact that both T and the triangulation resulting from the flip of e in T are indeed triangulations. The edge e' resulting from the lift of e in T admits the segment $[\tilde{v}_1, \tilde{v}_2]$ as a lift so $l(e')$ is the L_2 norm of $\tilde{v}_1 - \tilde{v}_2$. Recall also that $l(e)$ is the L_2 norm of $\tilde{p}_z^0 - \tilde{p}_{z'}^1$. By the triangular inequality the difference between the L_2 norms of $\tilde{v}_1 - \tilde{v}_2$ and $\tilde{p}_z^0 - \tilde{p}_{z'}^1$ cannot exceed the sum of the L_2 norms of $\tilde{v}_1 - \tilde{p}_z^0$ and $\tilde{v}_2 - \tilde{p}_{z'}^1$. The latter are both equal to $1/n$ by construction. That proves $l(e') - l(e) \geq -2/n$.

To prove (d) consider a lift \tilde{e} of a free edge e of T and the two vertices \tilde{v}_1 and \tilde{v}_2 of \tilde{e} . Let τ_1 be the translation by the vector $(1, 0)$ (one of the two translations defining \mathbb{T}_\square). The four points of \mathbb{R}^2 that are \tilde{v}_1 , \tilde{v}_2 , $\tau_1(\tilde{v}_2)$ and $\tau_1(\tilde{v}_1)$ are the vertices of a closed parallelogram P_\diamond . The closed parallelogram P_\diamond contains a lift of every free edge of T . Indeed every free edge f of T other than e admits a lift \tilde{f} whose relative interior intersects the interior of P_\diamond ², and the relative interior of \tilde{f} cannot intersect a side of P_\diamond because that would imply that the relative interior of the edge f intersects another edge of the triangulation T . To conclude observe that by construction the sides of P_\diamond are of length 1 (for the sides $\tilde{v}_1\tau_1(\tilde{v}_1)$ and $\tilde{v}_2\tau_1(\tilde{v}_2)$) and of length $l(e)$ (for the sides $\tilde{v}_1\tilde{v}_2$ and $\tau_1(\tilde{v}_1)\tau_1(\tilde{v}_2)$). Thus every free edge of T has its length between $l(e) - 2$ and $l(e) + 2$. \square

11.3 Upper bound

In this section we show that the construction of Section 11.2 was actually “the worst possible”, the lower bound of Proposition 11.1 is asymptotically matched by a general upper bound over all possible starting triangulations on a flat torus. This will prove Theorem 8.3.

The upper bound follows from a key proposition, Proposition 11.2 below, that says, informally, the following. Given two “long” edges e_1 and e_2 among the edges flipped in a sequence of Delaunay flips, if e_1 and e_2 have “comparable” lengths, then they must be “roughly parallel”. To formalize this, we first introduce the notion of *signature points* in Section 11.3.1. We state and prove Proposition 11.2 in Section 11.3.2. We finally prove Theorem 8.3 in Section 11.3.3.

11.3.1 Signature points

Consider a flat torus \mathbb{T}_Γ . We map every segment s of \mathbb{T}_Γ to a pair $\{\tilde{p}, -\tilde{p}\}$ of opposite nonzero points of \mathbb{R}^2 as follows. We consider the endpoints \tilde{u} and \tilde{v} of a lift of s and define the point \tilde{p} as the image of $0_{\mathbb{R}^2}$ under the translation that maps \tilde{u} to \tilde{v} . The resulting pair $\{\tilde{p}, -\tilde{p}\}$ does not depend on the choice of \tilde{u} and \tilde{v} . We call these two points the **signature points** of the segment s . Of course:

Lemma 11.2. *In a flat torus \mathbb{T}_Γ there cannot be more than two distinct segments with the same endpoints and the same signature points.*

Proof. Consider two segments s and s' of \mathbb{T}_Γ and assume that s and s' have the same endpoints u and v (u and v may be equal) and the same signature points \tilde{p} and $-\tilde{p}$. Consider also a lift \tilde{u} of u . For $\epsilon \in \{1, -1\}$ let \tilde{v}_ϵ denote the image of \tilde{u} under the translation that maps $0_{\mathbb{R}^2}$ to $\epsilon\tilde{p}$. There are $\epsilon, \epsilon' \in \{1, -1\}$ such that the segment $[\tilde{u}, \tilde{v}_\epsilon]$ of \mathbb{R}^2 is a lift of s and such that the segment $[\tilde{u}, \tilde{v}_{\epsilon'}]$ of \mathbb{R}^2 is a lift of s' . If $\epsilon = \epsilon'$, then $s = s'$. \square

²The closed parallelogram P_\diamond is a fundamental domain for the flat torus \mathbb{T}_\square .

11.3.2 The key proposition

In this section we prove provide our key proposition. In the following, we say that a segment s of a flat torus \mathbb{T}_Γ follows a segment s' of \mathbb{T}_Γ (possibly with $s = s'$) if there are triangulations T and T' of \mathbb{T}_Γ (possibly with $T = T'$) such that s is an edge of T , s' is an edge of T' , and there is a sequence of Delaunay flips (possibly of length 0) starting from T' and ending at T . Our key proposition is:

Proposition 11.2. *Given a flat torus \mathbb{T}_Γ there are $\kappa > 0$ and $l_0 > 0$ depending only on \mathbb{T}_Γ such that the following holds. If a segment s of \mathbb{T}_Γ follows a segment s' of \mathbb{T}_Γ and if $l(s) > l_0$ and $l(s') \in [l(s)/2, 2l(s)]$, then the signature points of s' are at distance at most κ from the line containing the signature points of s .*

See Figure 11.5 for an illustration of Proposition 11.2.

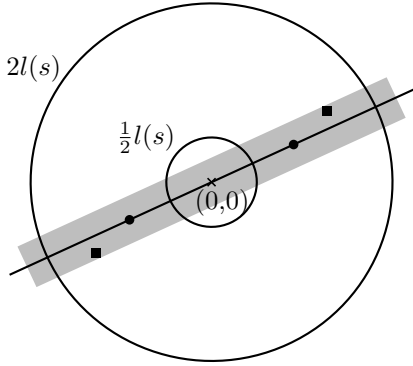


Figure 11.5: Illustration of Proposition 11.2. (Black disks) Signature points of s . (Black squares) Signature points of s' . (Gray) Points at distance at most κ from the line containing the signature points of s .

The rest of this section is devoted to the proof of Proposition 11.2. First we need two lemmas.

Lemma 11.3. *Assume that a segment s of a flat torus \mathbb{T}_Γ follows a segment s' of \mathbb{T}_Γ and consider a lift \tilde{s} of s and a lift \tilde{s}' of s' . If \tilde{s} and \tilde{s}' intersect in their respective relative interiors and if there is an open disk \tilde{D} whose boundary $\partial\tilde{D}$ contains the two endpoints of \tilde{s} and one of the endpoints of \tilde{s}' , then the other endpoint of \tilde{s}' lies outside \tilde{D} .*

Observe that in Lemma 11.3 if a point lies outside the open disk \tilde{D} it may still lie within the boundary circle $\partial\tilde{D}$. In particular the conclusion of the lemma holds when $s = s'$ and $\tilde{s} = \tilde{s}'$.

Proof. Let \tilde{u}, \tilde{v} denote the two endpoints of \tilde{s} , and \tilde{u}', \tilde{v}' denote the two endpoints of \tilde{s}' . Assume that the points \tilde{u}, \tilde{v} , and \tilde{u}' belong to the circle $\partial\tilde{D}$. The projection $\pi(\partial\tilde{D})$ is the intersection with $\mathbb{S}_2 \setminus \{P\}$ of a plane $\mathcal{P} \subset \mathbb{R}^3$. The plane \mathcal{P} bounds two closed half-spaces whose union is \mathbb{R}^3 and whose intersection is \mathcal{P} . We will show that $\pi(\tilde{v}')$ belongs to the half-space \mathcal{R} containing the point P .

There are triangulations T and T' of \mathbb{T}_Γ such that s is an edge of T , s' is an edge of T' , and there is a sequence of Delaunay flips starting from T' and ending at T . The lift \tilde{T} of T and the lift \tilde{T}' of T' are infinite triangulations of \mathbb{R}^2 ; \tilde{s} is an edge of \tilde{T} and \tilde{s}' is an edge of \tilde{T}' .

Let S and S' be stereographic surfaces associated to T and T' respectively. Lemma 11.1 and the transitivity of the above-below relation imply that S is above S' (possibly with $S = S'$). Thus any point $\tilde{p} \in \mathbb{R}^2$ of the intersection of \tilde{s} and \tilde{s}' is such that $\pi_{S'}(\tilde{p})$ lies on the segment $[P, \pi_S(\tilde{p})]$ of \mathbb{R}^3 on the line $I_{\tilde{p}}$. (Section 11.1). The point $\pi_S(\tilde{p})$ is the intersection with the line $I_{\tilde{p}}$ of an edge of S : this edge is the segment $[\pi(\tilde{u}), \pi(\tilde{v})]$ of \mathbb{R}^3 . This segment is fully contained in the plane \mathcal{P} since its endpoints $\pi(\tilde{u})$ and $\pi(\tilde{v})$ both belong to \mathcal{P} . In particular $\pi_S(\tilde{p})$ belongs to \mathcal{P} and $\pi_{S'}(\tilde{p})$ belongs to the half-space \mathcal{R} . Since $\pi_{S'}(\tilde{p})$ is distinct from $\pi(\tilde{u}')$ and belongs to the segment $[\pi(\tilde{u}'), \pi(\tilde{v}')]$ of \mathbb{R}^3 and since both $\pi_{S'}(\tilde{p})$ and $\pi(\tilde{u}')$ belong to \mathcal{R} then so does $\pi(\tilde{v}')$. \square

Lemma 11.4. *Let $\varepsilon > 0$ and $d > 20\varepsilon$. Let $\tilde{u} \in \mathbb{R} \times]-\infty, 0[$ and $\tilde{v} \in \mathbb{R} \times]0, +\infty[$ such that $\|\tilde{u}\| < \varepsilon$ and $\|\tilde{v} - \tilde{u}\| < 4d$. There is a unique open disk \tilde{D} whose boundary contains \tilde{u} and the points $(d, 0)$ and $(-d, 0)$. If \tilde{v} lies outside \tilde{D} , then $y_{\tilde{v}} < 100\varepsilon$ where $y_{\tilde{v}}$ denotes the second coordinate of \tilde{v} .*

Observe that in Lemma 11.4 if the point \tilde{v} lies outside the open disk \tilde{D} it may, still, belong to its boundary. See Figure 11.6 for an illustration of Lemma 11.4.

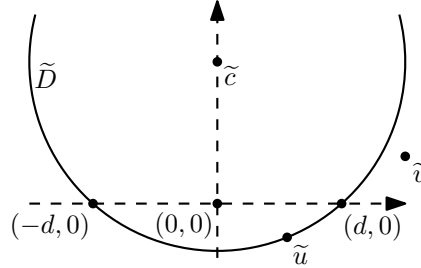


Figure 11.6: Illustration of Lemma 11.4.

Proof. We write $\tilde{u} = (x_{\tilde{u}}, y_{\tilde{u}})$ and $\tilde{v} = (x_{\tilde{v}}, y_{\tilde{v}})$ and recall that $y_{\tilde{v}} > 0$ and $y_{\tilde{u}} < 0$ both hold by assumption. The latter enforces the existence of the open disk \tilde{D} . Now let \tilde{c} denote the center of \tilde{D} . The segment $[-d, d] \times \{0\}$ is a chord of \tilde{D} and its midpoint is the point $(0, 0)$. Thus the first coordinate of \tilde{c} is 0 and the radius of \tilde{D} is $\sqrt{y_{\tilde{c}}^2 + d^2}$ where $y_{\tilde{c}}$ denotes the second coordinate of \tilde{c} . As shown below, one easily gets $y_{\tilde{c}} > 0$ from the assumptions $y_{\tilde{u}} < 0$, $\|\tilde{u}\| < \varepsilon$, and $d > \varepsilon$. See Figure 11.6.

We first prove a few inequalities that may seem arbitrary at first but will be used in the end of the proof. Pythagorean Theorem gives $(y_{\tilde{c}} - y_{\tilde{u}})^2 + x_{\tilde{u}}^2 = y_{\tilde{c}}^2 + d^2$ which simplifies to $-2y_{\tilde{u}}y_{\tilde{c}} = d^2 - x_{\tilde{u}}^2 - y_{\tilde{u}}^2$. We assumed $\|\tilde{u}\| < \varepsilon$ and $d > \sqrt{2}\varepsilon$, that implies $x_{\tilde{u}}^2 + y_{\tilde{u}}^2 < d^2/2$ and $-y_{\tilde{u}} < \varepsilon$ and thus

$$4\varepsilon y_{\tilde{c}} > d^2. \quad (11.1)$$

Equation (11.1) combined with the assumption that $d > 20\varepsilon$ implies

$$y_{\tilde{c}} > 100\varepsilon. \quad (11.2)$$

The triangle inequality gives $\|\tilde{v}\| \leq \|\tilde{v} - \tilde{u}\| + \|\tilde{u}\|$. The latter is smaller than $4d + \varepsilon < 5d$ by assumptions. So $\|\tilde{v}\|^2 < 25d^2$ and by Equation (11.1) we obtain

$$\|\tilde{v}\|^2 < 100\varepsilon y_{\tilde{c}}. \quad (11.3)$$

The combination of Equation (11.3) and Equation (11.2) imply

$$\|\tilde{v}\| < y_{\tilde{c}}. \quad (11.4)$$

Now we prove $y_{\tilde{v}} < 100\varepsilon$. Since \tilde{v} lies outside \tilde{D} then $(y_{\tilde{c}} - y_{\tilde{v}})^2 + x_{\tilde{v}}^2 \geq y_{\tilde{c}}^2 + d^2$, which simplifies to $y_{\tilde{v}}^2 - 2y_{\tilde{c}}y_{\tilde{v}} + x_{\tilde{v}}^2 - d^2 \geq 0$. We study this inequality to derive a bound on $y_{\tilde{v}}$. Equation (11.4) implies $4(y_{\tilde{c}}^2 + d^2 - x_{\tilde{v}}^2) > 0$ hence the polynomial $X^2 - 2y_{\tilde{c}}X + x_{\tilde{v}}^2 - d^2$ univariate in X admits two real roots $y_{\tilde{c}} \pm \sqrt{y_{\tilde{c}}^2 + d^2 - x_{\tilde{v}}^2}$. Equation (11.4) enforces $y_{\tilde{v}} \leq y_{\tilde{c}} - \sqrt{y_{\tilde{c}}^2 + d^2 - x_{\tilde{v}}^2}$, which implies

$$y_{\tilde{v}} < y_{\tilde{c}} \left(1 - \sqrt{1 - x_{\tilde{v}}^2/y_{\tilde{c}}^2} \right).$$

Equation (11.3) and Equation (11.2) successively infer

$$y_{\tilde{v}} < y_{\tilde{c}} \left(1 - \sqrt{1 - 100\varepsilon/y_{\tilde{c}}} \right) \leq 100\varepsilon.$$

This completes the proof. \square

Now we prove Proposition 11.2 using Lemmas 11.3 and 11.4.

Proof of Proposition 11.2. There exists $\varepsilon > 0$ such that every open disk of diameter ε intersects the Γ -orbit of every point of \mathbb{R}^2 . The value of ε depends on Γ only. We set $\kappa = 101\varepsilon$ and $l_0 = 40\varepsilon$.

Assume that a segment s of a flat torus \mathbb{T}_Γ follows a segment s' of \mathbb{T}_Γ . Consider a lift \tilde{s} of s . We may assume, by applying a rotation or translation if necessary, that \tilde{s} is a horizontal segment whose center is the point $(0, 0)$. We claim that there exists a lift \tilde{s}' of s' whose endpoints $\tilde{u} = (x_{\tilde{u}}, y_{\tilde{u}})$ and $\tilde{v} = (x_{\tilde{v}}, y_{\tilde{v}})$ satisfy the following three conditions: $\|\tilde{u}\| < \varepsilon$, $y_{\tilde{u}} < 0$, and $y_{\tilde{u}} \leq y_{\tilde{v}}$. To prove this claim start with any lift of s' and let $\tilde{p} = (x_{\tilde{p}}, y_{\tilde{p}})$ and $\tilde{q} = (x_{\tilde{q}}, y_{\tilde{q}})$ denote the endpoints of this lift. We may assume, by exchanging \tilde{p} and \tilde{q} if necessary, that $y_{\tilde{p}} \leq y_{\tilde{q}}$. By definition of ε , there is a point $\tilde{u} \in \mathbb{R}^2$ at distance less than $\varepsilon/2$ from the point $(0, -\varepsilon/2)$ and a translation $\tau \in \Gamma$ such that $\tau(\tilde{p}) = \tilde{u}$. Setting $\tilde{v} = \tau(\tilde{q})$ proves the claim.

The signature points of s belong to x-axis (the line $\mathbb{R} \times \{0\}$). We consider one of the two signature points of s' , namely $\tilde{v} - \tilde{u}$. Since $-\varepsilon < y_{\tilde{u}} < 0$ and $y_{\tilde{u}} \leq y_{\tilde{v}}$ proving $y_{\tilde{v}} < 100\varepsilon$ will infer the proposition. Having $y_{\tilde{v}} \leq 0$ would conclude so we assume $y_{\tilde{v}} > 0$. There are two cases: either \tilde{s} and \tilde{s}' intersect in their relative interiors or they do not.

First assume that \tilde{s} and \tilde{s}' intersect in their relative interiors. We set $d = l(s)/2$ and we have $d > l_0/2 = 20\varepsilon$. Lemma 11.3 implies that \tilde{v} lies outside the open disk \tilde{D} whose boundary contains \tilde{u} and the endpoints $(d, 0)$ and $(-d, 0)$ of \tilde{s} . Thus the conditions of Lemma 11.4 are satisfied and $y_{\tilde{v}} < 100\varepsilon$.

If \tilde{s} and s' do not intersect in their relative interiors, then \tilde{v} lies outside \tilde{D} and the conditions of Lemma 11.4 are satisfied again. \square

11.3.3 Upper bound: proof of Theorem 8.3

In this section we finally prove Theorem 8.3. First, we need two lemmas and an observation. The following lemma is folklore, we give a proof for completeness:

Lemma 11.5. *Consider a flat torus \mathbb{T}_Γ , an integer $m \geq 0$, and a sequence of Delaunay flips T_0, \dots, T_m . For every $k \in \{1, \dots, m\}$, we let e_k denote the edge of T_{k-1} that is flipped to obtain T_k . The segments e_1, \dots, e_m of \mathbb{T}_Γ are pairwise distinct.*

Proof. Assume there are $k, k' \in \{1, \dots, m\}$ such that $k < k'$ and $e_k = e_{k'}$. Let S_{k-1} , S_k and $S_{k'-1}$ be the stereographic surfaces associated to T_{k-1} , T_k and $T_{k'-1}$, respectively. Consider the edge f of T_k resulting from the Delaunay flip of the edge e_k in T_{k-1} . Let $p \in \mathbb{T}_\Gamma$ be the intersection point of the relative interiors of f and e_k . Let also $\tilde{p} \in \mathbb{R}^2$ be a lift of p .

Since $e_k = e_{k'}$ then $\pi_{S_{k-1}}(\tilde{p}) = \pi_{S_{k'-1}}(\tilde{p})$. By Lemma 11.1 $S_{k'-1}$ is above S_k and S_k is above S_{k-1} . We deduce $\pi_{S_k}(p) = \pi_{S_{k-1}}(\tilde{p}) = \pi_{S_{k'-1}}(\tilde{p})$. But Lemma 11.1 also gives $\pi_{S_k}(\tilde{p}) \neq \pi_{S_{k-1}}(\tilde{p})$ hence a contradiction. \square

The edges flipped in a sequence of Delaunay flips are not longer than $2\Delta(T)$ where $\Delta(T)$ is a parameter measuring in some sense how “stretched” the starting triangulation T is [70, Lemma 10]. The arguments yielding a bound in terms of $\Delta(T)$ easily infer a bound in terms of the maximum length of an edge in T . This new bound is stated by the following lemma, whose proof of is only a slight adaptation of the anterior proof [70, Lemma 10]:

Lemma 11.6. *Consider triangulations T and T' of a flat torus \mathbb{T}_Γ and assume that there is a sequence of Delaunay flips starting from T' and ending at T . Then the edges of T cannot be more than twice as long as a longest edge of T' .*

Proof. Let L' be the maximum length of an edge of T' and assume that there is an edge e of T such that $l(e) > 2L'$. Consider a lift \tilde{e} of e and let $\tilde{p} \in \mathbb{R}^2$ be the middlepoint of \tilde{e} . There is a face \tilde{t}' of the lift \tilde{T}' of T' such that \tilde{p} belongs either to \tilde{t}' or to the boundary of \tilde{t}' . The three edges of the triangle \tilde{t}' are not longer than L so, by the triangle inequality, the distance from \tilde{p} to any vertex of \tilde{t}' is not greater than L and the closed disk $\tilde{D} \subset \mathbb{R}^2$ of diameter L and centered at \tilde{p} contains \tilde{t}' . Also the two endpoints \tilde{u} and \tilde{v} of \tilde{e} lie outside \tilde{D} .

Consider the stereographic surfaces S and S' associated to the T and T' , respectively. The projection $\pi(\partial\tilde{D})$ of the boundary $\partial\tilde{D}$ of \tilde{D} is the intersection with $\mathbb{S}_2 \setminus P$ of a plane $\mathcal{P} \subset \mathbb{R}^3$. The plane \mathcal{P} bounds two open half-spaces. The points $\pi(\tilde{u})$ and $\pi(\tilde{v})$ both belong to the half-space \mathcal{R} that contains P . Thus $\pi_S(\tilde{p}) \in \mathcal{R}$. The vertices \tilde{w}_1, \tilde{w}_2 and \tilde{w}_3 of \tilde{t}' all belong to $\partial\tilde{D}$ thus $\pi(\tilde{w}_1), \pi(\tilde{w}_2)$ and $\pi(\tilde{w}_3)$ all belong to \mathcal{P} and $\pi_{S'}(\tilde{p}) \in \mathcal{P}$. Consequently $\pi_{S'}(\tilde{p})$ does not lie on the segment $[P, \pi_S(\tilde{p})]$ of \mathbb{R}^3 , contradicting Lemma 11.1. \square

Finally, we prove Theorem 8.3. The core of the proof is an observation that we give here to help build the intuition. Consider a flat torus \mathbb{T}_Γ and $\kappa > 0$. The following is a straightforward application of the theorem of Pick [156]:

Observation 11.1. *There is $C > 0$ (depending on \mathbb{T}_Γ , and κ) satisfying the following. Let L be a line in \mathbb{R}^2 containing the point $(0, 0)$. Let $0 < r < R$. Let m be the number of points of the Γ -orbit of $(0, 0)$ that are at distance less than κ from L , and whose distance from $(0, 0)$ lies between r and R . Then $m \leq C(R - r)$.*

Proof of Theorem 8.3. Consider $m \geq 0$ and a sequence of Delaunay flips T_0, \dots, T_m such that $T_0 = T$. For every $k \in \{0, \dots, m\}$ the edges of T_k constitute a set E_k of segments of \mathbb{T}_Γ . We are interested in the union E of the sets E_0, \dots, E_m . By Lemma 11.5 the cardinality of E is greater or equal to m . We partition the elements of E into $n(n+1)/2$ subsets according to their endpoints, as follows. For every unordered pair $\{u, v\}$ of vertices of the triangulation

T , we consider the set of segments in E that end at u and v . For single vertex v of T , we consider the set of segments in E that admit v as their unique endpoint. We will prove that each of those subsets contains at most $C_\Gamma \cdot L$ segments for some C_Γ depending only on Γ . This will infer the result.

So consider such a subset $F \subseteq E$ in the partition that we just described and let u and v be the (possibly equal) endpoints of the segments in F . Let $\kappa > 0$ and $l_0 > 0$ be given by Proposition 11.2.

By Lemma 11.2 there cannot be more than two distinct segments of \mathbb{T}_Γ having the same endpoints and the same signature points. Fix a lift \tilde{u} of u and a lift \tilde{v} of v . For any signature point \tilde{p} of a segment in F there is $\tau \in \Gamma$ such that either \tilde{p} or $-\tilde{p}$ is equal to $\tau(\tilde{v}) - \tilde{u}$. Thus there is a finite number of such signature points that are at distance at most l_0 from the point $(0, 0)$, and this finite number depends only on \mathbb{T}_Γ (recall that l_0 depends only on \mathbb{T}_Γ). That implies that there is only a finite number of segments in F of length at most l_0 .

Consequently we let $F' \subseteq F$ be the set of segments in F that are longer than l_0 ; we will now bound the cardinality of F' . By Lemma 11.6 no segment in F' is longer than $2L$. We partition the segments in F' by their lengths as follows. We consider $j_0 = l_0 < j_1 < \dots < j_N = 2L$ for some integer $N \geq 1$ such that for every $k \in \{1, \dots, N\}$ the reals j_{k-1} and j_k differ by a factor of at most 2. For every $k \in \{1, \dots, N\}$, we let F'_k denote the set of segments in F' whose length belongs to $]j_{k-1}, j_k]$. We now fix k and claim that F'_k contains at most $C'_\Gamma \cdot (j_k - j_{k-1})$ segments, where $C'_\Gamma > 0$ depends only on Γ .

To prove this claim observe that if F'_k is not empty, then it contains a segment s that follows every other segment $s' \in F'_k \setminus \{s\}$. For another such segment s' , Proposition 11.2 states that the signature points of s' are at distance at most κ from the line containing the signature points of s . Also the distance to $(0, 0)$ of the two signature points of s' is the length of s' and thus lies between j_{k-1} and j_k . Finally, observe that the signature points of elements of F'_k all belong, by definition, to the Γ -orbit \mathcal{O} of some point of \mathbb{R}^2 . It follows from Observation 11.1 that the number of signature points of elements of F'_k is at most linear in $j_k - j_{k-1}$ and the constant coefficient depends only on \mathbb{T}_Γ (recall that κ depends only on \mathbb{T}_Γ).

That, together with Proposition 11.1 for the lower bound, concludes the proof of Theorem 8.3. \square

Chapter 12

Implementation of Delaunay Triangulations of Closed Hyperbolic Surfaces

12.1 Introduction

We developed a package [3] that has been integrated in the Computational Geometry Algorithms Library (CGAL), a standard open source software library. This package enables building and handling triangulations of closed hyperbolic surfaces. Rather than including the documentation of the package, available here [3], we provide a short introduction to its functionalities.

Prominently, the package can compute, from a triangulation T of a closed hyperbolic surface, a Delaunay triangulation of the surface of T with the same vertices than T . This can be used as a preliminary before any computation with a triangulation. Delaunay triangulations are obtained simply by performing Delaunay flips greedily.

Other convenient functionalities are offered such as lifting a portion of a triangulation T in the Poincaré disk, to visualize T for example.

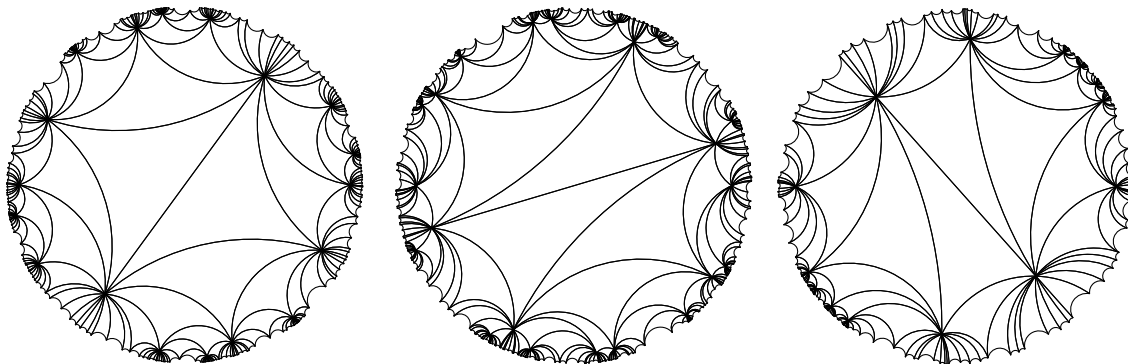


Figure 12.1: Delaunay triangulations of closed hyperbolic surfaces of genus two, partly lifted in the Poincaré disk, computed by the package.

The package also allows for *building* triangulations, in two levels. At one level the package implements **fundamental domains**, hyperbolic polygons with pairs of equal length sides

that can be glued to get a closed surface. A fundamental domain P is **convex** if its corner angles are all smaller than π . A method is offered that constructs a triangulation from P by triangulating the interior of P and gluing the paired sides. The assumption that P is convex ensures that the interior of P can be triangulated naively by insertion of any maximal set of pairwise-disjoint arcs of P . At a second level the package can randomly generate convex fundamental domains whose surfaces have genus two, and the set of surfaces that can be generated this way is dense in the space of surfaces of genus two. The user can thus either ask the package to generate and triangulate a fundamental domain all by itself, in which case the resulting surface has genus two, or he can come with its own convex fundamental domain and ask the package to triangulate it, without limitation on the genus.

Last but not least, the user can choose the number type used by the package. The only operations needed are the basic arithmetic ones (addition, subtraction, multiplication, and division), and the comparisons. More importantly, the fundamental domains generated by the package involve only rational numbers, and this a contribution of us, for then the user can choose any number type supporting the basic operations and constructible from rational numbers. This allows, for example, to perform all operations exactly, without rounding, which seems to be necessary in practice to execute even simple algorithms such as the Delaunay flips algorithm, perhaps because a high precision is needed to differentiate the numbers involved (think of a stretched fundamental domain with vertices very close to the boundary circle of the Poincaré disk). We do not know of a dense subset of the surfaces of genus $g \geq 3$ with a similar description by rational numbers, which is why the generation of fundamental domains is limited to genus two.

We detail the data structures in Section 12.2, and the generation of domains in Section 12.3. We denote by $\arg z$ the argument of any $z \in \mathbb{C} \setminus \{0_{\mathbb{C}}\}$. We denote by $\text{Re}[z]$ and $\text{Im}[z]$ respectively the real and imaginary parts of $z \in \mathbb{C}$.

12.2 Data structures

Each fundamental domain is represented by a polygon in the Poincaré disk \mathbb{D} , encoded by the list of its vertices, and by the list of its side pairings. Each vertex is a complex number. Each complex number is a pair of real numbers, its real and imaginary parts.

Each triangulation T is encoded by a combinatorial map whose edges are decorated with complex numbers, along with some optional data which we call anchor. The complex number $R_T(e) \in \mathbb{C}$ decorating an edge e of T is the *cross ratio* of e in T , defined as follows. Consider the lift \tilde{T} of T in the Poincaré disk \mathbb{D} . In \tilde{T} , let \tilde{e} be a lift of e . Orient \tilde{e} arbitrarily, and let $z_0 \in \mathbb{D}$ and $z_2 \in \mathbb{D}$ be the first and second vertices of \tilde{e} . In \tilde{T} , consider the triangle on the right of \tilde{e} , and let $z_1 \in \mathbb{D}$ be the third vertex of this triangle (the vertex distinct from z_0 and z_2). Similarly, consider the triangle on the left of \tilde{e} , and let $z_3 \in \mathbb{D}$ be the third vertex of this triangle. Then

$$R_T(e) = \frac{(z_3 - z_1)(z_2 - z_0)}{(z_3 - z_0)(z_2 - z_1)}.$$

Crucially, this definition does not depend on the choice of the lift \tilde{e} , nor on the orientation of \tilde{e} . Informally, the cross ratios encode the geometric information of the triangulation. We chose this particular encoding because it is simple to update when performing a Delaunay flip, and also because it allows for a simple test of whether an edge is Delaunay flippable. For example, if T' is obtained from T by flipping an edge e , and if e' is the resulting edge of

T' , then $R_{T'}(e') = R_T(e)/(R_T(e) - 1)$. Moreover, only the edges bounding the two triangles incident to e may have their cross ratio changed by the flip, and the changes are described by simple formulas as well. Finally, an edge e of T is Delaunay flippable if and only if $\text{Im}[R_T(e)]$ is positive.

As announced, the internal representation of T can contain some additional data, which we call *anchor*. The anchor is used when building a portion of the lift of T in the Poincaré disk \mathbb{D} . It contains a lift A of a triangle of T , represented by its three vertices in \mathbb{D} , and by the correspondence with a triangle in the combinatorial map of T . Once we have access to a first lift like A we can compute the other lifts using the cross ratios, informally by unfolding T along its edges, starting from A . We use the anchor because we do not know how to compute a first lift otherwise.

12.3 Generation of domains in genus two

To generate fundamental domains we use a construction of Aigon-Dupuy, Buser, Cibils, Künzle, and Steiner [8], which we now reformulate. A tuple of four complex numbers (z_0, z_1, z_2, z_3) is **pre-admissible** if $z_i \in \mathbb{D} \setminus \{0_{\mathbb{C}}\}$ for every i and $0 = \arg z_0 < \arg z_1 < \arg z_2 < \arg z_3 < \pi$. In that case the eight complex numbers $z_0, \dots, z_3, -z_0, \dots, -z_3$ are the vertices of a hyperbolic octagon $O(z_0, z_1, z_2, z_3)$ in \mathbb{D} . If the hyperbolic area of the octagon is equal to 4π then identifying the opposite sides of $O(z_0, z_1, z_2, z_3)$ results in a surface of genus two, and we say that the tuple (z_0, z_1, z_2, z_3) is **admissible**. Aigon Dupuy et al. also describe formulas to construct an admissible tuple [8, Section 3]. Start with $z_1, z_2, z_3 \in \mathbb{D}$ satisfying $0 < \arg z_1 < \arg z_2 < \arg z_3 < \pi$. Abbreviate $u = (1 - z_1\bar{z}_2)(1 - z_2\bar{z}_3)$, $a = \text{Im}[-u\bar{z}_1z_3]$, $b = \text{Im}[u(z_3 - \bar{z}_1)]$, and $c = \text{Im}[u]$. Assume $a + b + c < 0$ and let $z_0 = 2c/(-b + \sqrt{b^2 - 4ac})$. Then (z_0, z_1, z_2, z_3) is an admissible tuple. Note that the resulting z_0 may not be rational even if the real and imaginary parts of z_1, z_2 , and z_3 are, due to the square root.

Our contribution is to prove that the **rational** admissible tuples, in which the real and imaginary parts of the complex numbers are all rational, are dense in the space of admissible tuples. In detail we prove the following. For any $z \in \mathbb{D}$ and $\varepsilon > 0$, we denote by $B(z, \varepsilon)$ the open ball of points $z' \in \mathbb{D}$ whose hyperbolic distance to z is strictly smaller than ε . Then:

Theorem 12.1. *Let (z_0, z_1, z_2, z_3) be an admissible tuple and $\varepsilon > 0$. There exists an admissible tuple (Z_0, Z_1, Z_2, Z_3) such that $Z_k \in B(z_k, \varepsilon) \cap (\mathbb{Q} + i\mathbb{Q})$ for every k .*

We give a proof of Theorem 12.1 below. In the package we turned this proof into an effective procedure that takes a tuple (z_0, z_1, z_2, z_3) , not necessarily admissible but “very close to” an admissible one, and returns a rational admissible tuple (Z_0, Z_1, Z_2, Z_3) . This allows to generate a fundamental domain, in two stages. In a first stage we apply the formulas of Aigon Dupuy et al. [8] to generate a tuple (z_0, z_1, z_2, z_3) , but we use a real number type whose operations are inexact, in fact the native float type of C++. So (z_0, z_1, z_2, z_3) is not an admissible tuple, but it is very close to one. In a second stage we apply the procedure issued of Theorem 12.1 to construct a rational admissible tuple (Z_0, Z_1, Z_2, Z_3) very close to (z_0, z_1, z_2, z_3) . And we return the octagon $O(Z_0, Z_1, Z_2, Z_3)$ with opposite sides are paired. The set of surfaces that can be generated this way is dense in the “space” of surface of genus two. This follows from the fact that every surface of genus two can be obtained from an admissible tuple constructed with the formulas of Aigon Dupuy et al. [8]. We omit a formal proof for simplicity.

The rest of this section is devoted to the proof of Theorem 12.1. We denote by $\mathcal{P}(z_1, \dots, z_n)$ a hyperbolic polygon whose $n \geq 3$ vertices are $z_1, \dots, z_n \in \mathbb{D}$. We denote by $\mathcal{A}(X)$ the hyperbolic area of a hyperbolic polygon X . We use a result of Aigon Dupuy et al. [8, Lemma 3.2]. A pre-admissible tuple (z_0, z_1, z_2, z_3) is admissible if and only if $\mathcal{A}(\mathcal{P}(-z_0, z_1, z_2, z_3)) = 2\pi$, and this is equivalent to

$$\operatorname{Im} \left[\prod_{k=0}^3 (1 - z_k \overline{z_{k+1}}) \right] = 0. \quad (12.1)$$

The authors establish this condition after proving a preliminary result that we will also reuse [8, Appendix (A7)]. If $z, z' \in \mathbb{D} \setminus \{0_{\mathbb{C}}\}$ satisfy $0 \leq \arg z \leq \arg z' \leq \pi$ then

$$2 \arg(1 - z \overline{z'}) = \mathcal{A}(\mathcal{P}(0_{\mathbb{C}}, z, z')). \quad (12.2)$$

Proof of Theorem 12.1. We first choose for every $k \in \{0, 1, 2, 3\}$ a point $Z_k \in B(z_k, \varepsilon) \cap (\mathbb{Q} + i\mathbb{Q})$, with the constraint $\operatorname{Im}[z_0] = 0$, but without any other constraint. If ε is small enough then every such tuple (Z_0, Z_1, Z_2, Z_3) is pre-admissible. Assuming ε small enough, we shall further prove that we can replace Z_3 by a point $U \in B(z_3, \varepsilon) \cap (\mathbb{Q} + i\mathbb{Q})$ such that $\mathcal{A}(\mathcal{P}(-Z_0, Z_0, Z_1, Z_2, U)) = 2\pi$. This will prove the theorem for then (Z_0, Z_1, Z_2, U) is admissible.

To do so we first define an isometry $F : \mathbb{D} \rightarrow \mathbb{D}$ in the Poincaré disk: $F(z) = \frac{z+Z_0}{Z_0 z+1}$. Observe that $F(-Z_0) = 0_{\mathbb{C}}$. Since F and F^{-1} both map $\mathbb{D} \cap (\mathbb{Q} + i\mathbb{Q})$ to some subset of $\mathbb{D} \cap (\mathbb{Q} + i\mathbb{Q})$ our problem reduces to replacing $F(Z_3)$ by an element V of $B(F(Z_3), \varepsilon) \cap \mathbb{Q} + i\mathbb{Q}$ such that $\mathcal{A}(\mathcal{P}(0_{\mathbb{C}}, F(Z_0), F(Z_1), F(Z_2))) = 2\pi$. Indeed, by setting $U = F^{-1}(V)$ we obtain $U \in B(z_3, \varepsilon) \cap (\mathbb{Q} + i\mathbb{Q})$ and $\mathcal{A}(\mathcal{P}(-Z_0, Z_0, Z_1, Z_2, U)) = \mathcal{A}(\mathcal{P}(0_{\mathbb{C}}, F(Z_0), F(Z_1), F(Z_2), V)) = 2\pi$.

To find such a point V , we define a polynomial $P \in \mathbb{Q}[X]$ by setting

$$P(X) = \operatorname{Im} \left[(1 - F(Z_0) \overline{F(Z_1)})(1 - F(Z_1) \overline{F(Z_2)})(1 - X F(Z_2) \overline{F(Z_3)}) \right].$$

The degree of P is at most 1 so $P(X) = (P(1) - P(0))X + P(0)$.

We first show that if choose Z_k close to z_k for every k then $P(1)$ is close to 0 and $P(0)$ close to some $\kappa > 0$. Since $0 = \arg F(Z_0) < \arg F(Z_1) < \arg F(Z_2) < \arg F(Z_3) < \pi$ we can apply Equality (12.2) and obtain

$$\begin{aligned} & \arg \left[(1 - F(Z_0) \overline{F(Z_1)})(1 - F(Z_1) \overline{F(Z_2)})(1 - F(Z_2) \overline{F(Z_3)}) \right] \\ &= \arg(1 - F(Z_0) \overline{F(Z_1)}) + \arg(1 - F(Z_1) \overline{F(Z_2)}) + \arg(1 - F(Z_2) \overline{F(Z_3)}) \\ &= \frac{1}{2} \mathcal{A}(\mathcal{P}(0_{\mathbb{C}}, F(Z_0), F(Z_1))) + \frac{1}{2} \mathcal{A}(\mathcal{P}(0_{\mathbb{C}}, F(Z_1), F(Z_2))) + \frac{1}{2} \mathcal{A}(\mathcal{P}(0_{\mathbb{C}}, F(Z_2), F(Z_3))) \\ &= \frac{1}{2} \mathcal{A}(\mathcal{P}(0_{\mathbb{C}}, F(Z_0), F(Z_1), F(Z_2), F(Z_3))) = \frac{1}{2} \mathcal{A}(\mathcal{P}(-Z_0, Z_0, Z_1, Z_2, Z_3)). \end{aligned}$$

Every expression in between the equalities belongs to $[0, 2\pi[$ so those equalities are indeed equalities and not only congruences modulo 2π . By choosing Z_k close to z_k for every k we make the last expression approach $\frac{1}{2} \mathcal{A}(\mathcal{P}(-z_0, z_0, z_1, z_2, z_3)) = \pi$, which makes $P(1)$ tend to 0. Similarly, we obtain

$$\arg \left[(1 - F(Z_0) \overline{F(Z_1)})(1 - F(Z_1) \overline{F(Z_2)}) \right] = \frac{1}{2} \mathcal{A}(\mathcal{P}(-Z_0, Z_0, Z_1, Z_2)).$$

By choosing Z_k close to z_k for every k we make the last expression tend to $\frac{1}{2}A(\mathcal{P}(-z_0, z_0, z_1, z_2))$ which is not congruent to 0 modulo π . Thus $P(0)$ is close to some constant $\kappa > 0$. Whence we can assume that $P(1) \neq P(0)$.

To construct V set $\lambda = \frac{P(0)}{P(0)-P(1)}$ and let $V = \lambda F(Z_3)$; we have both $V \in \mathbb{Q} + i\mathbb{Q}$ and $P(\lambda) = 0$. We proved that $P(1)$ tends to 0 and that $P(0)$ tends to $\kappa > 0$ so λ tends to 1 and V tends to $F(Z_3)$. Finally, observe that $P(\lambda) = 0$, so $\mathcal{A}(\mathcal{P}(0_{\mathbb{C}}, F(Z_0), F(Z_1), F(Z_2), V)) = 2\pi$ by Equation (12.2). \square

Chapter 13

Conclusion

In this chapter we conclude the thesis by collecting possible continuations of our contributions. For example, our works concern orientable surfaces. A possible continuation would be to extend some of them to non-orientable surfaces. Apart from that, we discuss the two parts of the thesis independently, in two distinct sections.

13.1 Untangling graphs on surfaces

In this section we sketch the possible continuations of the first part of the thesis, concerning the problem of untangling graphs on surfaces.

13.1.1 Possible improvements

We start by listing three possible improvements of our works.

Certifying that a drawing cannot be untangled. First, some of the algorithms for testing the planarity of a graph G provide, in case G is not planar, a Kuratowski subgraph of G , to serve as a certificate that G is not planar. By contrast, our algorithms for untangling a drawing f do not provide anything in case f cannot be untangled. In this case, a natural extension would return some kind of smallest sub-drawing of f that cannot be untangled.

Attaching parts of a drawing. Second, the problem of determining whether a given drawing f can be untangled is naturally extended by allowing some parts of the drawing to be attached to the surface. We considered this extension, but only at the end of Chapter 8 (Section 8.4). The algorithm described there is exclusively on reducing triangulations, not on general embedded graphs, and we did not provide the conversion between the two models in this setting. The drawing can be attached only to the boundary of the surface, not to the interior. And, being based on harmonizing a drawing, the algorithm is not our most efficient untangling algorithm.

Further translating the method of Tutte. Finally, in Chapter 8 we defined harmonious drawings as a discrete analog of Tutte embeddings. However our algorithm for making a drawing harmonious by homotopy is not exactly an analog of the method of Tutte for producing a Tutte embedding. Our algorithm considers an input drawing, and modifies

this drawing with the only promise that it does not increase the length of any edge in the drawing. By contrast, the method of Tutte considers barycentric weights, and produces a Tutte embedding in which each vertex is a barycenter of its neighbors for the given choice of weights. A natural problem would be to understand whether this method of Tutte admits a translation in the framework of harmonious drawings.

13.1.2 Related problems

We now give two problems related to our work that we find interesting.

What is the complexity of untangling? The first problem is to understand the complexity of the untangling problem. Even though our algorithms for untangling graphs on surfaces are efficient, they are probably not optimal. One way to improve the complexities of our most efficient untangling algorithms (Theorem 3.2 and Theorem 3.3) would be to find more efficient conversions between models in Chapter 7. One bottleneck is that, when pushing the input drawing into a reducing triangulation for example, the size of the drawing usually increases by a factor that depends on the genus of the surface. On the other hand, pushing a drawing into a system of quads can be done without increasing the size of the drawing by more than a constant factor, which allows for the optimal linear time algorithms of Erickson and Whittlesey [88] on the different problem of testing curves for homotopy. Systems of quads are much weaker than reducing triangulations, so it is seems difficult to use them for solving the untangling problem on graphs. Nevertheless, the comparison motivates us to formulate the following question: Is there an algorithm that, given a closed surface S , a graph H of size m cellularly embedded on S , a graph G , and a drawing $f : G \rightarrow H$ of size n , determines whether f can be untangled in S in time (quasi-)linear in $m + n$? The same question can be asked with the problem of computing the intersection number of a collection of closed curves.

How unique reducing triangulations are? The second problem is to understand how unique reducing triangulations are. Reducing triangulations are one of the key contributions of this thesis. On a closed surface S , a reducing triangulation is, in particular, a graph T cellularly embedded on S that supports a collection of walks, which we called reduced walks, with the following properties. (1) Every subwalk of a reduced walk is also a reduced walk. (2) The reversal of a reduced walk is also a reduced walk. And (3) every walk is homotopic to exactly one reduced walk. It would be interesting to see if there exists any other kind of graph cellularly embedded on S that supports a collection of walks with all those properties.

13.1.3 Perspectives

We conclude this section by sketching two research directions related to untangling graphs.

Untangling by homotopy moves. First, some of the algorithms for minimizing the crossings of a collection of closed curves apply homotopy moves to the curves, like removing a monogon or a bigon [113, 62, 39, 38]. By contrast, our algorithms for untangling a drawing do not consider the untangling homotopy. A natural extension would be to define homotopy moves for drawings of graphs, and then design an algorithm that, given a drawing that can

be untangled, returns a sequence of homotopy moves untangling the drawing, with a care on the number of moves applied.

Minimizing crossings by homotopy. Beyond untangling, we considered minimizing crossings by homotopy, but only on closed curves, not on general drawings of graphs. We observed that this problem contains the crossing number problem, so it's decision version is NP-hard. But some particular cases can be solved efficiently, even beyond closed curves, for example minimizing the crossings between a system of loops and a cellularly embedded graph by deforming the system of loops [49]. Moreover, similarly to what has been done for the crossing number, one could aim for approximation or parameterized algorithms.

13.2 Computing Delaunay triangulations of surfaces

In this section we sketch the possible continuations of the second part of the thesis, concerning the problem of computing Delaunay triangulations of surfaces. We isolated three problems.

13.2.1 Lower bound for computing the Delaunay tessellation

We proved (Theorem 8.2) that the Delaunay tessellation of closed piecewise-flat surface can be computed from an arbitrary triangulation of the surface in time polynomial in n and $\log(r)$, where n is the number of vertices of the input triangulation, and r is its aspect ratio. A natural question is whether this result is matched by a lower bound, in a reasonable version of the Real RAM model of computation. This question is motivated by the fact that the classical machines of Blum, Shub, and Smale cannot compute the floor of a positive real number x in time $o(\log x)$ [21, Proposition 3]. We expect to prove the same lower bound on a recent model of computation such as the one described by Erickson, van Der Hoog, and Tillmann [87], and then reduce the problem of computing the floor of a positive real number to the problem of computing a Delaunay tessellation in order to transpose the lower bound.

13.2.2 Complexity of the flip algorithm

The complexity of the Delaunay flip algorithm on surfaces, piecewise-flat or hyperbolic, is vastly open. Our bound from Chapter 11 concerns only flat tori. On more general surfaces the only non-trivial bound we are aware of is by Despré, Schlenker, and Teillaud [70, Theorem 19]. They proved that, on a closed hyperbolic surface S of genus g , every sequence of Delaunay flips has length $O(n^2 \cdot \Delta^{6g-4})$, where n is the number of vertices, Δ is a geometric parameter of the input triangulation that we do not detail here, and the $O()$ notation depends on S . It seems reasonable to think that such a bound also holds on piecewise-flat surfaces. And Δ can probably be replaced by the maximum edge length of the input triangulation. The question is whether the exponent $6g - 4$ can be lowered to a constant. An intriguing question is whether better bounds can be achieved by starting from triangulations whose happiness is bounded. This assumption is reasonable for it applies to every triangulation carried by a mesh.

13.2.3 Generating hyperbolic surfaces of higher genus

In Chapter 12 we provided a method for generating closed hyperbolic surfaces of genus two. The resulting surfaces are described by rational numbers, which is crucial for performing exact and efficient computations. And they are dense in the space of genus two surfaces, which is important for generating inputs. We do not know of a dense set of higher genus surfaces described by rational numbers.

Contributions

- [1] É. Colin de Verdière, V. Despré, and L. Dubois. Untangling graphs on surfaces. In *Proceedings of the 2024 Annual ACM-SIAM Symposium on Discrete Algorithms (SODA)*, pages 4909–4941. SIAM, 2024.
- [2] É. Colin de Verdière, V. Despré, and L. Dubois. A discrete analog of Tutte’s barycentric embeddings on surfaces. In *Proceedings of the 2025 Annual ACM-SIAM Symposium on Discrete Algorithms (SODA)*, pages 5114–5146. SIAM, 2025.
- [3] V. Despré, L. Dubois, M. Pouget, and M. Teillaud. 2D triangulations on hyperbolic surfaces. In *CGAL User and Reference Manual*. CGAL Editorial Board, 6.1 edition, 2025.
- [4] L. Dubois. A bound for Delaunay flip algorithms on flat tori. *Computing in Geometry and Topology*, 2(2):6:1–6:13, 2023.
- [5] L. Dubois. Making multicurves cross minimally on surfaces. In *32nd Annual European Symposium on Algorithms (ESA 2024)*, volume 308, pages 50:1–50:15, 2024.
- [6] L. Dubois. Computing the intrinsic Delaunay tessellation of a closed piecewise-flat surface. *preprint*, 2025.
- [7] L. Dubois, G. Joret, G. Perarnau, M. Pilipczuk, and F. Pitois. Two lower bounds for p -centered colorings. *Discrete Mathematics & Theoretical Computer Science*, 22(Graph Theory), 2020.

Bibliography

- [8] A. Aigon-Dupuy, P. Buser, M. Cibils, A. F. Künzle, and F. Steiner. Hyperbolic octagons and Teichmüller space in genus 2. *Journal of Mathematical Physics*, 46(3), 2005.
- [9] H. A. Akitaya, G. Aloupis, J. Erickson, and C. D. Tóth. Recognizing weakly simple polygons. *Discrete & Computational Geometry*, 58:785–821, 2017.
- [10] H. A. Akitaya, R. Fulek, and C. D. Tóth. Recognizing weak embeddings of graphs. *ACM Transactions on Algorithms (TALG)*, 15(4):1–27, 2019.
- [11] S. Alamdari, P. Angelini, F. Barrera-Cruz, T. M. Chan, G. D. Lozzo, G. D. Battista, F. Frati, P. Haxell, A. Lubiw, M. Patrignani, et al. How to morph planar graph drawings. *SIAM Journal on Computing*, 46(2):824–852, 2017.
- [12] S. Alamdari, P. Angelini, T. M. Chan, G. Di Battista, F. Frati, A. Lubiw, M. Patrignani, V. Roselli, S. Singla, and B. T. Wilkinson. Morphing planar graph drawings with a polynomial number of steps. In *Proceedings of the Twenty-Fourth Annual ACM-SIAM Symposium on Discrete Algorithms*, pages 1656–1667. SIAM, 2013.
- [13] P. Angelini and G. Da Lozzo. Beyond clustered planar graphs. In *Beyond Planar Graphs: Communications of NII Shonan Meetings*, pages 211–235. Springer, 2020.
- [14] P. Angelini, F. Frati, M. Patrignani, and V. Roselli. Morphing planar graph drawings efficiently. In *Graph Drawing: 21st International Symposium, GD 2013, Bordeaux, France, September 23–25, 2013, Revised Selected Papers 21*, pages 49–60. Springer, 2013.
- [15] S. Angenent. Parabolic equations for curves on surfaces: part II. Intersections, blow-up and generalized solutions. *Annals of Mathematics*, pages 171–215, 1991.
- [16] M. A. Armstrong. *Basic Topology*. Springer Science & Business Media, 2013.
- [17] B. Aronov, R. Seidel, and D. Souvaine. On compatible triangulations of simple polygons. *Computational Geometry*, 3(1):27–35, 1993.
- [18] L. Auslander and S. Parter. On imbedding graphs in the sphere. *Journal of Mathematics and Mechanics*, pages 517–523, 1961.
- [19] M. C. Bell and R. C. Webb. Applications of fast triangulation simplification. *arXiv preprint*, 2016.
- [20] J. S. Birman and C. Series. An algorithm for simple curves on surfaces. *Journal of the London Mathematical Society*, 2(2):331–342, 1984.

- [21] L. Blum, M. Shub, and S. Smale. On a theory of computation and complexity over the real numbers: NP-completeness, recursive functions and universal machines. *Bulletin of the American Mathematical Society*, 21(1):1–46, 1989.
- [22] A. I. Bobenko and B. A. Springborn. A discrete Laplace–Beltrami operator for simplicial surfaces. *Discrete & Computational Geometry*, 38(4):740–756, 2007.
- [23] N. Bonichon, S. Felsner, and M. Mosbah. Convex drawings of 3-connected plane graphs. *Algorithmica*, 47(4):399–420, 2007.
- [24] K. S. Booth and G. S. Lueker. Testing for the consecutive ones property, interval graphs, and graph planarity using PQ-tree algorithms. *Journal of computer and system sciences*, 13(3):335–379, 1976.
- [25] J. M. Boyer and W. J. Myrvold. Simplified $O(n)$ planarity by edge addition. *Graph Algorithms Appl*, 5:241, 2006.
- [26] U. Brandes. The left-right planarity test. *Manuscript submitted for publication*, 3, 2009.
- [27] J. E. Bresenham. Algorithm for computer control of a digital plotter. *IBM Systems Journal*, 4(1):25–30, 1965.
- [28] U. Bronfenbrenner. The graphic presentation of sociometric data. *Sociometry*, 7(3):283–289, 1944.
- [29] Y. D. Burago and V. A. Zalgaller. Isometric piecewise-linear embeddings of two-dimensional manifolds with a polyhedral metric into \mathbb{R}^3 . *Algebra i analiz*, 7(3):76–95, 1995.
- [30] P. Buser. *Geometry and Spectra of Compact Riemann Surfaces*. Springer Science & Business Media, 2010.
- [31] S. Cabello. Hardness of approximation for crossing number. *Discrete & Computational Geometry*, 49(2):348–358, 2013.
- [32] S. Cabello, Y. Liu, A. Mantler, and J. Snoeyink. Testing homotopy for paths in the plane. *Discrete & Computational Geometry*, 31:61–81, 2004.
- [33] S. Cabello and B. Mohar. Adding one edge to planar graphs makes crossing number and 1-planarity hard. *SIAM Journal on Computing*, 42(5):1803–1829, 2013.
- [34] S. S. Cairns. Deformations of plane rectilinear complexes. *The American Mathematical Monthly*, 51(5):247–252, 1944.
- [35] E. W. Chambers, É. Colin de Verdière, J. Erickson, F. Lazarus, and K. Whittlesey. Splitting (complicated) surfaces is hard. *Computational Geometry: Theory and Applications*, 41(1–2):94–110, 2008.
- [36] E. W. Chambers, J. Erickson, K. Fox, and A. Nayyeri. Minimum cuts in surface graphs. *SIAM Journal on Computing*, 52(1):156–195, 2023.

- [37] E. W. Chambers, J. Erickson, P. Lin, and S. Parsa. How to morph graphs on the torus. In *Proceedings of the 2021 ACM-SIAM Symposium on Discrete Algorithms (SODA)*, pages 2759–2778. SIAM, 2021.
- [38] H.-C. Chang and A. de Mesmay. Tightening curves on surfaces monotonically with applications. *ACM Transactions on Algorithms*, 18(4):1–32, 2022.
- [39] H.-C. Chang, J. Erickson, D. Letscher, A. De Mesmay, S. Schleimer, E. Sedgwick, D. Thurston, and S. Tillmann. Tightening curves on surfaces via local moves. In *Proceedings of the Twenty-Ninth Annual ACM-SIAM Symposium on Discrete Algorithms*, pages 121–135. SIAM, 2018.
- [40] H.-C. Chang, J. Erickson, and C. Xu. Detecting weakly simple polygons. In *Proceedings of the twenty-sixth annual ACM-SIAM Symposium on Discrete Algorithms*, pages 1655–1670. SIAM, 2014.
- [41] J. Chen and Y. Han. Shortest paths on a polyhedron. In *Proceedings of the sixth annual symposium on Computational geometry*, pages 360–369, 1990.
- [42] J. Chen and Y. Han. Shortest paths on a polyhedron, part I: Computing shortest paths. *International Journal of Computational Geometry & Applications*, 6(02):127–144, 1996.
- [43] D. R. Chillingworth. Simple closed curves on surfaces. *Bulletin of the London Mathematical Society*, 1(3):310–314, 1969.
- [44] D. R. Chillingworth. An algorithm for families of disjoint simple closed curves on surfaces. *Bulletin of the London Mathematical Society*, 3(1):23–26, 1971.
- [45] J. Chuzhoy, S. Mahabadi, and Z. Tan. Towards better approximation of graph crossing number. In *2020 IEEE 61st Annual Symposium on Foundations of Computer Science (FOCS)*, pages 73–84. IEEE, 2020.
- [46] M. Cohen and M. Lustig. Paths of geodesics and geometric intersection numbers. I. *Combinatorial group theory and topology (Alta, Utah, 1984)*, 111:479–500, 1984.
- [47] É. Colin de Verdière and A. de Mesmay. Testing graph isotopy on surfaces. *Discrete & Computational Geometry*, 51:171–206, 2014.
- [48] É. Colin de Verdière and J. Erickson. Tightening nonsimple paths and cycles on surfaces. *SIAM Journal on Computing*, 39(8):3784–3813, 2010.
- [49] É. Colin de Verdière and F. Lazarus. Optimal system of loops on an orientable surface. *Discrete & Computational Geometry*, 33:507–534, 2005.
- [50] É. Colin de Verdière and T. Magnard. An FPT algorithm for the embeddability of graphs into two-dimensional simplicial complexes. *arXiv preprint*, 2021.
- [51] É. Colin de Verdière, T. Magnard, and B. Mohar. Embedding graphs into two-dimensional simplicial complexes. *Computing in Geometry and Topology*, 1(1):1–23, 2022.

- [52] Y. Colin de Verdière. Comment rendre géodésique une triangulation d'une surface ? *L'Enseignement Mathématique*, 37:201–212, 1991.
- [53] P. F. Cortese and G. Di Battista. Clustered planarity. In *Proceedings of the Twenty-First Annual Symposium on Computational Geometry*, SCG '05, page 32–34, New York, NY, USA, 2005.
- [54] P. F. Cortese, G. Di Battista, M. Patrignani, and M. Pizzonia. Clustering cycles into cycles of clusters. In *Graph Drawing: 12th International Symposium, GD 2004, New York, NY, USA, September 29-October 2, 2004, Revised Selected Papers 12*, pages 100–110. Springer, 2005.
- [55] P. F. Cortese, G. Di Battista, M. Patrignani, and M. Pizzonia. On embedding a cycle in a plane graph. *Discrete Mathematics*, 309(7):1856–1869, 2009.
- [56] M. Cygan, F. V. Fomin, Ł. Kowalik, D. Lokshtanov, D. Marx, M. Pilipczuk, M. Pilipczuk, and S. Saurabh. *Parameterized Algorithms*, volume 5. Springer, 2015.
- [57] M. de Berg, M. van Kreveld, M. Overmars, and O. Schwarzkopf. *Computational Geometry*, pages 147–218. Springer Berlin Heidelberg, Berlin, Heidelberg, 1997.
- [58] H. De Fraysseix, P. O. de Mendez, and P. Rosenstiehl. Trémaux trees and planarity. *International Journal of Foundations of Computer Science*, 17(05):1017–1029, 2006.
- [59] H. de Fraysseix, J. Pach, and R. Pollack. Small sets supporting Fáry embeddings of planar graphs. In *Proceedings of the twentieth annual ACM symposium on Theory of computing*, pages 426–433, 1988.
- [60] H. De Fraysseix, J. Pach, and R. Pollack. How to draw a planar graph on a grid. *Combinatorica*, 10:41–51, 1990.
- [61] H. de Fraysseix and P. Rosenstiehl. A depth-first-search characterization of planarity. In *North-Holland Mathematics Studies*, volume 62, pages 75–80. Elsevier, 1982.
- [62] M. de Graaf and A. Schrijver. Making curves minimally crossing by reidemeister moves. *Journal of Combinatorial Theory, Series B*, 70(1):134–156, 1997.
- [63] M. Dehn. Über unendliche diskontinuierliche gruppen. *Mathematische Annalen*, 71(1):116–144, 1911.
- [64] M. Dehn. Transformation der kurven auf zweiseitigen flächen. *Mathematische Annalen*, 72(3):413–421, 1912.
- [65] M. Dehn. On infinite discontinuous groups. In *Papers on Group Theory and Topology*, pages 133–178. Springer, 1987.
- [66] M. Dehn. Transformation of curves on two-sided surfaces. *Papers on Group Theory and Topology*, pages 183–199, 1987.
- [67] M. Dehn. *Papers on Group Theory and Topology*. Springer Science & Business Media, 2012.

- [68] O. Delgado-Friedrichs. Equilibrium placement of periodic graphs and convexity of plane tilings. *Discrete & Computational Geometry*, 33:67–81, 2005.
- [69] V. Despré and F. Lazarus. Computing the geometric intersection number of curves. *Journal of the ACM (JACM)*, 66(6):1–49, 2019.
- [70] V. Despré, J.-M. Schlenker, and M. Teillaud. Flipping geometric triangulations on hyperbolic surfaces. In *SoCG 2020-36th International Symposium on Computational Geometry*, 2020.
- [71] T. K. Dey. A new technique to compute polygonal schema for 2-manifolds with application to null-homotopy detection. In *Proceedings of the tenth annual symposium on Computational geometry*, pages 277–284, 1994.
- [72] T. K. Dey and S. Guha. Transforming curves on surfaces. *Journal of Computer and System Sciences*, 58(2):297–325, 1999.
- [73] G. Di Battista and F. Frati. From tutte to floater and gotsman: on the resolution of planar straight-line drawings and morphs. In *International Symposium on Graph Drawing and Network Visualization*, pages 109–122. Springer, 2021.
- [74] R. Diestel. *Graph Theory*. Springer-Verlag, 2000.
- [75] H. Djidjev and J. Reif. An efficient algorithm for the genus problem with explicit construction of forbidden subgraphs. In *Proceedings of the twenty-third annual ACM symposium on Theory of computing*, pages 337–347, 1991.
- [76] M. P. Do Carmo. *Riemannian Geometry*, volume 2. Springer, 1992.
- [77] R. Dyer, H. Zhang, and T. Möller. Voronoi-delaunay duality and delaunay meshes. In *Proceedings of the 2007 ACM symposium on Solid and physical modeling*, pages 415–420, 2007.
- [78] I. Dynnikov. Counting intersections of normal curves. *Journal of Algebra*, 607:181–231, 2022.
- [79] H. Edelsbrunner and J. Harer. *Computational Topology: An Introduction*. American Mathematical Soc., 2010.
- [80] A. L. Edmonds. Deformation of maps to branched coverings in dimension two. *Annals of Mathematics*, 110(1):113–125, 1979.
- [81] J. A. Ellis-Monaghan and I. Moffatt. *Graphs on Surfaces: Dualities, Polynomials, and Knots*, volume 84. Springer-Verlag, 2013.
- [82] D. Eppstein. Dynamic generators of topologically embedded graphs. In *Proceedings of the 14th Annual ACM-SIAM Symposium on Discrete Algorithms (SODA)*, pages 599–608, 2003.
- [83] D. B. A. Epstein. Curves on 2-manifolds and isotopies. *Acta Mathematica*, 115:83–107, 1966.

- [84] P. Erdős and R. K. Guy. Crossing number problems. *The American Mathematical Monthly*, 80(1):52–58, 1973.
- [85] J. Erickson. Ernie’s 3D pancakes: Shortest paths on PL surfaces. https://3dpancakes.typepad.com/ernie/2006/03/shortest_paths_.html, 2006.
- [86] J. Erickson and A. Nayyeri. Tracing compressed curves in triangulated surfaces. In *Proceedings of the twenty-eighth annual symposium on Computational geometry*, pages 131–140, 2012.
- [87] J. Erickson, I. Van Der Hoog, and T. Miltzow. Smoothing the gap between NP and ER. *SIAM Journal on Computing*, pages FOCS20–102, 2022.
- [88] J. Erickson and K. Whittlesey. Transforming curves on surfaces redux. In *Proceedings of the twenty-fourth annual ACM-SIAM symposium on Discrete algorithms*, pages 1646–1655. SIAM, 2013.
- [89] G. Even, S. Guha, and B. Schieber. Improved approximations of crossings in graph drawings and VLSI layout areas. *SIAM Journal on Computing*, 32(1):231–252, 2002.
- [90] S. Even and R. E. Tarjan. Computing an st-numbering. *Theoretical Computer Science*, 2(3):339–344, 1976.
- [91] B. Farb and D. Margalit. *A Primer on Mapping Class Groups*. Princeton university Press, 2012.
- [92] I. Fáry. On straight line representation of planar graphs. *Acta Sci. Math.(Szeged)*, 11:229–233, 1948.
- [93] Q. W. Feng, R. F. Cohen, and P. Eades. How to draw a planar clustered graph. In *Computing and Combinatorics: First Annual International Conference, COCOON’95 Xi’an, China, August 24–26, 1995 Proceedings 1*, pages 21–30. Springer, 1995.
- [94] Q.-W. Feng, R. F. Cohen, and P. Eades. Planarity for clustered graphs. In *Algorithms—ESA ’95: Third Annual European Symposium Corfu, Greece, September 25–27, 1995 Proceedings 3*, pages 213–226. Springer, 1995.
- [95] I. Filotti, G. L. Miller, and J. Reif. On determining the genus of a graph in $O(v^{O(g)})$ steps (preliminary report). In *Proceedings of the eleventh annual ACM symposium on Theory of computing*, pages 27–37, 1979.
- [96] M. S. Floater. Parametrization and smooth approximation of surface triangulations. *Computer aided geometric design*, 14(3):231–250, 1997.
- [97] M. S. Floater. Parametric tilings and scattered data approximation. *International Journal of Shape Modeling*, 4(03n04):165–182, 1998.
- [98] M. S. Floater and C. Gotsman. How to morph tilings injectively. *Journal of Computational and Applied Mathematics*, 101(1-2):117–129, 1999.
- [99] S. Fortune. Voronoi diagrams and delaunay triangulations. In *Handbook of discrete and computational geometry*, pages 705–721. Chapman and Hall/CRC, 2017.

- [100] R. Fulek and J. Kynčl. Hanani-Tutte for approximating maps of graphs. *arXiv preprint*, 2017.
- [101] R. Fulek and C. D. Tóth. Crossing minimization in perturbed drawings. *Journal of Combinatorial Optimization*, 40(2):279–302, 2020.
- [102] R. Fulek and C. D. Tóth. Atomic embeddability, clustered planarity, and thickenability. *ACM Journal of the ACM (JACM)*, 69(2):1–34, 2022.
- [103] M. R. Garey and D. S. Johnson. Crossing number is NP-complete. *SIAM Journal on Algebraic Discrete Methods*, 4(3):312–316, 1983.
- [104] A. Goldstein. An efficient and constructive algorithm for testing whether a graph can be embedded in a plane. In *Graph and Combinatorics Conference*, pages 16–18, 1963.
- [105] M. T. Goodrich, G. S. Lueker, and J. Z. Sun. C-planarity of extrovert clustered graphs. In *International Symposium on Graph Drawing*, pages 211–222. Springer, 2005.
- [106] S. J. Gortler, C. Gotsman, and D. Thurston. Discrete one-forms on meshes and applications to 3D mesh parameterization. *Computer Aided Geometric Design*, 23(2):83–112, 2006.
- [107] C. Gotsman and V. Surazhsky. Guaranteed intersection-free polygon morphing. *Computers & Graphics*, 25(1):67–75, 2001.
- [108] M. A. Grayson. Shortening embedded curves. *Annals of Mathematics*, 129(1):71–111, 1989.
- [109] M. Grohe. Computing crossing numbers in quadratic time. In *Proceedings of the thirty-third annual ACM symposium on Theory of computing*, pages 231–236, 2001.
- [110] J. L. Gross and T. W. Tucker. *Topological Graph Theory*. Wiley, 1987.
- [111] L. Guibas, J. Hershberger, D. Leven, M. Sharir, and R. Tarjan. Linear time algorithms for visibility and shortest path problems inside simple polygons. In *Proceedings of the second annual symposium on computational geometry*, pages 1–13, 1986.
- [112] L. J. Guibas and R. Sedgewick. A dichromatic framework for balanced trees. In *Proceedings of the 20th Annual IEEE Symposium on Foundations of Computer Science (FOCS)*, pages 8–21, 1979.
- [113] J. Hass and P. Scott. Intersections of curves on surfaces. *Israel Journal of mathematics*, 51:90–120, 1985.
- [114] J. Hass and P. Scott. Simplicial energy and simplicial harmonic maps. *arXiv preprint*, 2012.
- [115] A. Hatcher. *Algebraic topology*. Cambridge University Press, 2002.
- [116] P. S. Heckbert and M. Garland. Survey of polygonal surface simplification algorithms. In *Proceedings of the 24th annual conference on Computer graphics and interactive techniques*. Siggraph, 1997.

- [117] P. Hliněný. Crossing number is hard for cubic graphs. *Journal of Combinatorial Theory, Series B*, 96(4):455–471, 2006.
- [118] J. Hopcroft and R. Tarjan. Efficient planarity testing. *Journal of the ACM (JACM)*, 21(4):549–568, 1974.
- [119] F. Hurtado, M. Noy, and J. Urrutia. Flipping edges in triangulations. In *Proceedings of the twelfth annual symposium on Computational geometry*, pages 214–223, 1996.
- [120] C. Indermitte, T. M. Liebling, M. Troyanov, and H. Clémenton. Voronoi diagrams on piecewise flat surfaces and an application to biological growth. *Theoretical Computer Science*, 263(1-2):263–274, 2001.
- [121] M. Juvan, J. Marinček, and B. Mohar. Embedding graphs in the torus in linear time. In *International Conference on Integer Programming and Combinatorial Optimization*, pages 360–363. Springer, 1995.
- [122] S. Katok. *Fuchsian Groups*. University of Chicago press, 1992.
- [123] K.-I. Kawarabayashi, Y. Kobayashi, and B. Reed. The disjoint paths problem in quadratic time. *Journal of Combinatorial Theory, Series B*, 102(2):424–435, 2012.
- [124] K.-I. Kawarabayashi, B. Mohar, and B. Reed. A simpler linear time algorithm for embedding graphs into an arbitrary surface and the genus of graphs of bounded tree-width. In *2008 49th Annual IEEE Symposium on Foundations of Computer Science*, pages 771–780. IEEE, 2008.
- [125] K.-I. Kawarabayashi and B. Reed. Computing crossing number in linear time. In *Proceedings of the thirty-ninth annual ACM symposium on Theory of computing*, pages 382–390, 2007.
- [126] J. W. Kennedy, L. V. Quintas, and M. M. Sysło. The theorem on planar graphs. *Historia mathematica*, 12(4):356–368, 1985.
- [127] L. Kettner. Using generic programming for designing a data structure for polyhedral surfaces. *Computational Geometry: Theory and Applications*, 13:65–90, 1999.
- [128] D. Kirkpatrick. Optimal search in planar subdivisions. *SIAM Journal on Computing*, 12(1):28–35, 1983.
- [129] T. Korhonen, M. Pilipczuk, and G. Stamoulis. Minor containment and disjoint paths in almost-linear time. In *2024 IEEE 65th Annual Symposium on Foundations of Computer Science (FOCS)*, pages 53–61. IEEE, 2024.
- [130] C. Kuratowski. Sur le probleme des courbes gauches en topologie. *Fundamenta mathematicae*, 15(1):271–283, 1930.
- [131] M. Lackenby. Some fast algorithms for curves in surfaces. *arXiv preprint*, 2024.
- [132] Y. Ladegaillerie. Classes d’isotopie de plongements de 1-complexes dans les surfaces. *Topology*, 23(3):303–311, 1984.

- [133] F. Lazarus, M. Pocchiola, G. Vegter, and A. Verroust. Computing a canonical polygonal schema of an orientable triangulated surface. In *Proceedings of the seventeenth annual symposium on Computational geometry*, pages 80–89, 2001.
- [134] F. Lazarus and J. Rivaud. On the homotopy test on surfaces. In *2012 IEEE 53rd Annual Symposium on Foundations of Computer Science*, pages 440–449. IEEE, 2012.
- [135] F. Lazarus and F. Tallerie. A universal triangulation for flat tori. *Discrete & Computational Geometry*, 71(1):278–307, 2024.
- [136] A. Lempel. An algorithm for planarity testing of graphs. In *Theory of Graphs: International Symposium.*, pages 215–232. Gordon and Breach, 1967.
- [137] N. Linial, L. Lovasz, and A. Wigderson. Rubber bands, convex embeddings and graph connectivity. *Combinatorica*, 8:91–102, 1988.
- [138] H.-T. D. Liu, M. Gillespie, B. Chislett, N. Sharp, A. Jacobson, and K. Crane. Surface simplification using intrinsic error metrics. *ACM Transactions on Graphics*, 42(4), 2023.
- [139] Y.-J. Liu, Z. Chen, and K. Tang. Construction of iso-contours, bisectors, and voronoi diagrams on triangulated surfaces. *IEEE Transactions on Pattern Analysis and Machine Intelligence*, 33(8):1502–1517, 2010.
- [140] Y.-J. Liu, C.-X. Xu, D. Fan, and Y. He. Efficient construction and simplification of delaunay meshes. *ACM Transactions on Graphics (TOG)*, 34(6):1–13, 2015.
- [141] M. Löffler, T. Ophelders, R. I. Silveira, and F. Staals. Shortest paths in portalgons. In *39th International Symposium on Computational Geometry (SoCG 2023)*, volume 258, pages 48:1–48:16, 2023.
- [142] D. Lokshtanov, F. Panolan, S. Saurabh, R. Sharma, J. Xue, and M. Zehavi. Crossing number in slightly superexponential time (extended abstract). In *Proceedings of the 2025 Annual ACM-SIAM Symposium on Discrete Algorithms (SODA)*, 2025.
- [143] L. Lovász. *Graphs and Geometry*, volume 65. American Mathematical Soc., 2019.
- [144] A. Lubiw and M. Petrick. Morphing planar graph drawings with bent edges. *Journal of Graph Algorithms and Applications*, 15(2):205–227, 2011.
- [145] Y. Luo, T. Wu, and X. Zhu. The deformation space of geodesic triangulations and generalized Tutte’s embedding theorem. *Geometry & Topology*, 27(8):3361–3385, 2023.
- [146] M. Lustig. Paths of geodesics and geometric intersection numbers. II. *Combinatorial group theory and topology (Alta, Utah, 1984)*, 111:501–543, 1987.
- [147] K. Menger. Über plättbare dreiergraphen und potenzen nicht plättbarer graphen. In *Ergeb. Math. Kolloq*, volume 2, pages 30–31, 1929.
- [148] J. S. Mitchell. Shortest paths and networks. In *Handbook of Discrete and Computational Geometry*, pages 811–848. Chapman and Hall/CRC, 2017.

- [149] J. S. Mitchell, D. M. Mount, and C. H. Papadimitriou. The discrete geodesic problem. *SIAM Journal on Computing*, 16(4):647–668, 1987.
- [150] B. Mohar. A linear time algorithm for embedding graphs in an arbitrary surface. *SIAM Journal on Discrete Mathematics*, 12(1):6–26, 1999.
- [151] D. M. Mount. *Voronoi Diagrams on the Surface of a Polyhedron*. University of Maryland, 1985.
- [152] W. Myrvold and W. Kocay. Errors in graph embedding algorithms. *Journal of Computer and System Sciences*, 77(2):430–438, 2011.
- [153] W. Myrvold and J. Woodcock. A large set of torus obstructions and how they were discovered. *the electronic journal of combinatorics*, pages P1–16, 2018.
- [154] J. Pach and G. Tóth. Which crossing number is it anyway? *Journal of Combinatorial Theory, Series B*, 80(2):225–246, 2000.
- [155] H. Poincaré. Cinquième complément à l’analysis situs. *Rendiconti del Circolo Matematico di Palermo (1884-1940)*, 18(1):45–110, 1904.
- [156] H. W. Pullman. An elementary proof of Pick’s theorem. *School Science and Mathematics*, 79(1):7–12, 1979.
- [157] T. Quintanar. An explicit pl-embedding of the square flat torus into \mathbb{R}^3 . *Journal of Computational Geometry*, 11(1):615–628, 2020.
- [158] B. L. Reinhart. Algorithms for jordan curves on compact surfaces. *Annals of Mathematics*, 75(2):209–222, 1962.
- [159] J. Richter-Gebert. *Realization Spaces of Polytopes*. Springer, 2006.
- [160] R. D. Ringeisen. Survey of results on the maximum genus of a graph. *Journal of Graph Theory*, 3(1):1–13, 1979.
- [161] G. Ringel. Bestimmung der maximalzahl der nachbargebiete auf nichtorientierbaren flächen. *Mathematische Annalen*, 127(1):181–214, 1954.
- [162] G. Ringel. Das geschlecht des vollständigen paaren graphen. In *Abhandlungen aus dem Mathematischen Seminar der Universität Hamburg*, volume 28, pages 139–150. Springer, 1965.
- [163] G. Ringel and J. W. Youngs. Solution of the heawood map-coloring problem. *Proceedings of the National Academy of Sciences*, 60(2):438–445, 1968.
- [164] N. Robertson and P. D. Seymour. Graph minors. XIII. the disjoint paths problem. *Journal of combinatorial theory, Series B*, 63(1):65–110, 1995.
- [165] P. Rosenstiehl and R. E. Tarjan. Rectilinear planar layouts and bipolar orientations of planar graphs. *Discrete & Computational Geometry*, 1:343–353, 1986.
- [166] G. Rote. Strictly convex drawings of planar graphs. In *SODA*, volume 5, pages 728–734. Citeseer, 2005.

- [167] M. Schaefer. *Crossing Numbers of Graphs*. CRC Press, 2018.
- [168] M. Schaefer, E. Sedgwick, and D. Stefankovic. Computing Dehn twists and geometric intersection numbers in polynomial time. In *CCCG*, volume 20, pages 111–114, 2008.
- [169] H. Schipper. Determining contractibility of curves. In *Proceedings of the eighth annual symposium on Computational geometry*, pages 358–367, 1992.
- [170] W. Schnyder. Planar graphs and poset dimension. *Order*, 5:323–343, 1989.
- [171] W. Schnyder. Embedding planar graphs on the grid. In *Proceedings of the first annual ACM-SIAM symposium on Discrete algorithms*, pages 138–148, 1990.
- [172] N. Sharp and K. Crane. You can find geodesic paths in triangle meshes by just flipping edges. *ACM Transactions on Graphics (TOG)*, 39(6):1–15, 2020.
- [173] M. Shepard. *The Topology of Shortest Curves in Surfaces*. University of California, Berkeley, 1991.
- [174] Y. Shiloach. Arrangements of planar graphs on the planar lattice. *PhD thesis, Weizmann Institute of Science*, 1976.
- [175] S. K. Stein. Convex maps. *Proceedings of the American Mathematical Society*, 2(3):464–466, 1951.
- [176] J. Stillwell. The word problem and the isomorphism problem for groups. *Bulletin of the American Mathematical Society*, 6(1):33–56, 1982.
- [177] J. Stillwell. *Classical Topology and Combinatorial Group Theory*, volume 72. Springer Science & Business Media, 2012.
- [178] V. Surazhsky and C. Gotsman. Controllable morphing of compatible planar triangulations. *ACM Transactions on Graphics (TOG)*, 20(4):203–231, 2001.
- [179] K. Takayama. Compatible intrinsic triangulations. *ACM Transactions on Graphics (TOG)*, 41(4):1–12, 2022.
- [180] C. Thomassen. Deformations of plane graphs. *Journal of Combinatorial Theory, Series B*, 34(3):244–257, 1983.
- [181] C. Thomassen. The graph genus problem is NP-complete. *Journal of Algorithms*, 10(4):568–576, 1989.
- [182] C. Thomassen. Tutte’s spring theorem. *Journal of Graph Theory*, 45(4):275–280, 2004.
- [183] P. Turán. A note of welcome. *Journal of Graph Theory*, 1(1):7–9, 1977.
- [184] W. T. Tutte. How to draw a graph. *Proceedings of the London Mathematical Society*, 3(1):743–767, 1963.
- [185] G. Vegter and C. K. Yap. Computational complexity of combinatorial surfaces. In *Proceedings of the sixth annual symposium on Computational geometry*, pages 102–111, 1990.

- [186] K. Wagner. Bemerkungen zum vierfarbenproblem. *Jahresbericht der Deutschen Mathematiker-Vereinigung*, 46:26–32, 1936.
- [187] K. Wagner. Über eine eigenschaft der ebenen komplexe. *Mathematische Annalen*, 114(1):570–590, 1937.
- [188] H. Wang. A new algorithm for euclidean shortest paths in the plane. *Journal of the ACM*, 70(2):1–62, 2023.
- [189] H. Zhang and X. He. Compact visibility representation and straight-line grid embedding of plane graphs. In *Workshop on Algorithms and Data Structures*, pages 493–504. Springer, 2003.